

# STUDIES ON LECITHIN REVERSE MICELLAR SYSTEMS BY NMR AND OTHER SPECTROSCOPIC AND PHYSICAL TECHNIQUES

A Thesis Submitted  
in Partial Fulfilment of the Requirements  
for the Degree of  
DOCTOR OF PHILOSOPHY

By  
V. VENKATESWARA KUMAR

*to the*

DEPARTMENT OF CHEMISTRY  
INDIAN INSTITUTE OF TECHNOLOGY KANPUR  
FEBRUARY, 1982

*Dedicated*  
to  
*My Parents*

STATEMENT

I hereby declare that the work embodied in this thesis entitled, STUDIES ON LECITHIN REVERSE MICELLAR SYSTEMS BY NMR AND OTHER SPECTROSCOPIC AND PHYSICAL TECHNIQUES has been carried out by me under the supervision of Professor P. Raghunathan.

In keeping with scientific tradition, wherever work done by others has been utilised, due acknowledgement has been made.

V. Venkateswara Kumar

V. Venkateswara Kumar

4 JUN 1984

CENTRAL LIBRARY  
I. I. T., Kanpur.

Acc. No. A 82210

✓ CHM-1982-D-KUM-S

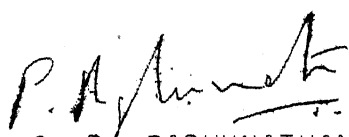


POSTGRADUATE CERTIFICATE  
24/2/82  
P.D.

iv

CERTIFICATE I

Certified that the work presented in this thesis entitled, STUDIES ON LECITHIN REVERSE MICELLAR SYSTEM BY NMR AND OTHER SPECTROSCOPIC AND PHYSICAL TECHNIQUES by Mr. V. Venkateswara Kumar, Department of Chemistry, IIT-Kanpur, has been carried out under my supervision and has not been submitted elsewhere for a degree.

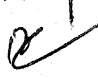
  
(Prof. P. RAGHUNATHAN)

Thesis Supervisor

Department of Chemistry

IIT-Kanpur - 208 016.

February 20, 1982.

POST GRADUATE OFFICE  
This thesis has been approved  
for the award of the Degree of  
Doctor of Philosophy (Ph.D.)  
in accordance with the  
regulations of the Indian  
Institute of Technology Kanpur  
Dated: 2-4-1983 

DEPARTMENT OF CHEMISTRY,  
INDIAN INSTITUTE OF TECHNOLOGY, KANPUR, INDIA

CERTIFICATE II

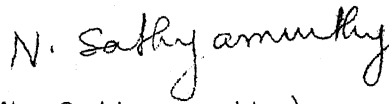
This is to certify that Mr. V. Venkateswara Kumar has satisfactorily completed all the courses required for the Ph.D. degree programme. The courses include:

Chm 500 Basic Course in Mathematics  
Chm 521 Chemical Binding  
Chm 524 Modern Physical Methods in Chemistry  
Chm 534 Electronics for Chemists  
Chm 626 Solid State Chemistry  
Chm 800 General Seminar  
Chm 801 Student Seminar  
Chm 900 Graduate Research

Mr. V. Venkateswara Kumar was admitted to the candidacy for the Ph.D. degree in March 1980 after he successfully completed the written and oral qualifying examinations.

  
(U.C. Agarwala)

Head,  
Department of Chemistry,  
IIT-KANPUR

  
(N. Sathyamurthy)

Convener,  
Departmental Post-  
Graduate Committee  
IIT-KANPUR

### ACKNOWLEDGEMENTS

It gives me great pleasure to place on record my deep sense of gratitude and indebtedness to Professor P. Raghunathan who introduced me to the field of Magnetic Resonance in general and the field of Biophysical Chemistry in particular. The past three years that I have been associated with him have gone a long way in shaping up my attitudes on academic as well non-academic issues. His valuable guidance and encouragement have been the prime factors responsible for the successful completion of this work. My sincere thanks are also due to Mrs. Vaijayanthi Raghunathan for her keen interest in my work and welfare.

I am deeply indebted to Dr. C. Kumar who has helped me out at innumerable stages of my work and whose knowledge and experience in the field of biophysical chemistry have been indispensable to me.

I humbly express my sincere gratitude to Professor D. Balasubramanian and Professor P.T. Manoharan for allowing me to utilise the NMR facilities at University of Hyderabad and at R.S.I.C., IIT-Madras, respectively.

I am very much thankful to my lab-mates Mr. K.K. Muraleedharan and Mr. Sandip K. Sur for their cooperation, help and encouragement. I also thank Dr. V. Harihara Subramanian for many helpful suggestions and discussions.

I wish to acknowledge the technical help provided by Mr. Das for Electron Microscopy, Mr. Jain for UV Spectroscopy,

M/s Bhaskaran for glass blowing, R.D. Singh for typing the manuscript, B.N. Shukla for cyclostyling, Gauri Singh for neat drawings and Ram Shankar Singh for help in the lab.

I thank all my friends and particularly Drs. P.B.K. Sarma, P. Subramanian, S.V.S. Murty, R. Ragunathan, S. Shankar, Rakesh, Vijaya Kumar, Scaria and messrs Khemani, Trinadha Rao, Subba Rao, Kamalakar, Mohan Rao, Narasimha Reddy, Swaminathan, Satyanarayana Raju, K.B.K. Rao, Muddukrishna, Keshava Murthy, BARC, Bhushan, Bajaj, Chowdhary, Mrs. Vidya Bhushan, and Mrs. Madhu Phull for helping me at various stages of this work.

I would like to thank Sri C.V. Subrahmanya Sastry, Secretary and Correspondent, C.S.R. Sarma College, Ongole, for sponsoring me as a Research Fellow under the FIP of UGC. I am also thank ful to Shri K. Bhuvaneswarachari, my colleague at Ongole for his suggestions and encouragement all these years.

Finally, I would be failing in my duty if I do not acknowledge the loving patronage and encouragement of my parents, sisters, brothers-in-law, brothers and sisters-in-law.

V. VENKATESWARA KUMAR

## SYNOPSIS

There has been a rapid growth of interest in recent years on the study of phospholipid aggregates in non-polar media since these aggregated structures often 'model' faithfully the nature of cell membranes. Such aggregation leads to reverse micelles with a polar interior and a non-polar outer surface. These aggregates can solubilise water in their interior as small water 'pools'. Despite the potential value accruing from a thorough understanding of reverse micellar arrangements of phospholipids, only a few detailed investigations have been reported to-date. In this thesis, an attempt is made at an exhaustive, in-depth investigation of a variety of physical and spectroscopic properties of the system lecithin (also known as phosphatidylcholine, PC) - water in three representative non-polar solvents, benzene, carbontetrachloride and cyclohexane.

In Chapter 1, the existing literature pertaining to phospholipid reverse micelles is reviewed. Chapter 2 contains results of the present work on the hydrodynamic and structural characterisation of PC-non polar solvent-water systems. It is shown by water uptake studies that about 0.37 g of water/1 g of PC is solubilised by a 5% w/v solution of PC in the non-polar solvent, resulting in a clear reverse micellar solution. Further addition of water causes phase separation. In cyclohexane solvent, a very interesting and novel behaviour is

observed in that a viscous and optically anisotropic liquid crystalline phase is detected at a water content of 0.11 g - 0.17 g of water/1 g of PC. Optical birefringence, viscosity, light scattering, electron microscopy and electrical conductivity techniques are utilised to characterise the reverse micellar and liquid crystalline phases and the transitions between them. In all the solvents studied the optically isotropic phase displays Newtonian viscosity, leading to the inference that highly symmetrical spherically-shaped structures are present. On the other hand, the anisotropic phase in cyclohexane exhibits a markedly non-Newtonian viscosity, typical of highly asymmetric structures. Positively stained electron micrographs presented in this chapter clearly demonstrate the formation of spherical structures in benzene (about 600 Å radius) and carbontetrachloride (about 500 Å radius), and of elongated 'tubular' structures containing aqueous canals in the cyclohexane medium.

Chapter 3 describes a detailed analysis of the water content in the pools by a variety of spectroscopic studies. The 1890 nm and 1930 nm near infrared bands reveal that most of the water resides in the 'pools' and only a negligible fraction remains in the non-polar 'oil' phases. A study of fluorescence emission wavelength (using 8-anilinonaphthalene sulfonic acid, ANSA, as a fluorescent probe) shows that, with increasing water concentration the polarity of the water 'pools' increases from an initially low value to that of bulk water.

This conclusion is further supported by the electronic absorption band of  $\text{NO}_3^-$ , a polarity probe dissolved in the water used in the system.

Chapter 3 also contains the NMR chemical shifts, spin-lattice ( $T_1$ ) and spin-spin ( $T_2$ ) relaxation times for the protons of trapped water and the PC head-group and  $T_1$  data for  $^{31}\text{P}$  of the latter. Proton  $T_1$  and  $T_2$  of water in carbontetrachloride and benzene systems increase linearly with added water upto the point of phase separation. In the case of cyclohexane, the corresponding values initially increase and then start to decrease at the proposed 'spherical-to-liquid crystalline' transition. In addition to providing clear evidence for the onset of the phase transition in cyclohexane medium, these data also provide a quantitative estimate of the bound and bulk water as well as of the mobility of water in the trapped or 'pool' state. Microviscosities and rotational correlation times of this trapped water at different water-concentrations are also reported.

The next two chapters present more specialised studies, based on NMR spectroscopy, pertaining to the liquid crystalline phase detected in the PC-cyclohexane-water system. In Chapter 4, the self-diffusion of water ( $D$ ) in the above system (relative to that of pure water,  $D_0$ , at the same temperature) is studied by using the magnetic-field gradient technique. At the micelle-liquid crystalline transition, the relative diffusion coefficient ( $D/D_0$ ) is sharply affected. In Chapter 5, quadrupolar

lineshapes of the  $D_2O$  are studied at various stages of water uptake by PC-cyclohexane reverse micelles. Also reported in this chapter is the lineshape analysis of the  $^{31}P$ -NMR spectrum of the PC-head group as the liquid crystalline phase is approached. For the sake of comparison computer simulation of the experimental  $^{31}P$  lineshapes is briefly discussed.

The thesis concludes with a brief chapter on the overall summary of this study and with suggestions for future work.



LIST OF FIGURES

FIGURE		<u>Page</u>
1.1	Structures of some phospholipids	... 4
1.2	Electron micrographs of vesicle and liposome	... 10
1.3	Electron micrograph of bilayer	... 11
1.4	Structure of lipid bilayer and fluid mosaic model of Singer and Nicolson	... 13
1.5	Structures of hydrated phospholipids	... 15
1.6	Structure representing the transformation of a bilayer into the reverse micellar structure during membrane fusion process	... 16
1.7	Schematics of a cell and reverse micelle	... 29
2.1	Variation of relative viscosity in benzene and carbontetrachloride systems as a function of added water	... 52
2.2	Variation of relative viscosity in cyclohexane system as a function of added water	... 53
2.3	Shear rate dependence of viscosity in cyclohexane system	... 57
2.4	Variation of dissymmetry parameter in benzene, carbontetrachloride and cyclohexane systems as a function of added water	... 62
2.5	Variation of dissymmetry parameter with radius of gyration for different shaped structures	... 64
2.6 and 2.7	Electron micrographs of benzene system at different water concentrations	... 67
2.8 and 2.9	Electron micrographs of carbontetrachloride system at different water concentrations	... 68
2.10 to 2.12	Electron micrographs of cyclohexane system at a different water concentrations	... to 70

FIGURE	<u>Page</u>
2.13 Variation of specific conductivity in benzene and carbontetrachloride systems as a function of added aqueous KCl solution	... 73
2.14 Variation of specific conductivity in cyclohexane system as a function of added aqueous KCl solution	... 74
3.1 Near IR spectra of benzene system at different water concentrations	... 85
3.2 Variation of $\lambda_{\max}$ of $n - \pi^*$ band of $\text{NO}_3^-$ in carbontetrachloride system as a function of added water	... 89
3.3 Fluorescence emission spectra of benzene system at various concentrations of added water	... 92
3.4 Fluorescence emission spectra of cyclohexane system at various concentrations of added water	... 93
3.5 Variation of fluorescence emission maximum of ANSA in benzene and cyclohexane systems as a function of added water	... 94
3.6 Variation of quantum yield of ANSA in benzene and cyclohexane systems as a function of added water	... 96
3.7 100 MHz proton NMR spectrum in the carbontetrachloride system at an R value of zero	... 98
3.8 100 MHz proton NMR spectrum in the carbontetrachloride system at an R value of 4.2	... 99
3.9 100 MHz proton NMR spectrum in the carbontetrachloride system at an R value of 8.3	... 100
3.10 100 MHz proton NMR spectrum in the carbontetrachloride system at an R value of 12.0	... 101
3.11 100 MHz proton NMR spectrum in the benzene system at an R value of zero	... 102
3.12 100 MHz proton NMR spectrum in the benzene system at an R value of 2.2	... 103

FIGURE	<u>Page</u>
3.13 100 MHz proton NMR spectrum in the benzene system at an R value of 6.5	... 104
3.14 100 MHz proton NMR spectrum in the benzene system at an R value of 10.0	... 105
3.15 100 MHz proton NMR spectrum in the cyclohexane system at an R value of zero	... 106
3.16 100 MHz proton NMR spectrum in the cyclohexane system at an R value of 4.0	... 107
3.17 Variation in NMR chemical shift of water protons in the three systems as a function of added water	... 109
3.18 Variation in NMR chemical shift of $^+N(CH_3)_3$ protons in the three systems as a function of added water	... 110
3.19 Structure of folded polar head group of lecithin according to (a) ref. 22; (b) ref. 23.	... 113
3.20 Interaction of water with folded polar head-group of lecithin	... 115
3.21 Variation in phosphorous NMR chemical shifts of lecithin head-group in benzene system as a function of added water	... 117
3.22 Variation in $T_1$ of water protons in the three systems as a function of added water	... 119
3.23 Hydration of head-group of lecithin in benzene system as a function of added water	... 121
3.24 Variation in $T_1$ of $^+N(CH_3)_3$ protons in the three systems as a function of added water	... 129
3.25 Variation in $T_1$ of $-CH_2N^+$ protons in carbon-tetrachloride and benzene systems as a function of added water	... 130
3.26 Variation in $T_2$ of water protons in carbon-tetrachloride and cyclohexane systems as a function of added water	... 132
3.27 Variation in $T_2$ of $^+N(CH_3)_3$ protons in carbon-tetrachloride and cyclohexane systems as a function of added water	... 133

FIGURE		<u>Page</u>
3.28	Variation in $^{31}\text{P}$ -NMR $T_1$ values of lecithin head group in the three systems as a function of added water	... 137
3.29	100.6 MHz $^{13}\text{C}$ -NMR spectrum of lecithin in $\text{CDCl}_3$ at an R value of zero	... 139
3.30	100.6 MHz $^{13}\text{C}$ -NMR spectrum of lecithin in $\text{CDCl}_3$ at an R value of 2.0	... 141
3.31	100.6 MHz $^{13}\text{C}$ NMR spectrum of lecithin in $\text{CDCl}_3$ at an R value of 6.0	... 142
3.32	100.6 MHz $^{13}\text{C}$ NMR spectrum of lecithin in $\text{CDCl}_3$ at an R value of 10.0	... 143
4.1	The $90^\circ$ - $\tau$ - $180^\circ$ $T_2$ experiment with formation of a spin echo	... 152
4.2	Spin echo amplitude <u>versus</u> $\tau^3$ for steady applied field gradient of 10.1 Gauss/cm	... 160
4.3	Spin echo amplitude <u>versus</u> $\tau^3$ for steady applied field gradient of 10.4 Gauss/cm	... 161
4.4	Spin echo amplitude <u>versus</u> $\tau^3$ for steady applied field gradient of 10.7 Gauss/cm	... 162
4.5	Spin echo decay rate <u>versus</u> $\tau^3$ . The solid line represents the fit of Eq.(4.7) to the experimental data	... 163
4.6	Variation of self-diffusion coefficient of water as a function of added water	... 165
5.1	Pulse sequence employed for recording DMR spectra	... 177
5.2	30.71 MHz DMR lineshape (i.e., FT of DMR quadrupolar echo) of PC-cyclohexane- $\text{D}_2\text{O}$ system at an R value of 1	... 179
5.3	30.71 MHz DMR lineshape of PC-cyclohexane- $\text{D}_2\text{O}$ system at an R value of 2	... 180
5.4	30.71 MHz DMR lineshape of PC-cyclohexane- $\text{D}_2\text{O}$ system at an R value of 3	... 181

FIGURE		<u>Page</u>
5.5	30.71 MHz DMR lineshape of PC-cyclohexane-D <sub>2</sub> O system at an R value of 4	... 182
5.6	30.71 MHz DMR lineshape of PC-cyclohexane-D <sub>2</sub> O system at an R value of 5	... 183
5.7	30.71 MHz DMR lineshape of PC-cyclohexane-D <sub>2</sub> O system at an R value of 6.5	... 184
5.8	30.71 MHz DMR lineshape of PC-cyclohexane-D <sub>2</sub> O system at an R value of 8	... 185
5.9	Polymorphic phases of phospholipids and the corresponding <sup>31</sup> P NMR spectra	... 191
5.10	32.44 MHz phosphorous NMR spectra of PC-cyclohexane-D <sub>2</sub> O system at an R value of 6.5	... 193
5.11	Computer simulated phosphorous NMR spectra of PC-cyclohexane-D <sub>2</sub> O system for different $\tau_c$ values	... 195

LIST OF TABLES

TABLE		<u>Page</u>
2.1	Water up-take by a 5% w/v solution of lecithin in benzene, carbontetrachloride and cyclohexane	... 46
2.2	Variation of relative viscosity in benzene, carbontetrachloride and cyclohexane systems as a function of added water	... 55
2.3	Radii of the spherical structures formed in benzene, carbontetrachloride and cyclohexane systems obtained from electron micrographs	... 71
3.1	Nitrate ion $n - \pi$ $\lambda_{\max}$ in different solvents	... 88
3.2	Details of the proton NMR spectra presented in Figs. 3.7 to 3.16.	... 97
3.3	Microviscosity of water environment in benzene system	... 124
3.4	Microviscosity of water environment in carbontetrachloride system	... 125
3.5	Microviscosity of water environment in cyclohexane system	... 125
3.6	Variation in proton NMR $T_1$ of $(-\text{CH}_2)_n$ in cyclohexane system	... 128
3.7	Calculated and experimental $T_2$ values of water protons in carbontetrachloride system at different water concentrations	... 135
4.1	Comparison of $T_2$ values from experimental spectral linewidth and from CPMG sequence at different R values for cyclohexane system	... 157
4.2	Self-diffusion coefficient, $D_0$ , of pure water at 25°C	... 158
4.3	Variation of self-diffusion coefficient of water as a function of R	... 164
5.1	$\tau_c$ values of PC-cyclohexane- $\text{D}_2\text{O}$ system at different R values	... 187

CONTENTS

	<u>Page</u>
STATEMENT	... iii
CERTIFICATE I	... iv
CERTIFICATE II	... v
ACKNOWLEDGEMENTS	... vi
SYNOPSIS	... viii
LIST OF FIGURES	... xii
LIST OF TABLES	... xvii
CHAPTER I - INTRODUCTION	... 1
CHAPTER II - PHYSICAL STUDIES	... 40
CHAPTER III - NMR AND OTHER SPECTROSCOPIC STUDIES	... 80
CHAPTER IV - NMR OF WATER DIFFUSION IN THE CYCLOHEXANE SYSTEM	... 149
CHAPTER V - $^2\text{H}$ and $^{31}\text{P}$ -NMR LINESHAPES IN THE CYCLOHEXANE SYSTEM	... 171
CONCLUSIONS AND SOME FURTHER PROSPECTS	... 199
VITAE	... 202
LIST OF PUBLICATIONS	... 203

...

CHAPTER I

I N T R O D U C T I O N



In the past two decades the study of biological membranes has acquired a key role in biochemical enquiries into the structure of living organisms. Biological membranes not only delineate the physical boundaries of cell and other cellular organelles, but in fact fulfil several other vital functions.

More recently, there has been a rapid growth of interest in biophysical studies of phospholipids and the polymolecular structures they form under various conditions (1-5), this interest undoubtedly stemming from the fact that these structures often model faithfully the nature of cell membranes.

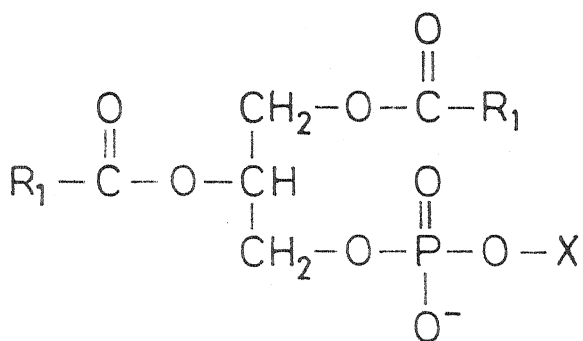
The two major structural elements of membranes are lipids and proteins. The diverse nature of the proteins and lipids found in natural membranes makes the study of their various interactions a difficult task. Nevertheless, a great deal of insight has been gained owing to the contributions of numerous workers in this field. The bulk of these research activities has been concerned with the significance for membranes of both the chemical (6) and physical (7-9) properties of phospholipids. Coherent models of the organisation of natural cell membranes, such as for example, the well known 'protein mosaic' model (10), have therefore become possible.

The fact that membranes contain large amount of lipids, particularly phospholipids, distinguishes them from most other cellular structures, and it is not surprising that until recent years the focus of membrane research has been primarily on the

lipid components. This focus on the membrane lipids was encouraged by the fact that the most obvious role of membranes is their barrier function. This requires that the unregulated passage of water-soluble materials be prevented, and the lipids, with their markedly hydrophobic hydrocarbon chains, would seem to be the logical candidates for this task. The use of sophisticated physical techniques to examine in detail the ways in which lipid molecules organise themselves in different environments would be both an interesting and rewarding exercise. The work to be described in this thesis is a contribution in this general direction.

It has long been known that phospholipids and glycolipids (i.e., glycerophosphatides and sphingolipids) form ordered multi-molecular structures when placed in aqueous surroundings (11). This reflects the fact that these molecules are classical amphiphiles or amphipaths (Greek: Amphi = dual, Pathi = sympathy, Phile = liking). Phospholipids are amphipathic, elongated molecules, much smaller in weight and size than polymers, but sufficiently large enough to have two distinct regions of greatly differing polarity. That is, one end of the lipid molecule is polar (hydrophilic) in nature which favours interaction with water, while the other end is non-polar (hydrophobic) region consisting of hydrocarbon chains. Fig. 1.1 shows the structures of some phospholipids.

The amphipathic nature of the lipids results in molecular association phenomena characteristic of lipids in both crystals

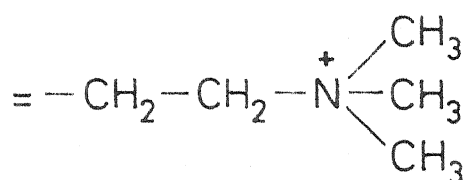


$\text{R}_1 = \text{R}_2 = \text{Fatty Acyl Groups}$

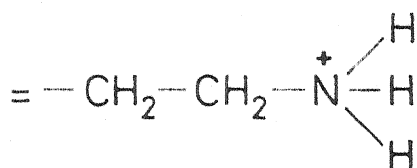
where



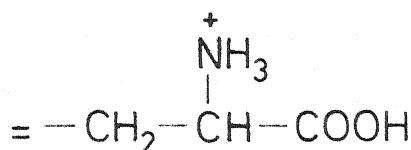
Phosphatidic Acid



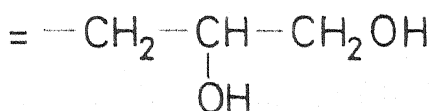
Phosphatidylcholine  
(Lecithin)



Phosphatidylethanolamine



Phosphatidylserine



Phosphatidylglycerol

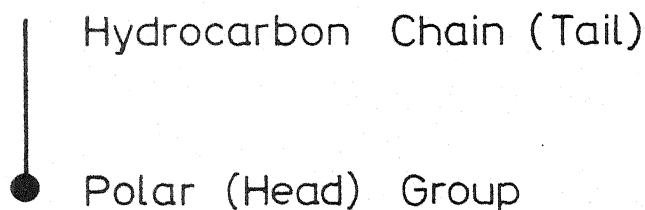


Fig. 1.1 Structures of some Phospholipids.

and lipid-water systems. The intermolecular forces of cohesion differ according to the nature of two regions. Van der Waals bonds are operative between the hydrocarbon chains of the neighbouring molecules ( $\sim 1.8 \text{ kcal mol}^{-1}$  of  $-\text{CH}_3$  and  $\sim 1 \text{ kcal mol}^{-1}$  of  $\text{CH}_2$ ) (12), while in the polar region hydrogen bonding and dipole-dipole interactions dominate, with interaction energies of the order of  $1\text{-}10 \text{ kcal mol}^{-1}$ . In the case of lipids with charged groups the principal interaction will be electrostatic, involving energies of about  $100\text{-}200 \text{ kcal mol}^{-1}$ . On the basis of energetic considerations it is expected that like regions interact with each other i.e., the polar head groups associate with each other and likewise apolar regions of the molecule cluster together when lipid molecules aggregate. In addition to the interaction energies mentioned above, the association of hydrocarbon chains is stabilised by a positive  $T\Delta S$  term ( $\Delta S$  is the entropy change) usually referred to as hydrophobic interaction (13,14).

### The Structure of Membranes

Among the major questions remaining unanswered regarding membrane organisation is that of lipid-water interaction at the membrane interface. Again, with structures containing many different molecules such as lipids, proteins, sugars, cholesterol and water, clearly a variety of structural arrangements is theoretically possible. It is, therefore, not surprising to find at present a wide range of speculations dealing with this question. These speculations often depend upon the emphasis given to one of the

components present. Thus an emphasis on lipid and its importance in determining structure leads to one possibility i.e., the bilayer model (15), while emphasis on protein leads to the protein mosaic model (10). In between there is a range of suggested structures dependent upon modifications of lipid structure by protein and vice versa. The emphasis also often depends upon which type of interaction dominates - electrostatic, hydrophobic or hydrogen bonding.

To limit the area of speculation, a great deal of experimental evidence about the organisation of components in the membrane is clearly required. The most direct information should be obtainable, of course, by examination of cell membranes themselves. However, since many components are present in intact membranes, studies of model systems involving interactions of selected components are necessary. Entirely in accordance with this spirit the work described in this thesis examines the structure and dynamics of lipid aggregates interacting with progressively increasing amounts of water in a variety of non-polar solvents by a variety of physical and spectroscopic techniques.

### Aggregates of Phospholipids

Phospholipids are seldom molecularly dispersed in solutions. They are present as aggregates of various sizes and shapes in solutions. At the interface of water and air or some immiscible organic solvent, the phospholipid molecules orient themselves

in such a way that the paraffin (hydrocarbon) chains remain in the organic solvent or air while only the polar groups interact with water; a hydrophilic 'head' and a hydrophobic 'tail' are thus distinguished.

Phospholipid aggregates are termed liposomes, vesicles, micelles and reverse micelles depending on the nature of the solvent, nature of the head group, the number, the length and the degree of unsaturation of the hydrocarbon chains and the phospholipid concentration. The size of the aggregates formed in a particular solvent can in general be related to the lipids' solubility. Short chain phospholipids form smaller micellar structures in polar solvents such as alcohols, acetone, etc. and are more soluble in these solvents; on the other hand, in non-polar solvents such as benzene and other hydrocarbons, they form larger reverse micellar structures. However, the situation with long chain phospholipids is just the reverse. Here, solubility would also depend on the degree of unsaturation of the fatty acid chain. For example, while the saturated long chain phospholipids are almost insoluble in acetone, ethyl ether and petroleum ether, their unsaturated counterparts are much more soluble in these solvents (11). The presence of one phospholipid can also markedly affect the solubility of another in a solvent.

#### Liposomes and Vesicles

Phospholipids exhibit very interesting behaviour in the presence of water. They are, in general, very hygroscopic

substances. About 10-20 molecules of water per molecule of lecithin can be absorbed at 25°C (16-18). When interacting with water, lipids do not directly pass from crystalline state to the solution. Depending on the water content, different hydrated phases exist until, at the limit of infinite dilution, an ideal solution of single lipid molecules occur. Such behaviour is called lyotropic mesomorphism. The lyotropic phases in turn exhibit thermotropic mesomorphism i.e., the particular phase observed will depend on both the water content and temperature. In addition to these two factors, the nature of the phase will be determined by the hydrophilic-hydrophobic balance (HLB) of the lipid molecule (19,20). An excellent treatment of the lyotropic and thermotropic mesomorphism of lipids is given in the articles by Hauser (2) and Williams and Chapman (21). Above the liquid-crystalline transition temperature, water can diffuse into the lattice to give a variety of different phases. The water penetrates into the polar regions of the crystal but not into the hydrocarbon regions. If the amphiphile is cooled below the liquid-crystalline transition after the water has penetrated the lattice, then the hydrocarbon chains again form an ordered crystalline lattice but the water need not necessarily be expelled. Gel is the name given to phases containing crystalline hydrocarbon chains and water (22,23).

The lamellar phase, made up of alternating layers of phospholipid and water is the most common of the lipid-water phases formed above the liquid-crystalline transition temperature. The

maximum hydration of the phosphatidylcholine-water system is about 40 weight per cent by water. When phosphatidylcholine is dispersed in water above its thermotropic phase transition temperature, large multilamellar closed sacs commonly referred to as liposomes are formed. Liposomes are composed of spherically concentric lamellae with water trapped between the bilayers (24). On irradiating suspensions of liposomes ultrasonically (high-frequency of about 20-100 kHz) these multiwalled aggregates are broken down to give smaller, unilamellar, single walled symmetrical aggregates called vesicles (25). Figs. 1.2 and 1.3 show the electron micrographs of phosphatidylcholine liposomes and vesicles (Fig. 1.2) and bilayer (Fig. 1.3). Vesicles are composed of a single continuous lipid bilayer membrane enclosing a volume of aqueous solution (26,27). A much more homogeneous dispersion can be obtained by gel filtration (27) or ultracentrifugation (28). Some simple methods for detecting the presence of large vesicles in small vesicle dispersions have been described recently (29,30). Lipid bilayers are the basis of a very large number of investigations based on methods such as X-ray crystallography (15,31,32), light scattering (33,34), infrared spectroscopy (35), differential thermal analysis (31), NMR (36-43), DMR (44-50),  $^{31}\text{P}$ -NMR (51,52),  $^{13}\text{C}$ -NMR (53), Neutron diffraction (54-56) etc., and will not be reviewed further here. A number of review articles on phospholipid-water systems are also available (1,2,11,57-60). Here we shall mention only in passing that liposomes are rapidly becoming popular as possible



Liposome



Vesicle

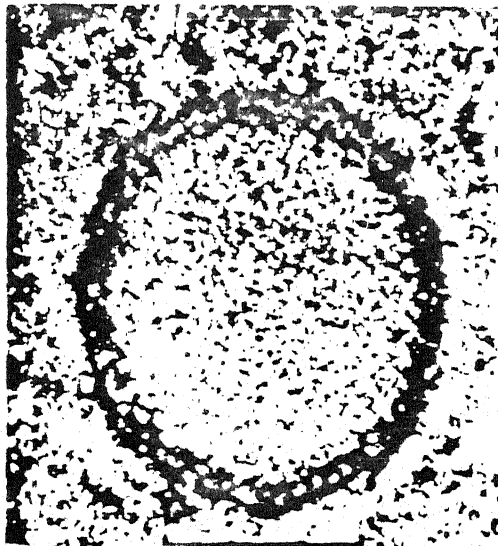


Fig. 1.2 Electron Micrograph of Vesicles

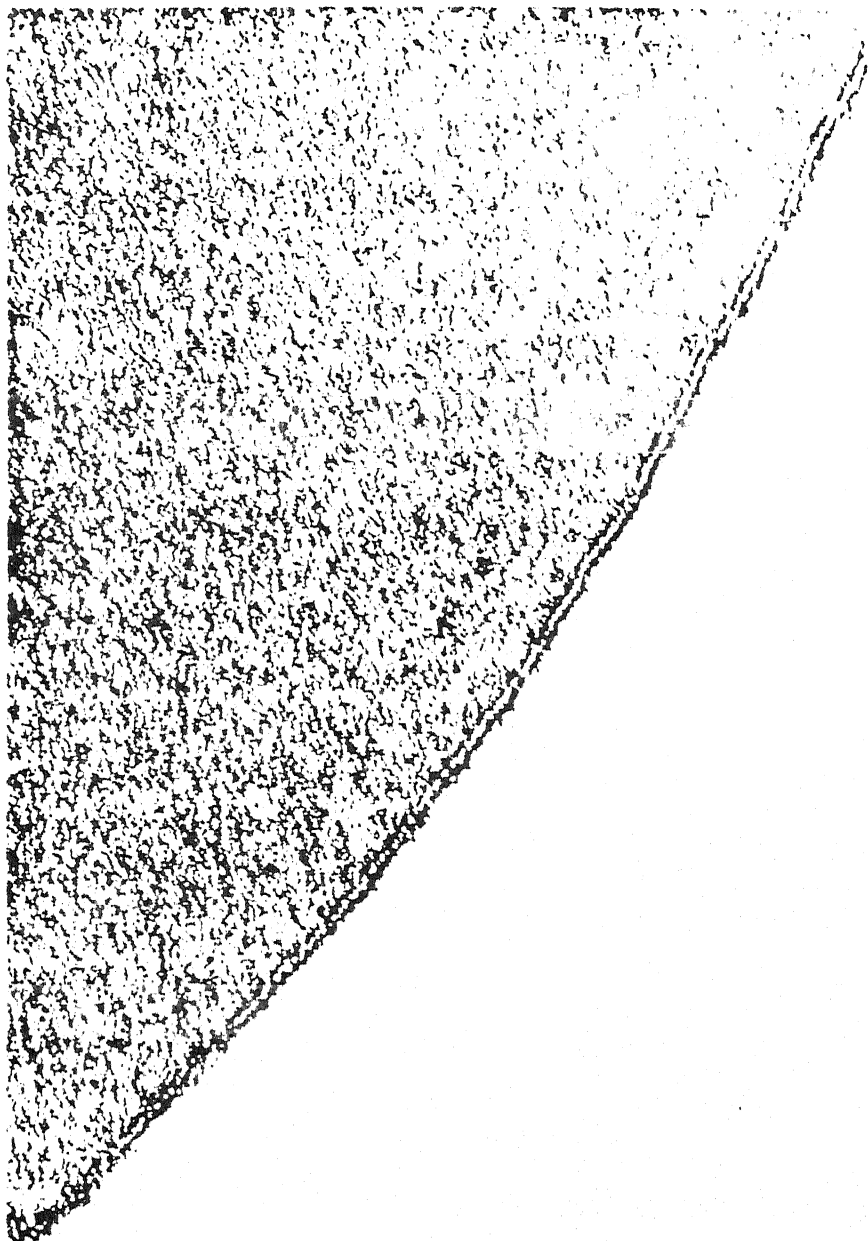


Fig. 1.3 Electron Micrograph of Bilayer .

drug carriers (61,62).

There is one other state of lipid aggregation which deserves a brief mention. Black lipid membranes (BLM) are lipid bilayer assemblies that are formed when a lipid solution in an organic solvent is applied on to a small (1 mm radius) hole in a polymer support immersed in an aqueous buffer. These systems are stable normally for a few hours. While not amenable to spectroscopic studies easily, BLMs are excellent models for studying the electrical characteristics of lipid membranes.

Liposomes (25) and the black lipid membranes (63) have superseded the older 'surface monolayers' (64) as more realistic model membranes. Of all the foregoing, however, the bilayer structure of biomembranes is perhaps the most popular, and membrane permeability is the only major functional role of lipids which may be regarded as firmly established to-date (27,65). Fig. 1.4 shows the structure of the lipid bilayer and the fluid mosaic model of Singer and Nicolson (18).

That hydrated phospholipids adopt a variety of phases in addition to the bilayer phase has been well documented in the literature extending over the past two decades. Luzzati and coworkers (66-69) have examined the structural characteristics of these alternative forms by employing X-ray diffraction techniques. Studies of lipid polymorphism have been significantly extended by the introduction of NMR (particularly  $^{31}\text{P}$ -NMR) methodology to both model and biomembrane systems (70,71). The hydrated lipids are now known to adopt a number of other phases

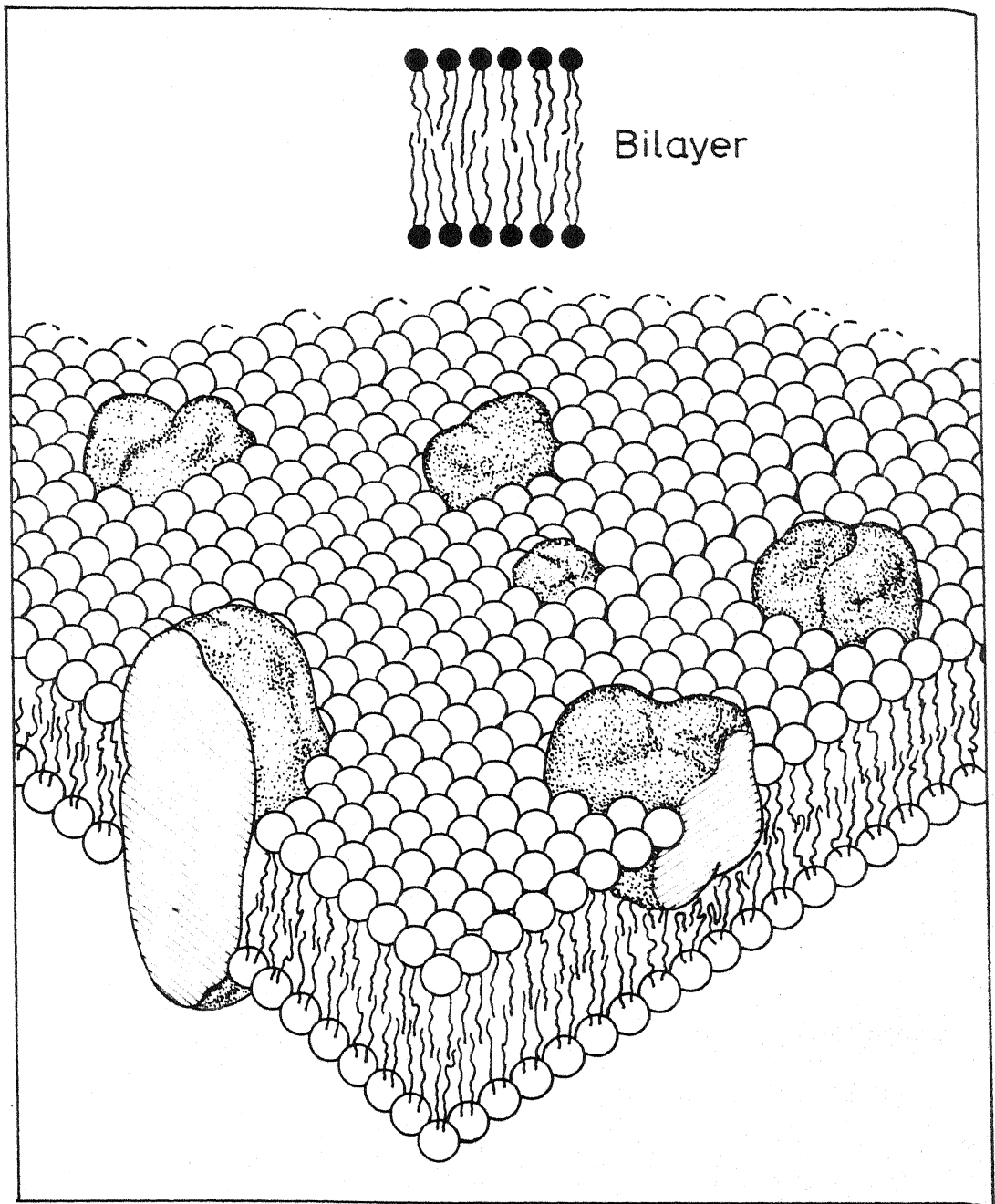


Fig. 1.4 Fluid mosaic model of cell membrane.

such as hexagonal  $H_I$  and  $H_{II}$  phases, the micellar phase, as well as those phases exhibiting cubic or rhombic structure. A particular preference for the short cylindrical segment ( $H_{II}$  configuration) by various lipids is well established (72-74). Fig. 1.5 shows the various structures that the hydrated phospholipids adopt.

The availability of such non-bilayer alternatives have not only opened up new vistas for rationalising the functional roles of lipids in biomembranes, but have also served to underscore the shortcomings of the bilayer model. For example, membrane fusion mechanisms (including related processes such as exo- and endocytosis) and transbilayer processes (including lipid flip-flop) are phenomena which cannot be reconciled with lipids remaining in a bilayer arrangement at all stages (70,71). As a model for these, the intra-bilayer reverse micelles have been proposed (70,71). Fig. 1.6 shows how the bilayer structure changes into the reverse micellar structure during membrane fusion process (70). However, it is equally clear that the hexagonal ( $H_{II}$ ) phase would not be expected to maintain the permeability barrier so vital to cellular function and integrity (70,71). Since the reverse micellar structure thus becomes a viable alternative to the bilayer arrangement of lipids, an understanding of the structure and properties of the reverse micellar system phosphatidylcholine-non polar solvent-water is sought in this thesis.

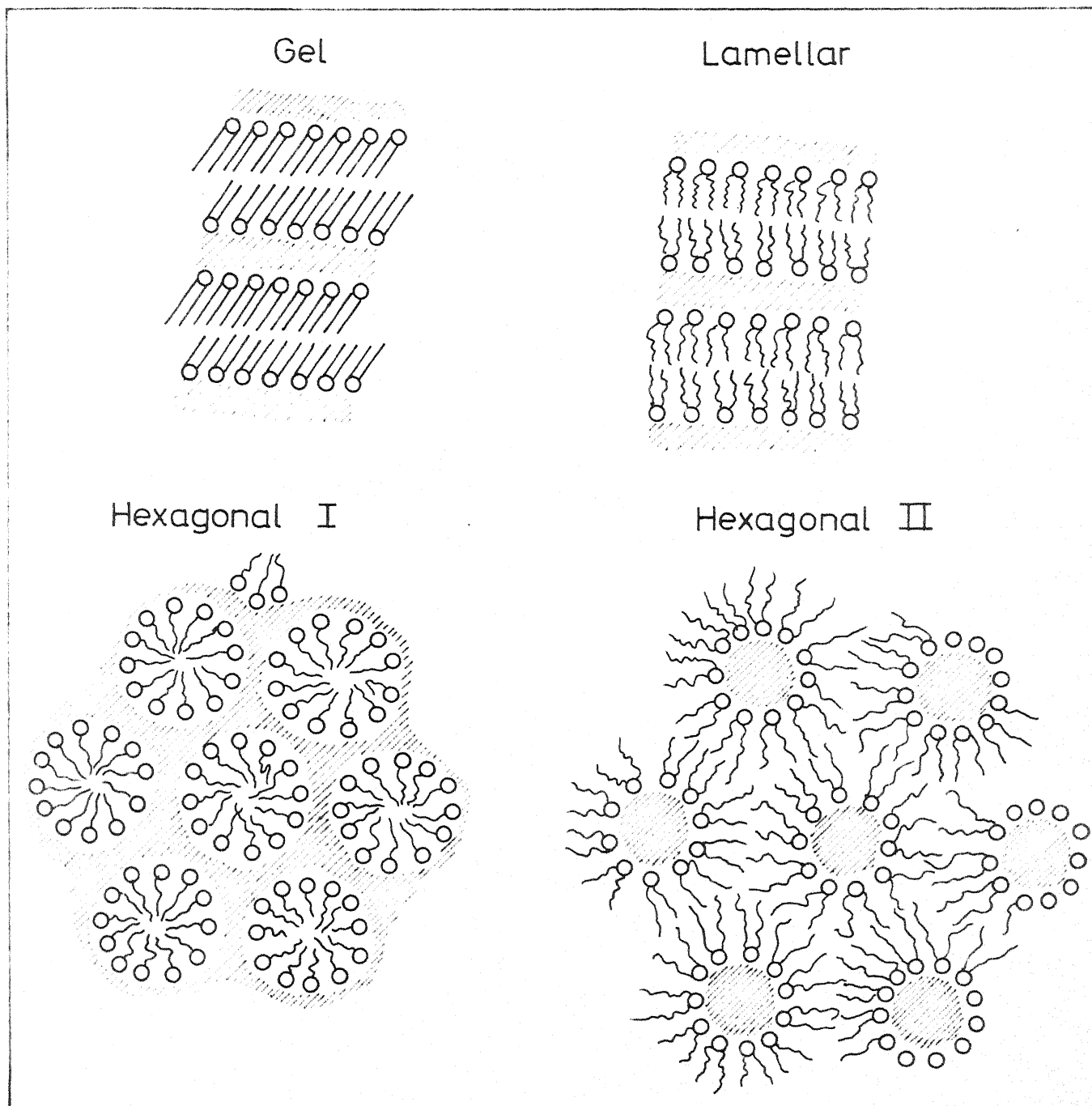


Fig 1.5 Structures of Hydrated Phospholipids

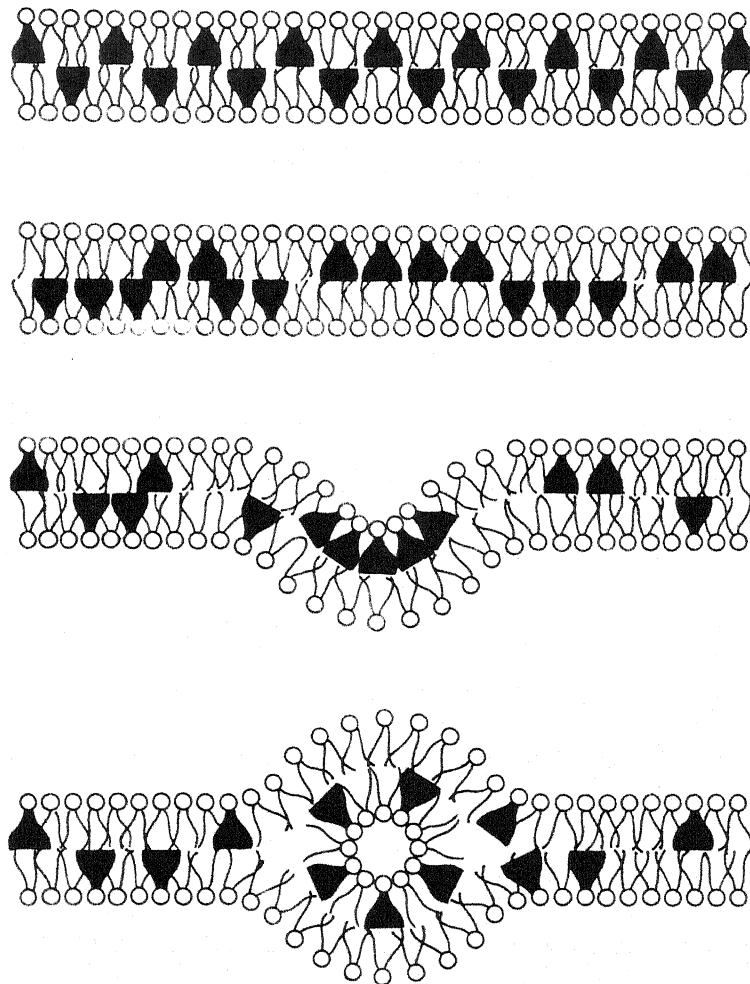


Fig. 1.6 Transformation of a bilayer into reverse micelle during membrane fusion.

In the following sections, a quick general survey will be made of the literature on micelles and reverse micelles of lipids and surfactant molecules, and the earlier work pertinent to our research will be critically reviewed.

### Micelles and Reverse Micelles

In general, micelles are the multimolecular aggregates of amphiphilic molecules (e.g. phospholipids and a variety of synthetic surfactants) in water and occasionally other polar media. The aggregation occurs above a particular concentration of the amphiphile in solution known as the critical micelle concentration (CMC).

Complementary to their aggregation behaviour in aqueous media, amphiphiles are also known to aggregate extensively in non-polar media. The important difference is that, in the latter, reverse micelles are formed by aggregation of the amphiphile through their polar head groups, with their hydrophobic tails projecting into the bulk solvent. Such reverse micelles are capable of solubilising significant amounts of polar solvents, specifically water.

A subject on which clarity has been lacking is the exact microstructural features of the micelles. The earlier 'boxlike' or 'double leaflet' structures proposed by McBain (75) were superseded by the proposal of a spherical micelle with a hydrocarbon interior and a smooth, hydrophilic surface (76). In studies using surfactant 'model' amphiphiles, it has been



suggested that an indefinite self-association model of step-wise aggregation may be more plausible (77). Further, at high concentrations of surfactant (20 times that required for CMC), the micelles enlarge and aggregate further, ultimately to produce liquid crystalline phases (78). Amphiphile aggregation in aqueous solution is very recently reviewed by Lindblom and Wennerstrom (79). Recently, Menger (80) has reviewed data relevant to the structure of ionic micelles and has shown that a 'pincushion-like' structure explains the known facts about micelles in a better way.

The reverse micellar surfactant aggregates have been the subject of a number of classic reviews (81-86). Among the synthetic surfactants, reverse micelles of aerosol OT (sodium bis(2-ethylhexyl)sulphosuccinate) (86), dodecyl ammonium-propionate (83), igepol CO-530 (83) and Triton X-100 (87-89) are the systems most thoroughly characterised. Though in the 'dry' systems there may be no surfactant association, addition of water or other polar substances may produce association or change the aggregation number (83,90). Indeed it has been suggested that the presence of water may be essential for reverse micelle formation (91). Of course, there are unusual exceptions where water prevents the association, e.g. polyoxyethylene-type surfactants in non-polar solvents (92).

In any event, the size of surfactant aggregates produced in non-polar solvents is generally small, the aggregation number being 2-40 (82,92). However, in these systems, the involvement

of a clearly-defined CMC has been questioned by Ruckenstein and Nagarajan (93) since the physical properties of the non-aqueous surfactant solutions change only gradually, without any sharp transition, as a function of surfactant concentration (84,94,95).

On the other hand, despite the potential value accruing from complete understanding of reverse micellar arrangements of phospholipids, a surprisingly small number of investigations have been reported to date (96-127). Indeed, some preliminary studies undertaken in the early seventies are cited in the literature under the general heading of 'micelles'. Almost all of these studies are somewhat cursory, and most of them are based on nuclear magnetic resonance chemical shift and linewidth measurements only.

A particular aspect of these studies which has generated some lively controversy is that of the interaction of water with the polar head groups of lecithin reverse micelles (100, 105, 111, 115, 116, 119-121, 123). In several articles referred to here, one comes across statements such as, "these results do not fully agree with those reported by other workers" (121), "our conclusions are quite different from the ones given by other authors" (123) and "this observation invalidates some of Henrikson's (105) conclusions" (121). The current situation is typified by the following two quotations from the literature:

- (i) ".... in our opinion, Elworthy's (96,97,99) results are not reliable due to imperfections in the measuring or calculating methods" (114).

(ii) "....most of our information on phospholipid micelles in solvents of low dielectric constant comes from the work of Elworthy (96,97,100)" (111).

In view of the above, we have undertaken an exhaustive and in-depth investigation of a variety of physical and spectroscopic properties of the polar head and its interaction with added water in three distinct 'oil' (continuous) phases. Indeed, several of the measurements to be reported in this work have been carried out for the first time to the best of our knowledge. Since this thesis embodies the results on phosphatidylcholine (also referred to as lecithin) - non polar solvent-water system, we present a brief summary of the relevant past work on this system.

Lecithin reverse micelle formation in benzene only (i.e., without added water) has been studied by Elworthy using colligative (96) and hydrodynamic techniques (97). The author proposes a laminar structure for the reverse micelles. Elworthy (96,97) has shown that reverse micelles of lecithin undergo a transition at about 0.08% lecithin, from 'small' micelles (molecular weight ~3500) to 'large' micelles (molecular weight ~50,000). Later Blei and Lee (98) indicated a true CMC,  $33 \times 10^{-5} \%$  for the formation of aggregates capable of solubilising water-soluble dyes. This CMC occurs at far lower concentrations than Elworthy's transition concentration of 0.73 g lit.<sup>-1</sup>. This work (98) also indicates a structural transition within the micelle in addition to its increase in size.

The first study on the interaction of water with Lecithin reverse micelles in benzene is due to Elworthy and McIntosh (100). When water was introduced into the lecithin-benzene system, it was solubilised by the solute. A maximum solubilisation of 0.33 g of water/1 g of lecithin, was recorded. This value is in agreement with that of Demchenko (101) who recorded a maximum solubilisation of water by lecithin to be 0.33 g of water/1 g of lecithin, and the solubilisation was found to be independent of solvents used (benzene, toluene and xylene). From their viscosity and diffusion measurements, Elworthy and McIntosh (100) also observed that the number of monomers in the micelle was independent of the solubilisate concentration between zero and 0.25 g of water/1 g of lecithin. Their viscosity results indicated an alteration in the reverse micellar structure and spherical micelles were present at high water contents. Later on, the validity of Elworthy's (100) results was severely questioned by Janson et al. (114) who investigated the static dielectric constant of phosphatidylcholine in benzene, carbontetrachloride and cyclohexane. For example, Elworthy and McIntosh (100) determined the apparent molecular weight of lecithin in benzene with the help of light scattering and found a molecular weight of about 60,000 i.e. aggregation number  $n = 73$  (taking 780 as the molecular weight of lecithin). These results are criticised by Janson et al. (114), who quote Debye and Coll (128) in stating that measurement of molecular weight lower than about  $1 \times 10^5$  in benzene with the help of light scattering is not possible. As a

check on Elworthy's (100) results Janson et al. (114) used vapour pressure osmometry for measuring the molecular weight of lecithin in benzene. By this method they (114) found the aggregation number to be  $\approx 15$ , in stark disagreement with Elworthy's value  $n \approx 73$ . Abramson and coworkers (102) obtained evidence from IR spectroscopy of dipalmitoylphosphatidylcholine in carbon-tetrachloride that the lipid is present in its zwitter-ionic form with one water molecule bonded to the phosphate group.

We also review the relevant NMR results now. Chapman and Morrison (103) assigned the various NMR spectral peaks to the functional groups present in egg phosphatidylcholine in  $\text{CDCl}_3$ . Later Haque et al. (112) have published the spectrum of lecithin in  $\text{CHCl}_3$ . They (112) also observed that as the solvent polarity increases the micellar size (i.e., aggregation number ' $n$ ') decreases. However, in view of the large difference in polarity between  $\text{CHCl}_3$  and  $\text{CH}_3\text{OH}$ , it is difficult to explain why Haque et al. (112) get the same value of  $n \approx 3$  in  $\text{CHCl}_3$  solvent which Elworthy and McIntosh (99) record for  $\text{CH}_3\text{OH}$ .

Henrikson (105) studied the interactions of water with lecithin reverse micelles in carbontetrachloride solution by proton NMR linewidth measurements. She finds that  $\sim 12$  water molecules per lecithin molecule are required to form a hydration shell around the phosphorylcholine part of the lecithin. Although no viscosity measurements are reported by her, a 'dramatic drop in viscosity' is claimed when 100 mg of water are added to a lecithin sample in carbontetrachloride. This is not verified

by our viscosity measurements to be presented in Chapter II.

Walter and Hayes (111) have studied the interaction of water with the polar region of phosphatidylcholine reverse micelles in benzene by proton NMR linewidth measurements. They suggest three regions of water. The first region is attributed to the existence of a first hydration shell of two to three molecules of water per molecule of lecithin, the second region corresponds to the next shell of four to six molecules of water per mole of lecithin and finally, a nearly constant region of simple bulk water filling the interior of the micelle. According to this work (111), addition of water increases the motion of trimethyl ammonium groups but slows down the motion of the hydrocarbon chains. (This, again, will be further examined in our observations presented in Chapter III.) They (111) observed the proton linewidth of the  $-N^+(CH_3)_3$  group in the choline residue was the same for  $H_2O$  and  $^2H_2O$  at low water concentrations, but was smaller for  $^2H_2O$  at higher water concentrations. Therefore, Walter and Hayes (111) suggest that  $^2H_2O$  has a different layer structure from that of  $H_2O$ . Subsequently, Fung and McAdams (123) suggested that the above difference in the behaviour of  $H_2O$  and  $^2H_2O$  is not surprising since the intermolecular dipolar interaction begins to contribute to the proton relaxation. Since  $^1H$ - $^2H$  dipolar interaction is  $\frac{1}{16}$ th of that of the  $^1H$ - $^1H$  interaction (129),  $T_1$  and  $T_2$  for the trimethylammonium group would naturally be longer, and the linewidth smaller, for reverse micelles filled with  $^2H_2O$ .

None of the above investigators, however, have studied the phospholipid-water interactions by measurements of proton chemical shifts. Shaw et al. (115) were the first to report such studies on the interaction of water with egg yolk phosphatidylcholine in carbontetrachloride. They (115) suggest that the sites of interaction in lecithin preferred by water are the choline nitrogen and the phosphate group. They also show that the water proton signal moves upfield on adding water, upto about 6 moles of  $H_2O$ /mole of PC, because of the electrostatic interaction between the  $N^+$  and the negative oxygen atom of the phosphate. The addition of water then decreases this electrostatic interaction, forming a hydrogen bonded complex. They also suggest that when water is in excess, self-aggregation of water takes place, resulting in a downfield shift of water proton signal beyond 10 moles of water/mole of lecithin.

Poon and Wells (119) and Wells (120) proposed that three distinct hydration states exist in ethereal solutions of phosphatidylcholine. The first requires about 7 water molecules, the second requires an additional 25-30 water molecules and the last requires a further 25-30 water molecules per lecithin molecule. The values of these hydration shells are considerably larger than in the case of benzene discussed earlier. This is because the amount of water that can be solubilised in PC-ether (1.1 g of  $H_2O$ /1 g of lipid) system is considerably higher than in the PC-benzene (0.33 g of  $H_2O$ /1 g of lipid) system. Wells (120) also states that there are numerous differences between the

micellisation processes, and the effect of water, in ether and in benzene. In view of the above facts, it is clear that micellisation takes place in entirely different ways in different solvents. It is, therefore, also not warranted to extrapolate the apparent physical state of the micelle (e.g., size, shape, aggregation number etc.) from one solvent to another. This is one of the main reasons for our choice of solvents, as will be discussed later.

Klose and Stelzner (116) investigated the interaction of water with lecithin in benzene solution using proton NMR (chemical shifts, linewidths) and phosphorous NMR (relaxation times,  $T_1$ ). They suggest that water interacts with the phosphate group of lecithin in two regions of different mobility and structure. The first region of strong interaction involves about 2 and the second of weaker interaction involves about 5 water molecules per lecithin molecule. When water is in excess a third region is formed and this third region is located beyond the two regions of interaction with the phosphate group, but within the micelle. A fast exchange of water molecules takes place between the first two regions. This hypothesis is also seriously questioned by Fung and McAdams (123).

Davenport and Fisher (121) have utilised phase contrast microscopy, IR spectroscopy and proton NMR (Transverse relaxation times,  $T_2$ ) to study the interaction of water with egg PC in benzene. By phase contrast microscopy, they observe that free water is present in the system above nine water molecules



per lecithin monohydrate molecule. This is in contrast with the well established observation of 1 mole of lecithin in benzene to 18 moles of water (97,101,123). Conceivably, Davenport and Fisher (121) have observed 'discrete' water pools that are formed in the system. The final picture that emerges from this study is that the first added water molecule is very strongly bound to the phosphate group. As more water is added, the molecules are less strongly bound, but still very much more restricted in motion than in 'free' or 'bulk' water. These authors (121), in fact, clearly rule out the existence of a series of hydration 'shells' as postulated by others (111, 116, 119, 120).

Fung and McAdams (123) have studied the interaction of water with polar head in reverse micelles of phosphatidylcholine in carbontetrachloride using  $^2\text{H}$  and  $^{31}\text{P}$ -NMR spin-lattice relaxation times ( $T_1$ ). From a quantitative analysis of their deuterium  $T_1$  data, they show that there is only one water molecule tightly bound to the polar head, and this is in rapid exchange with the rest of the water molecules. This supports the idea of Davenport and Fisher (121) quoted earlier.

Poon and Wells (125) estimate the molecular weight of egg lecithin in benzene solution by sedimentation equilibrium experiments and demonstrate that the aggregation increases with increasing addition of water. The molecular weight increases from about 14,000 in the anhydrous state (comparable to that of Janson, et al. (114)) to about 57,000 at a water/lecithin ratio of 0.31.

Klose et al. (126) report magnetic resonance, light scattering and visual observations (of viscosity) on lecithin-benzene system at a variety of temperatures and concentrations. At about 0°C the bulk of the benzene freezes, but a small amount of about 3 benzene molecules per lecithin molecule remains unfrozen to about -50°C. The systems studied show considerable temperature hysteresis and ageing effects. The overall conclusion of Klose et al. (126) is that small amounts of water drastically change the properties of lecithin-benzene system.

In view of the results of Klose et al. (126) it becomes possible to re-interpret the changes in the NMR parameters brought about by adding water as being due to changes in the structure and dynamics of the head group and/or the extent of lecithin aggregation, rather than as due to the presence of hydration shells as suggested by others (111,116,120,123).

More recently, Chen and Springer (127) have studied the effects of shift reagents on the  $^{31}\text{P}$ -NMR spectra of hydrated dipalmitoyllecithin reverse micelles in benzene, and they conclude that water exchange is fast on the NMR time-scale.

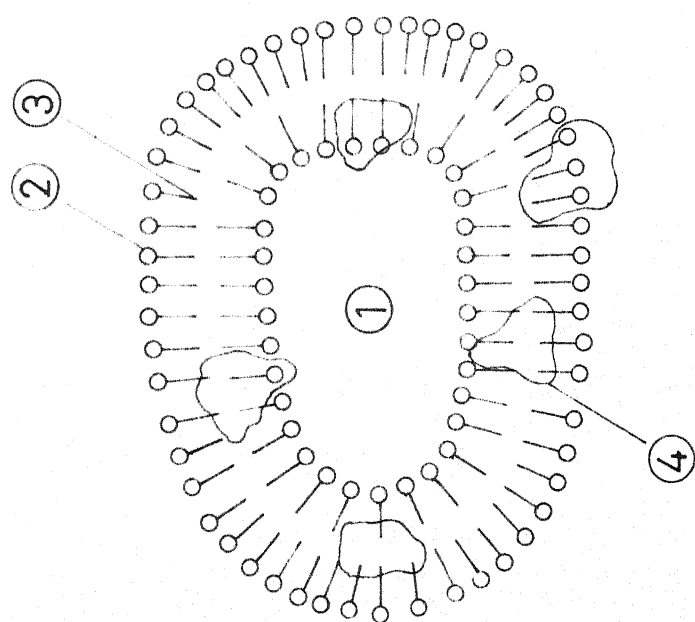
A proper understanding of molecular mobility and local ordering in bio- and model-membrane systems and of their relevance to clinical research is increasingly becoming important; this has been reviewed recently (130).

Our main interest in lecithin reverse micellar systems is to gain detailed information on the interaction between the choline head-group and individual water molecules, particularly

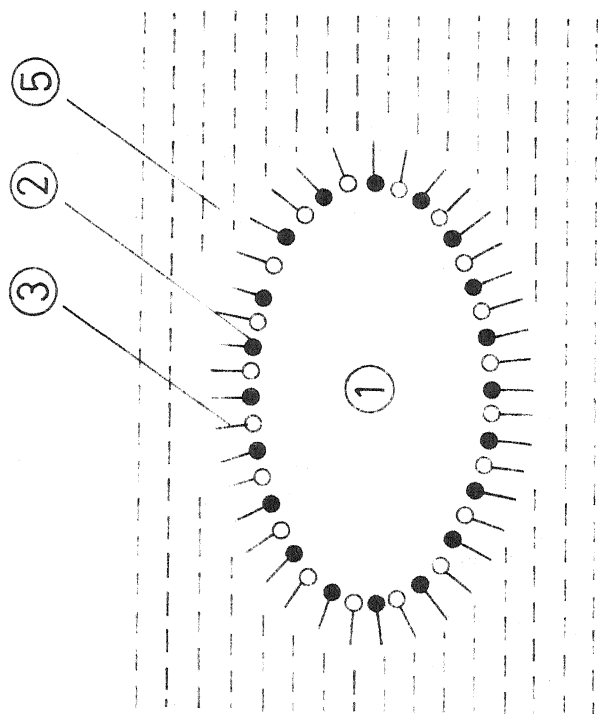
since the amount of water can be controlled to give small water/PC ratios. Also a number of similarities are present between reverse micelles containing water and the cell as a whole. The bilayer lipid membrane in the cells is modelled rather well by the phospholipid interfacial film of the reverse micelles. The water in the cell is similar to the central 'water pool' of the systems to be described herein. When viewed from inside the cell, the lipid membrane presents a surface sheath of polar head groups, backed up by a strongly hydrophobic non-polar region. An exactly identical picture of polar head groups backed up by a hydrophobic region emerges in the reverse micelles when viewed inside out. The formal similarity between the cell and the reverse micelle is shown in Fig. 1.7.

Keeping the above considerations in mind, we have studied the phosphatidylcholine-non polar solvent-water system. The three solvents chosen are benzene, carbontetrachloride and cyclohexane. The choice of the solvents is not random. Rather, each solvent has its own special significance, according to the rationale presented below:

Benzene: Generally it is supposed that in organic solvents the solvent molecules are solubilised only in the hydrocarbon region of lecithin (131,132). But benzene is a  $\pi$ -electron donor, which in principle can also interact with the polar head group of lecithin. Such interactions of aromatic compounds with tertiary nitrogen compounds have been reported (133-135).



A cell



Reverse micelle

- ① water    ② hydrophilic head group    ③ hydrophobic tails  
 ④ protein    ⑤ oil

Fig. 1.7 Schematics of a cell and reverse micelle.

Carbontetrachloride: In view of the numerous proton NMR line-width, chemical shift, spin-lattice, spin-spin relaxation time measurements that we have in mind, the entirely proton-free carbontetrachloride has become the logical candidate as one of the solvents.

Cyclohexane: Among saturated hydrocarbons, cyclohexane represents the typical behaviour of an oil in microemulsion systems (136). Further, such an important solvent has been very little exploited in PC reverse micellar systems. Since it does not have any  $\pi$ -electrons, the chance of the solvent molecules interacting with the head group is minimal and this contrasts rather well with benzene.

Chapter II deals with our experiments directed towards the establishment of phase boundaries and solution properties of the reverse micellar system in the three solvents. An important additional observation here is the formation of a new liquid crystalline phase when cyclohexane is the solvent.

Chapter III discusses the results of a variety of spectroscopic studies on the above systems. Many of the spectroscopic techniques are applied to these systems for the first time to the best of our knowledge.

The next two chapters are detailed studies, based on NMR spectroscopy alone, pertaining to the liquid crystalline phase detected in cyclohexane. In Chapter IV, the self-diffusion of water in the cyclohexane-lecithin-water is studied by using the

magnetic field gradient technique. In Chapter V, the quadrupolar lineshapes of the  $D_2O$  at various stages of water uptake by cyclohexane-lecithin reverse micelles are studied. Also reported in this chapter is a lineshape analysis of the phosphorous NMR spectrum of the PC head group in the vicinity of the liquid crystalline phase. The theory of Alexander, Baram and Luz (137) modified for a computer simulation of the observed lineshapes, is used.

REFERENCES

1. H. Hauser and M.C. Phillips, in 'Progress in Surface and Membrane Science,' Vol. 13, Eds. D.A. Cadenhead and J.F. Danielli, Academic Press, New York, 1979, p. 297.
2. H. Hauser, in 'Water - A Comprehensive Treatise', Vol. 4, Ed. F. Franks, Plenum Press, New York, 1975, p. 209.
3. W.L. Hubbell and H.M. McConnell, J. Am. Chem. Soc., 93, 310 (1971).
4. J.P. Reeves, in 'Biological Membranes', Ed. R.M. Dowben, Little Brown and Co., Boston, Mass., 1969, p. 223.
5. D. Chapman, 'Biological Membranes,' Academic Press, London, 1968, p. 125.
6. L.L.M. Van Deenen, Prog. Chem. Fats and Other Lipids, 8, 1 (1965).
7. A.D. Bangham, Prog. Biophys. Mol. Biol., 18, 29 (1968).
8. A.D. Bangham, Ann. Rev. Biochem., 41, 753 (1972).
9. C. Gilter, Ann. Rev. Biophys. Bioeng., 1, 51 (1972).
10. S.J. Singer and G.I. Nicolson, Science, 175, 720 (1972).
11. D.G. Dervichian, Prog. Biophys. Mol. Biol., 14, 263 (1964).
12. D. Chapman, 'The Structure of Lipids,' Methuen, London, 1965.
13. H.S. Frank and M.W. Evans, J. Chem. Phys., 13, 507 (1945).
14. W. Kauzmann, Adv. Protein. Chem., 14, 1 (1959).
15. V. Luzzati in 'Biological Membranes,' Ed. D. Chapman, Academic Press, New York, 1968, p. 71.
16. P.H. Elworthy, J. Chem. Soc., 815, 5385 (1961).
17. Z. Veksli, N.J. Salsbury and D. Chapman, Biochim. Biophys. Acta, 183, 434 (1969).
18. Y. Katz and J.M. Diamond, J. Memb. Biol., 17, 87 (1974).

19. D.G. Dervichian, *Molecular Crystals*, 2, 55 (1966).
20. D.M. Small, *Fed. Proc.*, 29, 1320 (1970).
21. R.M. Williams and D. Chapman, in 'Progress in the Chemistry of fats and other lipids,' Vol. XI, Ed. R.T. Holman, Pergamon Press, Oxford, 1970, p. 3.
22. A.D. Bangham, *Prog. Biophys. Mol. Biol.*, 18, 29 (1968).
23. Y.K. Levine, *Prog. Biophys. Mol. Biol.*, 24, 1 (1974).
24. A.D. Bangham and R.W. Horne, *J. Mol. Biol.*, 8, 660 (1964).
25. A.D. Bangham, M.W. Hill and N.C.A. Miller, in 'Methods in Membrane Biology,' Vol. 1 Ed. E.D. Korn, Plenum Press, New York, 1974, p. 1.
26. C. Huang, *Biochemistry*, 8, 344 (1969).
27. M.H.F. Wilkins, A.E. Blaurock and D.H. Engleman, *Nature New Biol.*, 230, 72 (1971).
28. Y. Barenholz, D. Gibbs, B.J. Litman, J. Goll, T.E. Thompson and F.D. Carlson, *Biochemistry*, 16, 2806 (1977).
29. D.A. Barrow and B.R. Lentz, *Biochim. Biophys. Acta*, 597, 92 (1980).
30. A.J.B.M.V. Ranswoude, R. Elumenthal and J.N. Weinstein, *Biochim. Biophys. Acta*, 575, 151 (1980).
31. D. Chapman, R.M. Williams and B.D. Ladbroke, *Chem. Phys. Lipids*, 1, 445 (1967).
32. H. Lecuyer and D.G. Dervichian, *J. Mol. Biol.*, 45, 39 (1969).
33. D.O. Tinker, *Chem. Phys. Lipids*, 8, 230 (1972).
34. D. Attwood and L. Saunders, *Biochim. Biophys. Acta*, 98, 344 (1965).
35. B.J. Bulkin and N.I. Krishnamachari, *Biochim. Biophys. Acta*, 211, 592 (1970).
36. Z. Veksli, N.J. Salsbury and D. Chapman, *Biochim. Biophys. Acta*, 183, 434 (1969).



37. E.G. Finer, A.G. Flook and H. Hauser, FEBS Lett., 18, 331 (1971).
38. J.T. Daycock, A. Darke and D. Chapman, Chem. Phys. Lipids, 6, 205 (1971).
39. E. Oldfield, J. Marsden and D. Chapman, Chem. Phys. Lipids, 7, 1 (1971).
40. E.G. Finer, A.G. Flook and H. Hauser, Biochim. Biophys. Acta, 260, 49 (1972).
41. E.G. Finer, A.G. Flook and H. Hauser, Biochim. Biophys. Acta, 260, 59 (1972).
42. G.L. Jendrsiak, Chem. Phys. Lipids, 9, 133 (1972).
43. Y.K. Levine, A.G. Lee, N.J.M. Birdsall, J.C. Metcalfe and J.D. Robinson, Biochim. Biophys. Acta, 291, 592 (1973).
44. N.J. Salsbury, A.D. Darke and D. Chapman, Chem. Phys. Lipids, 8, 142 (1972).
45. E.G. Finer, J. Chem. Soc. Faraday Trans. II, 69, 1590 (1973).
46. J. Seelig and A. Seelig, Biochem. Biophys. Res. Comm., 57, 406 (1974).
47. E.G. Finer and A. Darke, Chem. Phys. Lipids, 12, 1 (1974).
48. J. Ulminius, H. Wennerstrom, G. Lindblom and G. Arvidson, Biochemistry, 16, 5742 (1977).
49. G.W. Stockton and I.C.P. Smith, Chem. Phys. Lipids, 17, 251 (1976).
50. M.F. Brown, J. Seelig and U. Haberlen, J. Chem. Phys., 70, 5045 (1979).
51. R.W. Barker, J.D. Bell, G.K. Radda and R.E. Richards, Biochim. Biophys. Acta, 260, 161 (1972).
52. D.G. Davis, Biochem. Biophys. Res. Comm., 46, 1492 (1972).

53. Y.K. Levine, N.J.M. Birdsall, A.G. Lee and J.C. Metcalfe, *Biochemistry*, 12, 1416 (1972).
54. G. Buldt, H.U. Gally, A. Seelig, J. Seelig and G. Zaccai, *Nature*, 271, 182 (1978).
55. G. Buldt, H.U. Gally, J. Seelig and G. Zaccai, *J. Mol. Biol.*, 134, 673 (1979).
56. G. Zaccai, G. Buldt, A. Seelig and J. Seelig, *J. Mol. Biol.*, 134, 693 (1979).
57. D. Chapman, in 'Biological Membranes,' Vol. 2, Eds. D. Chapman and D.F.H. Wallach, Academic Press, New York, 1973, p. 91.
58. D. Chapman, *Quart. Rev. Biophys.*, 8, 185 (1975).
59. M. Montal, *Ann. Rev. Biophys. Bioeng.*, 5, 119 (1976).
60. D. Papahadjopoulos and H.K. Kimelberg, *Prog. Surface Sci.*, 4, 141 (1973).
61. G. Gregoriadis, *Ann. New York Acad. Sci.*, 308, 343 (1978).
62. C.D. Duwe, A. Trouet, D. Compemeere and R. Baurein, *Ann. New York Acad. Sci.*, 308, 226 (1978).
63. H.T. Tien, 'Bilayer Lipid Membrane', Marcel Dekker, New York, 1974.
64. N.L. Gershfeld, in 'Methods in Membrane Biology,' Vol. 1, Ed. E.D. Korn, Plenum Press, New York, 1974, p. 68.
65. H.F. Lodish and J.E. Rothman, *Scientific American*, 240, 38 (1979).
66. V. Luzzati and R.F. Husson, *J. Felle. Biol.*, 12, 207 (1962).
67. V. Luzzati, T. Gulik-Krzywicki, and A. Tardieu, *Nature*, 218, 1031 (1968).
68. V. Luzzati and A. Tardieu, *Ann. Rev. Phys. Chem.*, 25, 79 (1974).

69. V. Luzzati, R.F. Husson, E. Rivas and T. Gulik-Krzywicki, Ann. New York Acad. Sci., 137, 409 (1966).
70. P.R. Cullis and B. De Kruijff, Biochim. Biophys. Acta, 559, 399 (1979).
71. B. De Kruijff, P.R. Cullis and A.J. Verkleij, Trends. Biochem. Sci., March, 79 (1980).
72. F. Reiss-Husson, J. Mol. Biol., 25, 363 (1967).
73. R.D. Rand, D.O. Tinker and P.G. Fast, Chem. Phys. Lipids, 6, 333 (1971).
74. P.R. Cullis and B. De Kruijff, Biochim. Biophys. Acta, 507, 207 (1978).
75. J.W. McBain and O.A. Hoffman, J. Phys. Colloid. Chem., 63, 39 (1949).
76. G.S. Hartley, Q. Rev. Chem. Soc., 2, 152 (1948).
77. J.S. Clunie, J.F. Goodman and P.C. Symons, Trans. Faraday Soc., 63, 754 (1967).
78. S.I. Ahmad and S. Friberg, J. Am. Chem. Soc., 94, 5196 (1972).
79. B. Lindman and H. Wennerstrom, in 'Topics in Current Chemistry - 87', Eds, M.J.S. Dewar, K. Hafner, E. Heilbronner, S. Ito, J.M. Lehn, K. Niedenzee, C.W. Rees, K. Schafer and G. Wittig, Springer-Verlag, Berlin Heidelberg, 1980, p. 1.
80. F.M. Menger, Accts. Chem. Res., 12, 111 (1979).
81. K. Shinoda, 'Solvent Properties of Surfactant Solutions,' Marcel Dekker, New York, 1967.
82. See relevant sections in MTP international review of science, series one, Physical Chemistry, Volume on Surface and Colloid Chemistry, Ed. M. Kerker, Butterworths, London, 1973.
83. J.H. Fendler, Accts. Chem. Res., 9, 153 (1976).
84. A.S. Kertes and H. Gutman, in Surfactant and Colloid Science, Vol. 8, Ed. E. Matijevic, Wiley, New York, 1976, p. 193.

85. See relevant sections in MTP international review of science, series two, Physical Chemistry, Volume on Surface and Colloid Chemistry, Ed. M. Kerker, Butterworths, London, 1976.
86. H.F. Eicke, ref. 79, page 85.
87. C. Kumar and D. Balasubramanian, J. Colloid Interface Sci., 69, 271 (1979).
88. C. Kumar and D. Balasubramanian, J. Colloid Interface Sci., 74, 64 (1980).
89. C. Kumar and D. Balasubramanian, J. Phys. Chem., 84, 1895 (1980).
90. E. Gonick, J. Colloid Sci., 1, 393 (1946).
91. H.F. Eicke and H. Christen, Helv. Chim. Acta, 61, 2258 (1978).
92. P.S. Sheih, Ph.D., Thesis, Texas A & M University, 1976.
93. E. Ruckenstein and R. Nagarajan, J. Phys. Chem., 84, 1349 (1980).
94. G.Y. Markovitz, O. Levy and A.S. Kertes, J. Colloid Interface Sci., 47, 424 (1974).
95. H. Gutmann and A.S. Kertes, J. Colloid Interface Sci., 51, 406 (1975).
96. P.H. Elworthy, J. Chem. Soc., 813 (1959).
97. P.H. Elworthy, J. Chem. Soc., 1951 (1959).
98. I. Blei and R.F. Lee, J. Phys. Chem., 67, 2085 (1963).
99. P.H. Elworthy and D.S. McIntosh, Kolloid Z., 195, 27 (1964).
100. P.H. Elworthy and D.S. McIntosh, J. Phys. Chem., 68, 3448 (1964).
101. P.A. Demchenko, Colloid J. USSR, 22, 309 (1960).
102. M.B. Abramson, R. Katzman and R. Curci, J. Colloid Sci., 20, 777 (1965).

103. D. Chapman and A. Morrison, J. Biol. Chem., 241, 5044 (1966).
104. Z. Veksli, N.J. Salsbury and D. Chapman, Biochim. Biophys. Acta, 183, 434 (1969).
105. K.P. Henrikson, Biochim. Biophys. Acta, 203, 228 (1970).
106. J.W. Kellaway and L. Saunders, Biochim. Biophys. Acta, 210, 185 (1970).
107. G.L. Jendrasiak, Chem. Phys. Lipids, 4, 85 (1970).
108. V.F. Bystrov, N.I. Dubrovina, L.I. Barsul'kov and L.D. Bergelson, Chem. Phys. Lipids, 6, 343 (1971).
109. H. Trauble and E. Grell, Neurosciences Res. Prog. Bull., 9, 373 (1971).
110. G.L. Jendrasiak, Chem. Phys. Lipids, 6, 215 (1971).
111. W.V. Walter and R.G. Hayes, Biochim. Biophys. Acta, 249, 528 (1971).
112. R. Haque, I.J. Tinsley and D. Schmedding, J. Biol. Chem., 247, 157 (1972).
113. A.G. Lee, N.J.M. Birdsall, Y.K. Levine and J.C. Metcalfe, Biochim. Biophys. Acta, 255, 43 (1972).
114. J.P.M. Janson, M. Kunst, A. Rip and P. Bordewijk, Chem. Phys. Lipids, 9, 147 (1972).
115. Y-H. Shaw, L-S. Kan and N.C. Li, J. Mag. Res., 12, 209 (1973).
116. G. Klose and F. Stelzner, Biochim. Biophys. Acta, 363, 1 (1974).
117. J.D. McKinney, Chem. Phys. Lipids, 13, 249 (1974).
118. R.L. Misiorowski and M.A. Wells, Biochemistry, 13, 4921 (1974).
119. P.H. Poon and M.A. Wells, Biochemistry, 13, 4928 (1974).
120. M.A. Wells, Biochemistry, 13, 4937 (1974).

121. J.B. Davenport and L.R. Fisher, Chem. Phys. Lipids, 14, 275 (1975).
122. M.P.N. Gent, I.M. Armitage and J.H. Prestegard, J. Am. Chem. Soc., 98, 3749 (1976).
123. B.M. Fung and J.L. McAdams, Biochim. Biophys. Acta, 451, 313 (1976).
124. R.G. Griffin, J. Am. Chem. Soc., 98, 851 (1976).
125. P.H. Poon and M.A. Wells, Chem. Phys. Lipids, 18, 205 (1977).
126. G. Klose, G. Hempel and T.H.V. Zglinicki, Chem. Phys. Lipids, 21, 261 (1978).
127. S.T. Chen and C.S. Springer Jr., Chem. Phys. Lipids, 23, 23 (1979).
128. P. Debye and H. Coll, J. Colloid Sci., 17, 220 (1960).
129. A. Abragam, 'Principles of Nuclear Magnetism,' Oxford University Press, London, 1961, p. 289-295.
130. M.T. Yang, E.I. Ochiai, P. Raghunathan and R.W. Spitzer, Clinical Biochemistry, 11, 90 (1978).
131. J.C. Metcalfe, N.J.M. Birdsall, A.G. Lee, J. Feeney, Y.K. Levine and P. Partington, Nature, 233, 199 (1971).
132. Y.K. Levine, N.J.M. Birdsall, A.G. Lee and J.C. Metcalfe, Biochemistry, 11, 1416 (1972).
133. J.C.H. Eriksson and G. Gillberg, Acta Chem. Scand, 20, 2019 (1966).
134. W.T. Ford and D.J. Hurt, J. Am. Chem. Soc., 96, 3261 (1974).
135. E.J. Fendler, V.G. Coustin and J.H. Fendler, J. Phys. Chem., 79, 917 (1975).
136. K. Shinoda and H. Kunieda, in 'Microemulsions Theory and Practice,' Ed. L.M. Prince, Academic Press, New York, 1977, p. 64.
137. S. Alexander, A. Baram and Z. Luz, J. Chem. Phys., 61, 992 (1974).

## CHAPTER II

### PHYSICAL STUDIES

Among the physical measurements that are useful for identifying and characterising reverse micellar systems are optical birefringence, rheology, light scattering, electrical conductivity, centrifugation, sedimentation and, more recently, electron microscopy. While each of the above measurements leads to some specific information about the system, consideration of two or more measurements together goes a long way in putting our understanding of the amphiphile-oil-water systems on a much firmer basis. The system we have selected is lecithin (phosphatidylcholine, PC)-water in three representative non-polar solvents, namely, benzene, carbontetrachloride and cyclohexane. The reasons for the choice of these systems and the proposed goal of this study have already been discussed in Chapter I. In this chapter, we present evidence to show the formation of lecithin reverse micelles in the three solvents and also analyse at some length the changes in physical properties of the reverse micellar structures formed as a function of added water. We have utilised here many of the physical techniques mentioned at the beginning of this chapter.

### Materials and Methods

The chromatographically homogeneous lecithin used in our studies was extracted from fresh egg yolks by the method of Singleton et al. (1). The extracted lecithin was kept at  $-20^{\circ}\text{C}$  in a 9:1 v/v mixture of chloroform and methanol. Thin layer chromatography (TLC) was used for checking the purity of the



extracted lipid. Silica gel G (Merck) for thin layer chromatography was used for the TLC analysis. A paste consisting of 47.5 g of silica gel G in 100 ml of water was spread to a thickness of 0.5 mm on glass plates. The silica gel coated plates were air dried and activated at 105-110°C for 30 minutes prior to use, the activated plates were stored in a desiccator. The phosphatide extractions from egg-yolk in 9:1 chloroform-methanol, mixture were first applied to the plates and then developed by the solvent system chloroform-methanol-water (65:25:4, v/v) in a saturated chamber. Iodine vapour was used for the identification of the chromatographed materials. A single spot on TLC plates confirmed the purity of the extracted lipid. After evaporating away the solvent mixture under vacuum, the residual solid lipid was left in vacuum (~ 50 microns) for about 6 hrs. The solid lipid thus isolated was dissolved in the required dry solvent for further studies. The molecular weight of egg lecithin reported in most studies is in the range 750-770. We have assumed a value of 760 in our studies.

Solvents used were of AR grade and these were further dried by the following methods:

Benzene: After a preliminary distillation, AR grade benzene was refluxed in the presence of added sodium wire for about 3 hours and then redistilled (b.p. 80.6°C). This was stored in a bottle, with a tight stopper, over sodium wire.

Carbontetrachloride: AnalaR grade carbon-tetrachloride was distilled. The distillate was kept in contact with anhydrous calcium chloride overnight. The solution was decanted and redistilled (b.p.  $76.5^{\circ}\text{C}$ ).

Cyclohexane: The drying procedure used here was similar to that of benzene. The dried hydrocarbon boiled at  $81^{\circ}\text{C}$ .

All the salts used in this work were of AR grade. The water used was deionised and double glass-distilled.

The maximum uptake of water was found by the following method. Solutions of 2%, 5%, 8% and 10% w/v lecithin in non-polar solvent were prepared. Using Sigma Chemical Company recalibrated microlitre pipettes, different volumes of water were added to these solutions. The samples were shaken thoroughly to ensure homogeneous mixing, allowed to stand for fifteen minutes and centrifuged at 800 rpm in a Clay-Adams table-top centrifuge and then inspected for phase separation. The optical anisotropy of the solutions was tested by viewing the centrifugates held between two crossed polarisers against a strong source of light. The amount of water added was increased in fixed steps. Based on the results of water uptake studies, the 5% w/v solution of lecithin in non-polar solvent was chosen for further investigations by other techniques.

A Systronics 303 electrical conductivity meter standardised regularly against a 0.135 M KCl solution was used for conductivity measurements. The KCl solution used as an indicating electrolyte

in the titrations had a specific conductance of  $0.0176 \text{ mho cm}^{-1}$ . These measurements were carried out slowly by the addition of a measured quantity of KCl solution to a fixed volume of lecithin in the non-polar solvent. After each addition, the solution was thoroughly mixed and its conductivity measured. All measurements were repeated at least three times and the results averaged.

For the viscosity measurements, a Rheotest II rotating cup viscometer with measuring system N was used. All the measurements were made on freshly prepared solutions. All the measurements were carried out at a number of shear rates ranging from  $48.6 \text{ sec}^{-1}$  to  $1312 \text{ sec}^{-1}$ . For calculating relative viscosity of non-Newtonian samples, values of viscosity at a shear rate of  $1312 \text{ sec}^{-1}$  were used.

A Brice-Phoenix Model-2000 light scattering photometer, with appropriate accessories obtained from the same manufacturer, was used for the light scattering studies. A standard cylindrical cell C-105, 15 ml maximum capacity, and the narrow beam geometry were used. Addition of water and mixing were carried out in the cell itself. As is well known, dust particles play havoc in the light scattering measurements; therefore, in addition to keeping the work area as dust-free as possible, all the solutions, including solvents and water, were filtered at least thrice using  $0.22 \mu$  millipore filters with a Swinnex filtration assembly. At the final stage, the solutions were again filtered directly into the cell. All the glassware and cells

were repeatedly washed with detergent solution, filtered water and then with filtered acetone. Drying was done in a clean box.

Electron micrographs were recorded on a Phillips EM-301 transmission electron microscope operated at 80 or 100 kV. For purposes of 'staining' the micrographs, a 1 per cent aqueous solution of ammonium molybdate, pH 7.5, was substituted in place of the water normally added while preparing PC-solvent-water reverse micelles. The samples with different volume percentages of the stain added were applied on carbon coated copper grids, air dried and examined in the electron microscope.

In the case of all the above techniques, measurements were carried out at  $25 \pm 1^\circ\text{C}$ .

### Results and Discussion

Table 2.1 gives the amount of water solubilised by lecithin in the three non-polar solvents studied. The value of water uptake reported for benzene (Table 2.1) solvent is comparable to that of Demchenko (2) who found a value of 0.31 - 0.33 g of water per gram of lecithin. Our value above in benzene is also in agreement with that of Elworthy (3), who recorded a maximum of 0.33 g of water per gram of lecithin in benzene. In carbon-tetrachloride, the amount of water solubilised is 15.8 moles per mole of lecithin while in cyclohexane one observes a maximum of 15.0 moles of water per mole of lecithin.

Table 2.1

Water up-take by a 5% w/v solution of lecithin in benzene, carbontetrachloride and cyclohexane

Solvent	Lecithin concentration	Water Solubilised	
		$\frac{\text{g of water}}{1 \text{ g of PC}}$	$\frac{\text{mole of water}}{1 \text{ mole of PC}}$
Benzene	5% w/v	0.38	16.2
Carbontetra- chloride	5% w/v	0.37	15.8
Cyclohexane	5% w/v	0.35	15.0

A very interesting observation in cyclohexane is the existence of a slightly turbid, viscous, anisotropic region at a water content of 5-7 moles of water per mole of lecithin. This anisotropic region extends from 5-7 moles of water per mole of lecithin to 15 moles of water where phase separation occurs.

Lecithin solution in non-polar solvents can take up water to produce clear dispersions in two distinct ways: (a) when the water is either molecularly dispersed in the system; or (b) when water is contained in nearly spherical reverse micelles with radii that are small in comparison with the wavelength of visible light. If we assume the presence of ordered and highly asymmetric structures the optical anisotropy of the turbid region in cyclohexane solvent can be explained. Such structures can be either water cylinders or lamellae surrounded by a

phospholipid film. The phospholipid molecules are oriented at the water-solvent interface with their hydrophobic part into the non-polar continuous phase and the hydrophilic part into the aqueous phase. In analogous cases of surfactant-cosurfactant-hydrocarbon-water systems (microemulsion systems), such liquid crystalline assemblies are well known (4-7).

We have utilised optical birefringence for the confirmation of the optically anisotropic phase found in cyclohexane system starting from a water concentration of 5-7 moles of water per mole of PC. In this technique, a drop of the dispersion is placed between two microscopic slides and squeezed to produce flow and examined between two crossed nicols, at right angles to each other, against a strong source of light. The solutions of lecithin in the three solvents at different water concentrations are checked by this technique. Benzene and carbontetrachloride systems at all water concentrations appear dark when viewed through the crossed nicols. However, in the case of cyclohexane, the system appears black upto a water content of 6 moles of water per mole of lecithin. Thereafter, the illuminated background field starts to show beautifully coloured patterns.

When the small aggregates are anisotropic with one dimension longer than the other, as in rodlike or disklike aggregates, dispersions of them become doubly refracting when they are stirred or allowed to stream. This is due to the scattering and repolarisation of the polarised light. A particularly striking illustration of birefringence in liquid crystalline

phases may be found in a paper by Wilton and Friberg (8). The appearance of birefringence is a very good indicator of the fact that the dispersed phase of an oil-amphiphile-water system is no longer in spherical form and that a liquid crystalline phase is present. As long as the aggregates are spherical or isotropic, of course, the system appears dark due to total interference when viewed through crossed nicols. These arguments suggest that the aggregates formed in benzene and carbontetrachloride are spherical and isotropic whereas the aggregates formed in cyclohexane above a water content of six moles per mole of lecithin are anisotropic structures.

Though Friberg (9) points out that such liquid crystalline structures in surfactant systems fall in the multiphasic region of the phase diagram, we have treated the liquid crystalline anisotropic phase in cyclohexane as if it were a single homogeneous phase for the following reason. Storage of samples in the liquid crystalline region for one month did not lead to any phase separation because of the high phase stability of the system in this region.

Another important inference drawn from our study of water uptake values is that the high values of water solubilised per mole of lecithin indicate that all the water in the system will not be in a form 'bound' to the polar head group of lecithin. It is much more likely, in fact, that discrete 'pools' of free, unbound water contained by a lecithin film, exist in the system.

Before proceeding to the details of our viscosity studies, mention should be made of the quantity  $R$  which is used in this thesis. Since our main aim is to study the changes in properties of the system, lecithin-non polar solvent, as a function of added water, we have kept the concentration of lecithin constant at 0.067 M i.e., a 5% w/v solution of lecithin in the solvent. Water is then added in fixed increments. The quantity  $R$  is then defined as the molar concentration ratio of water to lecithin.

$$R = \frac{[H_2O]}{[PC]}$$

This definition of  $R$  is maintained throughout this thesis. The following additional naming system has also been used in this work: phosphatidylcholine-benzene-water system, for example, will be sometimes referred to simply as benzene system with obvious extensions for systems containing carbontetrachloride and cyclohexane as solvents. Further, the terms phosphatidylcholine (PC) and lecithin have been used interchangeably.

### Viscosity Studies

The principle of this method is based on the fact that when dispersed aggregates are other than spherical in shape, they offer more resistance to flow than their spherical counterparts. This manifests itself as a sudden and sharp increase in the viscosity of the dispersion.



Since our primary interest is to examine the effect of dispersed particles on the viscosity of the system, we include here a very brief outline of viscosity theory for the smooth flow of a liquid parallel to a stationary boundary. The velocity of the liquid will vary with distance from the boundary because of the viscous properties of the liquid. If  $V$  is the velocity gradient of the liquid, and  $X$  is the distance from the boundary, the instantaneous force  $F$  acting per unit area  $A$  in a layer of flowing liquid is given by

$$\frac{F}{A} = \eta \frac{dV}{dX} \quad \dots (2.1)$$

where  $\eta$  is the absolute or apparent viscosity. This, of course, is Newton's law modified for viscosity. The fluids which obey the form predicted by equation (2.1) are said to be Newtonian. The velocity gradient  $\frac{dV}{dX}$  in equation (2.1) is called the rate of shear, since  $\frac{dV}{dX}$  has units of reciprocal time,  $\text{sec}^{-1}$ . For a Newtonian fluid, a plot of  $F/A$  versus  $dV/dX$  should give a straight line of zero intercept and the slope equalling  $\eta$ . Non-Newtonian fluids generally show deviations from the linear plot. Their viscosity is then equal to the slope of the curve to the tangent at various points and is a function of the rate of shear. Summarising, systems whose apparent viscosity is independent of the rate of shear are said to be Newtonian, while systems whose apparent viscosity is a function of shear rate are said to be non-Newtonian.

Experimentally it is customary to report viscosity as relative viscosity,  $\eta_r$ , which is the ratio of apparent viscosity to that of solvent viscosity.

$$\eta_r = \frac{\eta}{\eta_0}$$

where  $\eta_0$  is the viscosity of the pure solvent. Inspection of equation (2.1) reveals that apparent viscosity  $\eta$ , has the dimensions of mass time<sup>-1</sup> length<sup>-1</sup>. In cgs units 1 g sec<sup>-1</sup> cm<sup>-1</sup> is defined equal to 1 poise. At room temperature (298 K) pure water has a viscosity of 0.01 poise. Relative viscosity,  $\eta_r$ , being a ratio, is dimensionless.

Figure 2.1 shows the variation in the relative viscosity of the benzene and CCl<sub>4</sub> systems as a function of added water. Similarly, viscosity data for the cyclohexane system are presented in Fig. 2.2.

From Fig. 2.1 it is evident that the relative viscosities of benzene and carbontetrachloride systems increase slowly with addition of water upto the phase separation point. Initially when no water is added, the solution is homogeneous. When water is introduced as a dispersed phase, it is a natural consequence that viscosity will increase (10). Benzene and carbontetrachloride systems displayed Newtonian viscosity at all concentrations of water. This suggests that the dispersed phase is present in highly symmetrical, i.e., spherically-shaped droplets.

CENTRAL LIBRARY  
K. N. R.

82710

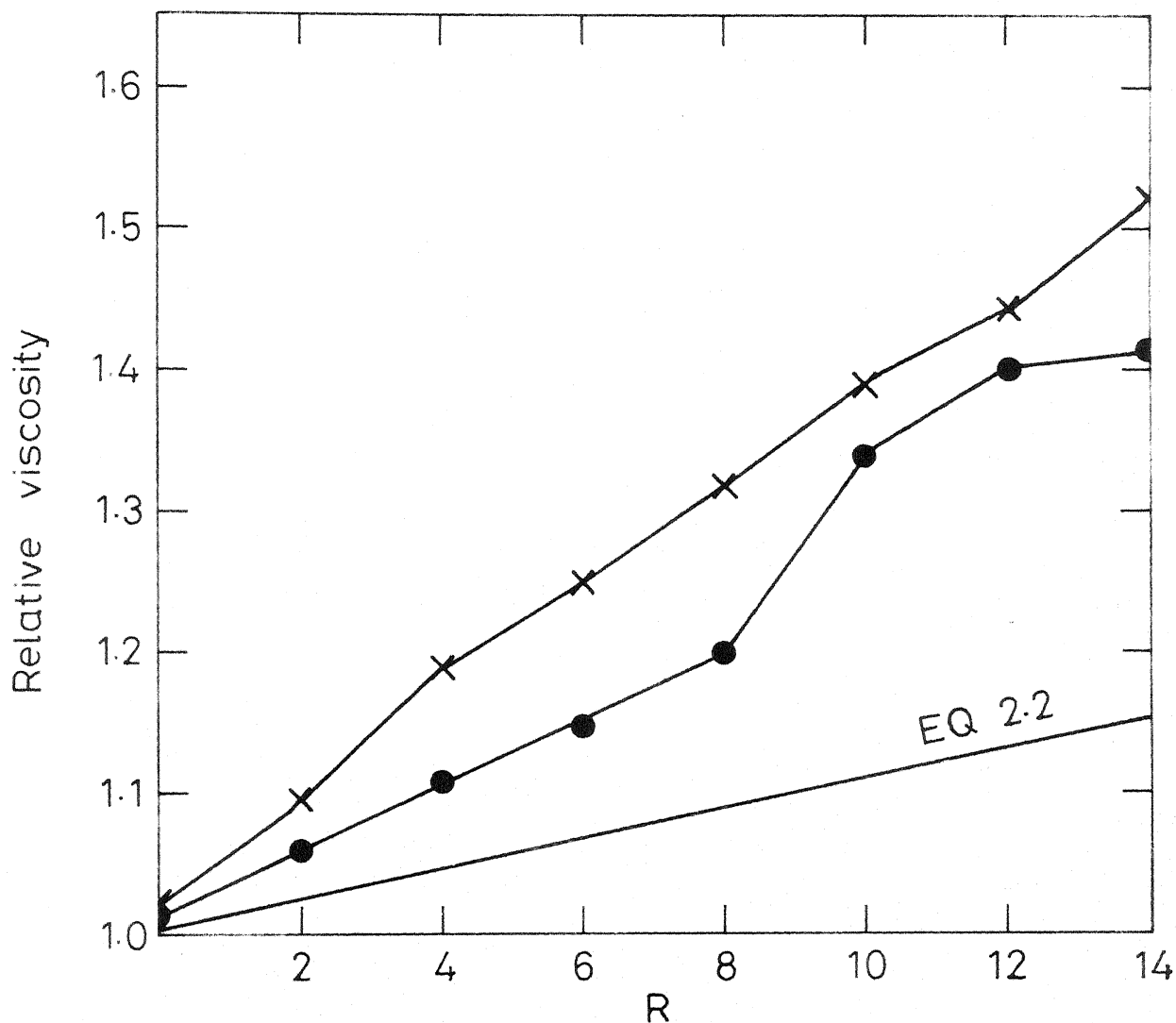


Fig. 2.1 Variation of relative viscosity in Benzene and Carbontetrachloride systems as a function of added water. ● ---- Carbontetrachloride points, X ---- Benzene points

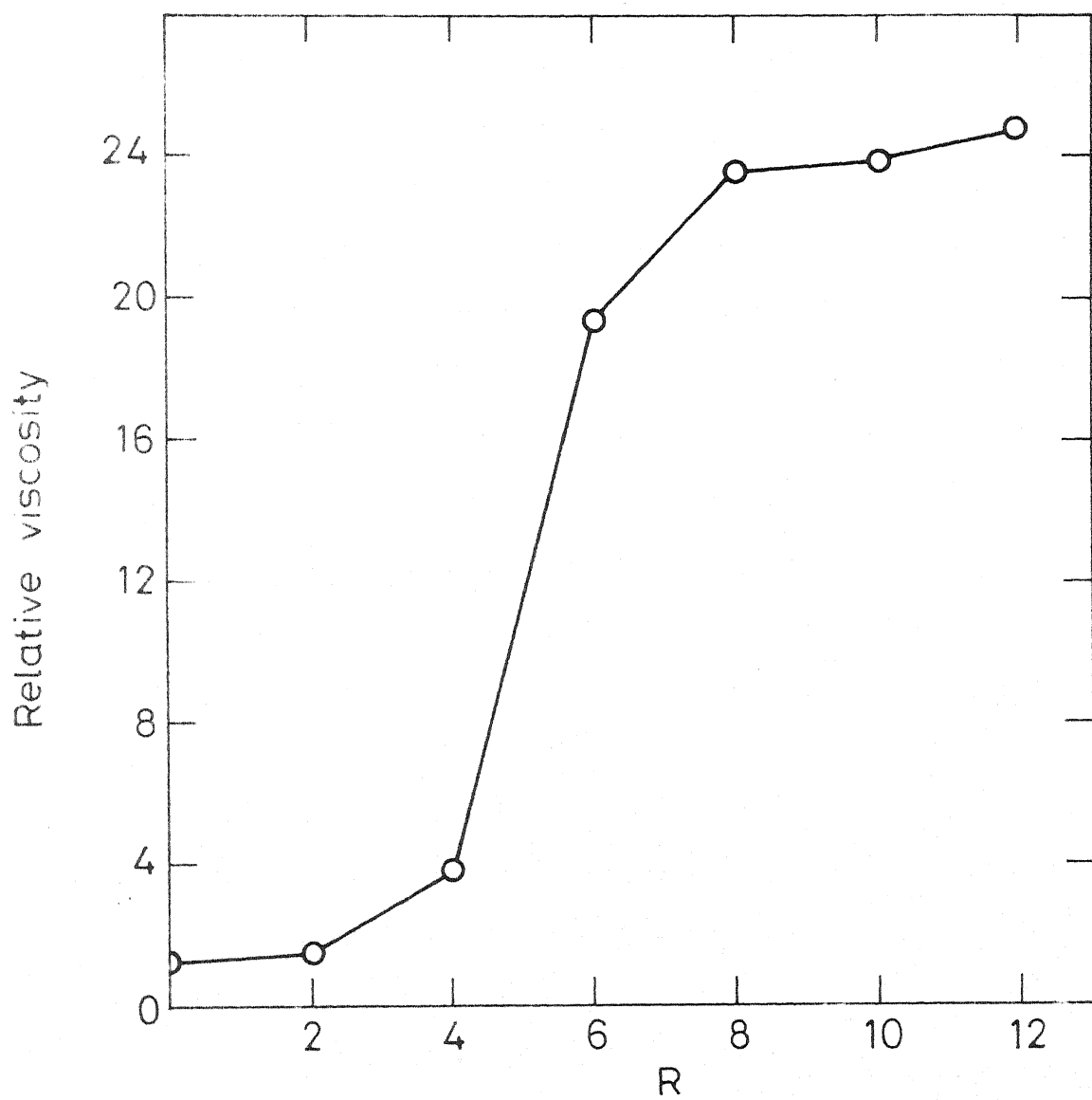


Fig. 2.2 Variation of relative viscosity in Cyclohexane system as a function of added water.

In contrast to our results in benzene system, Elworthy and McIntosh (11) in their earlier report state that the intrinsic viscosity of lecithin in benzene solution increases to a peak value upto a water content of 0.055 g of water per gram of lecithin or 2 moles of water per mole of lecithin followed by a subsequent decrease with further water incorporation. In a later publication, the validity of Elworthy and McIntosh's work was thoroughly questioned by Janson et al. (12).

In another study, Henrikson (13) claims a 'dramatic drop in viscosity' when 10 mg of water is added to a lecithin sample in carbontetrachloride; although no viscosity measurements are actually reported by her. In fact our present observations, revealing as they do an increase in viscosity in the carbon-tetrachloride system, clearly invalidate the claim of Henrikson. Table 2.2 gives the values of relative viscosities of the three systems. The viscosity values reported in Table 2.2 are reproducible within an error of 7-8%. In each case, the values are averages of at least two measurements.

We see from Table 2.2 and Fig. 2.2 that relative viscosity values are much higher for the cyclohexane solvent system than in the case of benzene and  $\text{CCl}_4$  systems at corresponding R values. One notices from Fig. 2.2 a sudden and sharp increase in the viscosity at an R value of 6, where a possible phase change from isotropic to anisotropic phase has been indicated by our earlier optical birefringence results. These viscosity data add support

to the observation that phase change is occurring in the cyclohexane system around an  $R$  value of 6. All the solutions in the cyclohexane system below values of  $R \sim 6$  exhibit Newtonian behaviour. On the other hand, solutions with  $R > 6$  display strongly non-Newtonian behaviour. This non-Newtonian behaviour typical of only asymmetric structures may be interpreted as being due to the presence of cylinders of lamellae under these conditions (13).

Table 2.2

Variation of relative viscosity in benzene, carbontetrachloride and cyclohexane systems as a function of added water

R	Relative Viscosity $\eta_r$			$\eta_r$ from Eq. 2.1
	Benzene	Carbon tetrachloride	Cyclohexane	
0	1.02	1.01	1.19	1.008
1	-	-	1.32	1.013
2	1.10	1.06	1.58	1.017
4	1.18	1.11	3.67	1.035
6	1.25	1.15	19.45	1.052
8	1.32	1.20	23.57	1.069
10	1.39	1.34	23.91	1.090
12	1.45	1.40	24.75	1.130
14	1.52	1.41	24.75	1.150

When the spherical aggregates begin to transform to cylindrical or lamellar ones, the new forms tend to obstruct the flow of aggregates past one another in the dispersion medium. Fig. 2.3 shows the shear rate dependence of cyclohexane system at  $R = 4$  and  $R = 10$  values.

A quantitative treatment of the above viscosity data will now be attempted. We have interpreted the data with water as the dispersed phase and lecithin in the solvent as the continuous phase. Roscoe (15) gives an expression for the relative viscosity of uniform spheres as:

$$\eta_r = (1 - 3.5 \phi)^{-2.5} \quad \dots (2.2)$$

where  $\phi$  is the volume fraction of the dispersed phase. However, in view of the likelihood of some of the dispersed component being present in the bulk phase as molecular solute, Matsumoto and Sherman (16) have argued that  $\phi$  must be corrected. Shah et al. (17) use an equation of the form given below which allows a correction to  $\phi$ :

$$\eta_r = [1 - 3.5 (\phi - \phi_0)]^{-2.5} \quad \dots (2.3)$$

where  $\phi_0$  is the correction term. Since in many cases the relative viscosity is found to be dependent not only on the volume fraction but on the size distribution as well, Attwood et al. (18) have used the equation:

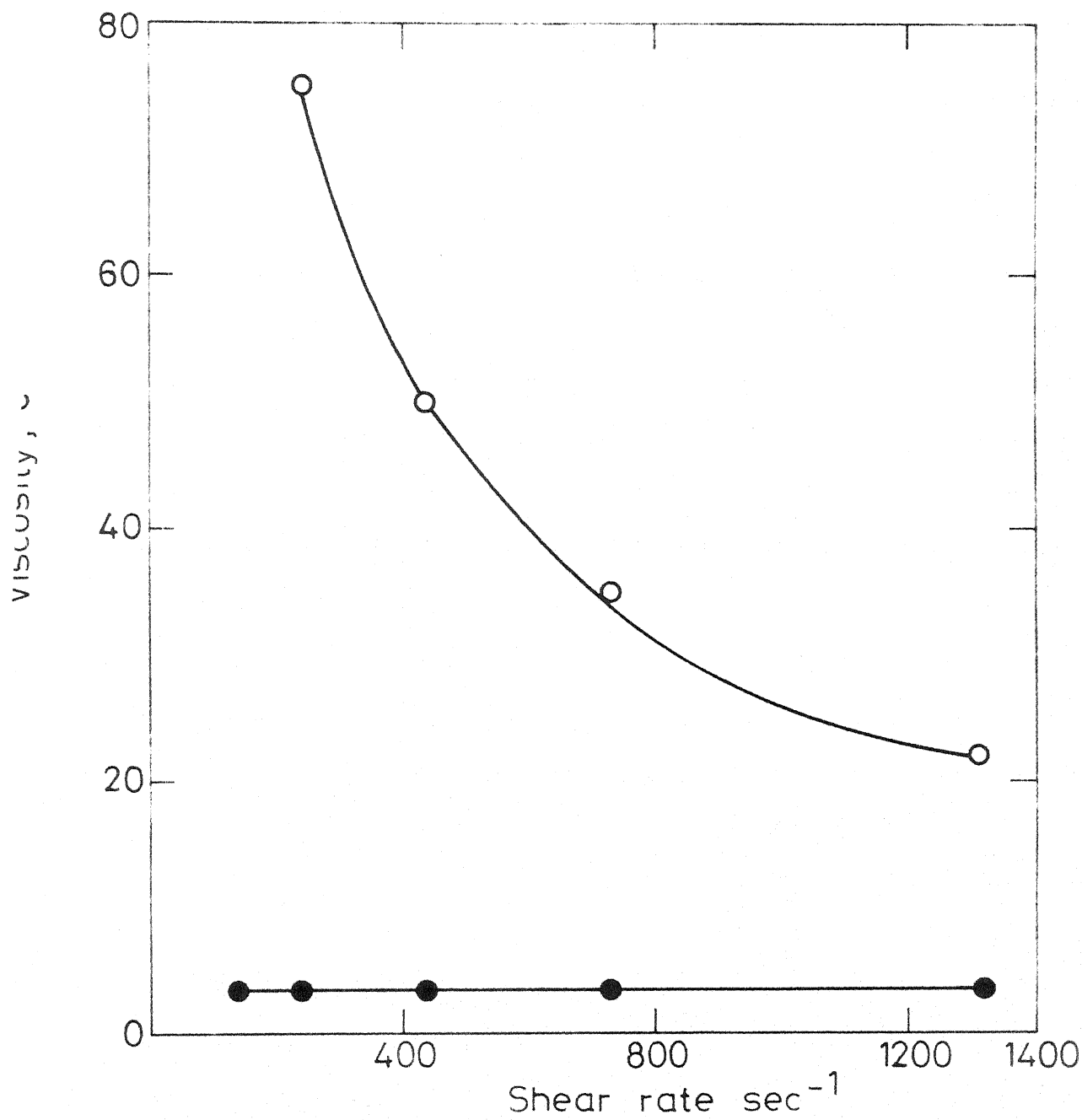


Fig. 2.3 Shear rate dependence of viscosity in Cyclohexane system ● ----  $R=4$ , ○ ----  $R=10$



$$\eta_r = \exp [a \phi / (1 - K \phi)] \quad \dots (2.4)$$

where  $a$  is a constant,  $K$  an interaction term and  $\phi$  the hydrodynamic volume of the dispersed phase.

The relative viscosity values calculated using Roscoe's expression (Eq. 2.2) are shown in the last column of Table 2.2 and also in Fig. 2.1 along with the experimental values. The experimental values in benzene and  $\text{CCl}_4$  systems agree well with the values calculated through Roscoe's expression. Since Roscoe's expression, in principle, applies to spheres only, this suggests again that the dispersed phase in these two systems is present in the form of spheres.

In the case of cyclohexane, the experimentally measured values are found to be consistently higher than the values calculated. This deviation increases with increasing water concentration and a sharp and sudden increase is found at  $R = 6$ . We advance the following explanation for this behaviour: For a model based solely on spherical geometry, the volume fraction of the dispersed phase and the effective hydrodynamic radius should increase at low  $R$  values because of the effect of the interfacial layer. The dimensions of the interfacial layer become small in comparison with that of the water pool as more and more water is added (i.e., as  $R$  increases) and therefore deviations arising from interfacial effects diminish. But we find here that deviations are increasing with water content. Therefore, we suggest that

increasing asymmetry in the shape of the micelle must be becoming important enough to override other effects. Indeed, our optical birefringence studies discussed earlier support this view.

It will be shown from the results to be presented in the next chapter, that most of the water resides in the water pools only and a negligible fraction of water is present in the bulk organic phase. We, therefore, have not used equation 2.3 for the analysis of our data. In equation 2.4 again the constants mentioned are size and shape dependent and since in our system it would appear from the forthcoming sections that the size of the micelles change as water is added and so we have not analysed our data using equation 2.4.

### Light Scattering Studies

The available theories of light scattering (19) quantitatively discuss only the light scattered by particles in dilute solution, when the range of droplet size distribution is wide, that, is when the system is heterodisperse, the scattering by a few large droplets may mask the scattering pattern caused by many small ones. The concentrations of lipid and water used in our studies are rather high which may lead to multiple scattering. Therefore, special precaution is to be exercised in interpreting the light scattering data. Hence, only a general and qualitative treatment of the light scattering data is attempted.

The basic concepts of light scattering have been expounded more than half a century ago by Rayleigh (20), Mie (21) and

Debye (22). It is convenient to divide light scattering by independent particles into three classes: (i) Rayleigh scattering, (ii) Debye scattering and (iii) Mie scattering. The class into which a given case falls is determined by two parameters of the scattering particles, namely, their size relative to the wavelength of the incident light ( $\lambda$ ) and the refractive index of the particles relative to that of the medium. The basic idea underlying the above three theories is that when a beam of light falls upon matter, the electric field associated with the light induces periodic oscillations of the electron clouds of the atoms of the material. The atoms then serve as secondary sources of light and radiate the light in the form of scattered radiation. The intensity of this scattered light at any angle depends on  $\lambda$ , the size and shape of the scattering particles, the optical properties of the scatterers as well as  $\theta$ , the angle of observation.

Particles that have a linear dimension comparable to or greater than  $\lambda$  scatter more light in the forward direction than in the backward direction. This asymmetry arises from the fact that in the forward direction ( $\theta < 90^\circ$ ) the wavelets scattered from two or more points in the material are closer in phase than in the backward ( $\theta > 90^\circ$ ) direction, resulting in increased intensity in the forward direction and decreased intensity in the backward direction. A measure of the extent through which the intensity is attenuated with angle of observation is the dissymmetry of scattering, which is the ratio of the intensities

at some angle and its supplement. In practice it is customary to represent dissymmetry as the intensity ratio of light scattered at  $45^\circ$  to that at  $135^\circ$ ,

$$\text{Dissymmetry} = \frac{I_{45}}{I_{135}} .$$

In Fig. 2.4, the variation of dissymmetry is plotted as a function of  $R$  for benzene, carbontetrachloride and cyclohexane systems.

From Fig. 2.4 we find that dissymmetry increases from 1.6 to 2.3 in the case of  $\text{CCl}_4$  system, in  $\text{C}_6\text{H}_6$  system it ranges from 1.9 to 2.1, while it varies from 1.2 to 3.4 in the cyclohexane system at corresponding  $R$  values.

In light scattering phenomena the radius of gyration,  $R_g$ , of the scattering particles plays an important role and we shall therefore, devote a brief section to this topic (23,24).

We assume that the particle whose radius of gyration is under discussion may be subdivided into a number of volume elements of mass  $m_i$ . The moment of inertia,  $I$ , about the axis of rotation is then given by

$$I = \sum_i m_i r_i^2 \quad \dots (2.5)$$

where  $r_i$  is the distance of the  $i$ th volume element from the axis of rotation.

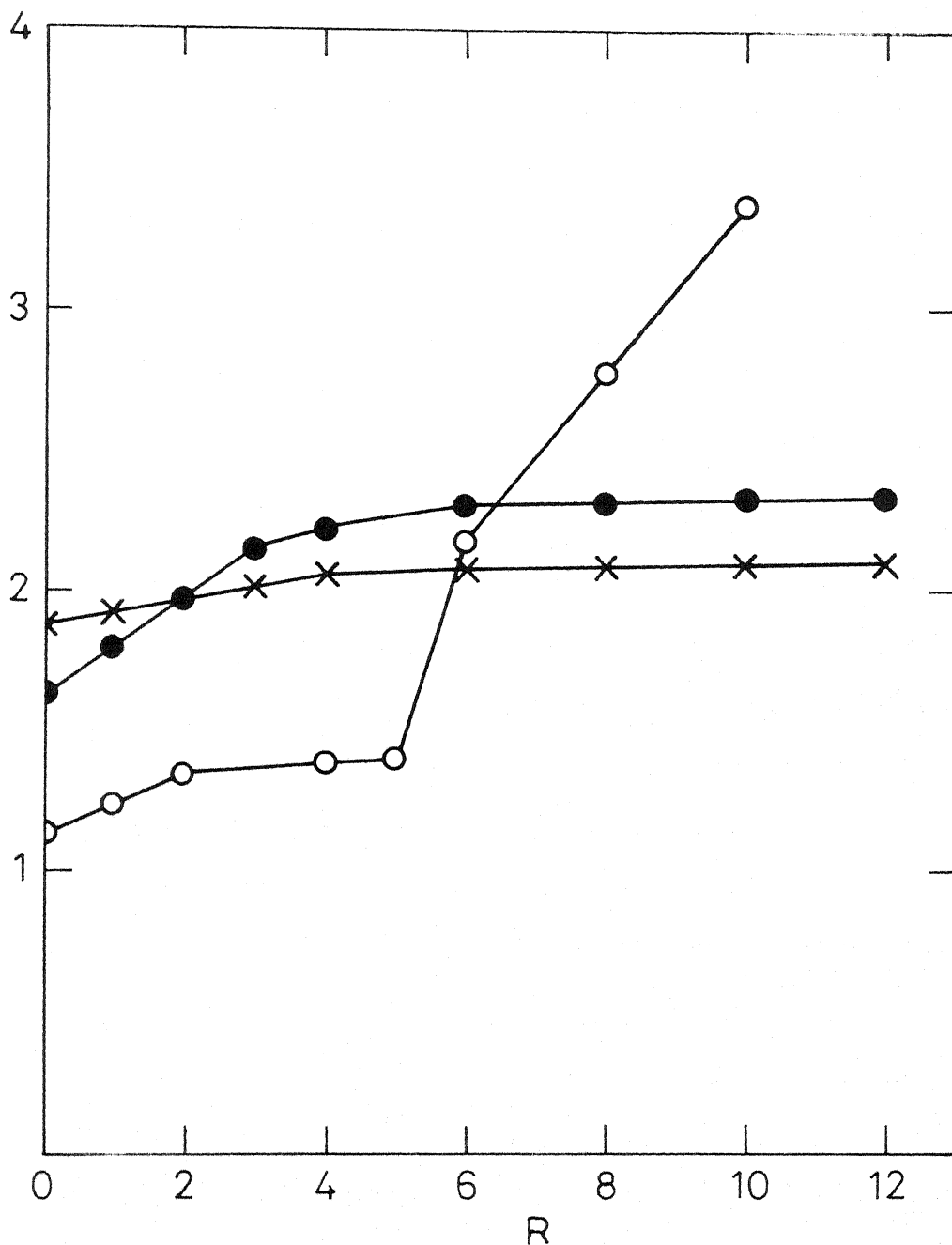


Fig 2.4 Variation of dissymmetry parameter in Benzene, Carbontetrachloride and Cyclohexane systems as a function of added water. ● ---- Carbontetrachloride points, ○ ---- Cyclohexane points, x ---- Benzene points

Regardless of the shape of the particle, there is a radial distance at which the entire mass of the particle could be located ('centre-of-mass') such that the moment of inertia would be the same as that of the actual distribution of the mass. This distance is the radius of gyration  $R_g$ . According to this definition, it is clear that

$$R_g^2 \sum_i m_i = I = \sum_i m_i r_i^2 \quad \dots (2.6)$$

The relationship between the radius of gyration of a particle and its actual dimensions depends on the shape of the particle. A more common procedure, however, is to plot the dissymmetry ratio versus  $D/\lambda$ , where  $D$  is a characteristic particle dimension and  $\lambda$  is the wavelength of light used. A number of plots could be constructed for different shapes such as spheres, disks, random coils, rods etc.

In Fig. 2.5 we present the variations in dissymmetry values for differently shaped structures with the radius of gyration of the scattering centre (24).

As is clearly seen from Fig. 2.5, the dissymmetry parameter constitutes a very sensitive indicator of the particle size above a minimum value of radius of gyration of the particle.

We shall now compare the features of Fig. 2.5 with those of Fig. 2.4. In  $\text{CCl}_4$  system, from Fig. 2.4, the dissymmetry varies from 1.6 to 2.3 in the  $R$  range 0 to 10. From Fig. 2.5 such

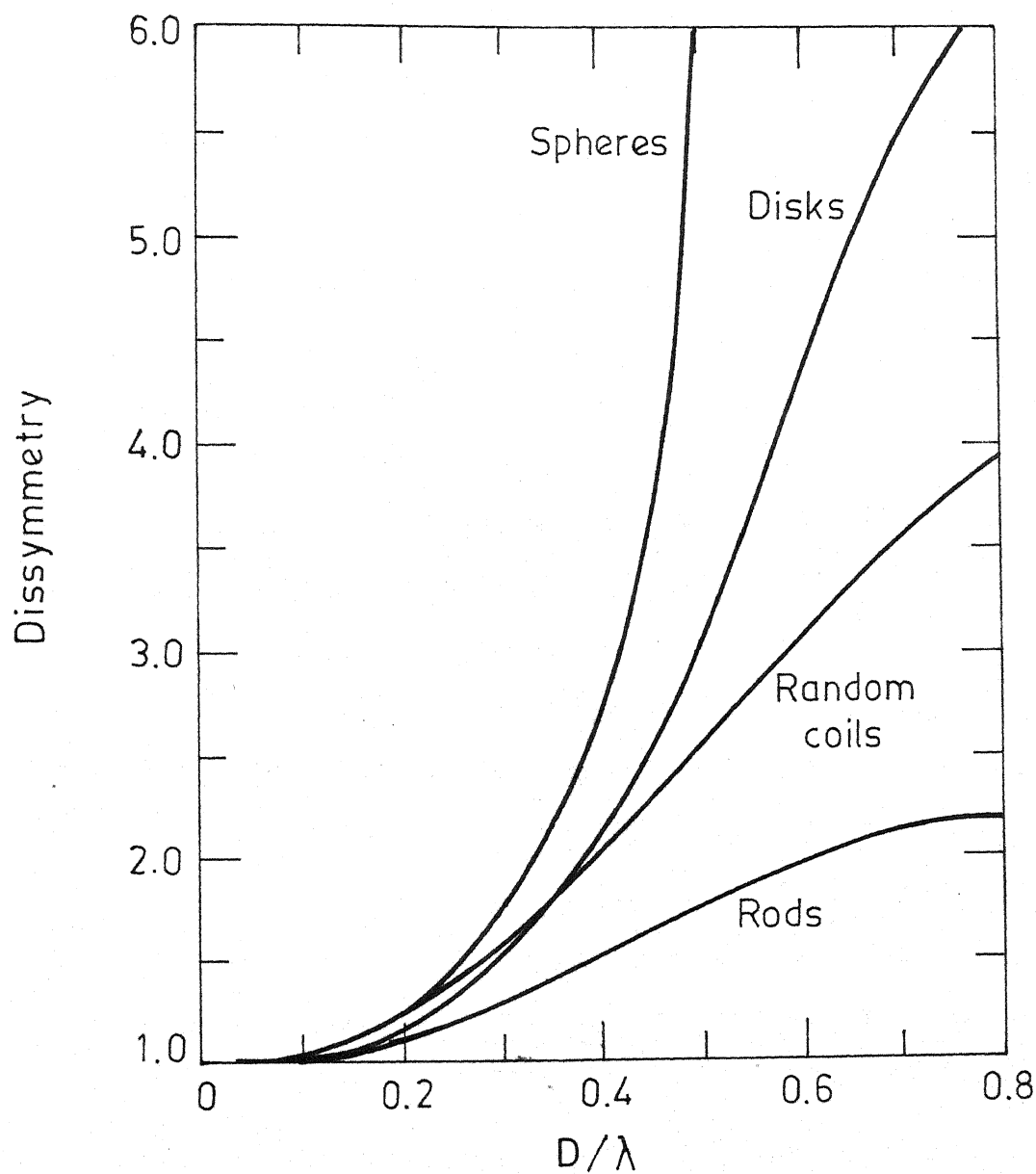


Fig.2.5 Variation of dissymmetry with the radius of gyration of the scattering particles for different shapes.

variation in dissymmetry values indicates that the average radius of gyration of the scattering centres lies between  $550 \text{ \AA} - 650 \text{ \AA}$  for spherically shaped structures. In the benzene system the radius of gyration varies between  $600 \text{ \AA} - 700 \text{ \AA}$  for the spherically shaped structures.

On the other hand, in cyclohexane system upto an  $R$  value of 5, the radius of gyration is about  $350 \text{ \AA}$  for spherical structures. Above  $R = 5$ , where a phase transition is expected, the dissymmetry increases sharply and reaches a value of 3.4. From Fig. 2.5 again, it can be seen that such high dissymmetry values can be displayed by either spherical or disklike or randomcoil structures. The possibility of rodlike structures is ruled out because, for this geometry, dissymmetry values level off below 3.4 as their radii of gyration approach the value of the wavelength of the light used. Since the cyclohexane system, in this region exhibits anisotropy, a spherical structure for the micelle is also clearly ruled out, reducing our choice to only two, namely, the disklike or randomcoil structures.

It will become apparent in the next section on the results of our electron microscopy work that the anisotropic region found in cyclohexane system conforms neither to the disklike or randomcoil structures, but in fact requires a more specialised description.



### Electron Microscopy Studies

We now proceed to report further experiments which lead to more direct and visual proof of our inferences upto this point. In their studies on microemulsions, Schulman and coworkers (25,26) utilised the technique of 'negative staining' to obtain electron micrographs of their systems. In our systems, we have found that 'positive staining' can be utilised for visualising lecithin reverse micelles. That is, if a suitably chosen stain is present in the aqueous phase, it will be localised within the core of the reverse micellar and liquid crystalline phases. The polar head group of lecithin may also be stained to some extent since it is in intimate contact with the water pool. Hence, if we include the stain in the aqueous phase of a spherical reverse micelle, the electron micrograph will show dark, electron impermeable circles. The bulk organic phase i.e., the 'background', will be transparent to the electron beam because the ionic stain will not dissolve in the organic phase. The radius of the above dark circle should correspond to the radius of the aqueous core plus the thickness of the head group. A number of such positively stained electron micrographs for the three systems at different  $R$  values have been carefully recorded and presented in Fig. 2.6 to 2.12.

In Table 2.3, we set forth representative values of the radii of different spherical structures formed in the three solvents for two limiting  $R$  values.

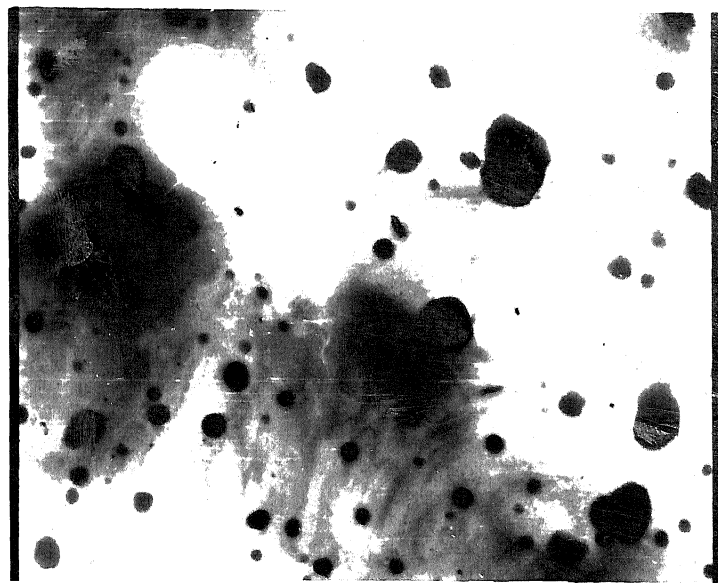


Fig. 2.6 Electron Micrograph of Benzene System  
at an R value of 5. Magnification:  $1 \times 10^4$

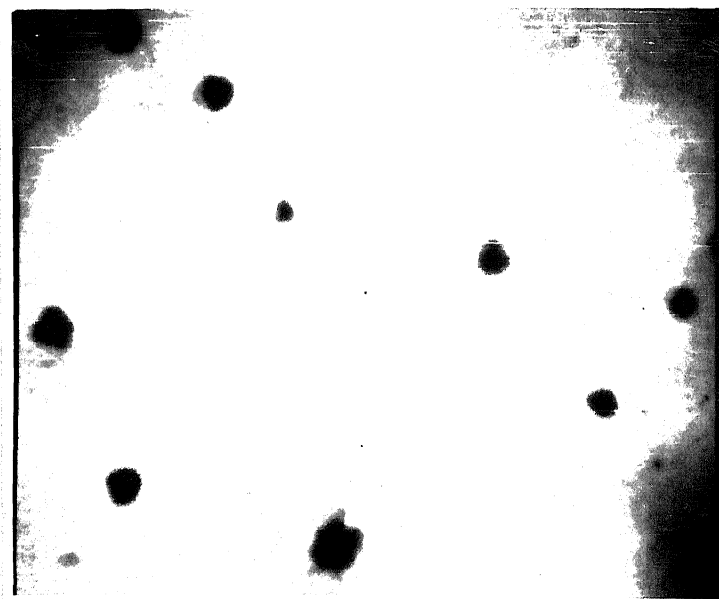


Fig. 2.7 Electron Micrograph of Benzene System at an  
R value of 12. Magnification:  $1 \times 10^4$

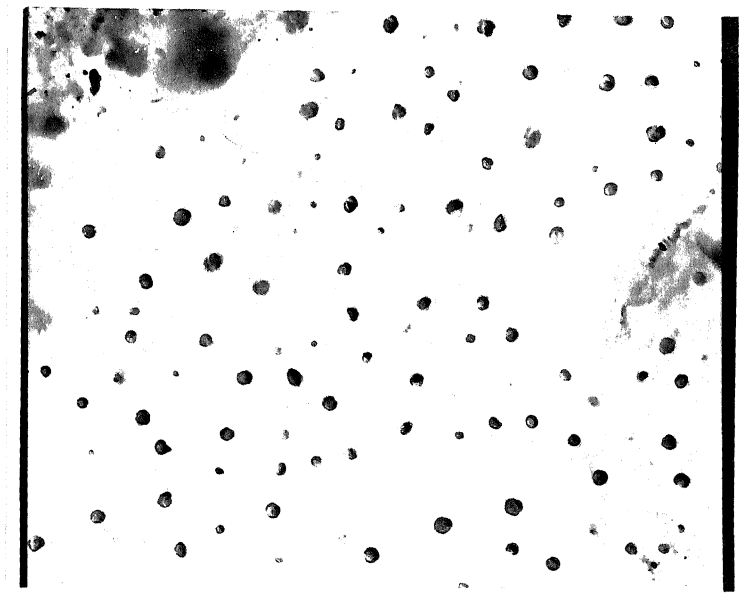


Fig. 2.8 Electron Micrograph of Carbontetrachloride System at an R value of 5. Magnification: 63217

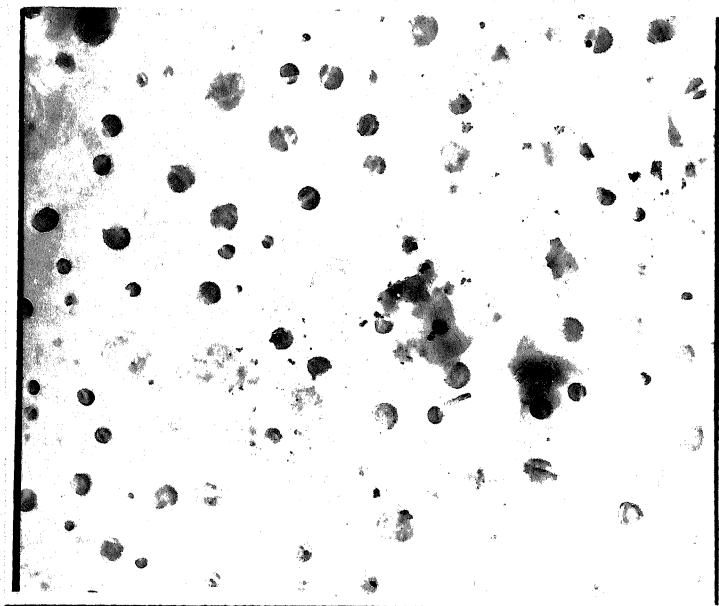


Fig. 2.9 Electron Micrograph of Carbontetrachloride System at an R value of 11. Magnification:  $1 \times 10^4$

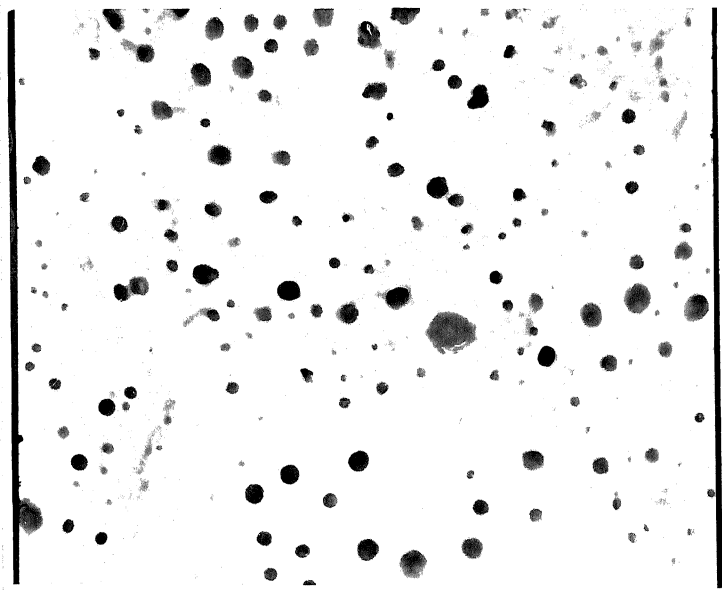


Fig. 2.10 Electron Micrograph of Cyclohexane System at an R value of 3. Magnification: 63217

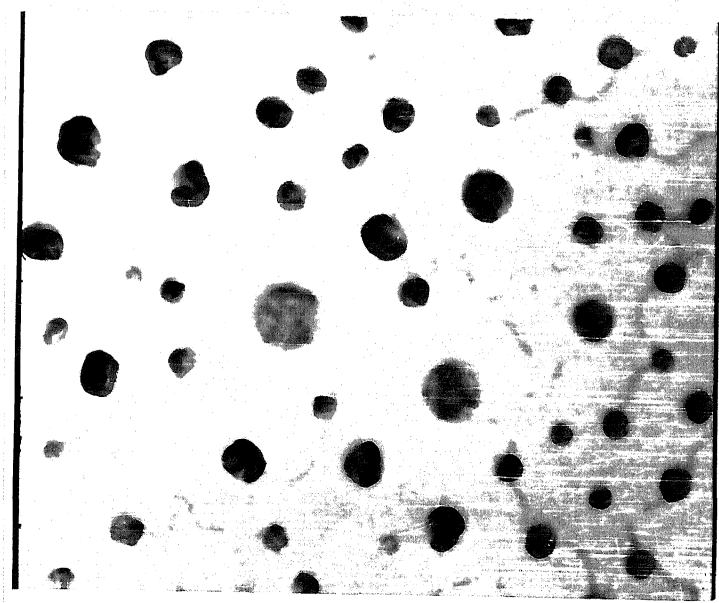


Fig. 2.11 Electron Micrograph of Cyclohexane System at an R value of 5. Magnification:  $7.8 \times 10^4$

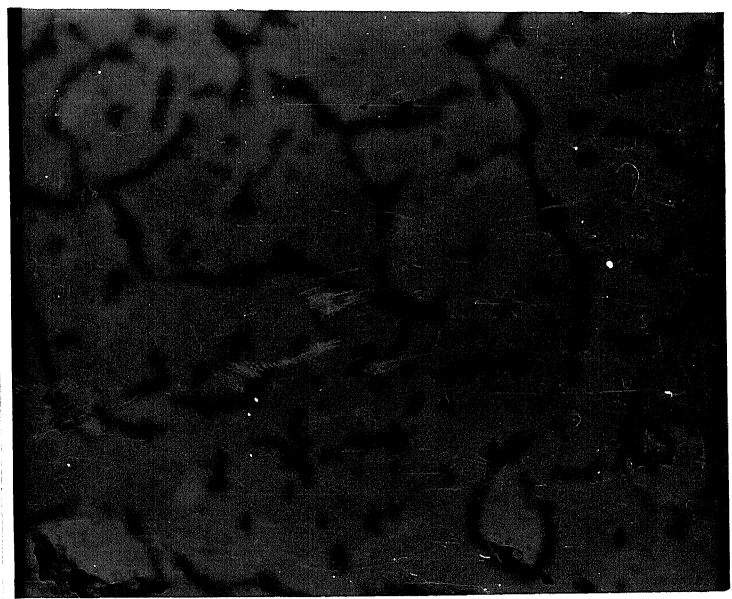


Fig. 2.12 Electron Micrograph of Cyclo-  
hexane System at an R value of 12.  
Magnification :  $7.8 \times 10^4$ .

Table 2.3

Radii of the spherical structures formed in benzene, carbontetrachloride and cyclohexane systems obtained from electron micrographs

Benzene		Carbontetrachloride		Cyclohexane	
R	Radius $\text{\AA}$	R	Radius $\text{\AA}$	R	Radius $\text{\AA}$
5	375-500	5	75-120	3	240
12	650	11	375-500	5	320

From Table 2.3 it can be seen that at an R value of 5, the spherical structures formed in carbontetrachloride are of smallest size while those formed in benzene are the biggest. In all the three cases, the size of spherical structures is found to increase as a direct consequence of the size of the water pool increasing with added water.

The non-spherical structures formed in the anisotropic region of cyclohexane system are shown in Fig. 2.12. The thick, curved, lines seen in Fig. 2.12 represent the aqueous channels that are formed in the liquid crystalline region of cyclohexane system. The thickness of these aqueous channels is about 60  $\text{\AA}$ . We describe these structures as 'tubular structures containing aqueous canals'.

The visual proof given by the electron micrographs presented in this section enhances the validity of our

conclusions arrived at from our other studies discussed so far.

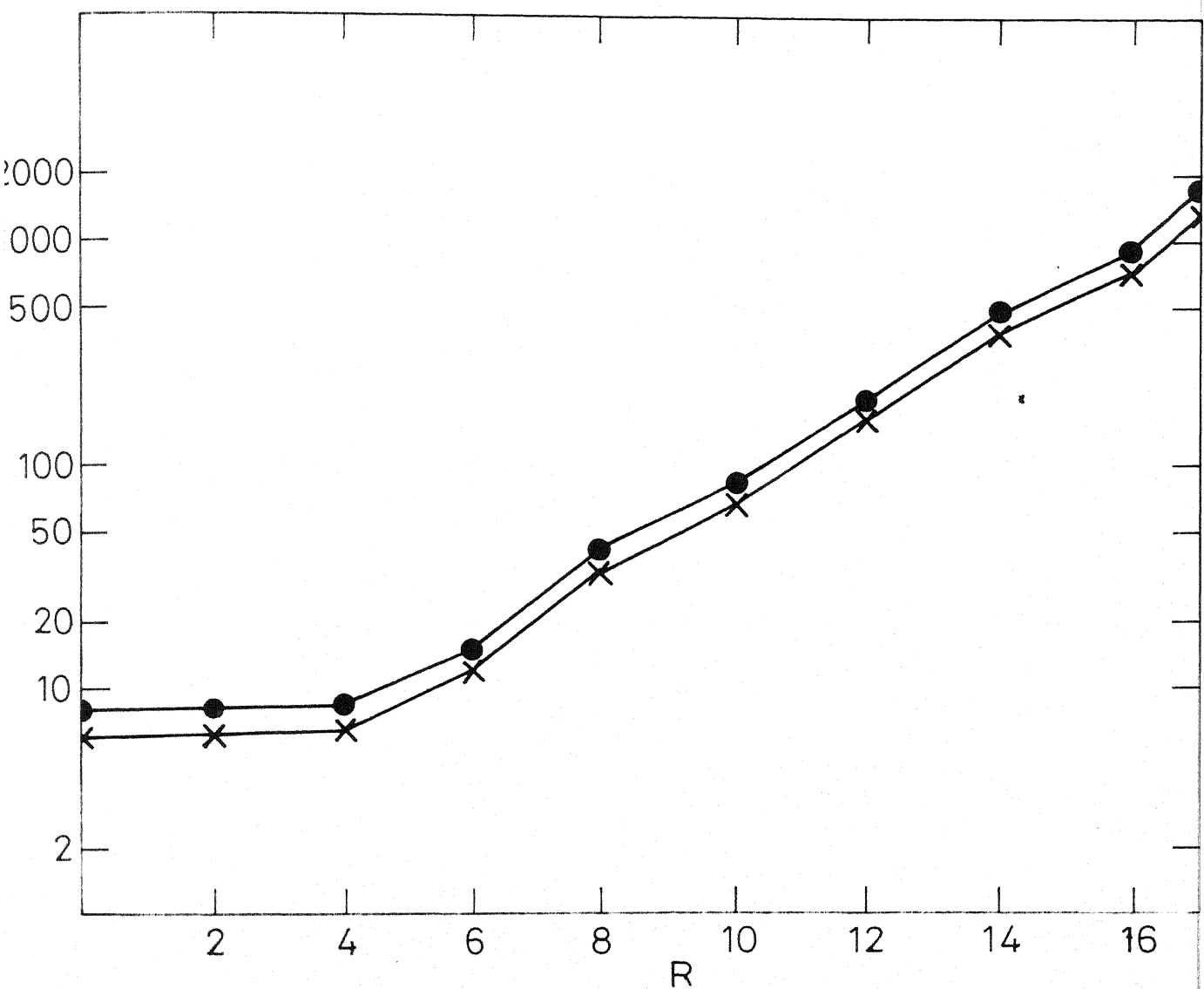
### Electrical Conductivity Studies

In Figs. 2.13 and 2.14 we present the variation in the electrical conductivity of the three systems as aqueous KCl is added.

From Fig. 2.13, it is seen that for benzene and carbon-tetrachloride systems the specific conductivity remains almost constant during the initial addition of aqueous KCl upto an R value = 4. Beyond this, the specific conductivity values start increasing, and the increase continues even beyond the phase separation.

If the electrolyte added is molecularly dispersed through the bulk of the solvent, even for additions of small volumes of electrolyte solution, basic electrochemical concepts lead us to expect that the specific conductivity should rise steeply. This is, of course, because of the number of carriers available for electrical conduction. The constancy of specific conductivity upto an R value of 4 in our systems indicates that the aqueous phase is not molecularly dispersed.

If we assume, in benzene and carbontetrachloride systems, that the aqueous electrolyte is contained in specific water pools surrounded and stabilised by a phospholipid film, the insensitivity of specific conductivity to added electrolyte can be explained. The interfacial phospholipid film and the continuous



13 Variation of specific conductivity in Benzene and C tetrachloride systems as function of added aqueous solution. ●---- Carbondetrachloride points, X---- Benz points



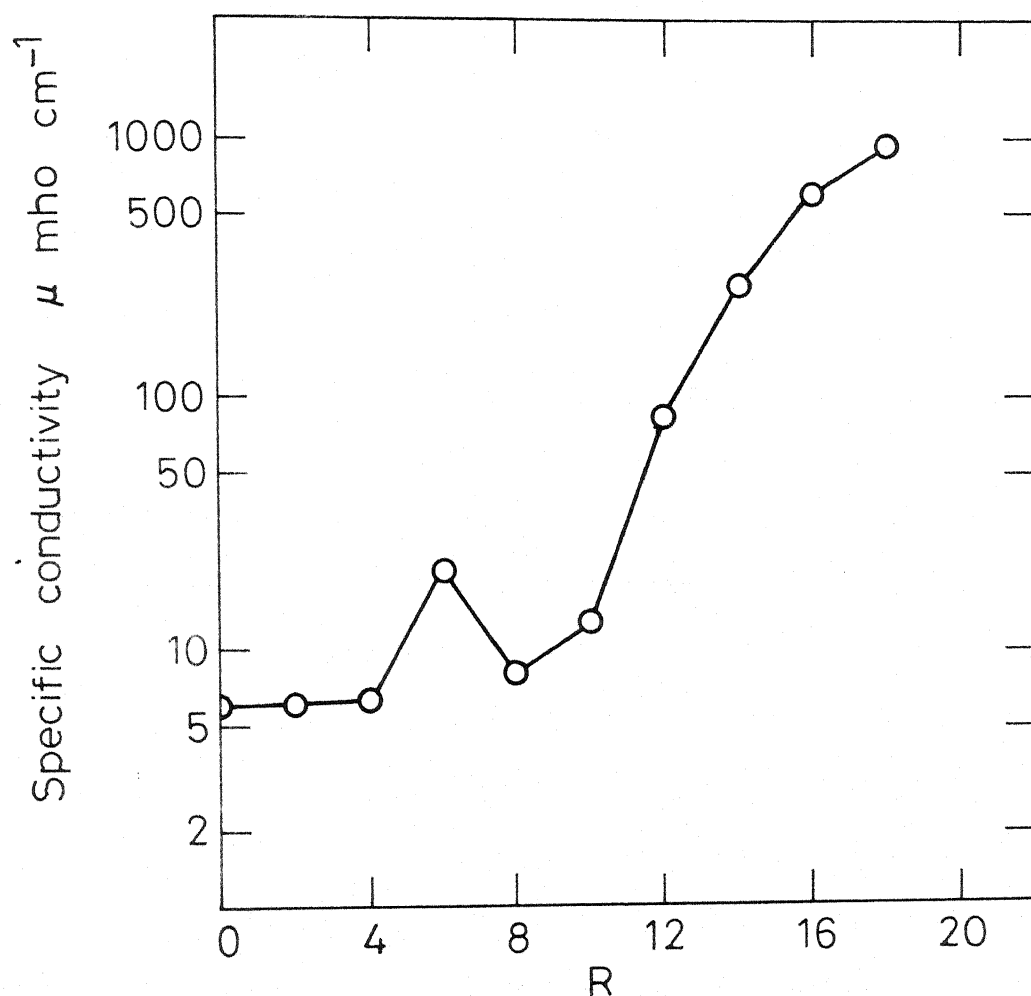


Fig. 2.14 Variation of specific conductivity in Cycohexane system as a function of added aqueous KCl solution.

organic phase between such water pools would form a significant barrier to conduction. We conclude that the added electrolyte solution is contained in discrete water pools that are formed in the interior of the reverse micelles; as long as the specific water pools are not in contact with electrodes, conduction can not occur. Schulman (27) and Shah et al. (28) have utilised just such conductivity measurements in the past to distinguish between solubilisation that occurs through microemulsion formation and that through molecular dispersion. The increase in conduction prior to phase separation in these systems can be interpreted to indicate that an enlargement of the size of the water pools occurs. After the phase separation point, free KCl solution is present, there is no significant barrier to conduction and hence the conductivity increases.

From Fig. 2.14 it is seen that in the case of the cyclohexane system, the conductivity is invariant upto an  $R$  value of 4. It then increases at first, followed by a decrease to intermediate values and again increases upto and beyond the phase separation. The specific conductivity shows a decrease at  $R$  values between 6-8, where the formation of an anisotropic phase is warranted from our results of earlier sections. Based on our electron microscopy observations, we have termed the structures formed in the anisotropic phase of cyclohexane system as 'elongated tubular structures containing aqueous canals'. It is then only natural to expect that the continuous aqueous canals formed in these structures should make conduction more facile

than in the isotropic region. However, we have seen earlier that our viscosity values undergo an enormous increase around an R value of 6. This increase in macroscopic viscosity of the system would reduce the mobility of the conducting ions through the aqueous canals. The combined observations of our conductivity and viscosity measurements are reconciled as follows: Initially, in the anisotropic region, the viscosity effect offsets the effect of water canals causing a net decrease in the conductivity. As more and more aqueous KCl solution is added, the ease of conduction increases and there is an increase in specific conductance due to the bigger size of the aqueous canals.

### Conclusions

The following conclusions can be drawn on the basis of experimental results presented in this chapter.

(1) A 5% w/v solution of lecithin in benzene or carbon-tetrachloride or cyclohexane solubilises about 0.37 g of water per 1 g of lecithin or about 16 moles of water per 1 mole of lecithin. In the case of cyclohexane system, an anisotropic liquid crystalline phase formation sets in around 6 moles of water per mole of lecithin.

(2) The anisotropic phase of cyclohexane system exhibits optical birefringence indicating non-spherical structures in this region while  $\text{CCl}_4$  and benzene system and the initial isotropic region (upto an R value of 6) of cyclohexane system conform to spherical structures.

(3) Viscosity, light scattering and electrical conductivity measurements as a function of added water, in benzene,  $\text{C}$  carbontetrachloride and the initial isotropic region of cyclohexane media, show that the reverse micelles contain dispersed water in small spherical droplets surrounded by a phospholipid layer. On the other hand, the anisotropic region of cyclohexane system exhibits a structuring effect that could be best described as 'elongated tubular structures containing aqueous canals'.

(4) The electron micrographs recorded in this chapter not only permit a direct visual evidence of the various structures mentioned above, but also enhance the validity of the results obtained through the techniques of viscosity, light scattering and electrical conductivity.

REFERENCES

1. W.S. Singleton, M.S. Gray, M.L. Brown and J.L. White, J. Am. Oil Chem. Soc., 42, 53 (1965).
2. P.A. Demchenko, Colloid J. USSR, 22, 309 (1960).
3. P.H. Elworthy and D.S. McIntosh, J. Phys. Chem., 68, 3448 (1964).
4. C. Kumar and D. Balasubramanian, J. Colloid Interface Sci., 69, 271 (1978).
5. P. Ekwall, L. Mandell and K. Fontell, Mol. Cryst. Liq. Cryst., 8, 157 (1969).
6. P. Ekwall, L. Mandell and F. Fontell, Acta Chem. Scand., 22, 373 (1968).
7. P.A. Winsor, Chem. Rev., 68, 1 (1968).
8. I. Wilton and S. Friberg, J. Am. Oil Chem. Soc., 48, 771 (1971).
9. S. Friberg, in 'Microemulsions, Theory and Practice', Ed. L.M. Prince, Academic Press, New York, 1977, p. 133.
10. P.C. Hiemenz, 'Principles of Colloid and Surface Chemistry', Marcel Dekker, New York, 1977, pp. 43-44.
11. P.H. Elworthy and D.S. McIntosh, Kolloid Z., 195, 27 (1964).
12. J.P.M. Janson, M. Kunst, A. Rip and P. Bordewijk, Chem. Phys. Lipids, 9, 147 (1972).
13. K.P. Henrikson, Biochim. Biophys. Acta, 203, 228 (1970).
14. P. Sherman, 'Rheology of emulsions' in 'Emulsion Science', Ed. P. Sherman, Academic Press, New York, 1968.
15. R. Roscoe, Brit. J. Appl. Phys., 3, 267 (1952).
16. S. Matsumoto and P. Sherman, J. Colloid Interface Sci., 30, 525 (1969).

17. D.O. Shah, A. Tamjeedi, J.W. Falco and R.W. Walker Jr.,  
Am. Inst. Chem. Eng. J, 18, 1116 (1972).
18. D. Attwood, C.R. Curie, P.H. Elworthy, J. Colloid Interface  
Sci., 46, 261 (1974).
19. M. Kerker, 'Scattering of Light and Other Electromagnetic  
Radiation', Academic Press, New York, 1969.
20. Lord Rayleigh, Phil. Mag., 12, 81 (1881) quoted in ref. 24.
21. G. Mie, Ann. Physik, 25, 377 (1908).
22. P. Debye, Ann. Physik, 30, 59 (1908).
23. See reference 10, pp. 160-204.
24. G. Oster, in 'Physical Methods of Chemistry', Vol. 1,  
Part IIIA, Eds. A. Weissberger and B.W. Rossiter, Wiley  
Interscience, New York, 1972.
25. J.H. Schulman, W. Stoecknius and L.M. Prince, J. Phys. Chem.,  
83, 1677 (1959).
26. W. Stoecknius, J.H. Schulman and L.M. Prince, Koll. Zeil.  
169, 170 (1971).
27. J.H. Schulman and D.P. Riley, J. Colloid Sci., 3, 383  
(1948).
28. D.O. Shah, R.D. Walker Jr., W.C. Hsieh, N.J. Shah,  
S. Dwivedi, J. Nelander, R. Pepinsky and D.W. Deamer,  
'Structural aspects of microemulsions and cosolubilised  
systems', SPE-5815, Paper presented at Improved Oil Recovery  
Symposium, Tulsa, U.S.A., March, 1976.

### CHAPTER III

#### NMR AND OTHER SPECTROSCOPIC STUDIES

In this chapter is presented a detailed analysis of the water content in the water 'pools' by means of a variety of spectroscopic techniques, namely, near infrared, ultraviolet, fluorescence emission, proton nuclear magnetic resonance ( $^1\text{H}$ -NMR) phosphorous nuclear magnetic resonance ( $^{31}\text{P}$ -NMR) and carbon nuclear magnetic resonance ( $^{13}\text{C}$ -NMR).

### Materials and Methods

The extraction of lecithin, drying of solvents and distillation of water is as described earlier in Chapter II.

Near IR spectra have been recorded using a Cary-17D spectrometer. A solution containing lecithin in non-polar solvent of the same concentration as that of the sample solution is used as a reference in order to record the spectra of solubilised water in reversed micellar system. Values of  $\lambda_{\text{max}}$  presented here were reproducible to within  $\pm 0.5$  nm. UV absorption spectra have also been recorded on the same Cary-17D spectrometer. The potassium nitrate salt used in polarity probe studies was of AnalaR grade.

Fluorescence emission spectra have been run on an Aminco-Bowman spectrofluorimeter Model SPF-125S. 8-Anilinonaphthalene sulfonic acid (ANSA), purchased as an AnalaR product from Sigma Chemical Company, was converted to the magnesium salt and recrystallised from water after charcoal treatment and the resulting product was used as a fluorescent probe. Quantum yields have



been calculated according to standard methods (1). The  $\lambda_{\max}$  values obtained in the fluorescence spectra were reproducible to  $\pm 1$  nm and the quantum yields are accurate upto  $\pm 0.01$ .

All the  $^1\text{H}$ -NMR spectra on the benzene system have been recorded using the JEOL-FX-100 FT-NMR spectrometer of the University of Hyderabad, India. The spin-lattice relaxation time measurements have been carried out with  $\text{D}_2\text{O}$  as external lock by the inversion recovery method ( $180^\circ$ - $\tau$ - $90^\circ$  pulse sequence) under the control of FX-100 'Autostacking' program. The  $90^\circ$  pulsewidth was 38 microseconds. Pulse repetition time was 10 seconds and the number of pulses in the sequence was eight.

The  $^1\text{H}$ -NMR spectra of  $\text{CCl}_4$  and cyclohexane systems were recorded on the Varian XL-100 FT NMR spectrometer at the Regional Sophisticated Instrumentation Centre, Indian Institute of Technology, Madras, India. In the case of cyclohexane system, the solvent was replaced by its deuterated counterpart ( $\text{d}_{12}$  cyclohexane, 99.5 atom % D, from Sigma Chemicals). Here again, the relaxation times were determined by the  $180^\circ$ - $\tau$ - $90^\circ$  pulse sequence. The  $90^\circ$  pulse width in these cases was 39 microseconds. Pulse repetition time was 10 seconds and the number of pulses in the sequence was ten. A  $\text{C}_6\text{D}_6/\text{TMS}$  capillary was used as an external lock in these experiments.

The  $^{31}\text{P}$ -NMR spectra were also recorded on the Varian XL-100 FT NMR spectrometer operated at 40.5 MHz for  $^{31}\text{P}$  nuclei. 85% phosphoric acid in a capillary tube was used as a reference.

Relaxation time measurements were carried out in the same way as that of  $^1\text{H}$ -NMR in  $\text{CCl}_4$  and cyclohexane systems.

The  $^{13}\text{C}$ -NMR spectra were run on Bruker WH-400 at a carbon frequency of 100.6 MHz at the Department of Chemistry, University of British Columbia, Vancouver, Canada.

### Near Infrared Studies

In the near infrared region, water exhibits relatively strong absorption bands due to the  $\nu_2$  (scissoring) plus  $\nu_3$  (asymmetric stretching) combination mode of vibration (2). In vacuum, this band is observed at 1875 nm, which corresponds to the absorption at 1876 nm theoretically calculated. This value refers to  $\text{H}_2\text{O}$  that is completely free of hydrogen bonding (2). If the water molecule interacts with other polar molecules or ions, the band will shift to the lower energy side, i.e., longer wavelength side. In pure (bulk), normally hydrogen bonded, liquid water this band occurs at 1930 nm (3). In non-polar solvents containing amphiphiles, a part of the cosolubilised water gets located in the bulk organic phase, where the water molecules are mostly freed from hydrogen bonding themselves and others in contact with the head group of the amphiphile. In the near IR region, the former exhibits absorption band around 1900 nm and the latter over a range of 1920 - 2020 nm (3,4). Sano et al. (4) and Sunamoto et al. (5) have utilised these near IR bands as a convenient handle for studying the state of water in

surfactant reverse micelles and other analogous systems.

The near IR spectra of the benzene system are presented in Fig. 3.1 for low amounts of water added.

An important feature of the spectra shown in Fig. 3.1 is that a shoulder is seen around 1890 nm at the very low concentration of water apart from the dominant 1930-1960 nm band. It is observed that this shoulder weakens and vanishes into the trailing portion of the 1930 - 1960 nm band at higher water concentrations. The results of Fig. 3.1 may be interpreted according to the following arguments. The shoulder at 1890-1900 nm is assigned to free or extremely weakly bonded water (3). This assignment suggests that the shoulder at about 1890-1900 nm is not due to the water solubilised in the polar region of lipid, but to the water dispersed in the non-polar organic phase. Further support of this assignment derives from the fact that this shoulder coincides in spectral position with that of water dispersed in pure benzene (4).

The band occurring at wavelengths greater than 1900 nm is thought to be due to bonded water (3). Thus the broad band observed between 1930-1960 nm in Fig. 3.1 is assigned to the water solubilised in the reverse micelles because of the following reasons: a) the band-shape resembles that expected for pure water, and water solubilised in the micelles could of course be supposed to form a 'bulk' water phase, whereas water dispersed in the organic solvent region will be hardly expected to form

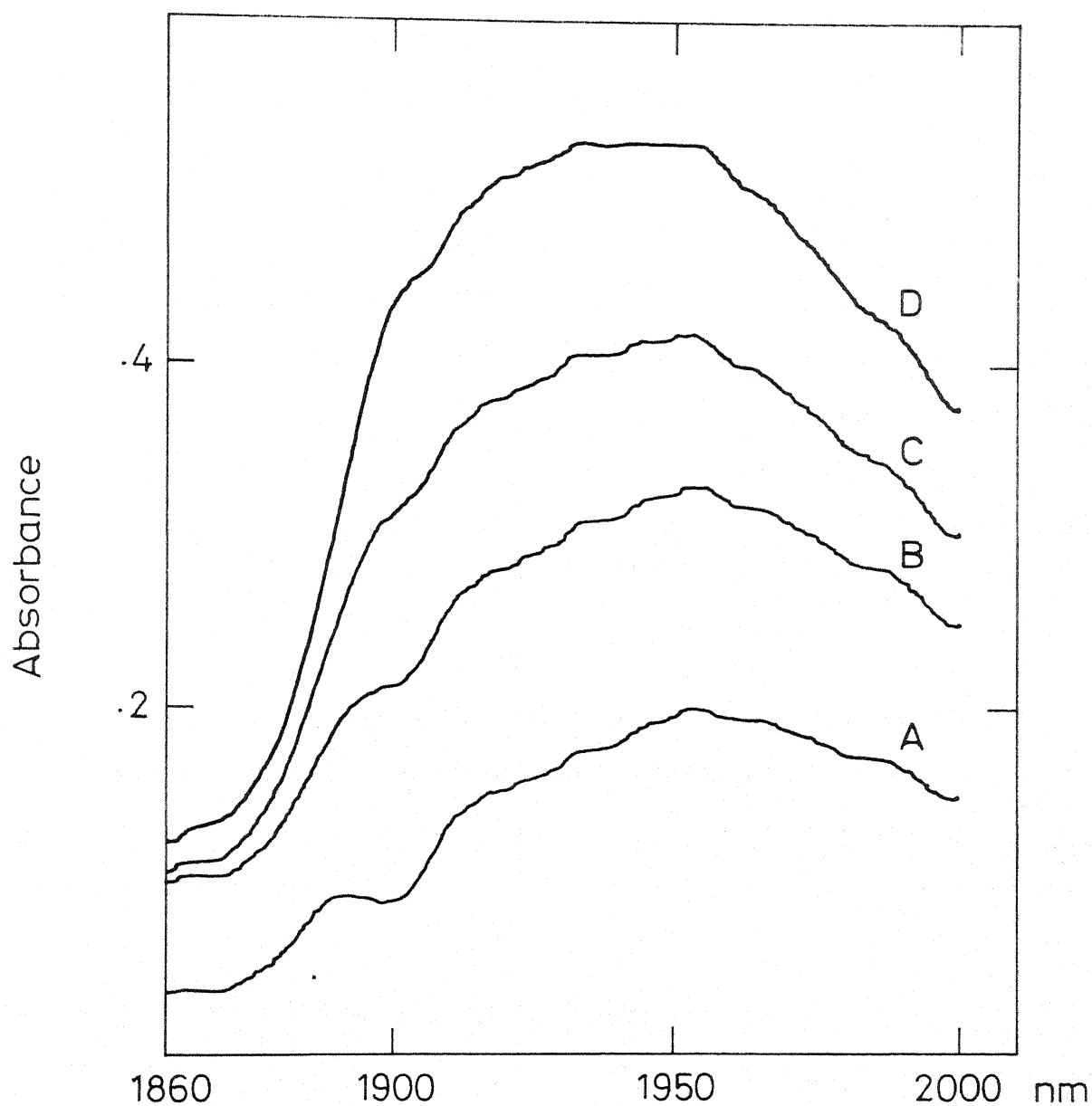


Fig. 3.1 Near IR spectra of Benzene system at different water concentrations.

A----- R= .17, B----- R= .34,

C----- R= .66, D----- R= .99.

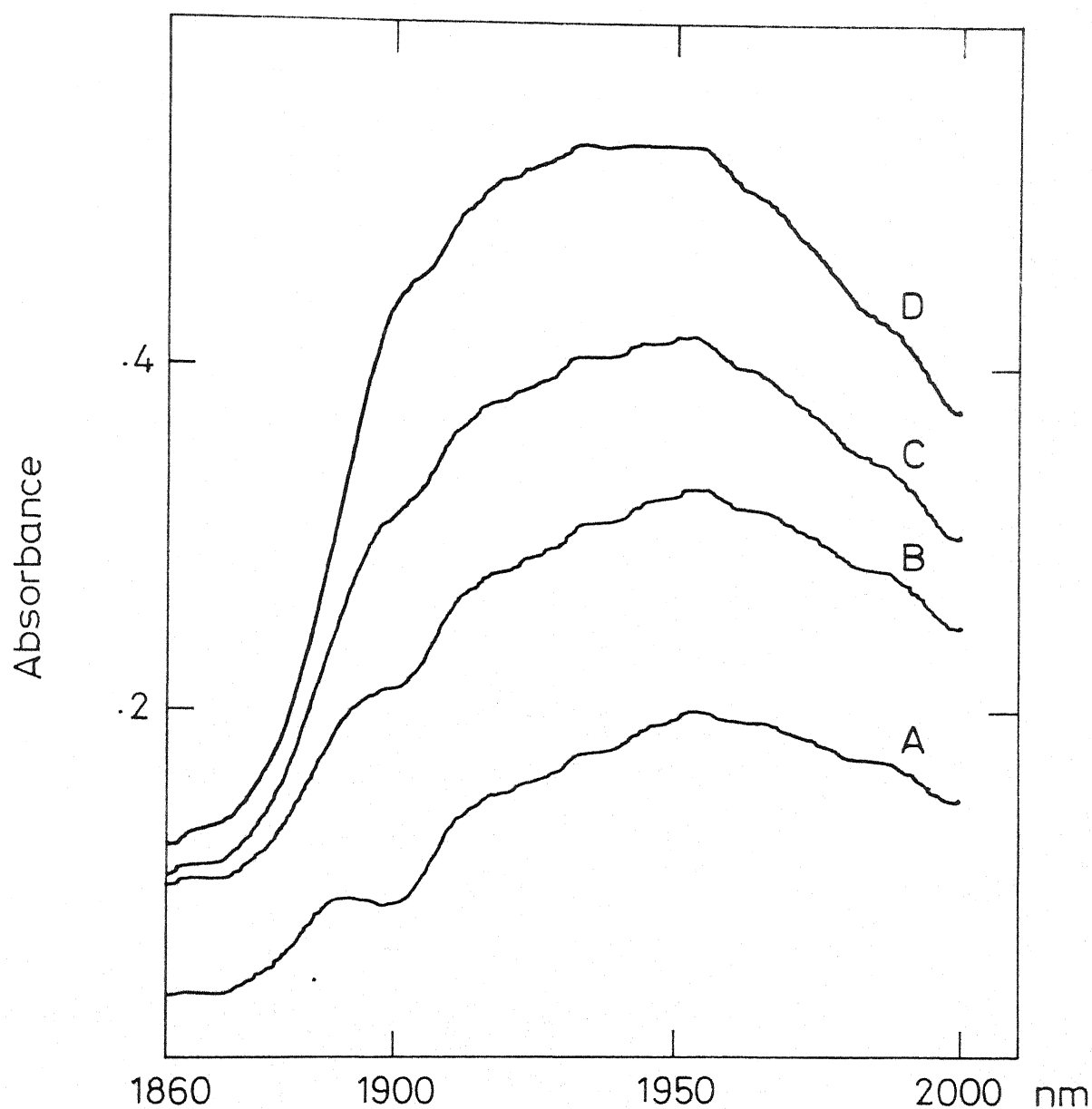


Fig. 3.1 Near IR spectra of Benzene system at different water concentrations.

A----- R= .17, B----- R= .34,

C----- R= .66, D----- R= .99.

such a phase; b) the increase in the amount of water over and beyond the solubility of water in the organic solvent results exclusively in the increase in intensity of this absorption band. Further, the position of this band ( $\lambda_{\text{max}}$ : 1930-1960 nm) is shifted a little to the longer wavelength side as compared with that of the pure specimen ( $\lambda_{\text{max}}$ : 1930 nm). This is explained by postulating that at low water concentrations the interaction between water and the polar head groups of lipid is very strong and consequently the band shifts to longer wavelength side. As more and more water is added, however, the strength of the above interaction decreases causing this band to shift to lower wavelength side.

The above arguments and explanations may be re-cast as follows: Two types of water exist in the lecithin reverse micellar solutions; One is water dispersed in the organic phase which shows a shoulder at about 1890 nm and the other is the water solubilised in the reverse micelles which shows a broad-band at 1930-1960 nm.

The data above are further utilised to make a quantitative estimate of the relative amount of water present in the bulk organic phase and in the reverse micellar interior (as 'pools'). The relative intensities of the 1890 nm shoulder and 1930-1960 nm band, assessed from expanded plots, should correspond to the ratio of water in the water pools to water in the solvent phase. From this it is estimated that not more than 0.05% v/v of water

enters the bulk solvent phase at any water concentration in these systems. This means that at water concentrations  $R \geq 1$  the fraction of water that is distributed in the bulk phase (organic) can be neglected and all the water treated as being present in the water pools. These low values for the concentration of water in the bulk phase are similar to those obtained for dodecylammonium propionate reverse micelles in benzene (4) and much lower than the 2.8% v/v obtained for potassium oleate-hexanol-hexadecane system (6). The above arguments are for benzene system and qualitatively hold good for carbontetrachloride and cyclohexane systems also.

### Polarity Probe Studies

The nitrate ion has an  $n-\pi^*$  band around 300 nm which is quite sensitive to the polarity of the solvent used (7). The position of this peak together with dielectric constant of the solvents which reflect their polarity, taken from the literature (7), are recorded in Table 3.1.

The general blue shift of the  $n-\pi^*$  band of nitrate ion with increase in polarity of the solvent is evident from Table 3.1. The solvent sensitivity of this band seems to arise from the differences in the H-bonding ability of the ground and excited states of the nitrate oxygen electrons. The solvent shift is therefore, a measure of the hydrogen bonding ability of the solvent. Keeping these facts in mind, we have utilised the  $n-\pi^*$  band of the nitrate ion as a probe of the polarity of water.

Table 3.1Nitrate ion  $n-\pi^*$   $\lambda_{\max}$  in different solvents

Solvent	Nitrate $n-\pi^*$ ( $\lambda_{\max}$ nm)	Dielectric Constant
H <sub>2</sub> O	301.5	80
HO(CH <sub>2</sub> ) <sub>2</sub> OH	302.5	39
CH <sub>3</sub> OH	303.0	33
C <sub>2</sub> H <sub>5</sub> OH	303.4	25
(CH <sub>3</sub> ) <sub>2</sub> CHOH	305.2	19
(CH <sub>3</sub> ) <sub>3</sub> COH	306.6	13
CHCl <sub>3</sub>	308.7	4.8

pools formed in the three solvent systems that we have studied. It has generally been observed that the polarity of the water pool is very low at low water concentrations and increases to higher values at higher concentrations of water in reverse micellar systems (8).

Fig. 3.2 shows the variation in  $\lambda_{\max}$  of the  $n-\pi^*$  band of the nitrate ion in carbontetrachloride system as a function of R. At low R values the  $n-\pi^*$  band appears around 309 nm indicating a lower strength of interaction between the pool water and nitrate ion. At higher R values, the strength of the nitrate ion-water pool interaction increases, blue shifting the band to its normal value of around 301.5 nm as seen in bulk water.



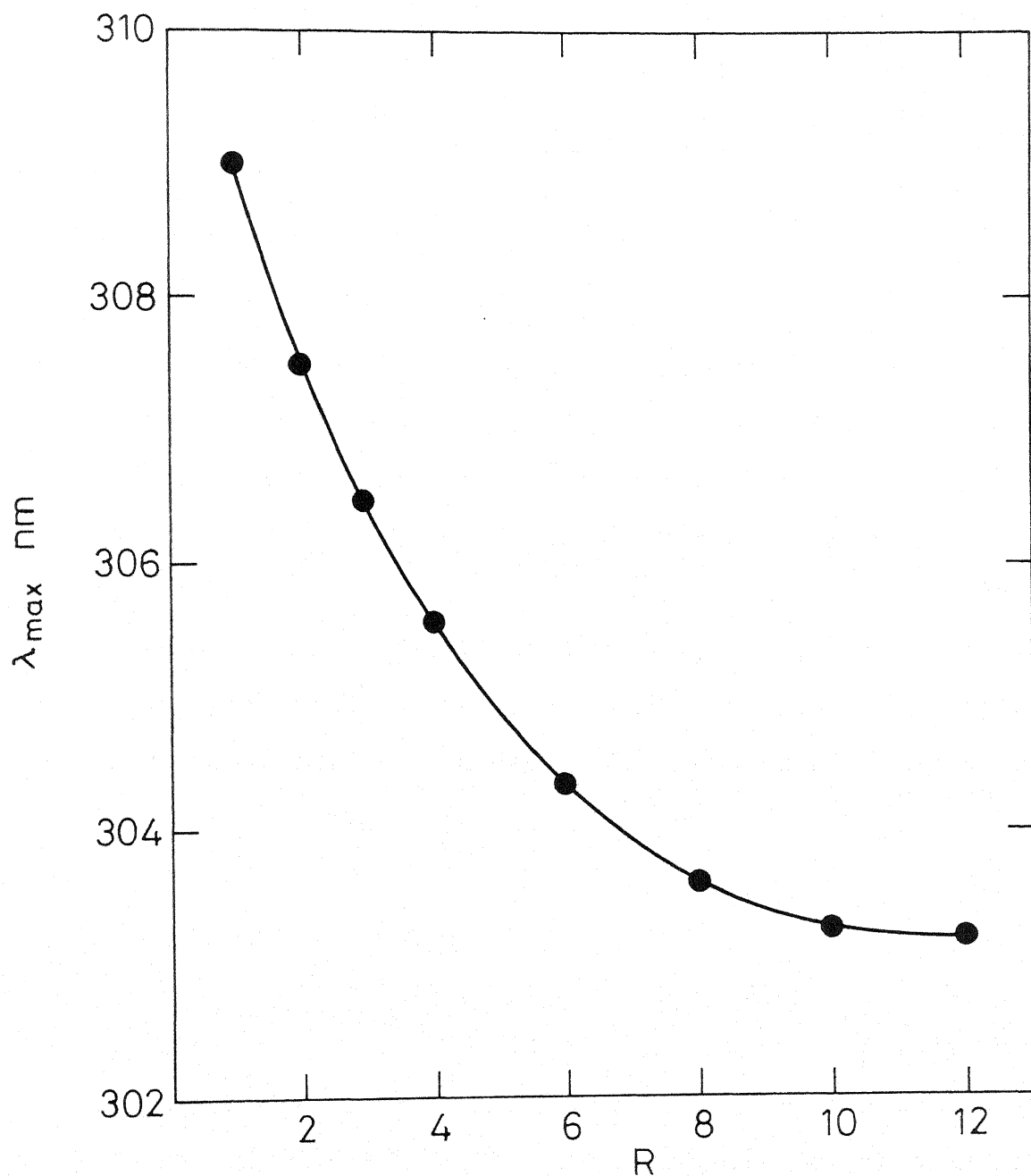


Fig 3.2 Variation of  $\lambda_{\max}$  of  $n \rightarrow \pi^*$  band of  $\text{NO}_3^-$  in Carbontetrachloride system as a function of added water.

It is clear that the weakened solvent-ion interaction is indicative of a lower effective polarity of the water pool, in comparison with bulk water, since at all times the  $(\text{H}_2\text{O}):(\text{NO}_3^-)$  ratio is at least 50 to 1. Qualitatively a similar behaviour is observed for benzene and cyclohexane systems also.

In similar studies, other solvent sensitive polarity probes have also been utilised. Menger et al. (9) used pyridine 1-oxide, and Fendler and coworkers (10-12) utilised 1-ethyl-4-carbomethoxy-pyridinium iodide, vitamin B<sub>12</sub> and hemin. These organic probes may not 'report' the unperturbed solvent polarity of the entire water pool, since these probes are large and are likely to be oriented at the interface. On the other hand, a small ionic inorganic probe such as the one used in our system is expected to dissolve completely in the water pool and report the average polarity of the entire pool.

### Fluorescence Probe Studies

Since fluorescence emission spectra are very sensitive to the polarity and polarisability of solvent molecules around the chromophore, the fluorescence emission spectra could be used in favourable circumstances to measure the polarity of the binding site (13). 8-Anilinonaphthalene sulfonic acid (ANSA) is one of the extensively used fluorescence probes. The emission maxima of ANSA and the quantum yield or efficiency  $\Phi$  are found to be very well related with the Kosower solvent polarity index,  $Z$  (14,15). The more polar the solvent, the more red shifted

(shift to longer wavelengths) the fluorescence emission maxima of ANSA and the lower the fluorescence quantum yield.

Viscosity, specifically microviscosity, plays an important role in the quantum yield and  $\lambda_{\max}$  of the emission spectrum (16). If the microviscosity of the monitored environment increases, it effectively freezes the solvent dipole and prevents the solvent dipole from reorienting itself about the excited state of ANSA molecules. This results in an increased overlap between absorption and emission with a concomitant increase in fluorescence quantum yield and a blue shift of the emission spectrum. Fluorescence quantum yields have been utilised in the past to measure the microviscosity of the binding site (17).

Figures 3.3. and 3.4 show the fluorescence emission spectra of ANSA at various R values in benzene and cyclohexane systems, respectively.

Fig. 3.5 shows the variation in the fluorescence emission maxima of ANSA-dissolved benzene and cyclohexane systems as a function of added water, R.

It can be seen from Fig. 3.5 that in the benzene system, the emission maxima,  $\lambda_{\max}$ , is red-shifted upon addition of water. This shift of  $\lambda_{\max}$  upon addition of water suggests that polarity of the water pools in which the ANSA molecules are localised increases with increasing concentration of water. The large  $\lambda_{\max}$  red shifts suggest that at low water concentrations, the polarity of the water pool as a whole is significantly less than

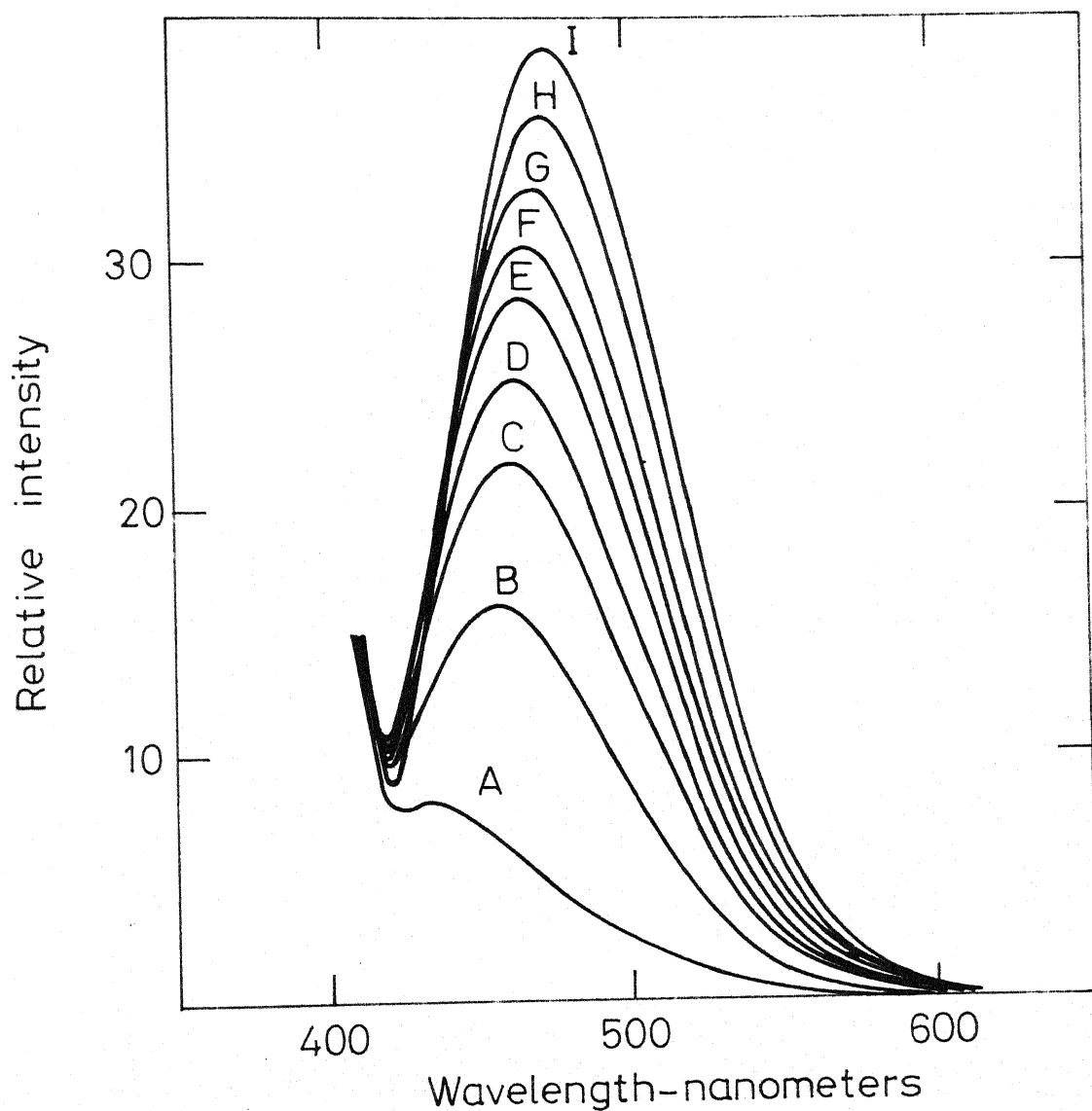


Fig.3.3 Fluorescence emission spectra of Benzene system at various concentrations of added water. A----R=0, B----R=1, C----R=2, D----R=3, E----R=4, F----R=5, G----R=6, H----R=8, I ----R=10.

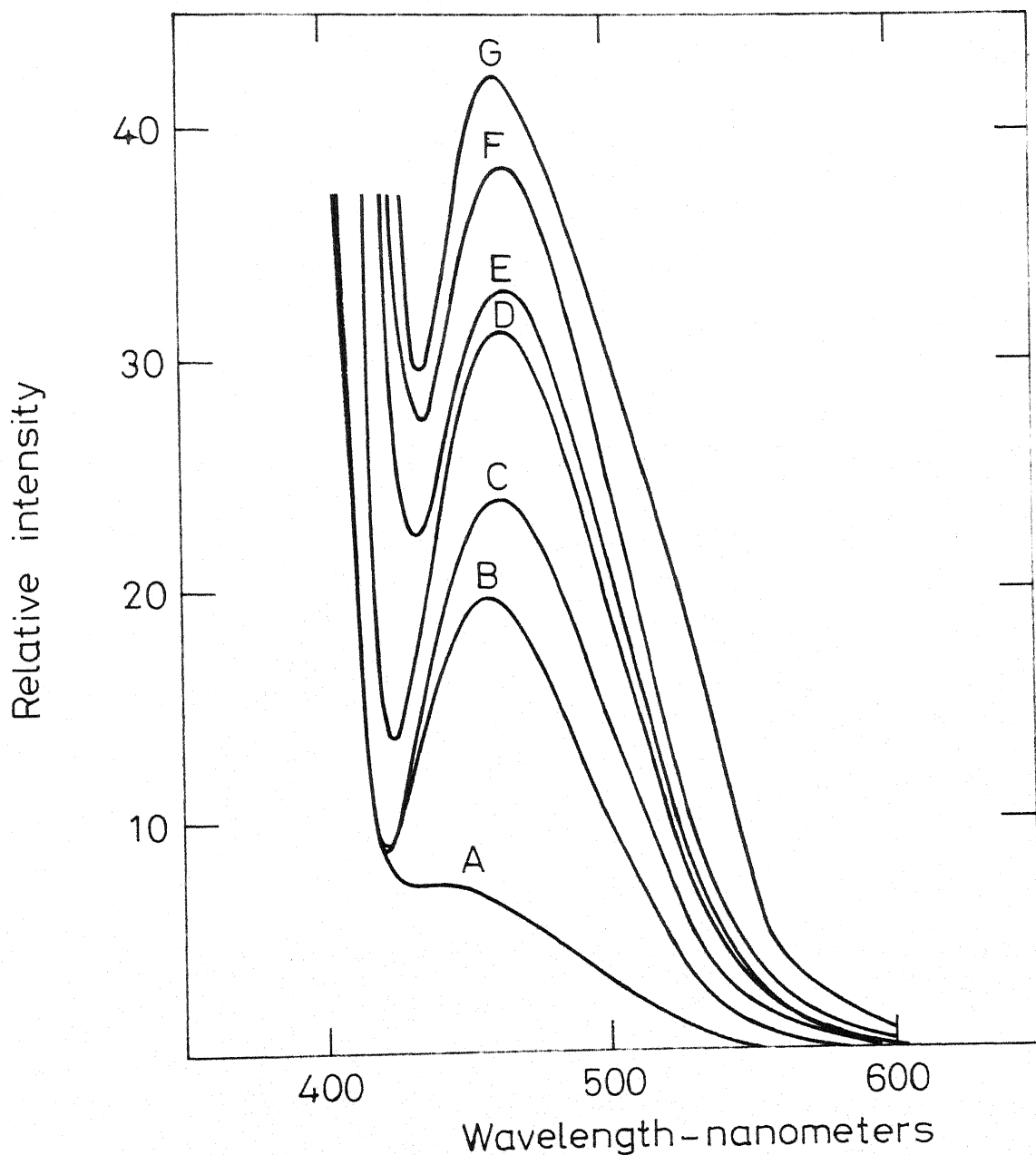


Fig. 3.4 Fluorescence emission spectra of Cyclohexane system at various concentrations of added water. A ---- R=0, B ---- R=1, C ---- R=2  
D ---- R=3, E ---- R=4, F ---- R=5, G ---- R=6

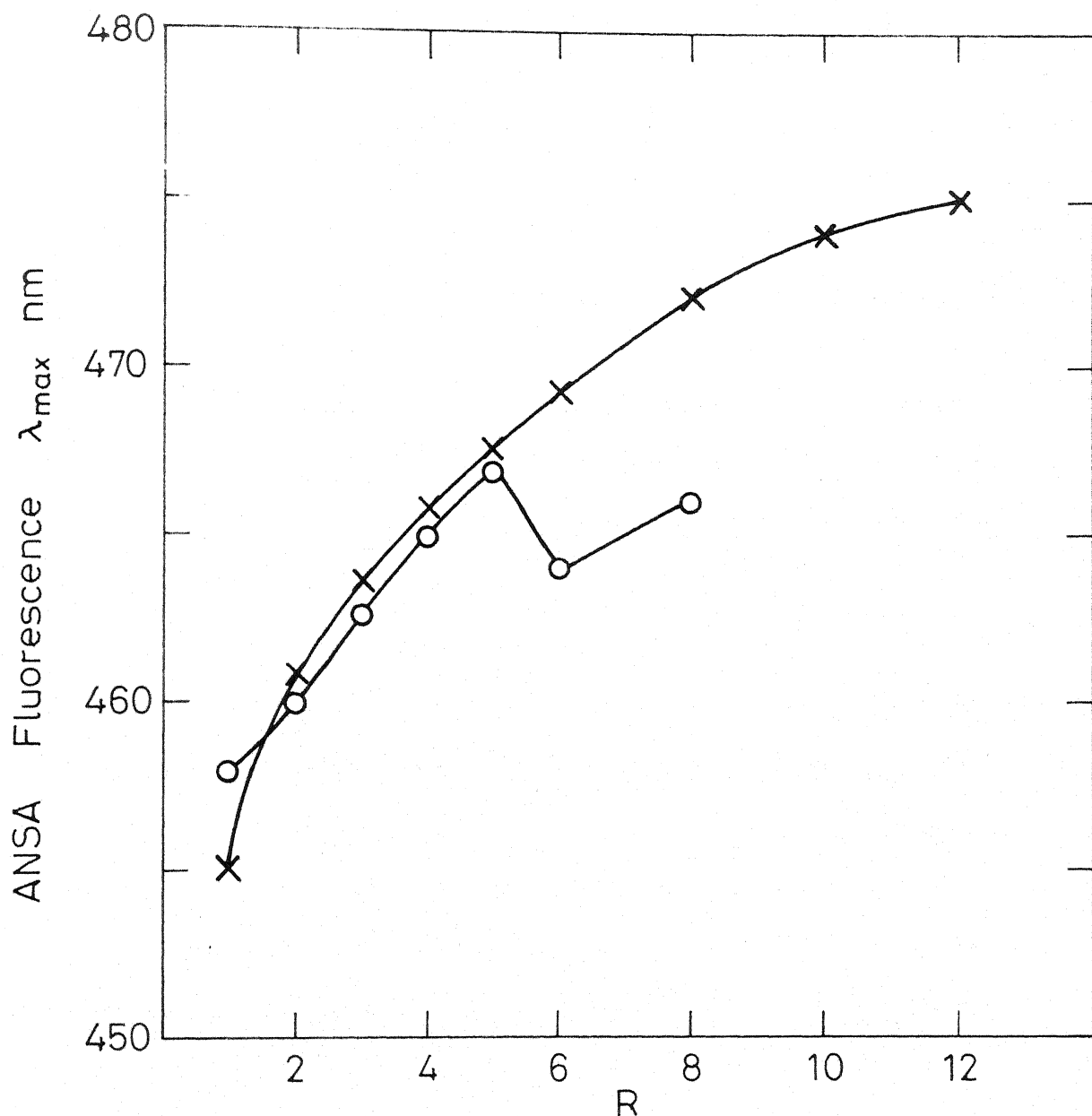


Fig 3.5 Variation of Fluorescence emission maximum of ANSA in Benzene and Cyclohexane systems as a function of added water.  
x ---- Benzene points, o ---- Cyclohexane points

that of bulk water. This result further supports our polarity probe studies presented in the previous section.

It can also be observed from Fig. 3.5 that in cyclohexane system, however,  $\lambda_{\max}$  shows a blue shift around an R value of 6. This blue shift indicates that the effective polarity of the water pool decreases around an R value of 6. It is difficult to visualise any mechanism by which the water pool becomes less polar with increasing water concentration in this region. However, this can be attributed to the formation of a liquid crystalline phase with an increase in microscopic as well as macroscopic viscosity in this region.

We have calculated the fluorescence quantum yield of ANSA in benzene and cyclohexane systems as a function of added water by standard methods (1). The results of the quantum yield as a function of R are presented in Fig. 3.6.

It can be seen from Fig. 3.6 that in the case of benzene system, the quantum yield continuously decreases with increasing R values. From this it is clear that the polarity of the water pool monitored by ANSA increases with increasing water concentration.

From Fig. 3.6 it may also be noted that in the case of cyclohexane system the quantum yield of the fluorescence probe decreases upto an R value of 6. At higher R values, the quantum yield shows an increase. This may be due to the formation of liquid crystalline phase with an increase in microviscosity

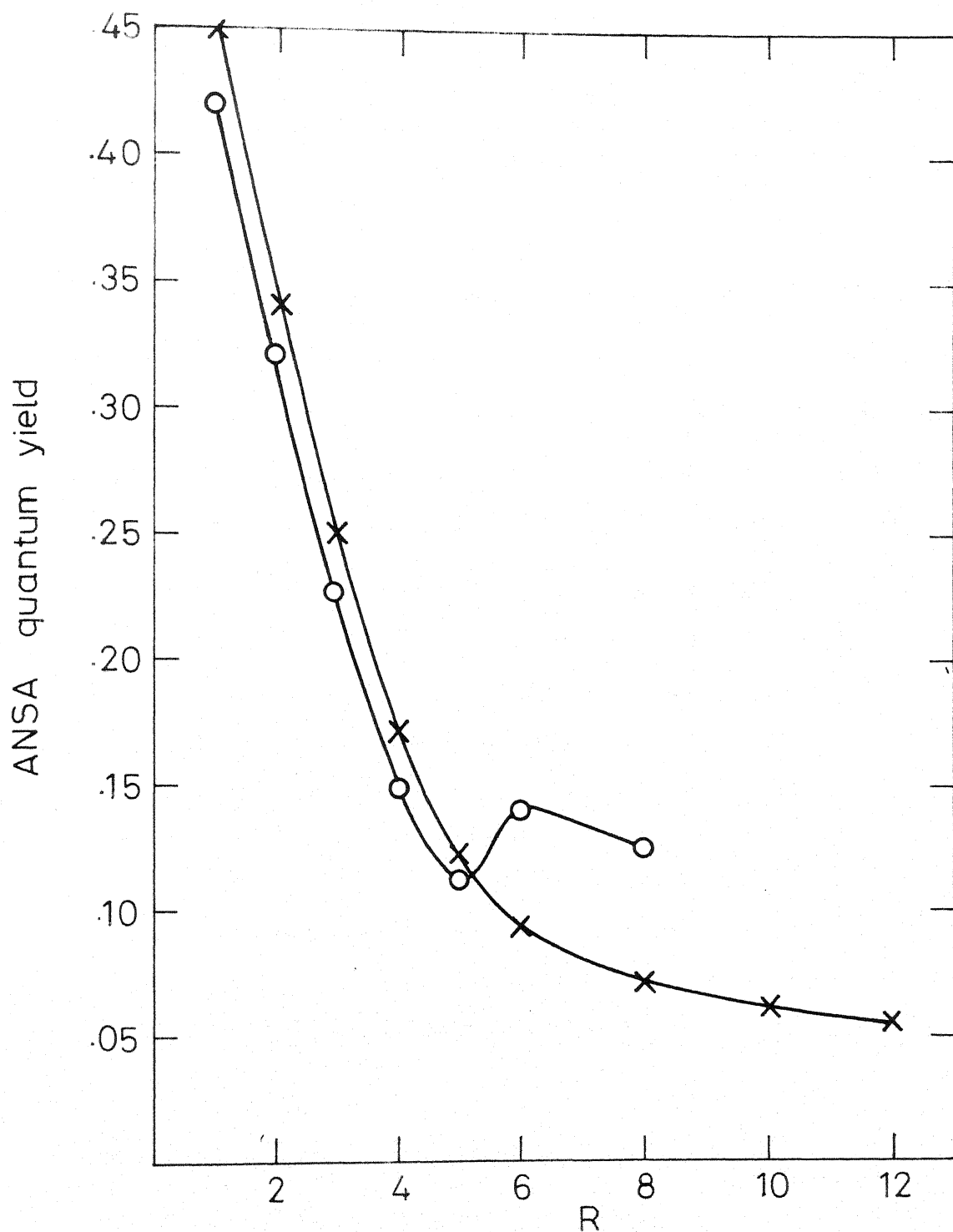


Fig 3.6 Variation of quantum yield of ANSA in Benzene and Cyclohexane systems as a function of added water. X-----Benzene points, O-----Cyclohexane points



and also macroviscosity. This increased microviscosity would indeed effectively 'freeze out' the solvent dipoles and thereby prevent their orientation about the excited state of ANSA molecules (16).

The behaviour of  $\text{CCl}_4$  system is qualitatively similar to that of benzene system.

In order to develop an understanding of the molecular organisation of the lecithin and water molecules in our three systems, we have carried out  $^1\text{H}$ -NMR,  $^{31}\text{P}$ -NMR and  $^{13}\text{C}$ -NMR studies.

In Figs. 3.7 to 3.16 we present a number of  $^1\text{H}$ -NMR spectra recorded at 100 MHz for the three systems at various R values. In Table 3.2 we present the details of these spectra, i.e., about the system and amount of water added.

Table 3.2

Details of the proton NMR spectra presented in Figs. 3.7 - 3.16

FIG. NO.	SYSTEM	R
3.7	PC- $\text{CCl}_4$ - $\text{H}_2\text{O}$	0.0
3.8	"	4.2
3.9	"	8.3
3.10	"	12.0
3.11	PC- $\text{C}_6\text{H}_6$ - $\text{H}_2\text{O}$	0.0
3.12	"	2.2
3.13	"	6.5
3.14	"	10.0
3.15	PC-Cyclohexane- $\text{H}_2\text{O}$	0.0
3.16	"	4.0

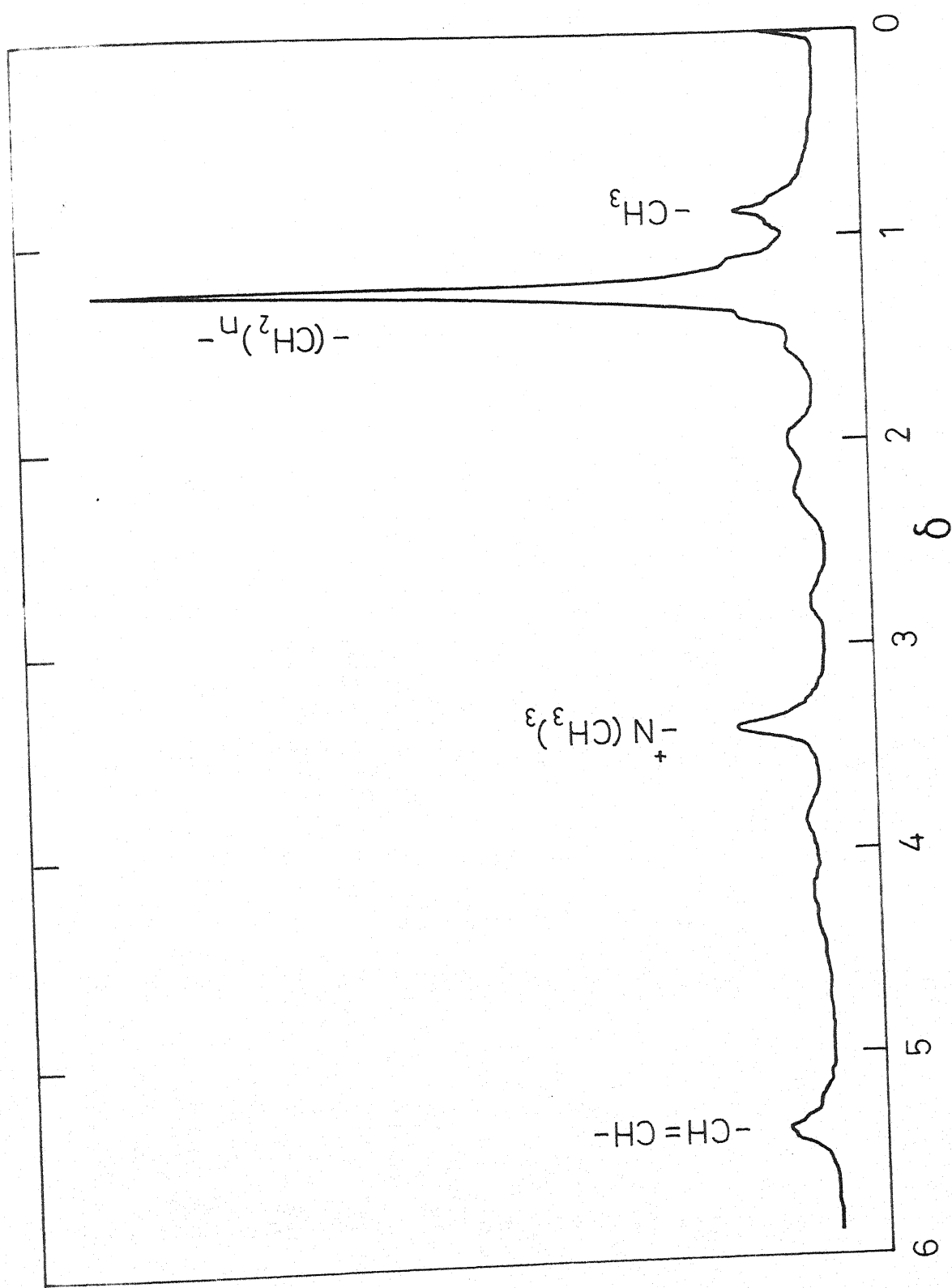


Fig 3.7 100MHz Proton NMR spectrum in the Carbontetrachloride system at an R value of 0.0

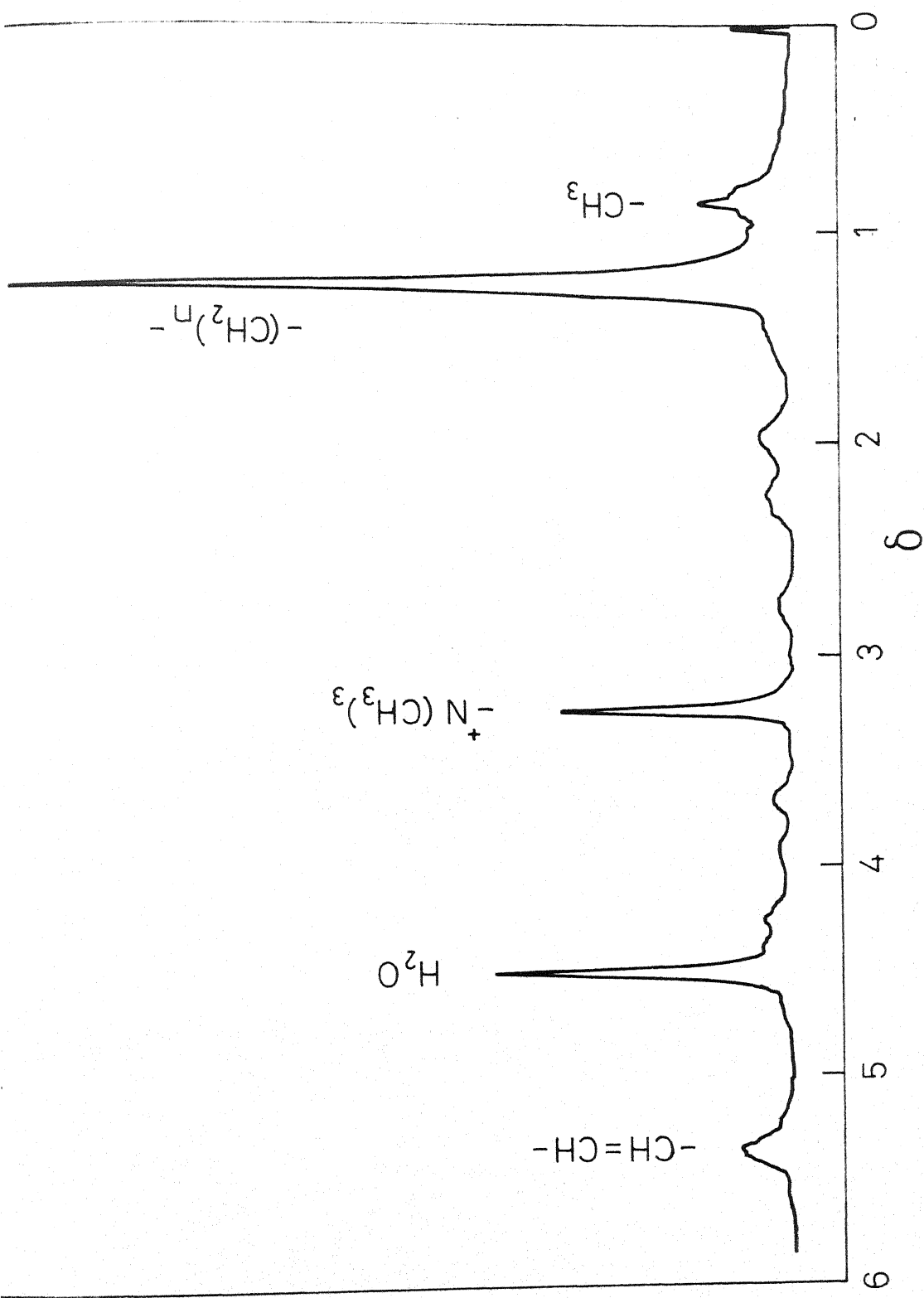
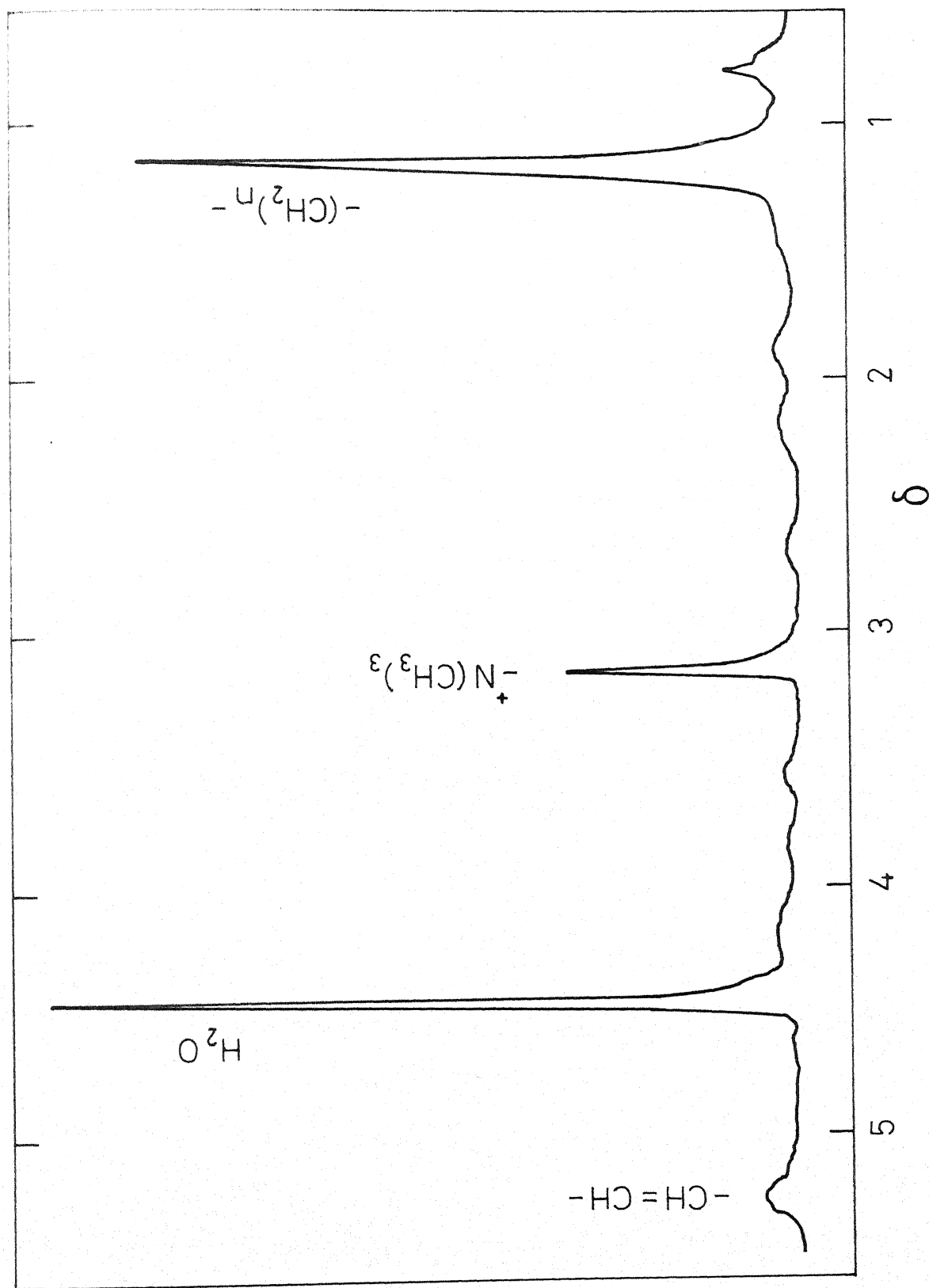


Fig 3.8 100MHz Proton NMR spectrum in the Carbontetrachloride system at an  $R$  value of 4.2



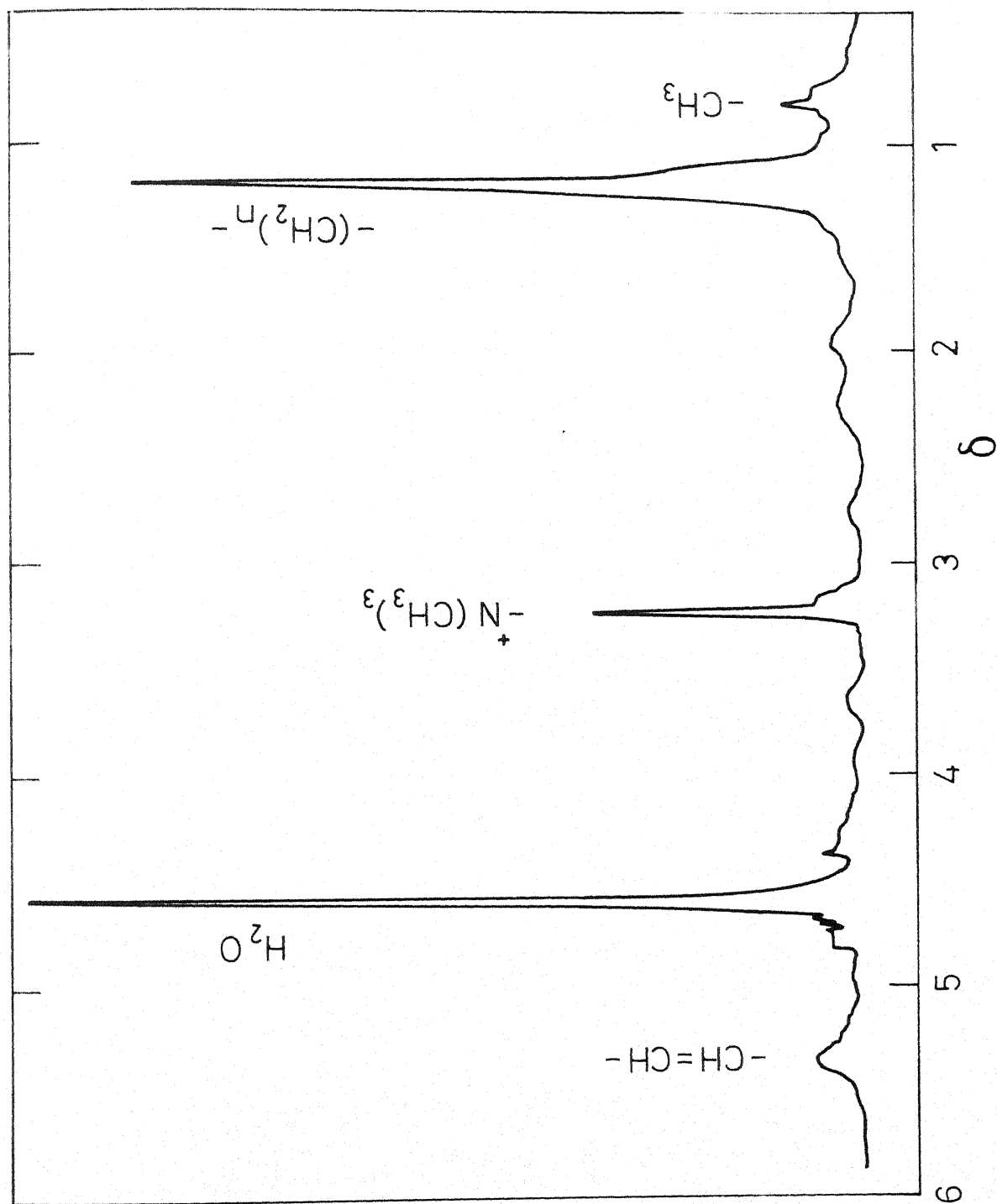


Fig.3.10 100MHz Proton NMR spectrum in the Carbondetrachloride system at an R value of 12.0

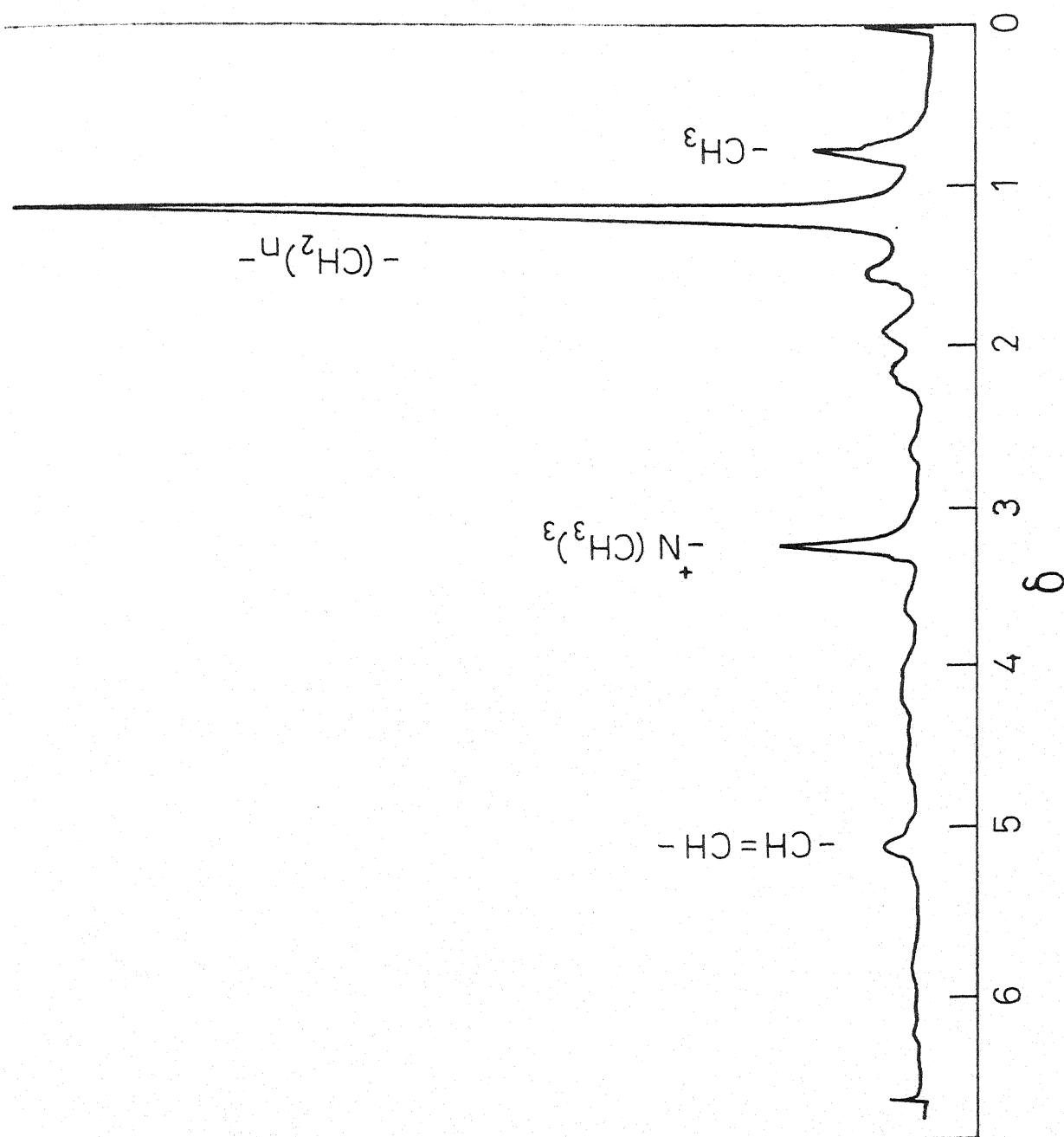


Fig 3.11 100MHz Proton NMR spectrum in the Benzene system at an R value of 0.0

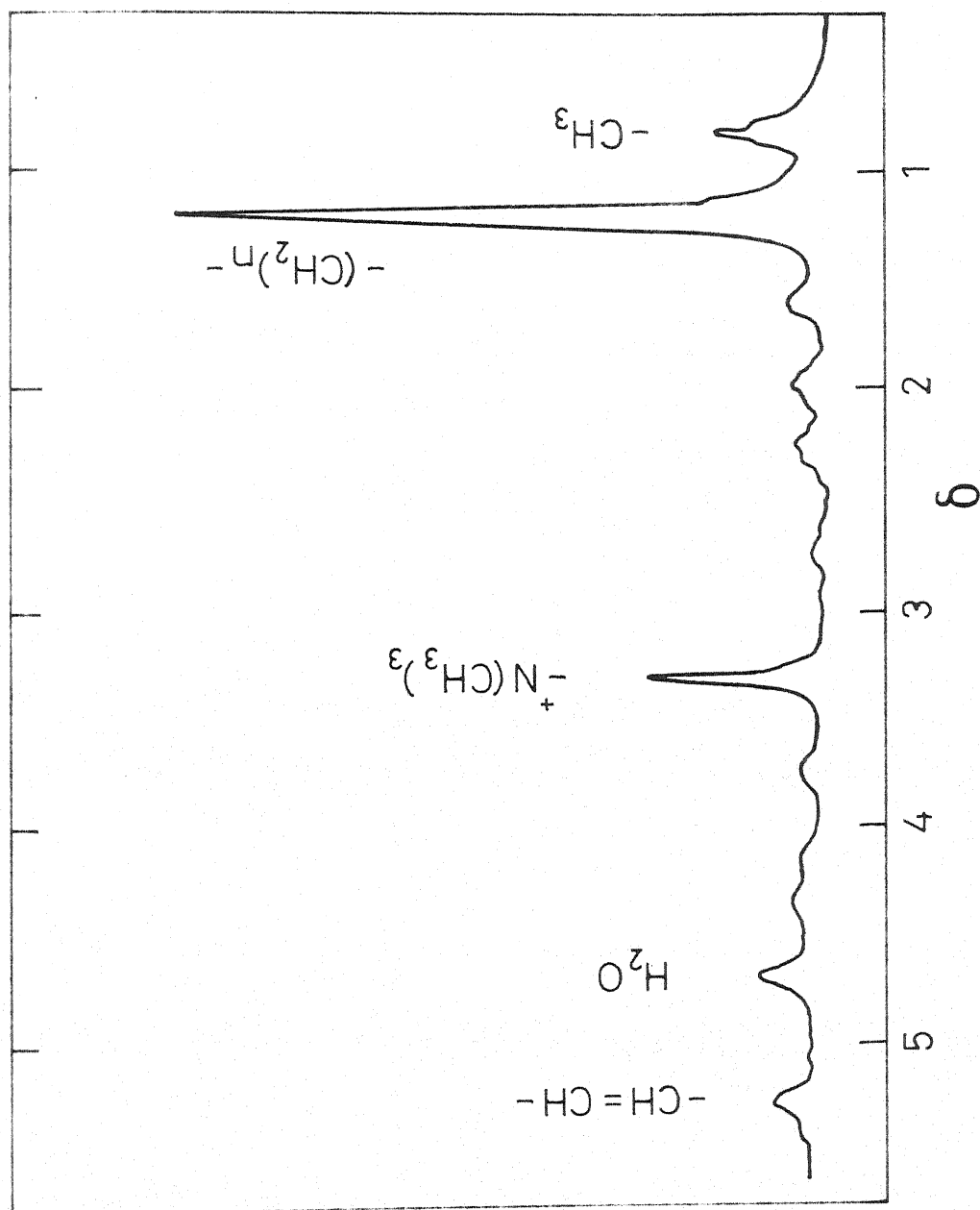


Fig. 3.12 100MHz Proton NMR spectrum in the Benzene system at an R value of 2.2

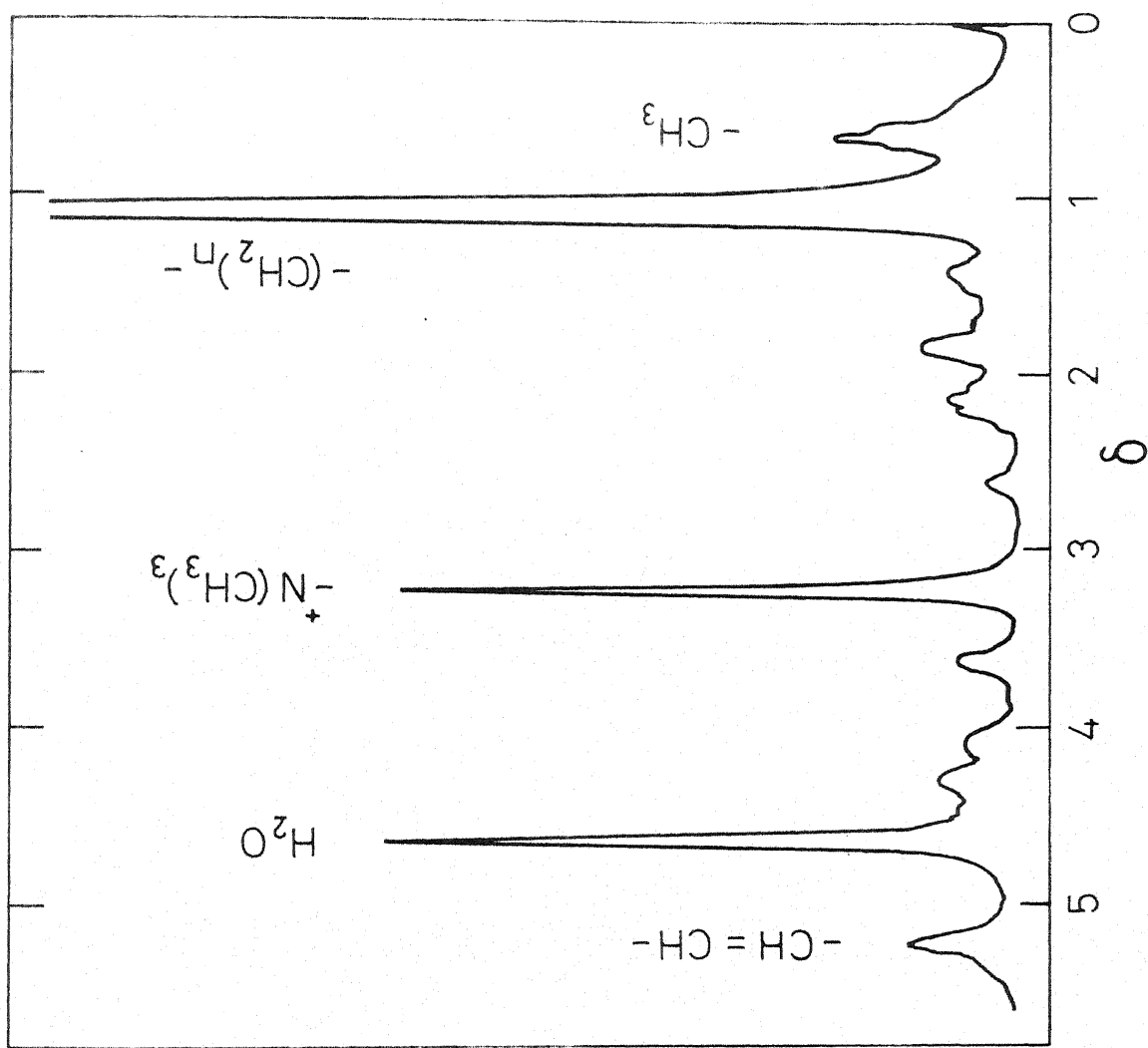
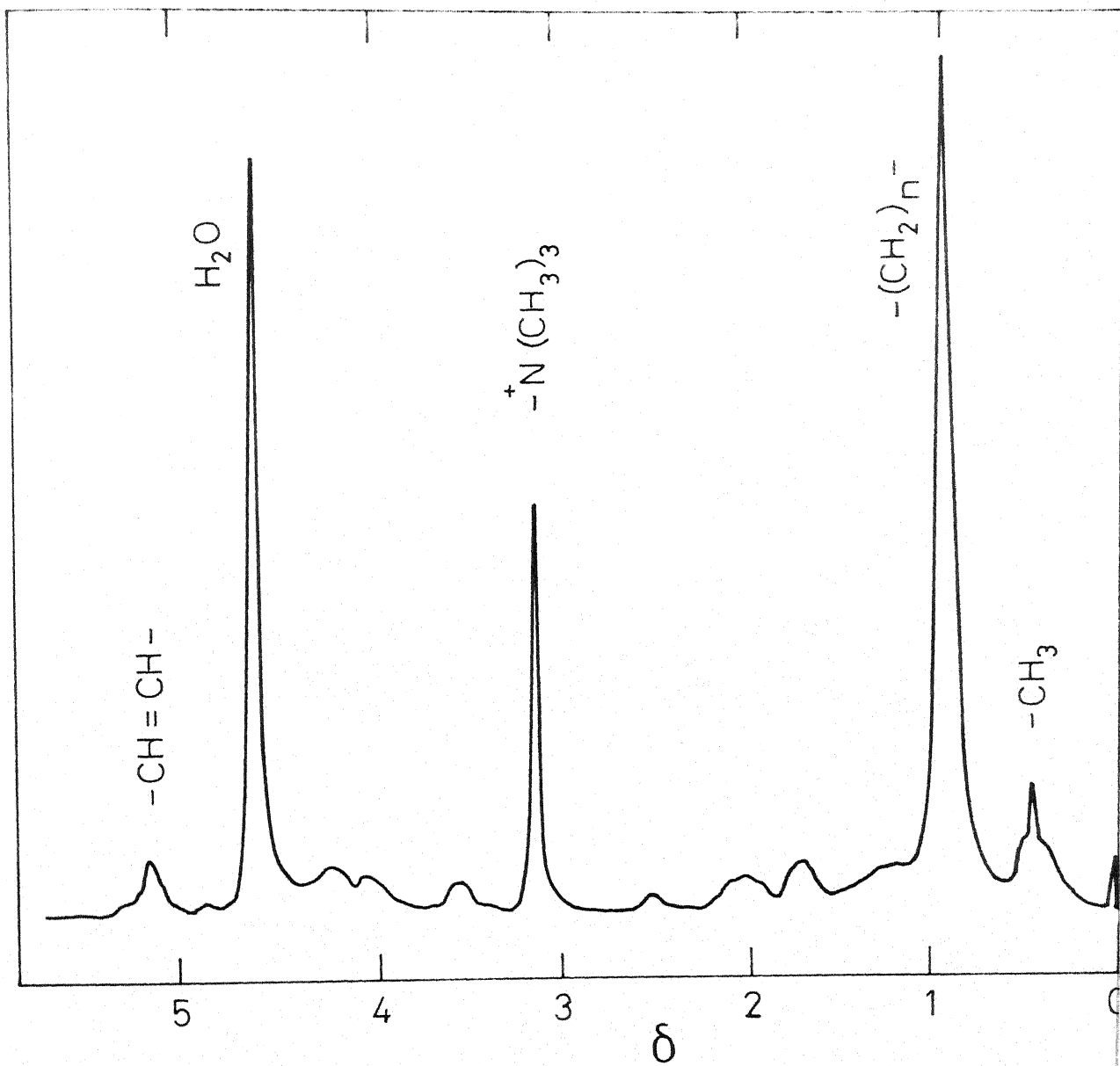


Fig. 3.13 100MHz Proton NMR spectrum in the Benzene system at an R value of 6.5





3.14 100MHz Proton NMR spectrum in the Benzene sys  
at an R value of 10.0

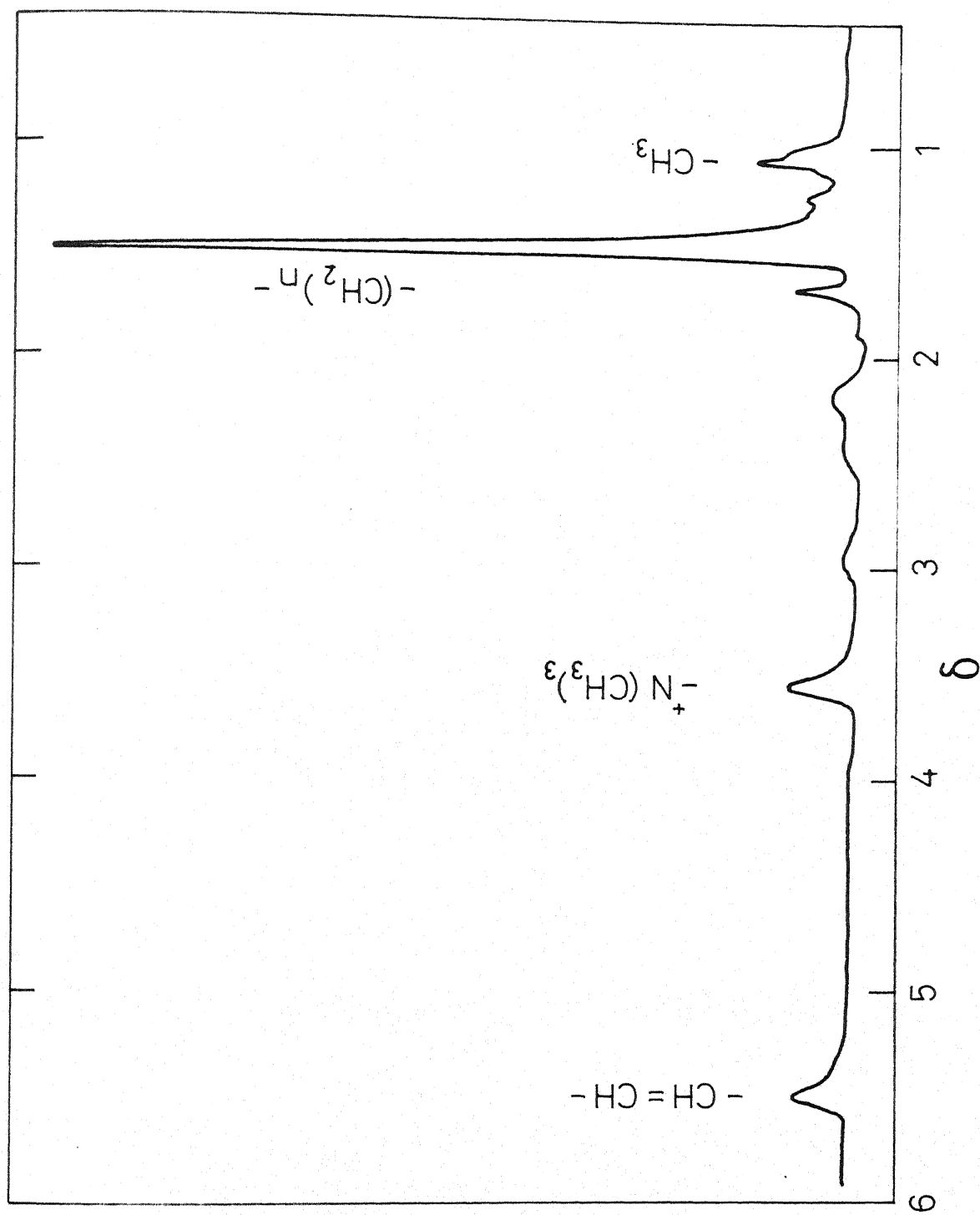


Fig. 3.15 100MHz Proton NMR spectrum in the Cyclohexane system at an R value of 0.0

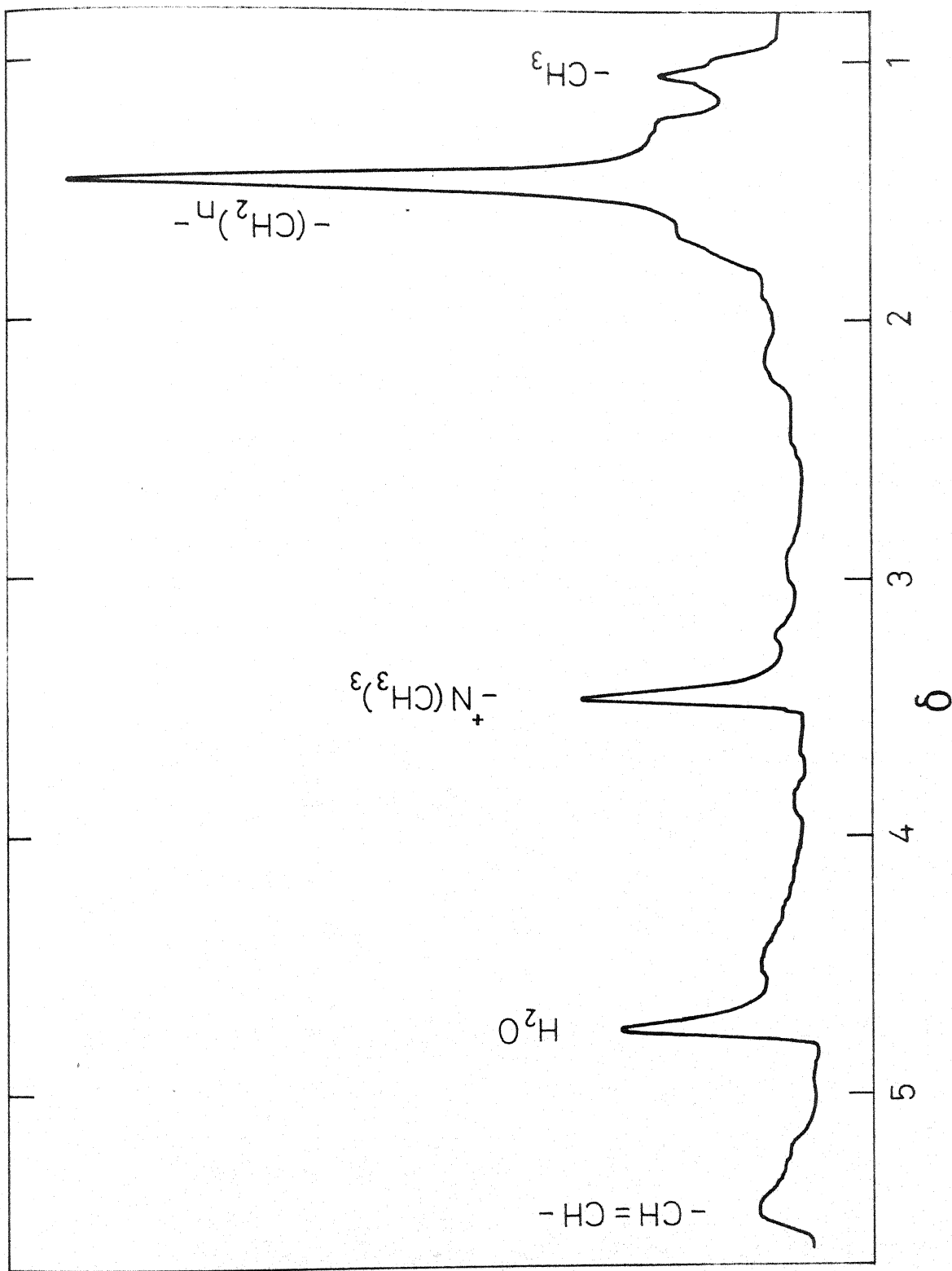


Fig 3.16 100MHz Proton NMR spectrum in the Cyclohexane system at an R value of 4.0

### Chemical Shift Studies

Figs. 3.17 and 3.18 show the variation in the  $^1\text{H}$ -NMR chemical shift of the water-OH protons and of the lecithin  $^+\text{N}(\text{CH}_3)_3$  protons respectively in benzene, carbontetrachloride and cyclohexane systems as functions of added water (R).

From Fig. 3.17 it is clear that at low water content, the water proton resonance is upfield compared to that for normal bulk water ( $\delta \sim 5$ ), which suggests minimal amount of hydrogen bonding. As the water concentration increases, there is an upfield shift of the -OH proton resonance followed by a downfield shift i.e., towards the normal bulk water value of around  $\delta 5.0$ .

From Fig. 3.18 it can be seen that the  $^+\text{N}(\text{CH}_3)_3$  proton resonance moves continuously upfield in all the three systems as a function of R.

The above trends in the -OH proton resonance arise because the chemical shifts of the -OH protons are strongly influenced by the following two factors: (a) changes in the hydrogen bonding state of the water molecule and (b) changes in the chemical environment of the water molecule, i.e., the ratio of water bound to the lecithin head group to the free, bulk water in the water pools.

The trend of the -OH proton chemical shifts reported by us at 100 MHz is in the same direction as that reported at 250 MHz by Shaw et al. (18) and at 100 MHz by Klose and Stelzner (19). Wells (20) also reported a similar trend in chemical shifts of

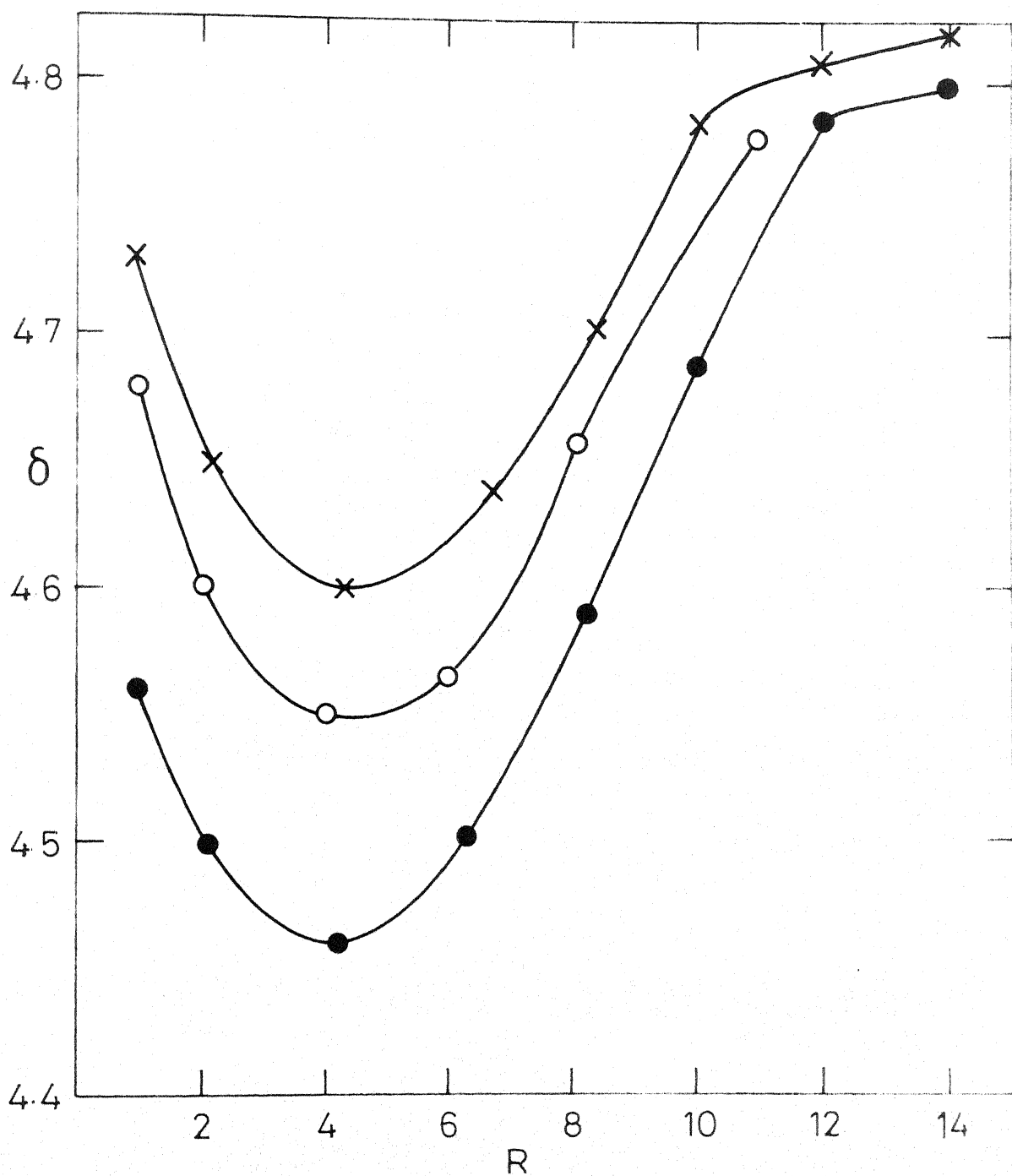


Fig. 3.17 Variation in NMR Chemical shift of water Protons in the three systems as a function of added water. X ---- Benzene points, • ---- Carbon tetrachloride points, O ---- Cyclohexane points.

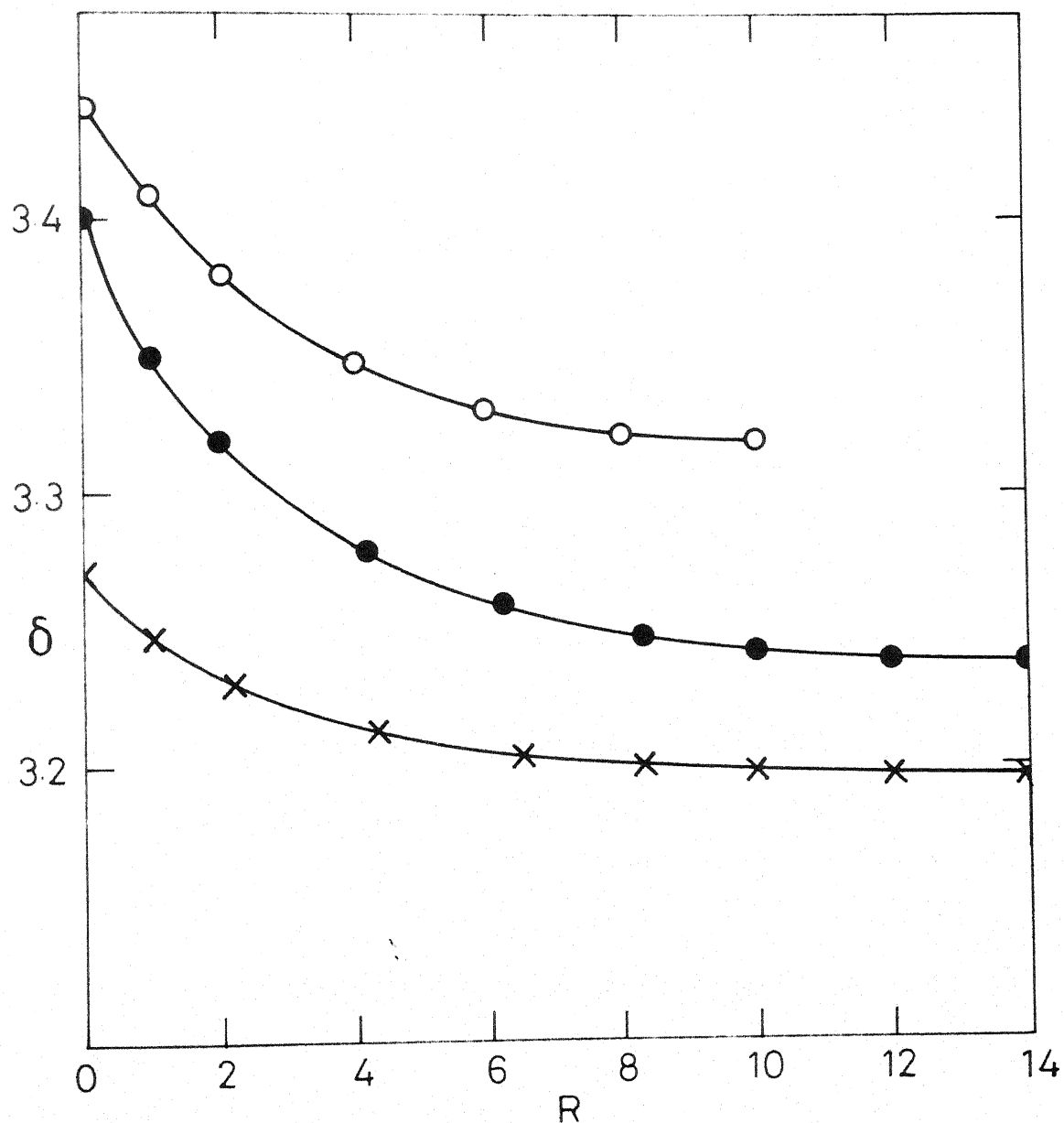


Fig. 3.18 Variation in NMR Chemical shift of  $^+\text{N}(\text{CH}_3)_3$  Protons in the three systems as a function of added water. X ---- Benzene points, ● ---- Carbon tetrachloride points, O ---- Cyclohexane points.

-OH protons in his  $^1\text{H}$ -NMR studies of the hydration of PC reverse micelles in diethyl ether. In the study of Shaw et al. (18), where the interaction of water with PC in carbontetrachloride has been examined, an upfield shift upto R values  $\approx 6$  and a downfield shift at a much higher value ( $R = 10$ ) have been observed for the water protons. In the region between  $R = 6$  to  $R = 10$  experimental observations do not appear to have been made in this study. The later work of Klose and Stelzner (19) on the chemical shift of water protons in lecithin in benzene as a function of added water once again indicates an upfield shift of -OH protons upto an R value of 4 followed by a subsequent downfield shift. Fung and McAdams (21), however, comment that the trends in the -OH proton chemical shifts in the above two studies (18,19) are opposite in direction although such is not the case. Both Shaw et al. (18) and Klose and Stelzner (19) used the  $\delta$  scale for reporting their chemical shift values of -OH protons. In both the studies, the  $\delta$  value decreases at first, i.e., -OH resonance shifts upfield, followed by a reversed trend at higher R values. Of the three investigations quoted above (18,19,21), that of Shaw et al. (18) perhaps gives the best clue as to the 'water-head group' interaction in lecithin reverse micelles. In the following, we attempt a more systematic and rational approach towards unravelling the interaction of water with polar head based on our own  $^1\text{H}$  chemical shift data at 100 MHz as well as  $^{31}\text{P}$ -NMR chemical shift data at 40 MHz.

Our discussion proceeds considering a plausible arrangement of the head group in the reverse micelle. This arrangement derives support from a couple of earlier studies, namely, those of Henderson et al. (22) on the  $^{31}\text{P}$  NMR studies of phospholipids in dry organic solvents and of Pullman and Berthod (23) on the quantum mechanical studies of energetically preferred conformations of the polar heads of the phospholipids. Both the above studies (22,23) have favoured the fact that the polar heads of the phospholipids are likely to adopt highly folded structures. Fig. 3.19 gives the structure of such folded polar head group of lecithin.

In the context of a water molecule (or molecules) getting 'bound' to the head group of lecithin, the electrostatic interaction model with positively charged terminal trimethyl-amino group ( $^+\text{N}(\text{CH}_3)_3$ ) and negatively charged phosphate oxygens suggested by the above studies (22,23) becomes useful.

When increasing amounts of water are added, the most probable effect will be disruption, at least in part, of the folded arrangement of the head group and the production of a more 'swollen' or extended conformations. Indeed, such a phenomenon is envisaged by Pullman and Berthod (24) in connection with the theoretical model of the zwitterionic gamma-aminobutyric acid (GABA).

When water is added, it reduces the electrostatic interaction between the positively charged trimethyl-amino group



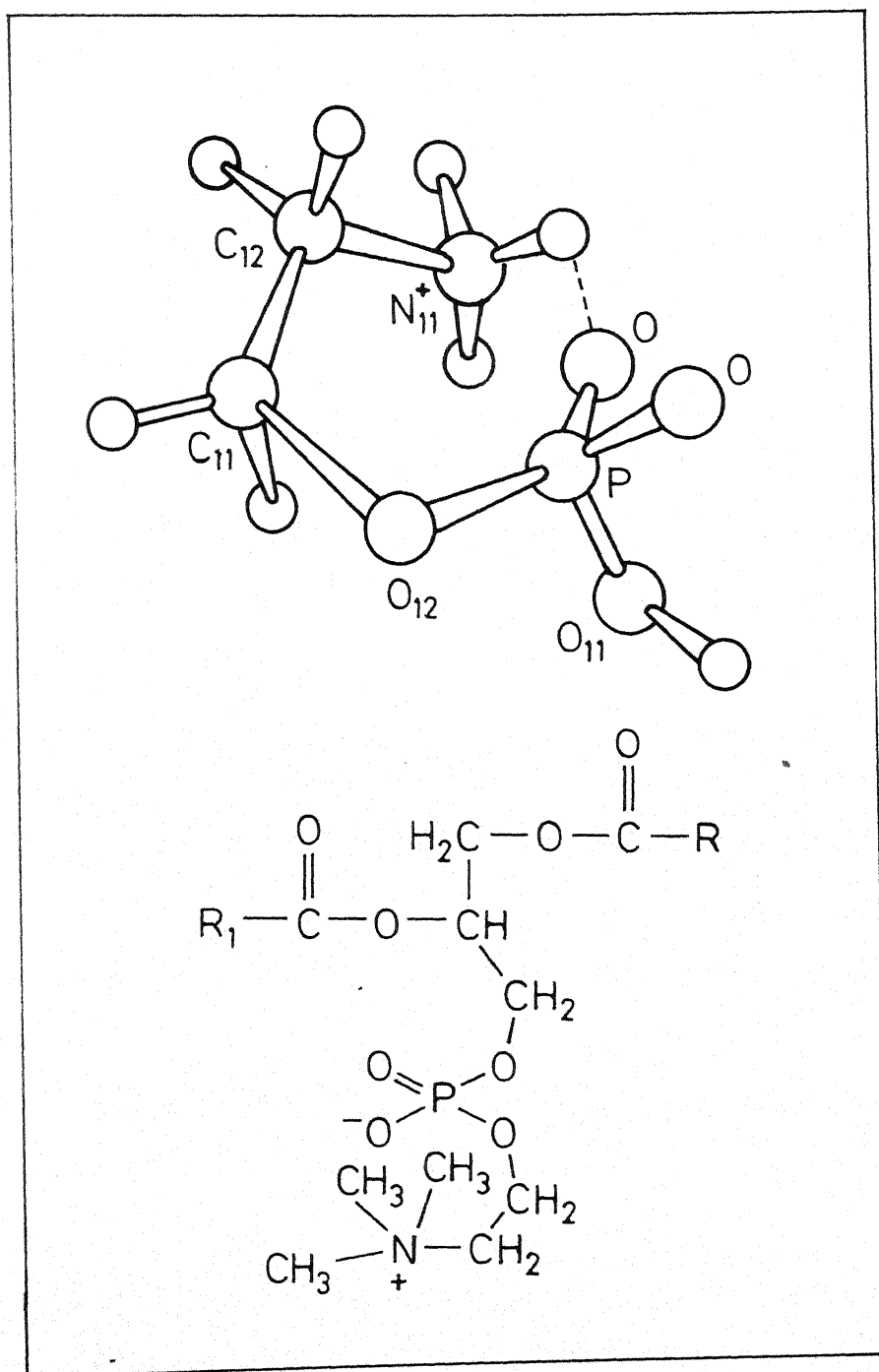


Fig 3.19 Structure of folded polar head group of Lecithin.

and the negatively charged phosphate oxygen atoms. Water is more likely to bind to the phosphate portion of the head group. The protons of water will thus form a weak bond to the phosphate group; likewise, the oxygen atoms of water will be in weak electrostatic interaction with  $^+\text{N}(\text{CH}_3)_3$ . Fig. 3.20 depicts the interaction of water molecule with polar head group of lecithin discussed above.

In such a model, the water is weakly hydrogen bonded with itself, or equivalently, the oxygen atoms are farther removed from the hydrogen atoms (20). Such a weak hydrogen bonding leads to an upfield shift of the -OH protons because it is shielded more thoroughly from the external magnetic field. This explains the initial upfield shift of the -OH proton resonance in Fig. 3.17. In fact, this shift is essentially very similar to that observed whenever structure breakers (i.e., electrolytes) are added to water (25,26). Also, it may be observed that the chemical shift trend reported in our study is similar to the upfield shift of the micellar solubilised water signal when water is added to Aerosol OT in octane (27).

At higher values of R i.e., when water is in excess, free water pools are formed with an increase in the average level of H-bonding of water due to water-water H-bonds (i.e., self-association) leading to down-field shift in the -OH resonance. This is in accordance with the result of Fig. 3.17.

From Fig. 3.18 it is evident that  $^+\text{N}(\text{CH}_3)_3$  proton resonances continuously move upfield as a function of added water upto a

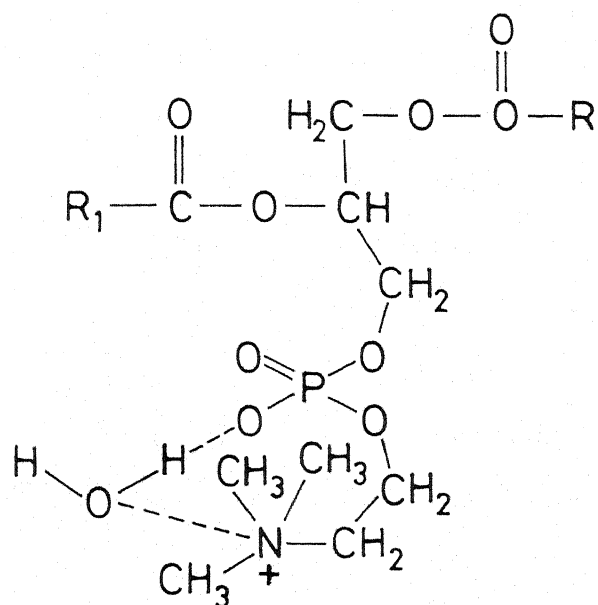


Fig. 3.20 Interaction of water with polar head group of Lecithin.

certain value and then level off for the three systems studied. This, again, is quite expected in view of the added water electrostatically shielding the trimethylamino group.

The arguments given above for the  $-OH$  and  $^+N(CH_3)_3$  proton chemical shifts are nicely complemented by our  $^{31}P$ -NMR chemical shifts of the lecithin head group presented below.

Fig. 3.21 shows the variation in the  $^{31}P$ -NMR chemical shift as a function of added water. It can be seen from Fig. 3.21 that, with added water, the  $^{31}P$ -NMR chemical shifts move downfield. As above, the explanation, of course, is that there will be a strong electrostatic interaction between the hydroxyl proton of the added water and the oxygen atom of phosphate of lecithin. Such an interaction would be expected to deshield phosphorous and hence result in a downfield shift. In their studies of methanol addition to phosphatidylcholine reverse micelles in chloroform, Henderson et al. (22) have also shown that  $^{31}P$  resonances of phosphatidylcholine head group moves as much as 25 Hz downfield. Above  $^{31}P$  chemical shift data is presented for benzene system and qualitatively apply to carbontetrachloride and cyclohexane systems also.

### Relaxation Studies

To elucidate further the role of water in these reverse micellar systems, the proton relaxation times of water molecules and those of the head group of lecithin, as well as the phosphorous relaxation times of the head group, are measured at various water

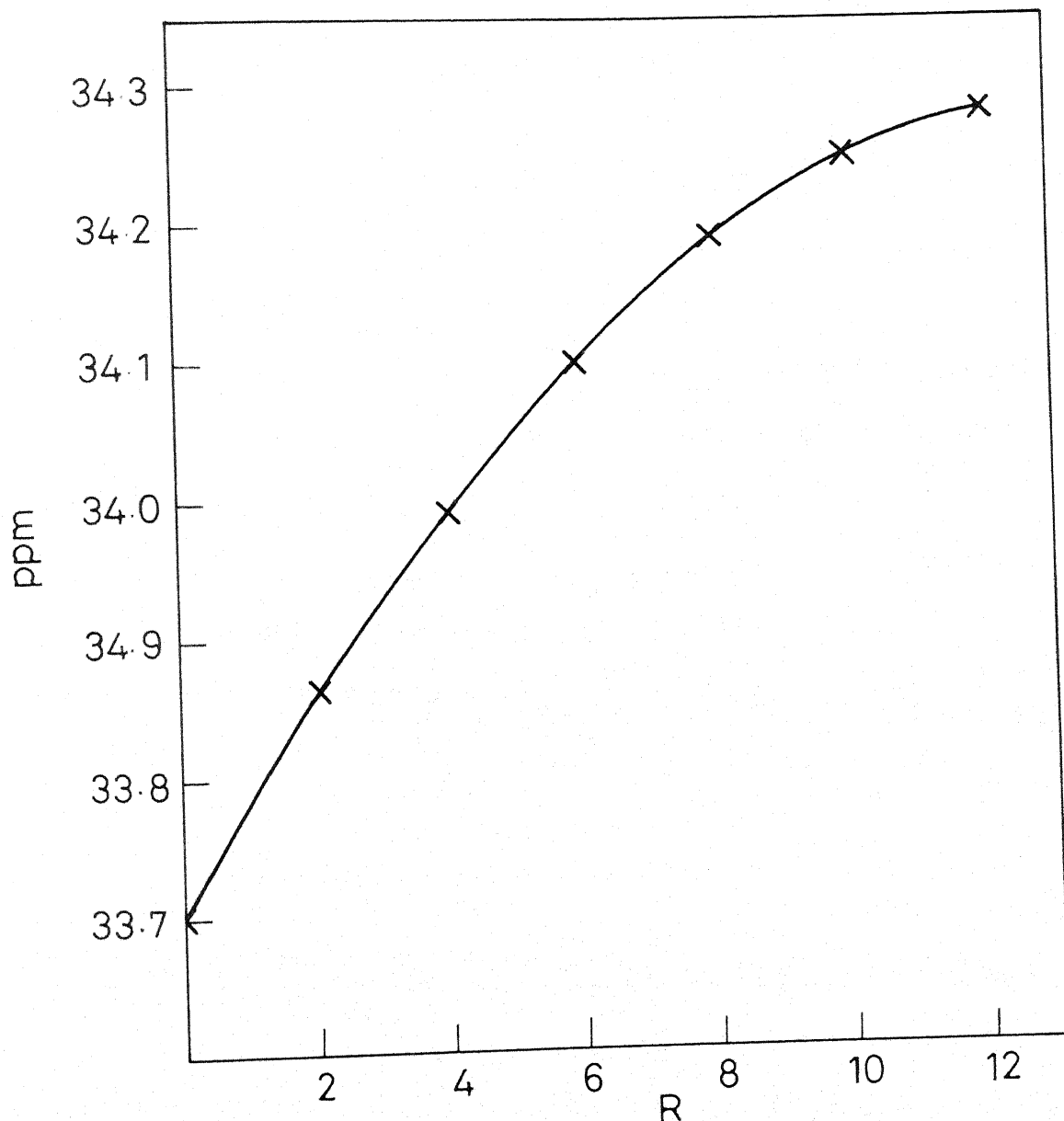


Fig. 3.21 Variation in  $^{31}\text{P}$  NMR Chemical shifts of Lecithin Head Group in Benzene system as a function of added water.

contents.

The longitudinal nuclear relaxation rate ( $\frac{1}{T_1}$ ), also known as spin-lattice relaxation rate, leads to information concerning the motion of molecules in solution (25). A change in molecular motion usually reflects a change in the structure of the medium (28) and/or the interactions between the molecules observed and the surroundings.

Fig. 3.22 shows the variation of the spin-lattice relaxation time,  $T_1$ , of the water protons as a function of added water in benzene, carbontetrachloride and cyclohexane systems.

From Fig. 3.22 we note that  $T_1$  of the water protons increases roughly linearly for the  $\text{CCl}_4$  and  $\text{C}_6\text{H}_6$  systems from  $R = 1$  to 14. For the cyclohexane system also, the overall trend is similar; but here, however, one observes a sharp 'peaking' in  $T_1$  in the range of  $R = 4$  to 8.

An attempt to analyse quantitatively the linear increase in  $T_1$  of the three systems is presented below. The rationalisation proceeds in terms of changes in the fraction of water molecules bound to the polar head group. For this purpose, the water proton signal is considered to be arising from two different populations of water, namely, (a) a fraction of water in intimate contact with the polar head group i.e., bound to the head group; this fraction may be called  $f_B$  characterised by a spin-lattice relaxation time,  $T_{1B}$  and (b) a second fraction consists of protons from free, fluid water which forms the core of the water pool;

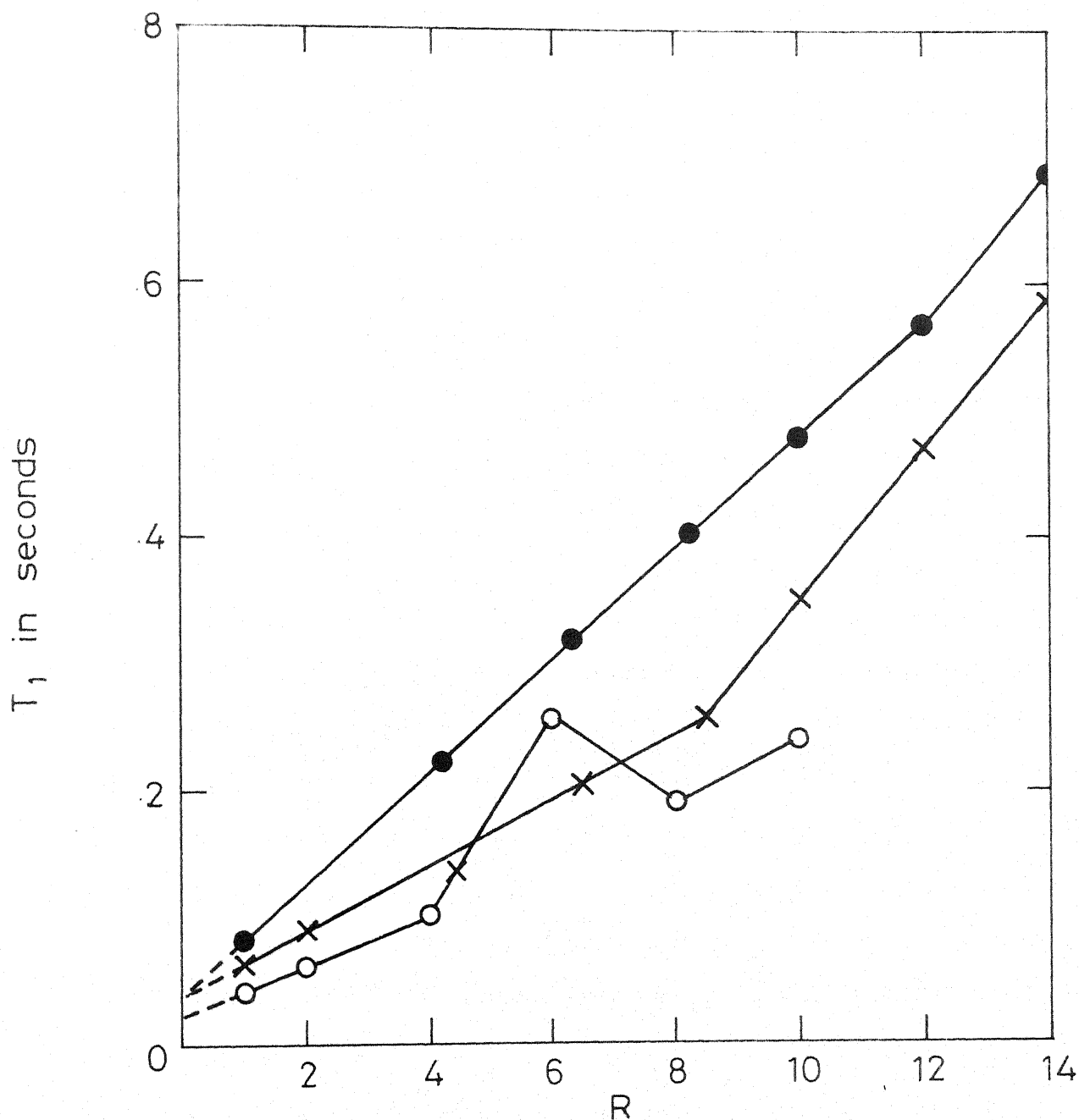


Fig. 3.22 Variation in  $T_1$  of water Protons in the three systems as a function of added water.  
 x ---- Benzene points, ● ---- Carbon tetrachloride points, ○ ---- Cyclohexane points.

this fraction may be termed  $f_F$  having a spin-lattice relaxation time,  $T_{1F}$ .

According to Woessner and Zimmermann (29), under conditions of fast exchange, we can write for the above two fractions

$$\frac{1}{T_1(\text{obs})} = \frac{f_B}{T_{1B}} + \frac{f_F}{T_{1F}} \quad \dots (3.1)$$

If it is assumed that  $T_{1B}$  and  $T_{1F}$  are approximately constant in the water concentration range corresponding to linear increase of  $T_1$ , we can calculate  $f_B$  and  $f_F$  provided that  $T_{1B}$  and  $T_{1F}$  are known.  $T_{1F}$ , the value of  $T_1$  for bulk water, is taken as 3.6 sec. as given by Krynicki (30).  $T_{1B}$  is assumed to be equal to the intercept of the  $T_1$  versus water concentration plot extrapolated to zero water concentration. This value turns out to be 0.040 sec. for benzene and carbontetrachloride systems and 0.025 seconds for cyclohexane system. The value of  $f_B$  thus calculated gives the amount of water immobilised or, in other words, amount of water bound to the polar head group. For the case of benzene system this  $f_B$  value has been converted into moles of water per mole of head group and plotted as a function of  $R$  in Fig. 3.23.

From Fig. 3.23 it is clear that the hydration of the PC head group increases slowly with increasing amounts of water added. This value, expressed as moles of water bound per mole of head group reaches a maximum of around 1 and levels off. Carbontetrachloride system and the reverse micellar region of cyclohexane system also displayed a similar behaviour. This



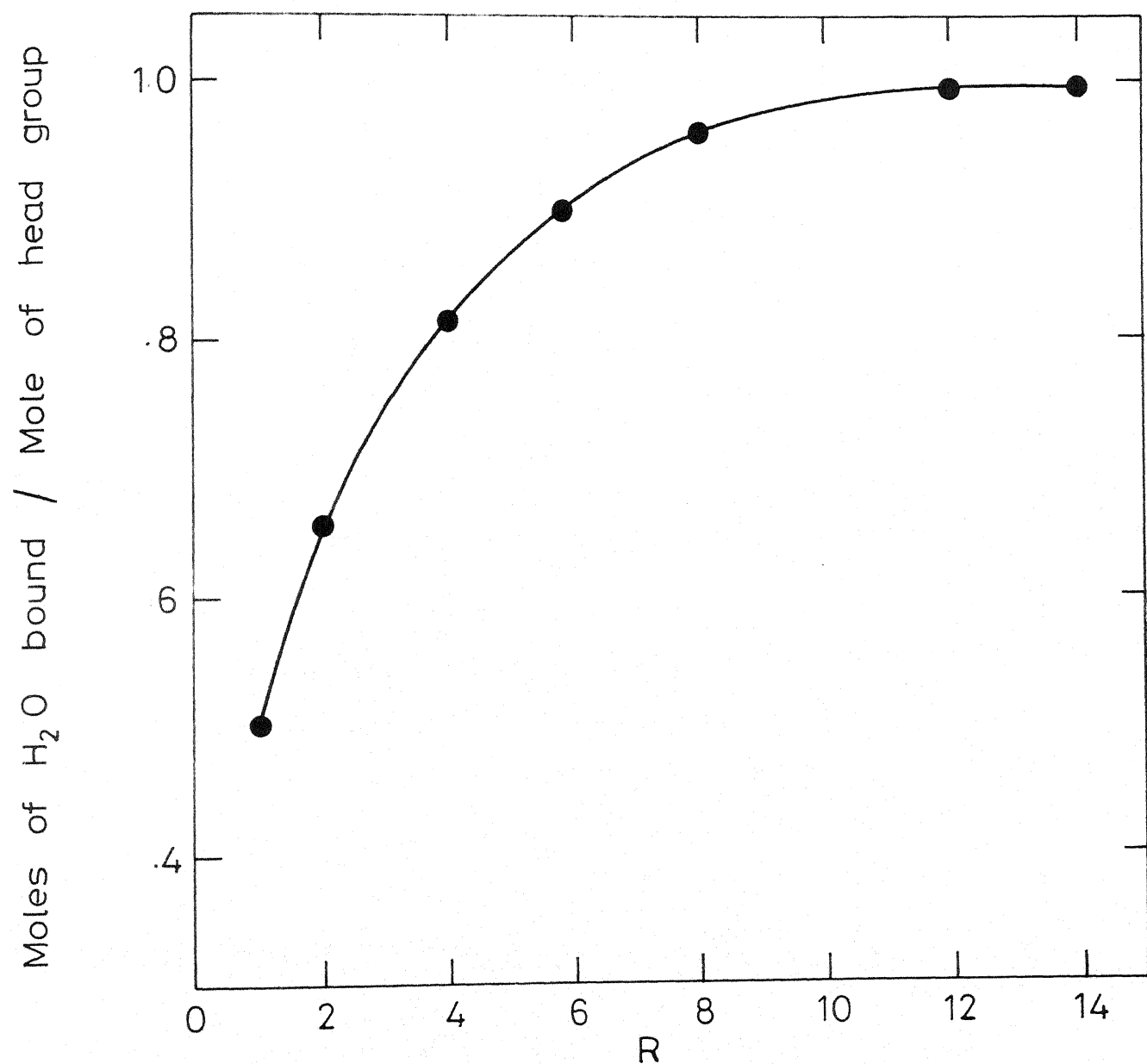


Fig. 3.23 Hydration of head group of Lecithin in Benzene system as a function of added water.

limiting value is in excellent agreement with one mole of water tightly bound to one mole of lecithin head group reported earlier by Fung and McAdams (21) from their deuterium relaxation study and that of Davenport and Fisher by NMR linewidth and infrared studies (31).

There is yet another approach to quantitatively analysing the water proton spin-lattice relaxation times presented above i.e., in terms of microviscosity values. The relaxation times are related to molecular motion by the rotational correlation time,  $\tau_c$ , which gives a measure of the mean residence time of the two proton nuclei in a given relative orientation. The correlation time in turn depends on the microviscosity. For any small molecule of two equal spins ( $I_1 = I_2 = \frac{1}{2}$ ), such as water, the spin-lattice relaxation time  $T_1$  may be considered to be the result of a combination of intramolecular and intermolecular relaxation effects, each of which can be theoretically evaluated. The intramolecular contribution to relaxation of nucleus I caused by dissipation of the nuclear spin energy to rotational motion (32). The relevant equations for intermolecular and intramolecular relaxation effects for the water molecule as developed in the classic work of Bloembergen, Purcell and Pound (33) are:

$$\frac{1}{T_{1 \text{ intra}}} = \frac{2\gamma^4 \hbar^2 I(I+1)}{5 r^6} \left[ \frac{\tau_c}{1 + \omega^2 \tau_c^2} + \frac{4\tau_c}{1 + 4\omega^2 \tau_c^2} \right] \dots (3.2)$$

$$\frac{1}{T_{1 \text{ inter}}} = \frac{9\pi^2 \gamma^4 \eta \hbar^2 N_0}{5 kT} \dots (3.3)$$

$$\frac{1}{T_1} = \frac{1}{T_{1 \text{ intra}}} + \frac{1}{T_{1 \text{ inter}}} \quad \dots (3.4)$$

where  $T_{1 \text{ intra}}$  and  $T_{1 \text{ inter}}$  are the intramolecular and intermolecular parts of the dipolar mode of relaxation,  $\gamma$  is the gyromagnetic ratio,  $r$  is the proton-proton distance in the water molecule,  $\tau_c$  is the rotational correlation time,  $\omega$  is the resonance frequency of the water molecule,  $\eta$  is the microviscosity and  $N_0$  the volume concentration of spins. Substituting the value of  $\tau_c$  thus obtained in the Debye-Stokes equation

$$\tau_c = \frac{4\pi \eta a^3}{3kT} \quad \dots (3.5)$$

where  $a$  is the radius of the water molecule approximated to a sphere, we can get  $\eta$ , the microviscosity of the water molecules whose  $T_1$  is known.

We have analysed the  $T_1$  data of water protons in two ways: 1) under the simplifying assumption that the intramolecular relaxation mode alone is dominant, from equations 3.2 and 3.5, and 2) under the assumption that both intra- and intermolecular relaxation mechanisms are operative, from equations 3.2, 3.3, 3.4 and 3.5. The results of such calculations are presented in Table 3.3 for benzene system, Table 3.4 for carbontetrachloride system and Table 3.5 for cyclohexane system.

Table 3.3

Microviscosity of water environment in benzene system

R	$\tau_c$ from Eq. 3.2, $10^{-10}$ s	$\eta$ from $\tau_c$ according to Eq. 3.2 (CP)	$\eta$ from Eq. 3.4 (CP)
1	2.70	68.0	38.0
2.2	2.00	50.0	29.0
4.3	1.30	33.0	18.0
6.5	0.92	23.0	13.0
8.7	0.70	18.0	10.0
10.0	0.52	13.0	7.4
12.0	0.40	11.0	5.7
14.0	0.31	7.5	4.5

CONSTANTS USED :  $a = 1.50 \times 10^{-8}$  cm;  
 $b = 1.58 \times 10^{-8}$  cm;  
 $h = 6.6242 \times 10^{-27}$  erg sec.  
 $N_0 = 6.75 \times 10^{22}$ ;  
 $k = 1.38 \times 10^{-16}$  erg/deg/molecule  
 $T = 298$  K

Table 3.4

Microviscosity of water environment in carbontetrachloride system

R	$\tau_c$ from Eq. 3.2, $10^{-10}$ s	$\eta$ from $\tau_c$ according to Eq. 3.2 (CP)	$\eta$ from Eq. 3.4 (CP)
1	2.40	60.0	34.0
2.1	1.50	38.0	22.0
4.2	0.83	21.0	12.0
6.2	0.55	14.0	7.8
8.3	0.46	12.0	6.6
10.0	0.39	9.4	5.6
12.0	0.33	8.3	4.7
14.0	0.27	6.8	3.8

Table 3.5

Microviscosity of water environment in cyclohexane system

R	$\tau_c$ from Eq. 3.2, $10^{-10}$ s	$\eta$ from $\tau_c$ according to Eq. 3.2 (CP)	$\eta$ from Eq. 3.4 (CP)
2	3.10	78	44
4	1.70	43	25
6	0.70	18	10
8	0.97	24	14
10	0.76	19	11

From Tables 3.3 to 3.5 it is seen that for benzene and carbontetrachloride systems and for the initial reverse micellar region of cyclohexane (i.e. upto an R value  $\sim 6$ ), the  $\tau_c$  of the proton nuclei of water molecules decreases as a function of added water. This indicates that the mobilities of the water molecules engaged in binding to the polar head groups is significantly reduced and hence these  $\tau_c$  values at low R values are much higher than that of normal bulk water,  $\tau_c = 3 \times 10^{-12}$  seconds (34). Addition of further water to the systems gradually reduces  $\tau_c$  to a value approaching that of free water.

Even at low water concentrations, i.e.,  $R = 2$ , the rotational correlation time of water protons is greater by a factor of 200 than the rotational correlation time of the overall micelle in benzene,  $\tau_c = 6 \times 10^{-8}$  secs, estimated by using the Debye-Stokes equation by Walter and Hayes (35). Hence, even at low concentrations of water the rotational motion of water is not influenced by the overall tumbling of the micelle. At higher water concentrations, additional water is 'free' and  $\tau_c$  approaches a value measured for the bulk water,  $\tau_c = 3 \times 10^{-12}$  secs. This bound water exchanges rapidly with the water in the pool and dominates the observed relaxation processes. It is of interest to note that similar conclusions have been made regarding the water in cells and protein solutions (34). Cooke and Kuntz (34) show that a small fraction of water is firmly bound to macromolecules and exhibits extremely short relaxation times i.e., rotational correlation times well in excess of  $10^{-12}$  secs.

Chapter II. Bound water has a lower mobility than free water and consequently shows a higher microviscosity.

Figs. 3.24 and 3.25 show the variation in  $T_1$  of  $^+N(CH_3)_3$  and  $-CH_2N^+$  protons respectively as functions of added water. Increasing the water content in the micellar aggregates affects only the relaxation rates of those protons adjacent to the polar head groups. Since the water molecules are only in contact with the polar head groups, addition of water to the system increases the fluidity in the central aqueous pool and the interfacial region. Therefore, the relaxation times of water protons, as well as of those protons adjacent to the water, would be expected to increase, as found in Figs. 3.24 and 3.25. In this connection we may add that the  $T_1$  values of  $-(CH_2)_n$  group of lecithin remain constant and this is again expected because these protons are not in direct contact with the water phase. In Table 3.6 we present the  $T_1$  values of  $-(CH_2)_n$  group of cyclohexane system at various R values and it may be noted that  $T_1$  is constant.

Table 3.6

Variation in proton NMR  $T_1$  of  $-(CH_2)_n$  in cyclohexane system

R	$T_1$ of $-(CH_2)_n$ (seconds)
0	0.458
2	0.449
4	0.450
6	0.457
8	0.452
10	0.449

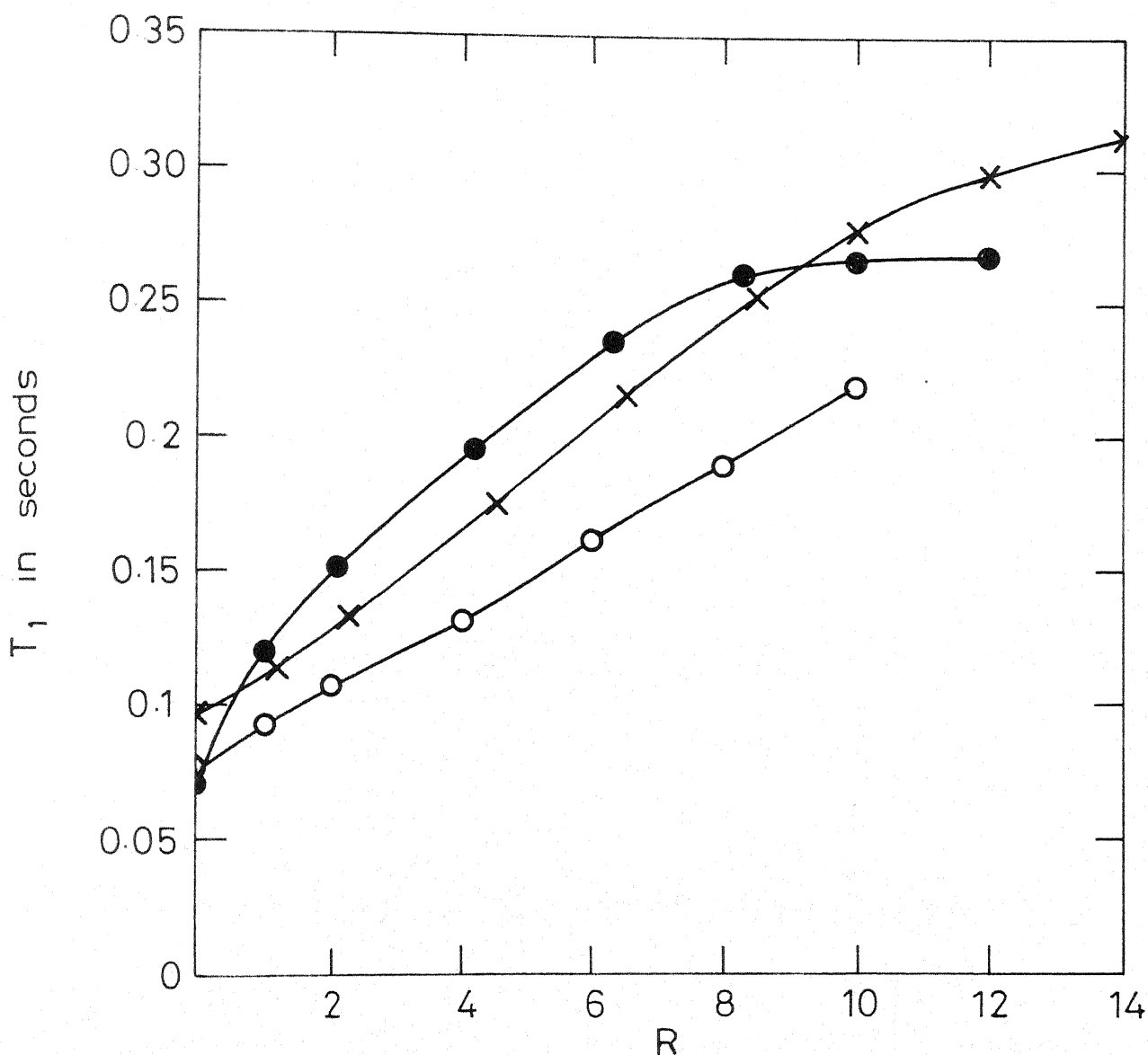


Fig. 3.24 Variation in  $T_1$  of  $^+N(CH_3)_3$  Protons in the three systems as a function of added water.  
 X ---- Benzene points, ● ---- Carbondetrachloride points, ○ ---- Cyclohexane points.



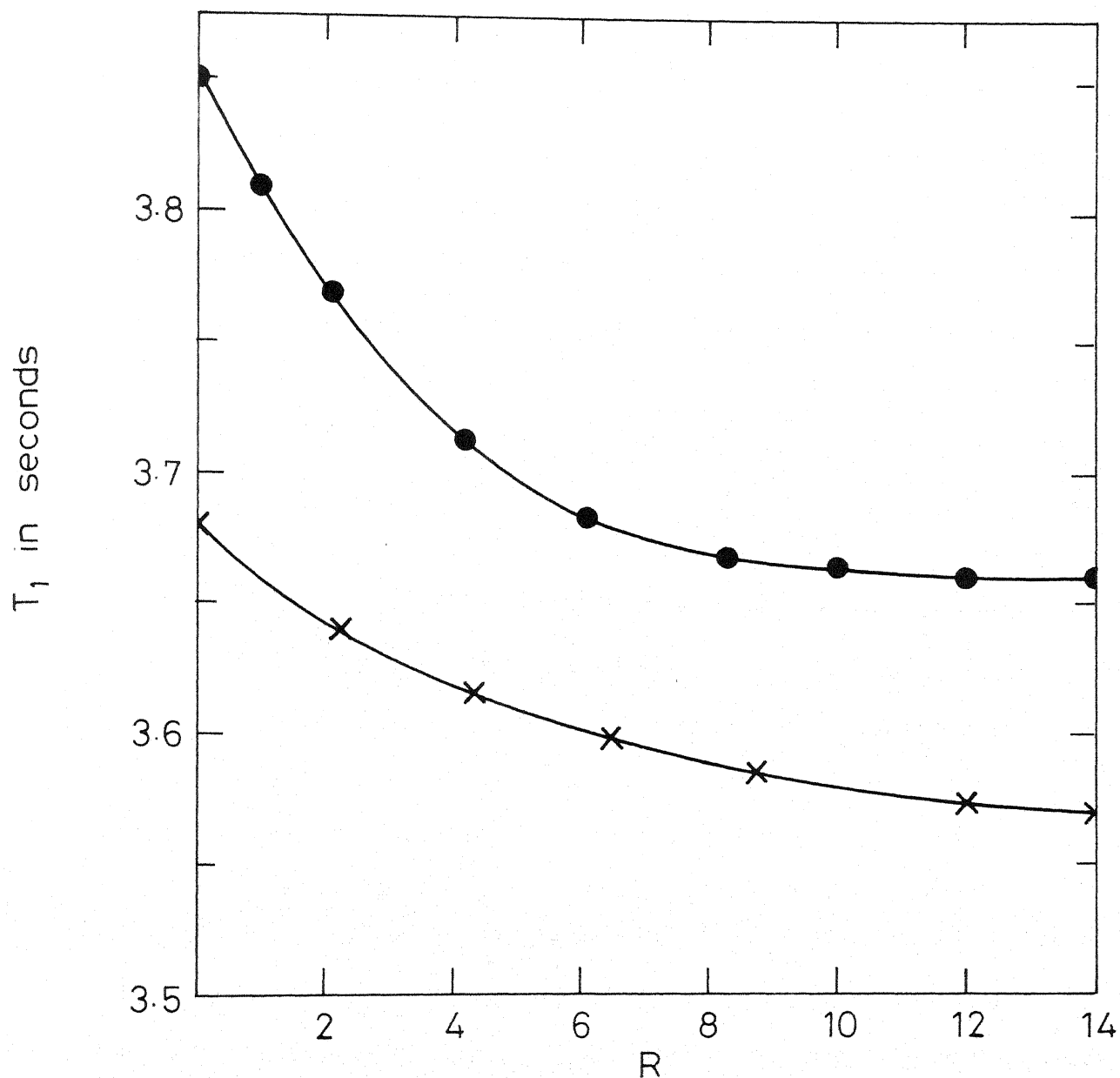


Fig. 3.25 Variation in  $T_1$  of  $-\text{CH}_2\text{N}^+$  Protons in Benzene and Carbontetrachloride systems as a function of added water. ● --- Carbontetrachloride points. X --- Benzene points.

Figs. 3.26 and 3.27 show the trends in the spin-spin relaxation times,  $T_2$ , for the water and  $^+N(CH_3)_3$  protons, respectively, in carbontetrachloride and cyclohexane systems as a function of added water.

It is evident from Fig. 3.26 that in carbontetrachloride system,  $T_2$  values of water protons show a linear increase with water concentration, whereas in the cyclohexane system the  $T_2$  values of water protons start decreasing from R value 6, which suggests that some of the molecular organisational rearrangements necessary for the phase transition take place in this region. It can be seen from Fig. 3.27 that the  $T_2$  values of the  $^+N(CH_3)_3$  protons of both carbontetrachloride and cyclohexane systems increase linearly with added water.

The changes in  $T_2$  values roughly parallel the changes in  $T_1$  values with the only difference that the  $T_2$  values are lower than the  $T_1$  values while still remaining in the same order of magnitude. In contrast, the  $T_1$  and  $T_2$  values of TritonX-100 reverse micelles are found to differ by an order of magnitude by Kumar and Balasubramanian (38). In the case of  $^+N(CH_3)_3$  protons (Fig. 3.27) the  $T_1$ - $T_2$  differences could be due to diffusional changes in the orientation of lecithin at the interface, a process that has been shown to affect  $T_1$  and  $T_2$  values differently (39).

The difference between  $T_1$  and  $T_2$  values of hydroxyl protons could indicate the presence of other modes of relaxation in

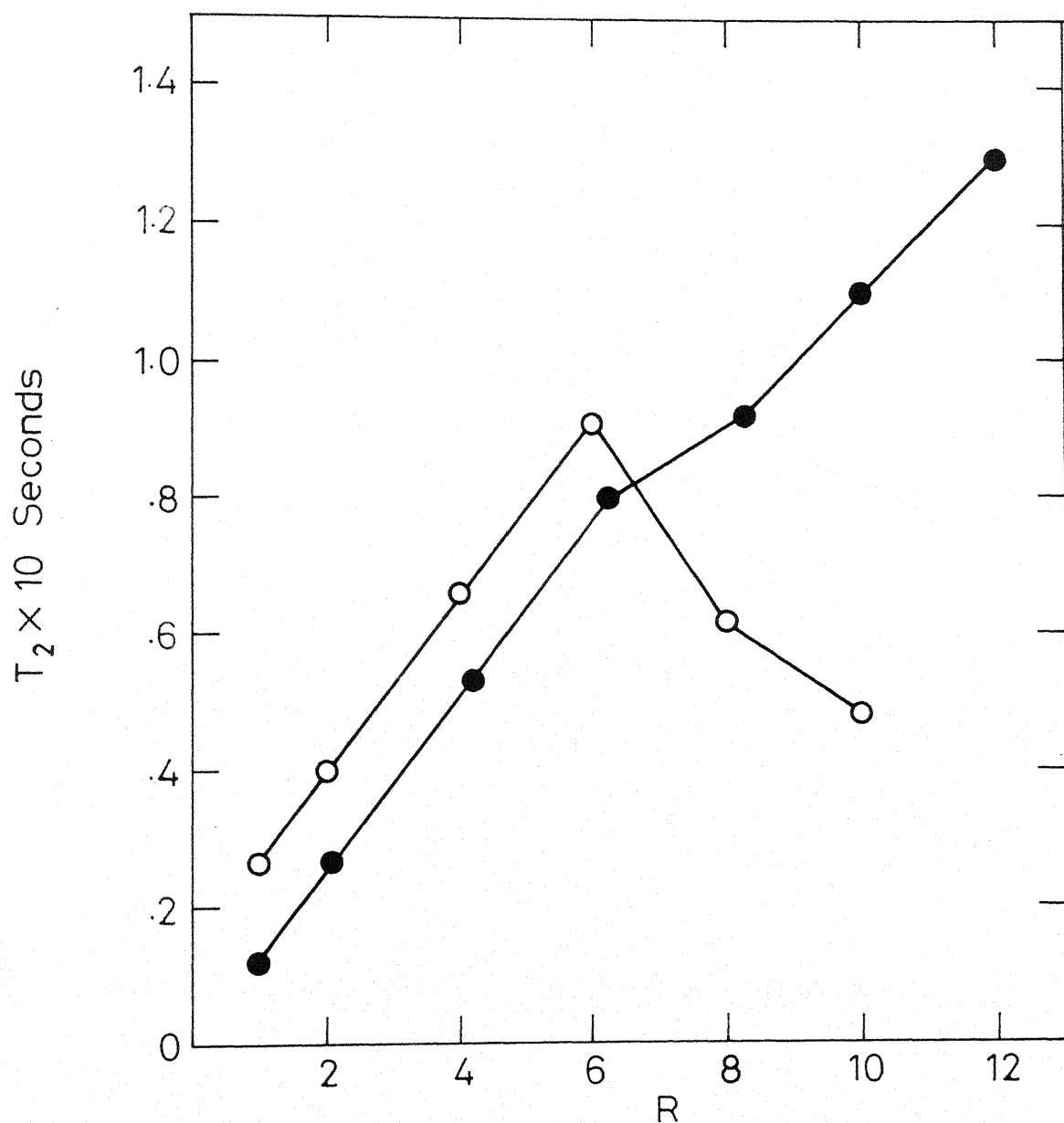


Fig. 3.26 Variation in  $T_2$  of water Protons in Carbon-tetrachloride and Cyclohexane systems as a function of added water.  
 ● ---- Carbontetrachloride points, X ---- Cyclohexane points.

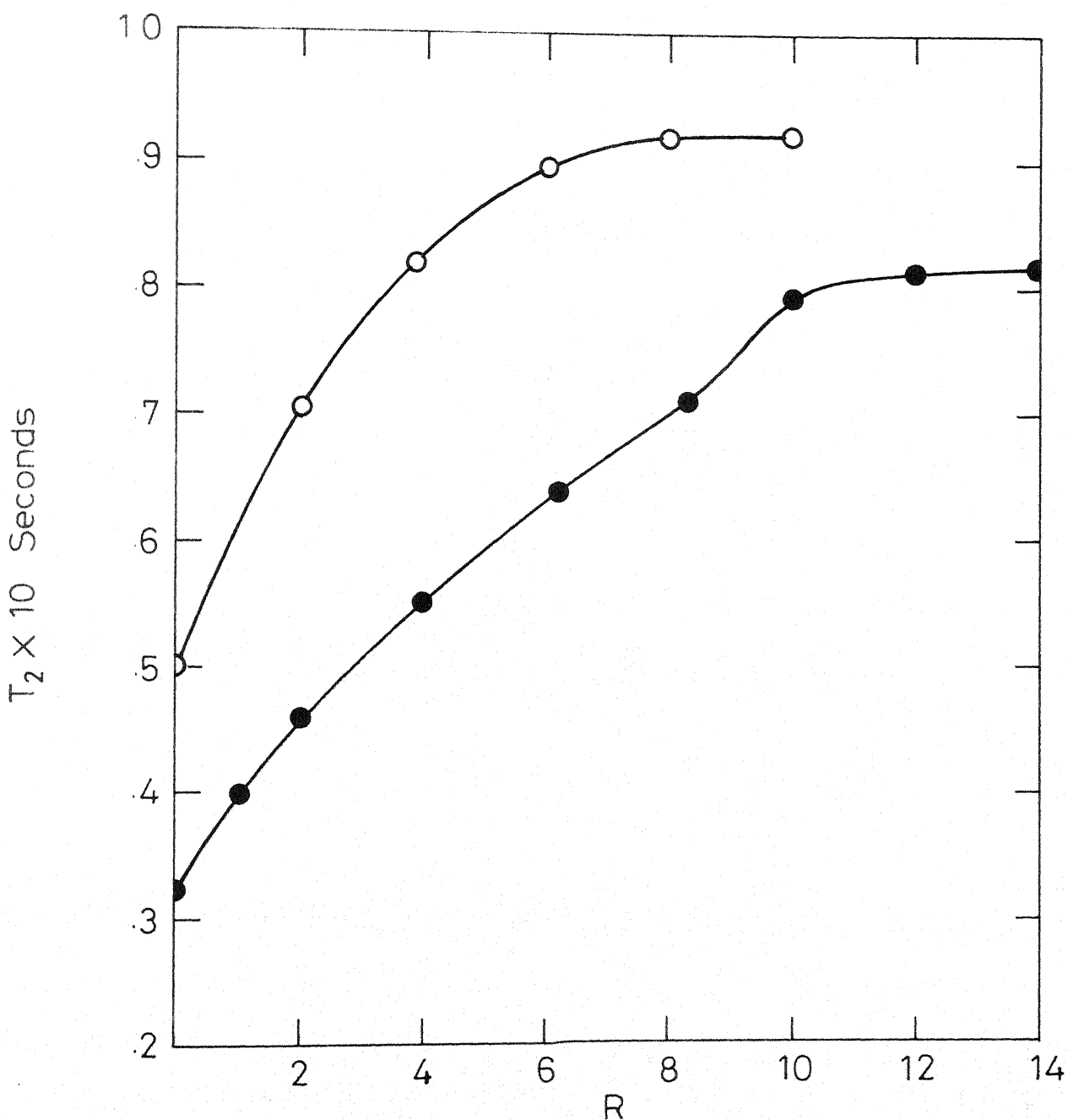


Fig. 3.27 Variation in  $T_2$  of  $^+N(CH_3)_3$  Protons in Carbon-tetrachloride and Cyclohexane systems as a function of added water.  $\bullet$ ---- Carbontetrachloride points,  $\circ$ ---- Cyclohexane points.

addition to intramolecular dipole-dipole relaxation. This view is rationalised by the argument given below.

The intramolecular contribution to  $T_2$  relaxation is given by (32):

$$\frac{1}{T_{2 \text{ intra}}} = \frac{\gamma^4 \hbar^2 I(I+1)}{5 r^6} \left[ 3 \tau_c + \frac{5 \tau_c}{1 + \omega^2 \tau_c^2} + \frac{4 \tau_c}{1 + 4\omega^2 \tau_c^2} \right] \quad \dots(3.6)$$

where all the symbols have the same meaning as given earlier.

The rotational correlation time,  $\tau_c$ , obtained from equation 3.2 is substituted in equation 3.6 to calculate the spin-spin relaxation time  $T_2$ . Table 3.7 gives the calculated and experimental  $T_2$  values (from spectra  $T_2 = \frac{1}{\pi \nu_{1/2}}$ , where  $\nu_{1/2}$  is the width at half height) at different concentrations of water for the carbontetrachloride system.

From Table 3.7 it is seen that the experimental  $T_2$  values (obtained from spectra) are lower than the  $T_2$  values calculated using Eq. 3.7. The validity of Eq. 3.7 in calculating  $T_2$  depends on the condition that intramolecular dipole-dipole relaxation dominates spin-spin relaxation. Hence, the deviation of the experimental  $T_2$  values from those calculated from Eq. 3.7 suggests that other relaxation mechanisms which cause a fluctuating magnetic field about the perturbed  $^1\text{H}$  nucleus also contribute to the overall spin-spin relaxation processes. Additional relaxation mechanisms other than dipole-dipole relaxation are thought to be operative here. These are most likely to be exchange narrowing,

spin-rotational and chemical shift anisotropy.

Table 3.7

Calculated and experimental  $T_2$  values of water protons in carbontetrachloride system at different water concentrations

R	$T_2$ Calculated from Eq. 3.7 (seconds)	$T_2$ Obtained from spectra $[T_2 = \frac{1}{\pi\nu_{1/2}}]$ (seconds)
1.0	0.032	0.011
2.1	0.051	0.027
4.2	0.092	0.053
6.2	0.139	0.080
8.3	0.166	0.091
10.0	0.196	0.107
12.0	0.232	0.130
14.0	0.283	0.130

One very likely mechanisms in view of our foregoing discussions is the following: the rapid spin exchange between the two environments, bound and free water, would cause an additional contribution to the transverse relaxation rate. The theoretical approach to this problem has been presented by Gutowsky, McCall and Slichter (40), McConnell (41) and Swift and Connick (42). Finally, one ought to remember that, since the

experimental  $T_2$  values are evaluated from the linewidth at half-maximum height, slight inhomogeneities in the magnetic field would cause additional line broadening and thereby result in a decrease in the apparent relaxation time. However, we eliminate this possibility since some of our measurements at 60 MHz with PC-CCl<sub>4</sub>-H<sub>2</sub>O system at four R values gave linewidths that are within  $\pm 5\%$  of those measured at 100 MHz. Indeed, the field independence of linewidth is a classical test for magnetic field homogeneity (43) and this has been taken into account in our case.

Fig. 3.28 shows the variation of  $^{31}\text{P}$  spin-lattice relaxation time of choline head group with increasing water concentration for the three system at 40.5 MHz.

From Fig. 3.28 it is clear that  $^{31}\text{P}$   $T_1$  in benzene and carbontetrachloride systems increase linearly with added water. This increase in  $T_1$  with added water is in agreement with the general trends reported by Klose and Stelzner (19) in benzene-lecithin-water system and also by Fung and McAdams (21) in carbontetrachloride system. In the "extreme narrowing" limit an increase in  $^{31}\text{P}$  relaxation time ( $T_1$ ) means a decrease in the rotational correlation time of the phosphate group i.e., an increase in the mobility of the phosphate group. At very low concentrations of water, the positively charged trimethylammonium group and the negatively charged phosphate group would interact with each other strongly as discussed earlier in this chapter (see chemical shift studies and figures 3.19 and 3.20). Hence, the internal rotation of the phosphate group is severely

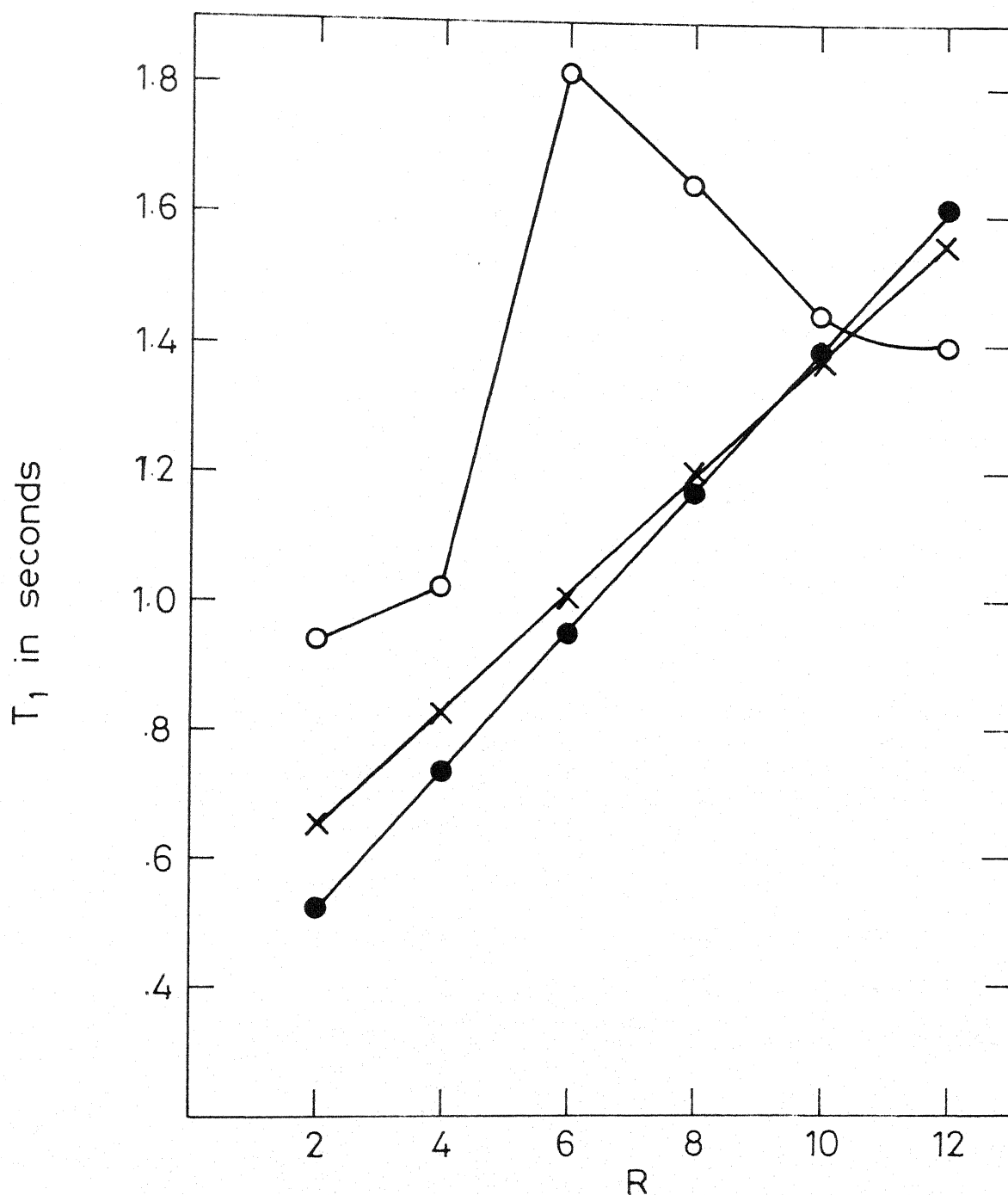


Fig. 3.28 Variation in  $^{31}\text{P}$  NMR  $T_1$  values of Lecithin head group in the three systems as a function of added water. X ---- Benzene points, ● ---- Carbon tetrachloride points, ○ ---- Cyclohexane points.



hindered by the trimethylammonium group. When more and more water is added this interaction will be weakened and consequently the phosphate group will be more mobile. This explains the linear increase in  $^{31}\text{P}$  spin-lattice relaxation times of benzene and carbontetrachloride systems with added water.

The other very remarkable feature of Fig. 3.28 is that phosphorous  $T_1$  values in cyclohexane solvent system increase upto an R value of 6 and then start decreasing. It is here pointed out that our proton NMR  $T_1$  values and  $T_2$  values in cyclohexane system also exhibit a similar behaviour in this region, i.e., around R value of 6. In this solvent, the increase in  $^{31}\text{P}$   $T_1$  upto an R value of 6 shows that the mobility of the phosphate group increases upto this point. At further concentrations of added water, there is a decrease in the mobility of the phosphate group, suggesting that some molecular rearrangements take place in the lecithin head group in cyclohexane system at an R value of 6. This once again confirms that there is a transition taking place in this region i.e., the "reverse micellar-liquid crystalline" transition proposed earlier. Thus the  $^{31}\text{P}$  data are in essential agreement with our proton NMR  $T_1$  values which arise due to a decrease in the mobility of water in the region  $R \geq 6$ .

In Fig. 3.29 we present the  $^{13}\text{C}$ -NMR spectrum of lecithin in dry  $\text{CDCl}_3$ . This spectrum has been recorded at a  $^{13}\text{C}$  resonance frequency of 100.6 MHz under conditions of proton noise decoupling. One very important feature of the spectrum presented in

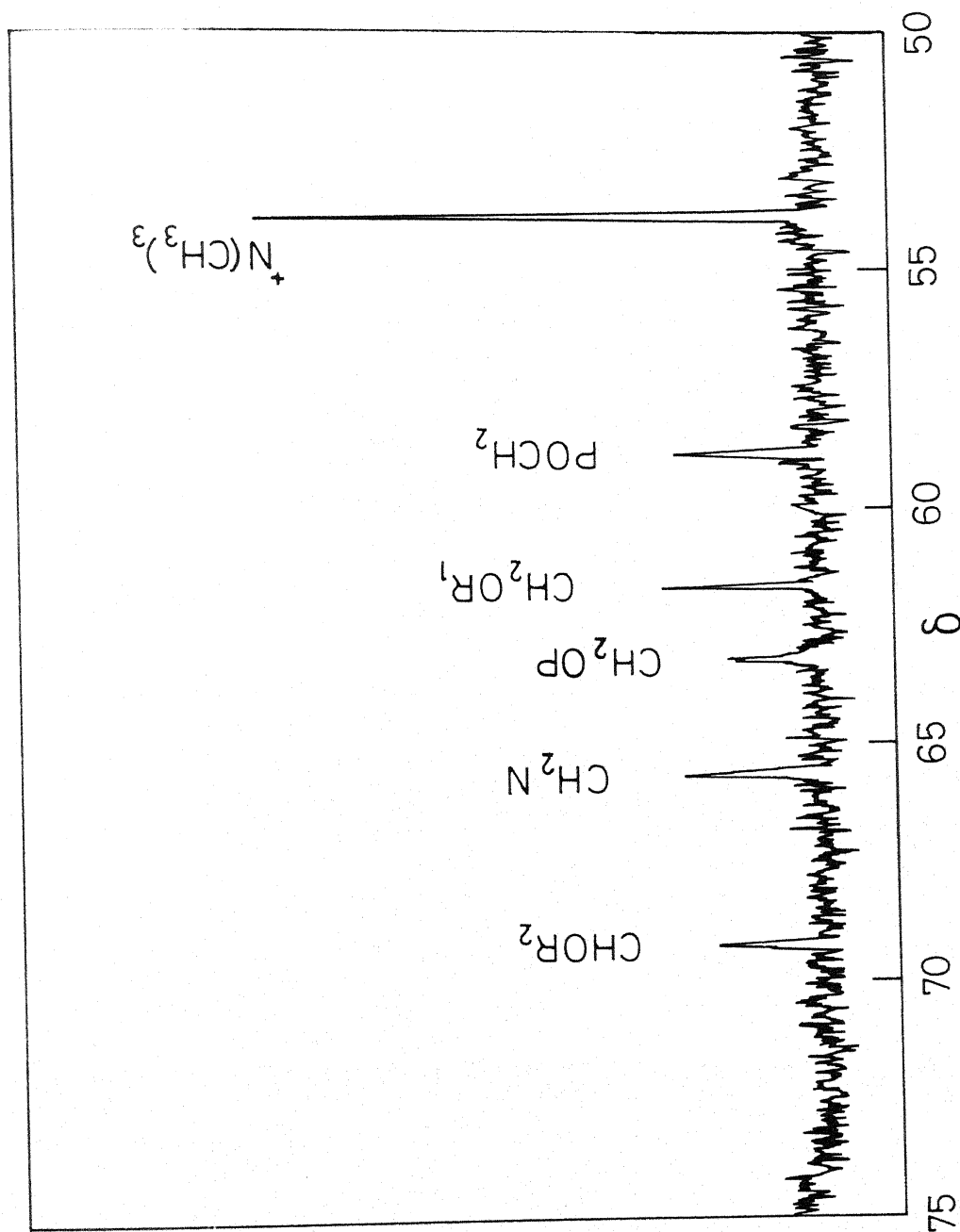


Fig. 3.29 100.6MHz  $^{13}\text{C}$  NMR spectrum of Lécithin in  $\text{CDCl}_3$  at an R value of 0.0

Fig. 3.29 is that the separation of  $-\text{CH}_2\text{OR}_1$  and  $-\text{CH}_2\text{OP}$   $^{13}\text{C}$  signals. These two peaks which are clearly chemical shifted by  $\sim 2.5 \delta$ , under our observing Larmor frequency, appear as a single peak in the early study of Birdsall et al. (44) (carbon resonance frequency 25.2 MHz) and the more recent study of Baumann and Murari (45) (carbon resonance frequency 20 MHz). These earlier studies have also been carried out in  $\text{CDCl}_3$  solvent. In all other respects, the agreement between our  $^{13}\text{C}$ -NMR spectra and those of the earlier workers is complete and we have assigned the peaks in our spectrum in the accepted fashion.

In Figs. 3.30 to 3.32 we present the  $^{13}\text{C}$ -NMR spectra of lecithin in  $\text{CDCl}_3$  with added water, i.e., at different R values.

From Figs. 3.30 to 3.32 it can be seen that at none of the R values studied resolved  $^{13}\text{C}$ - $^{14}\text{N}$  couplings for the choline methyls are observed. Also in Figs. 3.29 - 3.32 the linewidth at half height of  $^+\text{N}(\text{CH}_3)_3$  peak is found to be constant at 8.5 Hz. As concluded before (45), this is clearly due to aggregation and as more and more water is added the size of the micelle increases i.e., the aggregation number increases. In their work, Birdsall (44) suggested that this collapse of the lecithin  $^+\text{N}(\text{CH}_3)_3$  triplet in  $\text{CDCl}_3$  is as a result of shorter  $^{14}\text{N}$  relaxation times in micellar structures. London et al. (46) attributed the disappearance of resolved  $^{13}\text{C}$ - $^{14}\text{N}$  splittings in PC vesicles in  $\text{D}_2\text{O}$  at lower temperatures [ $< 60^\circ\text{C}$ ] to either dipolar broadening or a decrease in  $^{14}\text{N}$  relaxation times.

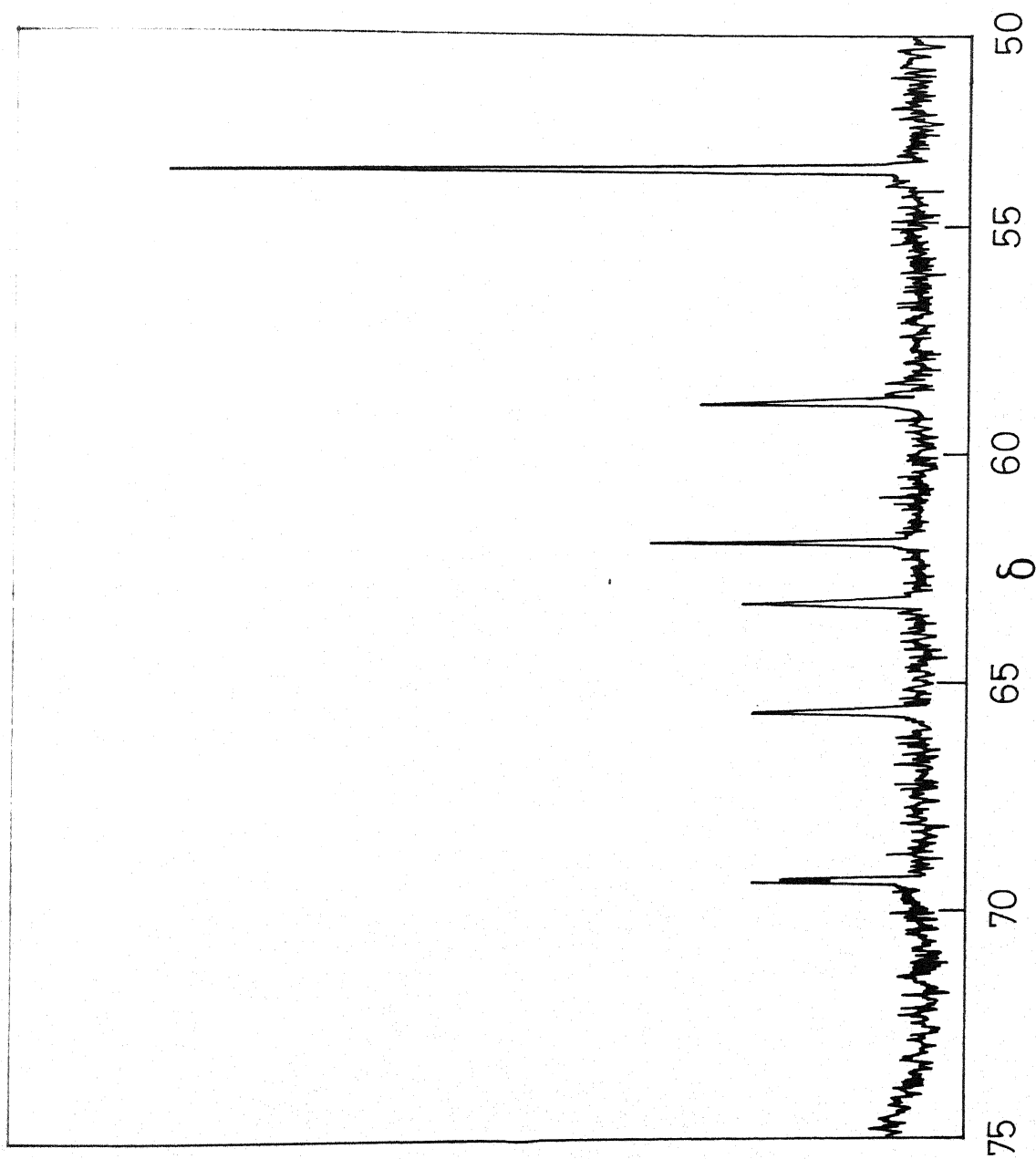


Fig. 3.30  $^{13}\text{C}$  NMR spectrum of Lecithin in  $\text{CDCl}_3$  at an R value of 2.0

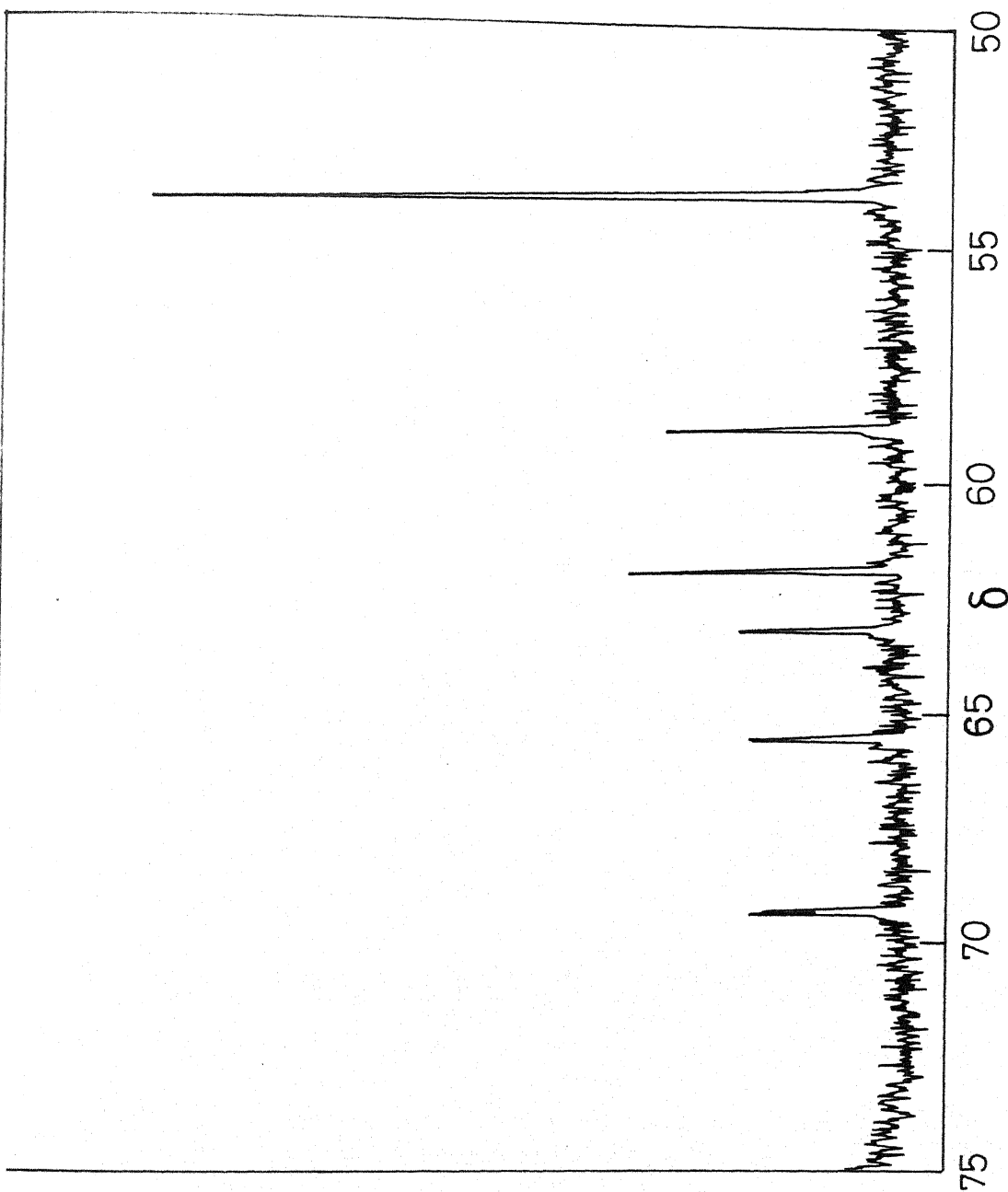


Fig. 3.31  $^{13}\text{C}$  100.6 MHz NMR spectrum of Lecithin in  $\text{CDCl}_3$  at an R value of 6.0

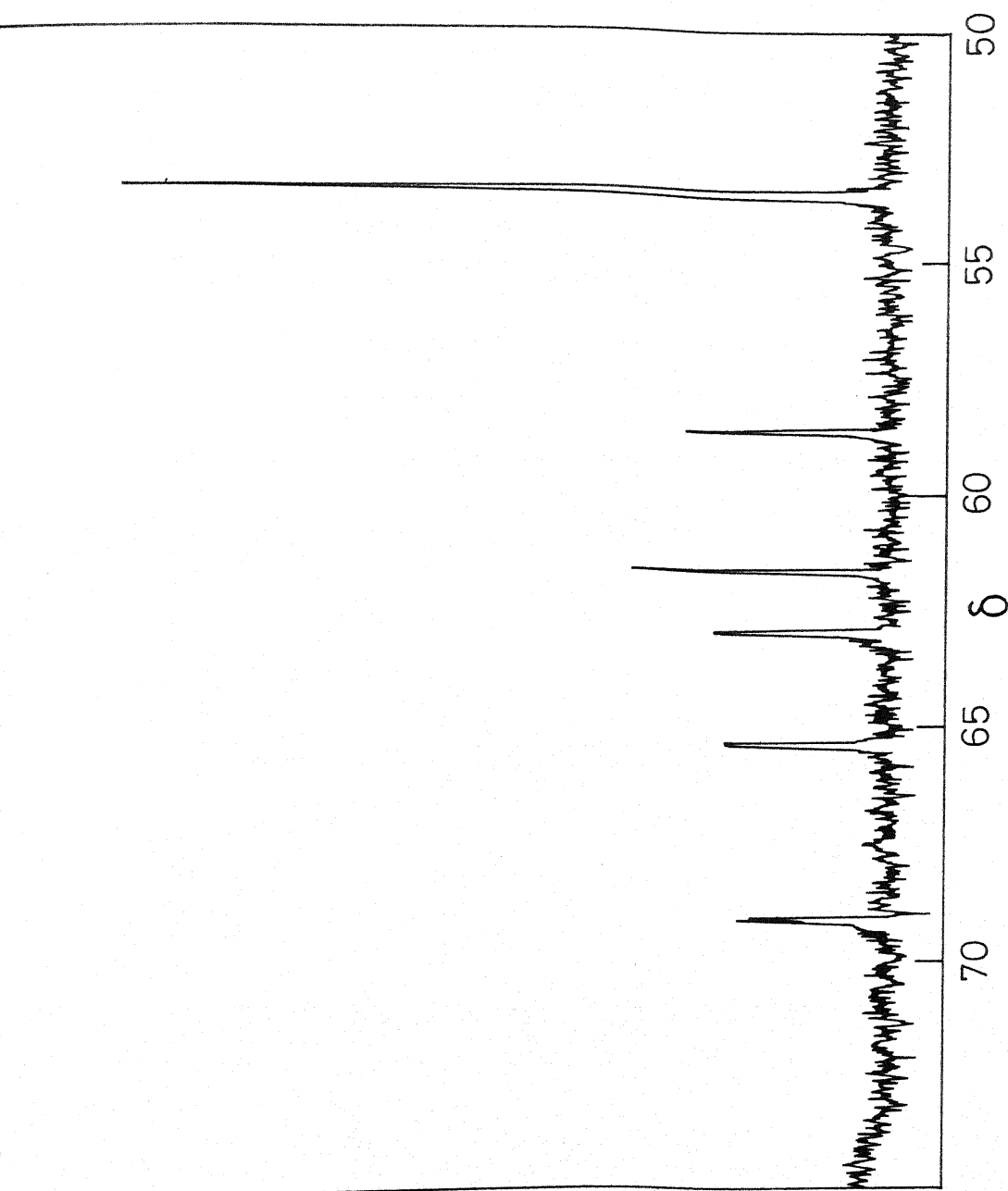


Fig 3.32 100MHz  $^{13}\text{C}$  NMR spectrum of Lecithin in  $\text{CDCl}_3$  at an R value of 10.0

In order to distinguish between the above two effects, Murari and Baumann (45) measured  $^{14}\text{N}$   $T_1$  and  $T_2^*$  values of several choline derivatives in various solvents and concluded that the nonobservation of  $^{13}\text{C}$ - $^{14}\text{N}$  splittings could be rationalised on the basis of reduction in  $^{14}\text{N}$   $T_1$  alone rather than dipolar broadening. These authors (45) have not, of course, reported any further results under conditions of water-uptake by the inverted micelles of lecithin in  $\text{CDCl}_3$ . Since we did not observe any  $^{13}\text{C}$ - $^{14}\text{N}$  couplings even with added water, the explanation given by the above authors (45) can be extrapolated to cases with added water as in our system.

### Conclusions

On the basis of the results of extensive spectroscopic studies on the three systems the following conclusions can be made:

(1) Near infrared studies show that the amount of water present in the bulk organic solvent phase is negligible at all water concentrations studied in all the three systems.

(2) The results of polarity probe and ANSA fluorescence emission maxima studies reveal that the polarity of the water pool is much lower than that of bulk water. The difference in polarity between the water pool and bulk water decreases with increasing water concentration in benzene and carbontetrachloride systems. However, in the cyclohexane system, at the point of 'reverse micelle-liquid crystalline' transition, the polarity

of the water pool is found to decrease.

(3) Proton NMR chemical shift studies indicate that at low water concentrations the water molecules are weakly hydrogen bonded in these systems.

(4) Proton NMR spin-lattice relaxation time studies show that one water molecule is tightly bound to the polar head group.

(5) From proton NMR spin-lattice relaxation times it is found that the rotational correlation time ( $\tau_c$ ) of the water pool is long at low water concentrations and that, as a function of added water,  $\tau_c$  approaches the value for normal, bulk water ( $3 \times 10^{-12}$  secs.).

(6) The microviscosity of the water environment is very high at low water concentrations and falls off rapidly with added water.

(7) Proton NMR spin-spin relaxation time studies reveal that in addition to intramolecular dipole relaxation the observed relaxation processes are possibly strongly influenced by exchange narrowing, spin-rotational and chemical shift anisotropy.

(8)  $^{13}\text{C}$ -NMR studies confirm that aggregation leads to the collapse of the N-methyl triplet.



REFERENCES

1. G. Guilbault, in 'Practical Fluorescence,' Marcel Dekker, New York, 1973, p. 14.
2. G. Herzberg, in 'Molecular Spectra and Molecular Structure, II, Infrared and Raman Spectra of Polyatomic Molecules,' Van Nostrand Reinhold Co., New York, 1945, p. 280.
3. O.D. Bonner and Y.S. Choi, J. Phys. Chem., 78, 1723 (1974).
4. M. Seno, K. Araki, S. Shiraishi, Bull. Chem. Soc. Japan, 49, 899 (1976).
5. J. Sunamoto, T. Hamada, T. Seto and S. Yamamoto, Bull. Chem. Soc. Japan, 53, 583 (1980).
6. J.W. Falco, R.D. Walker Jr. and D.O. Shah, Am. I. Chem. Eng. J., 20, 510 (1974).
7. E. Rotlevi and A. Treinin, J. Phys. Chem., 69, 2645 (1965).
8. J.H. Fendler, Acc. Chem. Res., 9, 153 (1976).
9. F.M. Menger, J.A. Donohue and R.F. Williams, J. Am. Chem. Soc., 95, 286 (1973).
10. J.H. Fendler and L.J. Liu, J. Am. Chem. Soc., 97, 999 (1975).
11. J.H. Fendler, F. Nome and H.C. Van Woert, J. Am. Chem. Soc., 96, 6745 (1974).
12. W. Hinze and J.H. Fendler, J. Chem. Soc. Dalton Trans., 238 (1975).
13. L. Brand, in 'Probes and Membrane Function,' Eds. B. Chance, C.P. Zee and J.K. Blasie, Academic Press, New York, 1971, p. 17.
14. D.C. Turner and L. Brand, Biochemistry, 7, 3381 (1968).
15. E.M. Kosower, 'An Introduction to Physical Organic Chemistry,' Wiley, New York, 1968.

16. B. Chance and G.K. Radda, in Ref. 13, p. 13.
17. M. Nishimura, in Ref. 13, p. 227.
18. Y.H. Shaw, L.S. Kan and N.C. Li, J. Mag. Res., 12, 209 (1973).
19. G. Klose and F. Stelzner, Biochim. Biophys. Acta, 363, 1 (1974).
20. M.A. Wells, Biochemistry, 13, 4937 (1974).
21. B.M. Fung and J.L. McAdams, Biochim. Biophys. Acta, 451, 313 (1976).
22. T.O. Henderson, T. Glonek and T.C. Myers, Biochemistry, 13, 623 (1974).
23. B. Pullman and H. Berthod, FEBS Lett., 44, 266 (1974).
24. B. Pullman and H. Berthod, C.R. Acad. Sci. Ser. D, 278, 1433 (1974).
25. H.G. Hertz, 'Progress in NMR Spectroscopy,' Vol. III, Pergamon Press, Oxford, 1967.
26. J.N. Shoolery and B.J. Alder, J. Chem. Phys., 23, 805 (1955).
27. S.G. Frank, Y.H. Shaw and N.C. Li, J. Phys. Chem., 77, 238 (1973).
28. H.G. Hertz, Ber. Bungenes, Phys. Chem., 68, 907 (1964).
29. D.E. Woessner and J.R. Zimmermann, J. Phys. Chem., 67, 1590 (1963).
30. K. Krynicky, Physica, 32, 167 (1966).
31. J.B. Davenport and L.R. Fisher, Chem. Phys. Lipids, 14, 275 (1975).
32. T.L. James, 'NMR in Biochemistry,' Academic Press, New York, 1975, p. 43.
33. N. Bloembergen, E.M. Purcell and R.V. Pound, Phys. Rev., 73, 679 (1948).

34. R. Cooke and I.P. Kuntz, *Ann. Rev. Biophys. Bioeng.*, 4, 267 (1975).
35. W.V. Walter and R.G. Hayes, *Biochim. Biophys. Acta*, 249, 528 (1971).
36. M. Shinitzky, A.C. Dianoux, C. Gilter and G. Weber, *Biochemistry*, 10, 2106 (1971).
37. H.J. Pownall and L.C. Smith, *J. Am. Chem. Soc.*, 95, 3136 (1973).
38. C. Kumar and D. Balasubramanian, *J. Phys. Chem.*, 84, 1895 (1980).
39. E.J. Staples and G.J.T. Tiddy, *J. Chem. Soc., Faraday Trans. I*, 74, 2530 (1978).
40. H.S. Gutowsky, O.W. McCall and C.P. Slichter, *J. Chem. Phys.*, 21, 279 (1953).
41. H.M. McConnell, *J. Chem. Phys.*, 28, 430 (1958).
42. T.J. Swift and R.E. Connick, *J. Chem. Phys.*, 41, 2553 (1964).
43. E.R. Andrew, in 'Nuclear Magnetic Resonance,' Cambridge University Press, 1955, p. 109.
44. N.J.M. Birdsall, J. Feeney, A.G. Lee, Y.K. Levine and J.C. Metcalfe, *J. Chem. Soc. Perkin Trans. II*, 1441 (1972).
45. R. Murari and W.J. Baumann, *J. Am. Chem. Soc.*, 103, 1238 (1981).
46. R.E. London, T.E. Walker, D.M. Wilson and N.A. Matwiyoff, *Chem. Phys. Lipids*, 25, 7 (1979).

## CHAPTER IV

### NMR OF WATER DIFFUSION IN THE CYCLOHEXANE SYSTEM

From the results of the previous chapters, there is strong empirical evidence to indicate that, in the cyclohexane solvent system, at  $R$  values in excess of 6, a profound change occurs in the reverse micellar arrangement of the phospholipid head groups and the motional state of the trapped water pool. The change has been rationalised as being due to the onset of an ordered liquid crystalline phase, possibly complemented by the intercalation of cyclohexane molecules between successive hydrocarbon chains in the hydrophobic region. Granted that such an ordered arrangement does set in, the dynamics of water in the 'pool' should then be profoundly influenced at  $R \geq 6$ .

In this chapter, this aspect of the work is further highlighted by performing a very specific and sensitive magnetic resonance experiment, namely, the measurement of the self-diffusion coefficient of water at various  $R$  values. Elsewhere in the literature, measurements of diffusion coefficient of cell water in biological systems has disclosed reductions of as much as 50% in the diffusion coefficient of this water compared to that of pure bulk water (1-8).

Translational self-diffusion coefficients ( $D$ ) in single as well as multiphase systems are most conveniently measured by observing the loss of phase coherence of a set of precessing nuclear spins due to their random motion over a gradient in the magnetic field (9). This method (MFG-NMR) is the basis of the measurements presented in this chapter and hence a brief review of the method shall be presented.

As is well known (10,11) a general method for measuring nuclear transverse relaxation times  $T_2$  is by studying the decay of the transverse component of magnetisation - i.e., the component in the xy plane when the Zeeman field is along the z direction.

$$\vec{M}_\perp = \vec{i} M_x + \vec{j} M_y \quad \dots(4.1)$$

Hahn (12) has pioneered the use of the  $90^\circ$ - $\tau$ - $180^\circ$  r.f. pulse sequence for measuring  $T_2$ . Fig. 4.1 illustrates the basic mechanism of the process.

In Fig. 4.1A, the net magnetisation at equilibrium is polarised along the direction of the Zeeman field  $\vec{H}_0$ . When a  $90^\circ$  r.f. pulse is applied to such a system, Fig. 4.1B, the magnetic moment is mutated and aligned along  $y'$  axis giving a non-zero value to the transverse component of the magnetisation. Due to spin-spin relaxation process (time constant  $T_2$ ) and inhomogeneities in the magnetic field, however, the component along the  $y'$  axis begins to decay. The magnetic field is intentionally made slightly inhomogeneous such that the inhomogeneity effect overrides the  $T_2$  relaxation process. The decay of the component along  $y'$  axis by magnetic field inhomogeneity is represented by  $T_2^*$ , the decay constant. The individual spins will have different precessional frequencies because of the field inhomogeneity created, and hence start fanning out in  $x'y'$  plane because of the loss of phase coherence and this situation is

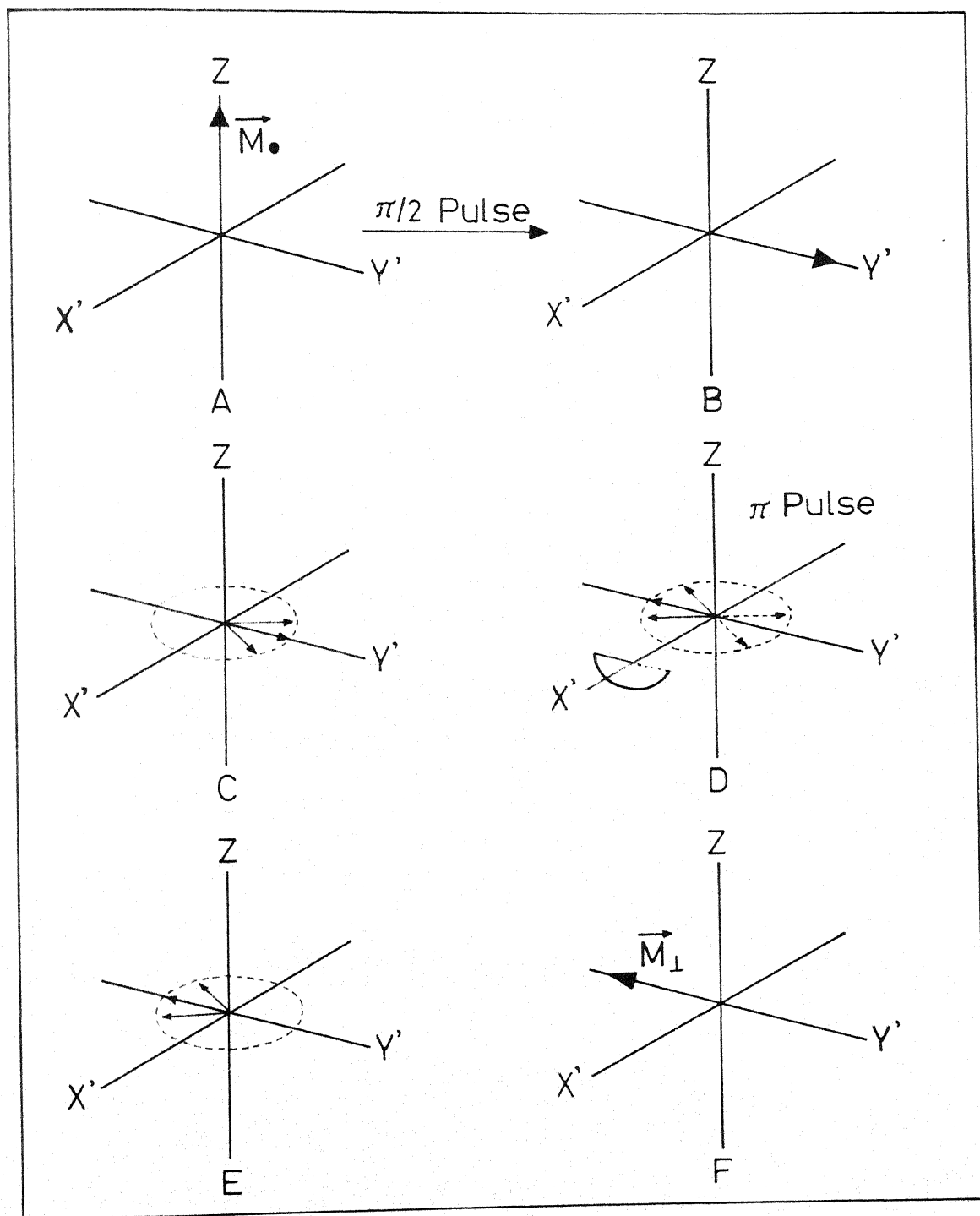


Fig. 4.1 The 90°- $\tau$ -180°  $T_2$  experiment with formation of a spin echo.

represented in Fig. 4.1C. After a time  $\tau$ , a  $180^\circ$  pulse is applied to flip the spins by  $180^\circ$  Fig. 4.1D. Now the individual spins will be precessing with the same individual Larmor frequencies as before, and this situation is shown in Fig. 4.1E. These precessing spins will again be in phase after a time  $2\tau$  but the orientation will be in the negative  $y'$  direction, Fig. 4.1F. This will result in an induced signal being detected in the absence of an r.f. field; and this signal is referred to as 'spin echo'. After the spin echo, the individual spins will again go out of phase and fan out in the  $x'y'$  plane, with a time constant  $T_2$ . The magnitude of  $\vec{M}_I$  as a result of this decay will be given by the amplitude of the spin echo. Therefore, a measurement of spin echo amplitudes for different values of  $\tau$ , the time between two pulses, provides a means for determining  $T_2$ .

A variation of Hahn's (12) spin echo method has been developed by Carr and Purcell (13). In this method, a  $90^\circ$  pulse at time  $t = 0$  is applied first, followed by a train of  $180^\circ$  pulses at times  $\tau$ ,  $3\tau$ ,  $5\tau$  etc. These  $180^\circ$  pulses refocus the individual spins to form echoes at times  $2\tau$ ,  $4\tau$ ,  $6\tau$ , etc. The major drawback of this Carr-Purcell (13) sequence is that any error in setting up the  $180^\circ$  pulse is cumulative. That is, if the ' $180^\circ$  pulse' only turns the magnetisation through  $(180-\alpha)^\circ$  on the first pulse, then after application of second pulse, the magnetisation will make an angle of  $2\alpha$  with the  $x'y'$  plane, and on the third  $3\alpha$  and so on. As the measured signal corresponds to the magnetisation in the  $x'y'$  plane, this becomes progressively more important.



To overcome this difficulty, Meiboom and Gill (14) modified the Carr-Purcell sequence. Here, the  $180^\circ$  pulses are not applied in phase with the  $90^\circ$  pulse, but rather with a phase shift of  $90^\circ$ . This modification of a  $90^\circ$  phase shift after the first  $90^\circ$  pulse renders the precise setting of the  $180^\circ$  pulse width less critical. The phase shift also eliminates effects caused by inhomogeneities in the r.f. field. At present, the common pulsed NMR method used for  $T_2$  measurements, and perhaps the most accurate, is the one utilising the Carr-Purcell-Meiboom-Gill (CPMG) pulse sequence.

Now the effects of diffusion enter the picture in the following way. In an isotropic environment, the peak amplitude of the water proton spin echo may be given by (15)

$$M(2\tau) = M(0) \exp\left[-\left(\frac{2\tau}{T_2}\right) - \left(\frac{2}{3}\right) \gamma^2 D \tau^3 G^2\right] \quad \dots (4.2)$$

where  $\tau$  is the time interval between the  $90^\circ$  and  $180^\circ$  pulses,  $G$  is the applied magnetic field gradient in gauss/cm, and  $D$  is the diffusion coefficient having the units of  $\text{cm}^2/\text{sec}$ . In Eq.4.2, the term involving  $D$  takes account of the extra damping suffered by the transverse nuclear magnetisation due to the change in the Larmor frequency resulting from the translational diffusion of the spins across the inhomogeneous magnetic field. Since we can choose  $G$  to have a fixed, precalibrated value over the sample volume in our experiment, and since we could measure  $T_2$  rather precisely by the above mentioned techniques (e.g., via the

familiar CPMG sequence)  $D$  can be determined directly from the slope of a plot of  $\log [M(2\tau) + \frac{2\tau}{T_2}]$  versus  $\tau^3$ .

For water diffusion in an anisotropic environment, Eq. 4.2 has to be modified (16). In the specific instance of a liquid crystalline or elongated 2-dimensional phase, the diffusion of trapped water will be mainly parallel to the long axis. An angular dependence is then imparted to the diffusion tensor (which will now be cylindrically symmetric) according to the formula

$$D_{\text{aniso}} = \langle D_{\perp} \rangle + (\langle D_{\parallel} \rangle - \langle D_{\perp} \rangle) \sin^2 \theta \quad \dots (4.3)$$

where  $\langle D_{\parallel} \rangle$  and  $\langle D_{\perp} \rangle$  are the components of the diffusion tensor parallel and perpendicular to the long axis of the anisotropic phase, and  $\theta$  is the angle between the field gradient direction and the normal to the preferred axis for diffusion (16). Since, for our assumed model,  $\langle D_{\parallel} \rangle \gg \langle D_{\perp} \rangle$ , the latter may be neglected and Eq. 4.3 may then be rewritten as

$$D_{\text{aniso}} = \langle D_{\parallel} \rangle \sin^2 \theta = D (1 - \mu^2) \quad \dots (4.4)$$

where  $D_{\text{aniso}} = D_{\parallel}$  and  $\mu = \cos \theta$ .

With the above redefinition, the echo amplitude, Eq. 4.2, may be modified to

$$M(2\tau) = M(0) \exp \left[ \left( -\frac{2\tau}{T_2} \right) - \left( \frac{2}{3} \right) \gamma^2 G^2 D (1 - \mu^2) \tau^3 \right] \quad \dots (4.5)$$

In our model, all values of  $\mu = \cos \theta$  are equally probable, and therefore, we have to perform an integration over the angular variable, namely,

$$M(2\tau) = M(0) \exp\left(-\frac{2\tau}{T_2}\right) \int_0^1 \exp\left(-\frac{2}{3} \gamma^2 G^2 D (1-\mu^2) \tau^3\right) d\mu \quad \dots (4.6)$$

$$= M(0) \exp\left(-\frac{2\tau}{T_2}\right) \exp\left(-\frac{2}{3} \gamma^2 G^2 D \tau^3\right) f(y) \quad \dots (4.7)$$

$$\text{where } y = \left(\frac{2}{3} \gamma^2 G^2 D \tau^3\right)^{1/2}$$

$$\text{and } f(y) = \frac{1}{y} \int_0^1 \exp(\mu^2) d\mu.$$

It is thus seen that the term  $f(y)$  supplies the requisite correction to Eq. 4.2 for our case of anisotropic diffusion in the randomly oriented canal structures.

Using a Bruker, B-KR 322S, pulse spectrometer and a precalibrated Bruker B-KR 300 Z18 field gradient unit,<sup>†</sup> we have measured the rate of decay of spin echo signals in the presence of known magnetic field gradients to estimate the self-diffusion coefficient of the water phase; the echoes were observed at time  $2\tau$  of a  $90^\circ$ - $\tau$ - $180^\circ$  ( $90^\circ$ ) NMR pulse train, where the subscript ( $90^\circ$ ) indicates that the phase of the r.f. carrier of the second pulse is shifted by  $90^\circ$  relative to the first.  $T_2$  was evaluated to an estimated accuracy of  $\pm 5\%$  using the Carr-Purcell-Meiboom-Gill

---

<sup>†</sup>The preliminary data on which this chapter is based were recorded by Prof. P. Raghunathan, during a summer visiting appointment at the Department of Chemistry, University of British Columbia, Vancouver, Canada.

pulse train (14) corrected for baseline drift by the procedure of Hughes (17). All signal amplitude measurements were either read out directly from a Tektronix storage oscilloscope or (for weaker signals) recorded by an electronic digital readout at the output of a high speed signal averager. In Table 4.1 we present the values of  $T_2$  obtained by this method and the  $T_2$  values calculated from the experimental spectra ( $T_2 = \frac{1}{\pi \Delta \nu_{1/2}}$ ), at different R values. Within the error limit of the two methods, agreement between the two  $T_2$  values is quite satisfactory.

Table 4.1

Comparison of  $T_2$  values from experimental linewidth and from CPMG sequence at different R values for cyclohexane system

R	$T_2$ from linewidth [ $T_2 = \frac{1}{\pi \Delta \nu_{1/2}}$ ] (seconds)	R	$T_2$ from CPMG Sequence (seconds)
1	-	1.0	0.045
2	0.040	2.0	0.066
4	0.071	4.3	0.080
6	0.091	6.5	0.112
8	0.053	8.6	0.063
10	0.043	10.8	0.045
		13.0	0.041

In our diffusion coefficient measurements, it was important that during each experiment the NMR probe was thermostated to within  $\pm 0.5$  K. Depending on the choice of field gradient strengths, probe temperatures ranged from  $23^{\circ}$  to  $25^{\circ}\text{C}$ . Larmor frequencies also had to be readjusted slightly from experiment to experiment around a central value of 30 MHz. The spacing between pulse trains was always greater than  $\sim 6$  times the  $T_1$  of the sample.

To minimise the errors due to the probe temperature and other variations to which absolute value of  $D$  may be sensitive, all results were converted to the dimensionless ratios  $D/D_0$ , the diffusion coefficient of the sample relative to that of triply distilled water; here the sample sizes and diameters of the tubes (5 mm OD) were chosen to be identical.

Table 4.2

Self-diffusion coefficient,  $D_0$ , of pure water at  $25^{\circ}\text{C}$

Value of $D_0$ $\text{cm}^2/\text{sec.}$	Temp ( $^{\circ}\text{C}$ )	Method of Measurement	Ref.
$2.51 \times 10^{-5}$	25	Pulsed field gradient spin echo	18
$2.40 \times 10^{-5}$	25	„	19
$2.23 \times 10^{-5}$	25	Steady field gradient spin echo	20
$2.28 \times 10^{-5}$	25	Pulsed field gradient spin echo	21
$2.37 \times 10^{-5}$ Average of six values	25	Steady field gradient spin echo	Our work

As an internal consistency check of our measurement, we compare in Table 4.2 our  $D_0$  value for pure water at  $24 \pm 1^\circ\text{C}$  (average of six measurements) with available literature values reported for distilled water at  $25^\circ\text{C}$ .

Figs. 4.2 to 4.4 show the plots of  $\ln M(2\tau) + \frac{2\tau}{T_2}$  versus  $\tau^3$  at different field gradients.

From the slopes of Figs. 4.2 to 4.4 the diffusion coefficient  $D$  of water in the water pools is calculated using

$$\text{slope} = \frac{2}{3} \gamma^2 G^2 D$$

The non-linear trend seen in Fig. 4.5 clearly corresponds to diffusion in the anisotropic phase. To calculate  $D$  from this curve, Eq. 4.7 was fitted to the data points by a two parameter ( $D, \tau$ ) non-linear least squares fit where the integral was numerically evaluated on the DEC 10 computer by a 'Simpson's  $\frac{1}{3}$  - rule' library subroutine (22). Fig. 4.5 shows the experimental points and the 'best fit' line through them. The ratio of this  $D$  to the  $D_0$  value (for triple-distilled water) obtained under identical experimental conditions) turns out to be 0.658, as shown in Table 4.3. The values of  $D$  thus obtained and the values of  $D_0$  for pure water are shown in Table 4.3 for different  $R$  values.

The variation of relative self-diffusion coefficient  $D/D_0$  versus  $R$  is pictorially represented in Fig. 4.6.

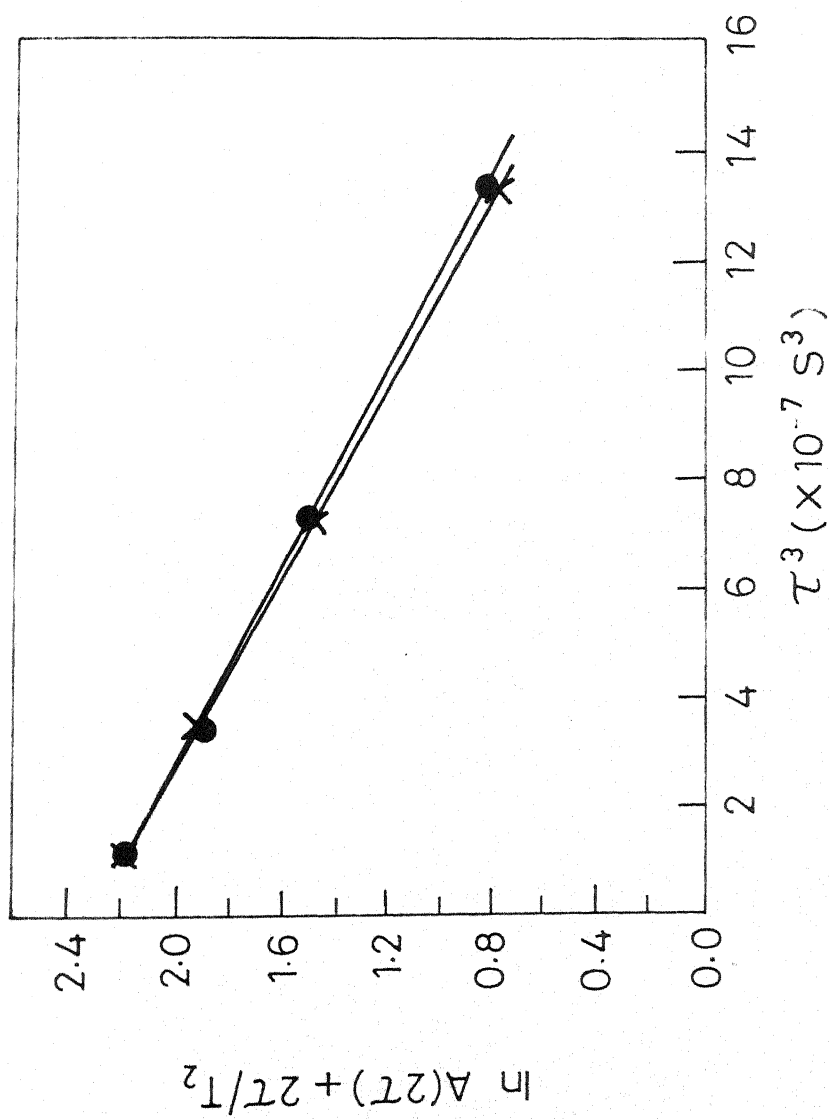


Fig. 4.2 Spin echo amplitude versus  $\tau^3$  for steady applied field Gradient of 10.1 Gauss/cm  
 $D_0 = (x-x-x) = 2.75 \text{ cm}^2/\text{s}$   
 $D = (\bullet-\bullet-\bullet) = 2.24 \text{ cm}^2/\text{s}$

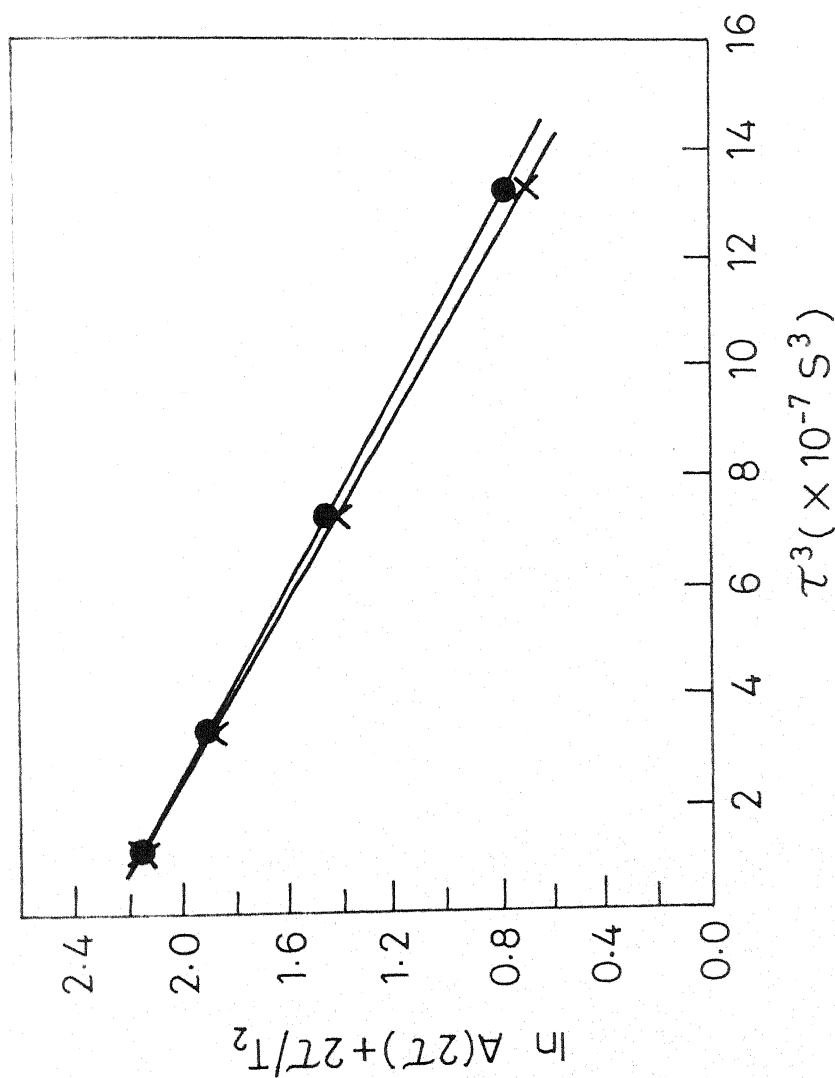


Fig. 4.3 Spin echo amplitude versus  $\tau^3$  for steady applied field Gradient of 10.4 Gauss/cm  
 $D_0 = 2.44 \text{ cm}^2 \text{ sec}^{-1} = (x-x-x)$   
 $D = 2.09 \text{ cm}^2 \text{ sec}^{-1} = (\bullet-\bullet-\bullet)$



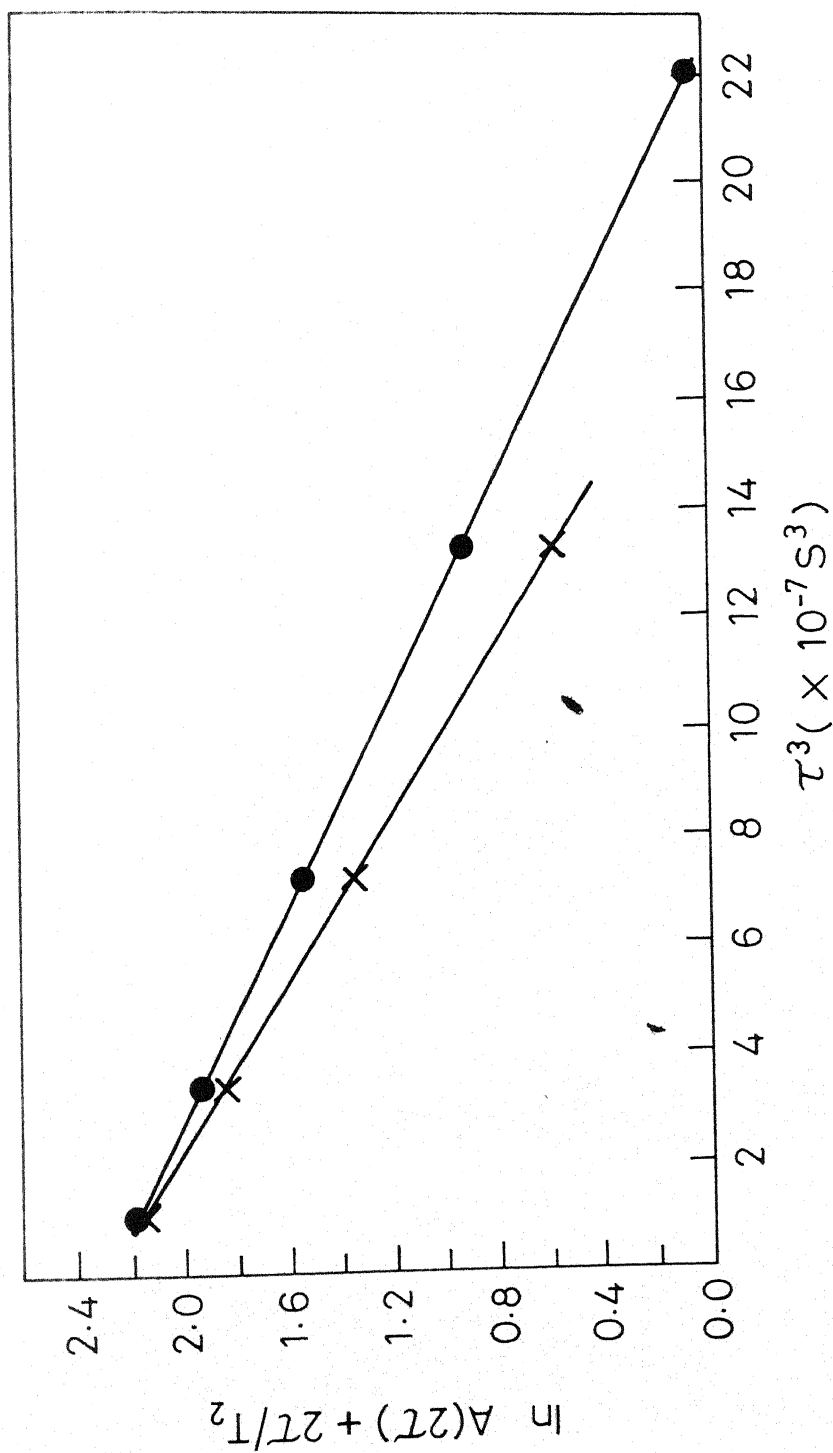


Fig 4.4 Spin echo amplitude versus  $\tau^3$  for steady applied field

Gradient of 10.7 Gauss/cm

$D_0 = 2.35 \times 10^{-5} \text{ cm}^2 \text{ sec}^{-1} = (\text{x}-\text{x}-\text{x})$

$D = 1.86 \times 10^{-5} \text{ cm}^2 \text{ sec}^{-1} = (\bullet-\bullet-\bullet)$

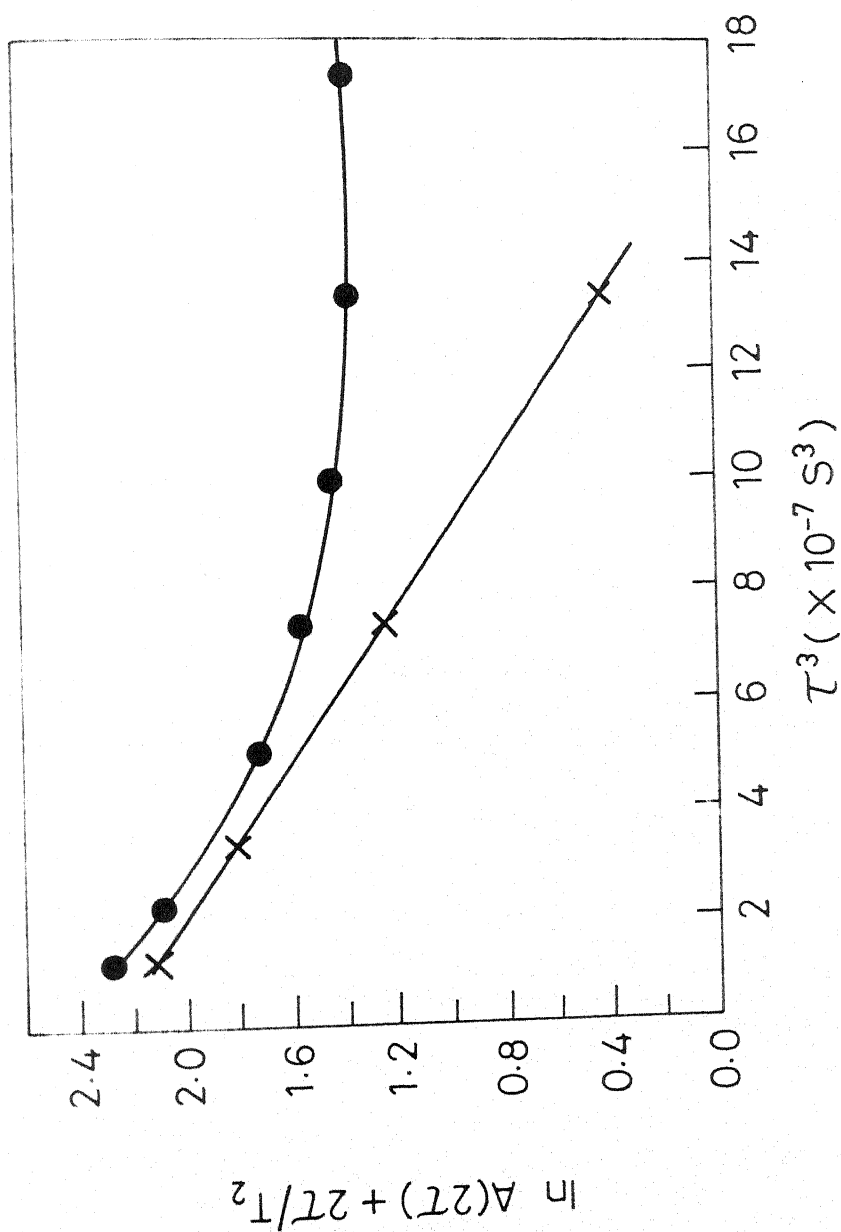


Fig 4.5 Spin echo decay rate versus  $\tau^3$ .  
 The solid line represents the fit of eq. 4.7  
 to the experimental data (●)  
 $D_0 = (x-x-x) = 2.37 \times 10^{-5} \text{ cm}^2/\text{s}$   
 $D = (\bullet-\bullet-\bullet) = 1.56 \times 10^{-5} \text{ cm}^2/\text{s}$  (best fit)

Table 4.3

Variation of self-diffusion coefficient of  
water as a function of R

R	D cm <sup>2</sup> sec <sup>-1</sup> , 10 <sup>-5</sup>	D <sub>0</sub> cm <sup>2</sup> sec <sup>-1</sup> , 10 <sup>-5</sup>	D/D <sub>0</sub>
1	2.0341	2.3523	0.865
2	2.2414	2.3521	0.953
4.3	2.2064	2.3448	0.941
6.5	2.1689	2.3343	0.929
8.6	2.0926	2.4414	0.857
10.8	1.8598	2.3577	0.790
13.0	1.5601	2.3724	0.658

From Fig. 4.6 one sees that the relative self diffusion coefficient increases first and then remains constant upto an R value of 6.5 followed by a sudden decrease in the D/D<sub>0</sub> value. This again confirms our idea, earlier presented in Chapters II and III, that in cyclohexane solvent system around an R value of 6 there is a transition from the isotropic reverse micellar to an anisotropic phase which affects the mobility of the water pool.

For water molecules diffusing in a barrier free system, the root mean square displacement of a water molecule in, say, the X direction,  $\langle(\Delta x)^2\rangle^{1/2}$  occurring during time t, is

related to the self-diffusion coefficient,  $D$ , by the well known Einstein relationship

$$\langle (\Delta x)^2 \rangle^{1/2} = 2 D t$$

If barriers that halt free motion (or obstructions that hinder free motion) are present, the measured value of  $D$  will of course be less than the corresponding value in the unhindered bulk fluid state. In theory, if  $2\tau$  can be made short enough (roughly less than the root mean square time for a molecule to diffuse between barriers or obstructions) (23,24), NMR pulse techniques should yield a 'faithful' measurement of the  $D$  value for the confined fluid.

Using the above analysis, if diffusion barriers are present and sufficiently close together,  $D$  becomes a function of the applied gradient and the echoes no longer decay as  $\tau^3$  (23). In our 'earlier' ( $R \leq 6$ ) measurements, value of  $D$  was constant when  $G^2$  was varied by a factor of  $\sim 20$  and all echo decays were linear in  $\tau^3$  to  $2\tau \sim 25$  msec. for the smallest gradient used. Hence any barrier must be more than  $[2D(25 \text{ msec})]^{1/2}$  apart, i.e., 10 microns apart. This is in agreement with the estimates of the upper limit of micellar size by our electron microscopy experiments presented in Chapter II (namely, 0.1 microns).

Although the above estimate of the diffusion of trapped water is somewhat crude, it should be here mentioned that more sophisticated NMR experiments such as the pulsed field gradient

technique (9) as well as more recent experimental refinements such as (i) Techniques for diffusion measurement in presence of small and large background gradients (25,26) and (ii) methods for absolute measurement of  $D$  without recourse to a standard sample (27) should further improve our understanding of the lecithin-cyclohexane-water systems.

In context of our present observation, a host of somewhat similar studies on biological cell and protein bound water may be cited (1-8, 24). Many of these studies have revealed that the diffusion coefficient of water molecules in the living tissue is reduced by a factor of approximately 2 compared with the value for pure water. Three explanations for the observed reduction in the diffusion coefficient have been frequently advanced:

- (i) The intracellular membrane systems serve to compartmentalise the cytoplasmic water.
- (ii) Intracellular protein structures serve as obstruction to diffusion of cytoplasmic water; and
- (iii) The water-protein interaction induce long-range changes in the water-water interaction in a substantial fraction of the intra cellular water.

Of the three above explanations an interaction of the last type, in our case the water-lipid interaction, is more likely to be significant in the low  $R$  value region of our experiment.

At low concentration of water, the initial portion of water binds to the phospholipid at the interface for a long time compared

with the correlation time for bulk water with a diffusion constant  $D_v = 2.03 \times 10^{-5} \text{ cm}^2/\text{sec}$ . A lower limit for  $D_v$  is the diffusion coefficient for the phospholipid reverse micelle aggregate itself. As far as we know, this diffusion coefficient has not been measured. Such an independent measurement, together with our present measurements of the diffusion coefficient of water as well as the proton relaxation rates as a function of added water (earlier presented in Chapter III) should be useful in formulating a complete theory of the 'head group versus water' dynamics at the interface.

REFERENCES

1. J.H. Wang, J. Am. Chem. Soc., 76, 4775 (1954).
2. T.L. James and K.T. Gillen, Biochim. Biophys. Acta, 286, 10 (1972).
3. E.E. Burnell, M.E. Clark, J.A.M. Hinke and N.R. Chapman, Biophys. J., 33, 1 (1981).
4. E.D. Finch, J.F. Harmon and B.H. Muller, Archives Biochem. Biophys., 147, 299 (1971).
5. J.R. Hansen, Biochim. Biophys. Acta, 230, 482 (1971).
6. D.C. Chang, C.F. Hazelwood, B.L. Nichols and H.E. Rorschach, Nature, 235, 170 (1972).
7. D.C. Chang, H.E. Rorschach, B.L. Nichols and C.F. Hazelwood, Ann. N.Y. Acad. Sci., 204, 434 (1973).
8. H.E. Rorschach, D.C. Chang, C.F. Hazelwood and B.L. Nichols, Ann. N.Y. Acad. Sci., 204, 444 (1973).
9. J.E. Tanner in 'Magnetic Resonance in Colloid and Interface Science', Eds. H.A. Resing and C.G. Wade. American Chemical Society Symposium Series 34, Washington, D.C., 1976, pp.16-30.
10. A. Abragam in 'Principles of Nuclear Magnetism,' Oxford University Press, London, 1961, pp. 59-67.
11. T.L. James in 'NMR in Biochemistry', Academic Press, New York, 1975, pp. 27-30.
12. E.L. Hahn, Phys. Rev., 80, 580 (1950).
13. H.Y. Carr and E.M. Purcell, Phys. Rev., 94, 630 (1954).
14. S. Meiboom and D. Gill, Rev. Sci. Instrum., 29, 688 (1958).
15. See ref. 10, page 61.
16. R. Blinc, M. Burgar, M. Luzar, J. Pirs, I. Zupancic and S. Zumer, Phys. Rev. Lett., 33, 1192 (1974).

17. D.G. Hughes, J. Mag. Res., 26, 481 (1977).
18. N.J. Trappeniers, C.J. Gerritsma and P.H. Oosting, Phys. Lett., 18, 256 (1965).
19. L.A. Abecedarskaya, F.G. Miftahutdinova and V.D. Fedotov, Biophysics (USSR), 13, 750 (1968).
20. K.T. Gillen, D.C. Douglas and M.J.R. Hoch, J. Chem. Phys., 57, 5117 (1972).
21. C.G. Cleveland, D.C. Chang, C.F. Hazelwood and H.F. Rorschach, Biophys. J., 16, 1043 (1976).
22. T.L. Isenhour and P.C. Jurs, in 'Introduction to Computer Programming for Chemists', Allyn and Bacon, Inc., Boston, 1972, p. 278.
23. R.C. Wayne and R.C. Cotts, Phys. Rev., 151, 264 (1964) and references cited therein.
24. D.E. Woessner, J. Phys. Chem., 67, 1365 (1963).
25. W.D. Williams, E.F.W. Seymour and R.M. Cotts, J. Mag. Res., 31, 271 (1978).
26. R.F. Karlicek and I.J. Lowe, J. Mag. Res., 37, 75 (1980).
27. M.I. Hrorath and C.G. Wade, J. Chem. Phys., 73, 2509 (1980).



CHAPTER V

$^2\text{H}$  AND  $^{31}\text{P}$ -NMR LINESHAPES  
IN THE  
CYCLOHEXANE SYSTEM

## Introduction

In this, the last chapter on experimental results, two further magnetic resonance studies of the lecithin-cyclohexane-water system are described. In the first part, the deuterium magnetic resonance (DMR) spectra of various  $D_2O$  concentrations in the PC-cyclohexane-heavy water obtained by fourier transforming the  $^2H$  quadrupolar 'echo' are discussed. In the second part, the lineshapes of the  $^{31}P$ -NMR spectra of the PC-cyclohexane-water systems are examined. Both these experiments are essentially aimed at obtaining information pertaining to the dynamics of water and the phospholipid head groups as the 'dry' reverse micellar system is progressively hydrated in the cyclohexane medium.

In similar contemporary experiments in aqueous media, DMR (1-6) and  $^{31}P$ -NMR (7-9) studies are extensive, and considerable improved techniques have been developed to demonstrate rather unambiguously that water near model and biomembranes possesses significantly more structure than, and dynamically very different from, aqueous phase 'bulk' water.

## General Theory

### Quadrupolar interaction as a first order perturbation to the Zeeman energy levels of an $I > \frac{1}{2}$ nucleus

In addition to its magnetic dipole moment, a nucleus of spin  $I > \frac{1}{2}$  possesses an electric quadrupole moment which has its origin in a non-spherically symmetric nuclear charge distribution (10-12). Consequently, in addition to the magnetic dipolar

'Zeeman' interaction between the applied magnetic field and the nuclear spin ( $\mathcal{H}_Z$ ), the nucleus has an electrostatic interaction with its environment when it is in an electric field gradient (efg) which does not possess too high a degree of symmetry. The total Hamiltonian now appears as

$$\mathcal{H} = \mathcal{H}_Z + \mathcal{H}_Q \quad \dots (5.1)$$

where  $\mathcal{H}_Q$  is the quadrupolar Hamiltonian due to the interaction between the quadrupole moment  $eQ$  associated with the spin  $I$  and the electric field gradient existing at the nuclear site. In the above Eq. (5.1), the chemical shift and dipole-dipole interactions have been ignored for simplicity.

Under conditions when  $\mathcal{H}_Q \ll \mathcal{H}_Z$ , it can be shown (10,11,13) that the first order perturbation to the Zeeman energy levels due to  $\mathcal{H}_Q$  are given (in frequency units) by

$$E_m^{(1)} = \frac{e^2 q Q}{4h I (2I-1)} \left[ \frac{3 \cos^2 \Theta - 1}{2} + \frac{\eta}{2} \sin^2 \Theta \cos 2\phi \right] [3m^2 - I(I+1)] \quad \dots (5.2)$$

where  $\Theta$  and  $\phi$  are the usual polar and azimuthal angles specifying the magnetic field direction in relation to the principal coordinate system of the efg,  $m$  is the magnetic quantum number in the representation where  $I_z$  is diagonal, and  $e^2 q Q/h$  is the quadrupole coupling constant involving the product of the Z-component of the efg ( $q = V_{ZZ}/e$ ) in the principal coordinate system, and the quadrupole moment  $eQ$  associated with the spin  $I$  nucleus. The

quantity  $\eta$ , defined by

$$\eta = [ |V_{YY}| - |V_{XX}| ] / V_{ZZ} \quad \dots (5.3)$$

is called the asymmetry parameter, where  $V_{XX} = \partial^2 V / \partial X^2$ , etc., and  $V$  is the net electrostatic potential at the nuclear site. Conventionally, the efg principal axes are ordered so that

$$|V_{ZZ}| \geq |V_{YY}| \geq |V_{XX}| \quad \dots (5.4)$$

and, consequently,  $0 \leq \eta \leq 1$ . The energy levels of the total Hamiltonian in frequency units as a result of the first order perturbation solution of Eq. (5.1) are given by

$$E_m = E_m^{(0)} + E_m^{(1)} \quad \dots (5.5)$$

where  $E_m^{(0)} = E_Z(m) / h = (-\gamma H_0 / 2\pi)$ ,  $m = -\nu_0 m$ , and  $\nu_0$  is the Larmor frequency. If one defines the parameter  $\nu_Q$  as

$$\nu_Q = \frac{3}{4} \frac{e^2 q Q}{h I (2I-1)} \quad \dots (5.6)$$

then Eq. (5.5) may be rewritten as

$$E_m = -\nu_0 m + \frac{\nu_Q}{3} \left[ \frac{3 \cos^2 \theta - 1}{2} + \frac{\eta}{2} \sin^2 \theta \cos 2\phi \right] [3m^2 - I(I+1)] \quad \dots (5.7)$$

### DMR in D<sub>2</sub>O

Since the deuterium nucleus has  $I = 1$ ,  $m$  will assume values of 1, 0 and -1 and the NMR spectrum arising from a particular deuteron will consist of two sharp peaks centred about  $\nu_0$  and separated by

$$\Delta\nu = \nu_Q (3 \cos^2 \theta - 1) + \eta \nu_Q \sin^2 \theta \cos 2\phi \quad \dots (5.8)$$

One notices from Eq. (5.8) that, for cases where the efg at a Deuteron site has cylindrical symmetry, the asymmetry parameter is practically zero, reducing Eq. (5.8) to the simpler form

$$\Delta\nu = \nu_Q (3 \cos^2 \theta - 1) \quad \dots (5.9)$$

For water deuterons, although the major contribution to the efg is from the intramolecular O-D bond, there can be other contributions of intermolecular origin such as the charge distribution in the vicinity of polar head group and other interactions. Furthermore, hydrogen bonding can reduce the contribution of the O-D bond from 312 kHz (as measured in the gas phase) to 213 kHz (14-16). For such reasons  $\nu_Q$  could be different for different sites. Also, chemical exchange can take place between nuclei in different environments. If the exchange rate is much faster than the quadrupole splitting  $\Delta\nu$ , the observed splitting is a weighted average over the different sites and is given by (2,17,18)

$$\Delta\nu = \left| \sum_i P_i \nu_Q^i \right| \quad \dots (5.10)$$

where  $P_i$  is the probability (defined by the fraction of nuclei in site  $i$ ) that a nuclei is in site  $i$  with a characteristic quadrupole coupling constant  $\nu_Q^i$ .

In the extreme limit, if the isotropic tumbling motion of the quadrupolar nuclei is fast compared to the static splitting frequency, the angular term in Eq. (5.9) is averaged to zero and no splitting is observed. On the other hand, the motion in a lamellar or liquid crystalline phase would in general be expected to be anisotropic, and a splitting of the first order spectrum will usually be observed.

In summary, then,  $\Delta\nu$  data can provide useful information for a qualitative interpretation of the quadrupole splittings of the first order DMR spectrum of water system.

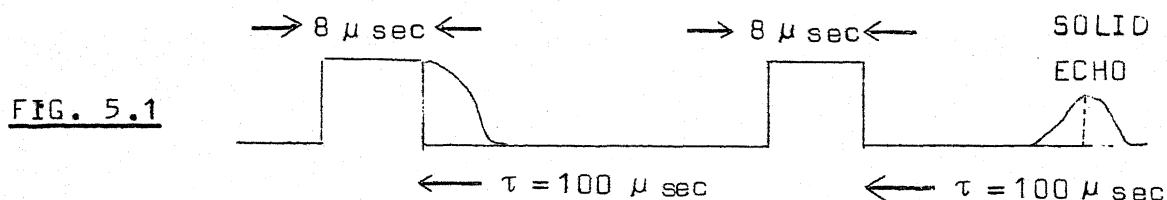
## Experimental

### DMR measurements

The conventional FT method of obtaining NMR spectra consists of applying a  $90^\circ$  rf pulse and then Fourier-transforming the free induction decay (FID). During the application of the rf pulse, the receiver of the NMR spectrometer gets saturated and a certain length of time (called the recovery time or dead time) has to elapse before it returns to its normal operating conditions. Therefore, the early part of the FID cannot be observed due to the recovery time of the rf receiver. To circumvent this problem, our DMR spectra have been obtained

using the 'solid echo' by the method of Davis et al. (19). This method consists of applying a  $90^\circ$  pulse (whose phase is zero with respect to the reference frequency) followed by another  $90^\circ$  pulse whose phase is shifted by  $90^\circ$  with respect to the first pulse at a time  $\tau$  (typically 100 microseconds or so) later. An echo is formed at  $2\tau$  due to the refocussing of the nuclear magnetisation. By Fourier transforming the echo starting at  $T = 2\tau$  the full spectrum is obtained.

The DMR spectra were obtained at a frequency of 30.71 MHz on the Bruker CXP-200 NMR pulse spectrometer/ASPECT-2000 computer system of the University of British Columbia, Canada. Storage and analysis of the data was done on a 'Diablo' model-31 single-density magnetic disc system interfaced to the ASPECT-2000. The signals were detected employing quadrature detection, and 500 scans of the solid echo were accumulated for the DMR of  $D_2O$  prior to FT. (Details of the pulse sequence employed are depicted in Fig. 5.1.)



The  $^{31}\text{P}$ -NMR spectra were recorded on a Bruker WP-80 spectrometer operating at 32.44 MHz for  $^{31}\text{P}$  nuclei.

## Results and Discussion

Figs. 5.2 to 5.8 show the DMR lineshapes in PC-cyclohexane- $D_2O$  system at various R values. In Figs. 5.2 to 5.6 a single peak is observed. In Fig. 5.7 a weak double splitting can be seen. However, in Fig. 5.8 i.e. at an R value of 8, where the spherical reverse micelle has been demonstrated by our other experiments to become anisotropic, i.e., elongated tubular structures containing aqueous canals, a deuterium doublet is observed. The characteristic double splitting in Fig. 5.8 is 4.8 kHz. The value of this splitting is much less than  $\sim 170$  kHz found in polycrystalline ice and hydrates by Soda and Chiba (20). Such low values of doublet splitting for  $D_2O$  in lecithin bilayer were observed previously by Finer and Darke (4). This low value of doublet splitting indicates that there must be some motional mechanism with a fast enough time scale to average out the electric field gradient to a certain extent.

In the spherical reverse micellar phase, i.e., upto an R value of 6, the motion is completely isotropic and produces a zero average electric field gradient (efg) and hence zero splitting. This causes a sharp singlet in Figs. 5.2 to 5.6. However, binding of  $D_2O$  to a macromolecule will produce a doublet in the deuterium NMR spectrum if the motion of the bound molecule is either slow, or is fast but anisotropic. In either case, the doublet splitting will depend on the corresponding residual efg felt by the deuterium nucleus of  $D_2O$ .



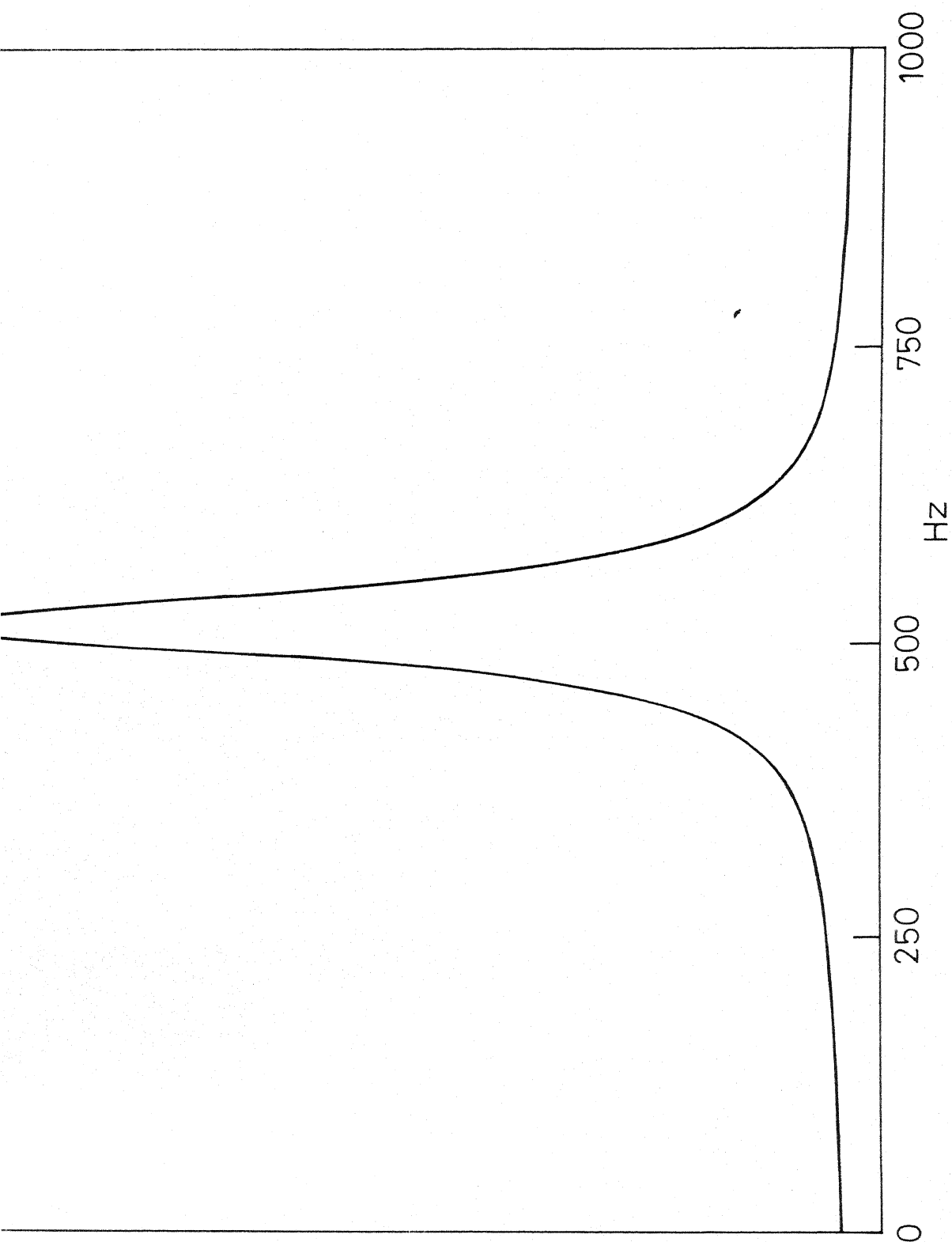


Fig. 5.2 30.71 MHz DMR Lineshape (i.e., FT of DMR Quadrupolar Echo) of PC-Cyclohexane -  $D_2O$  system at an R value of 1

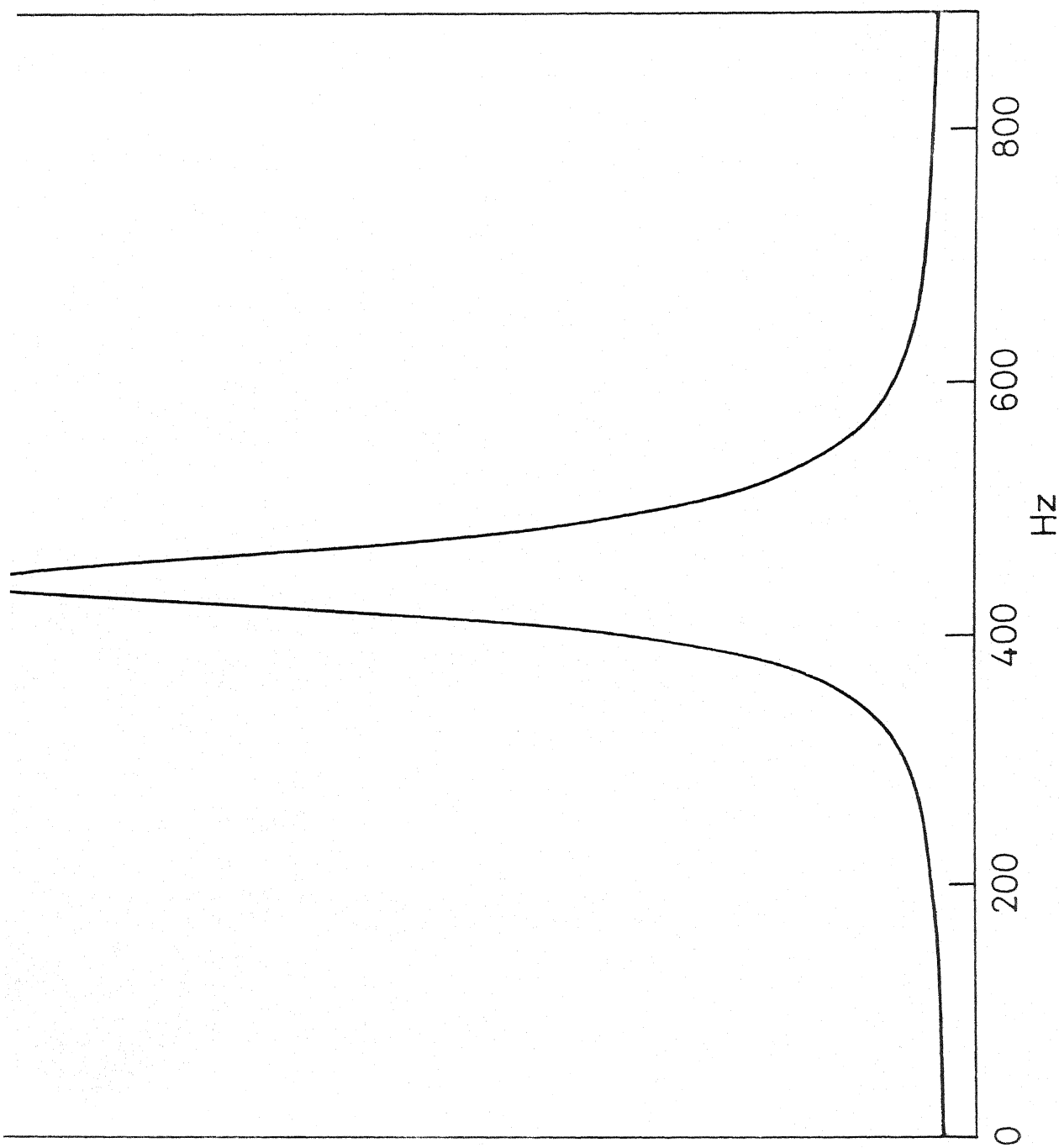


Fig. 5.3 30.71 MHz DMR Lineshape of PC-Cyclohexane - D<sub>2</sub>O system at an R value of 2

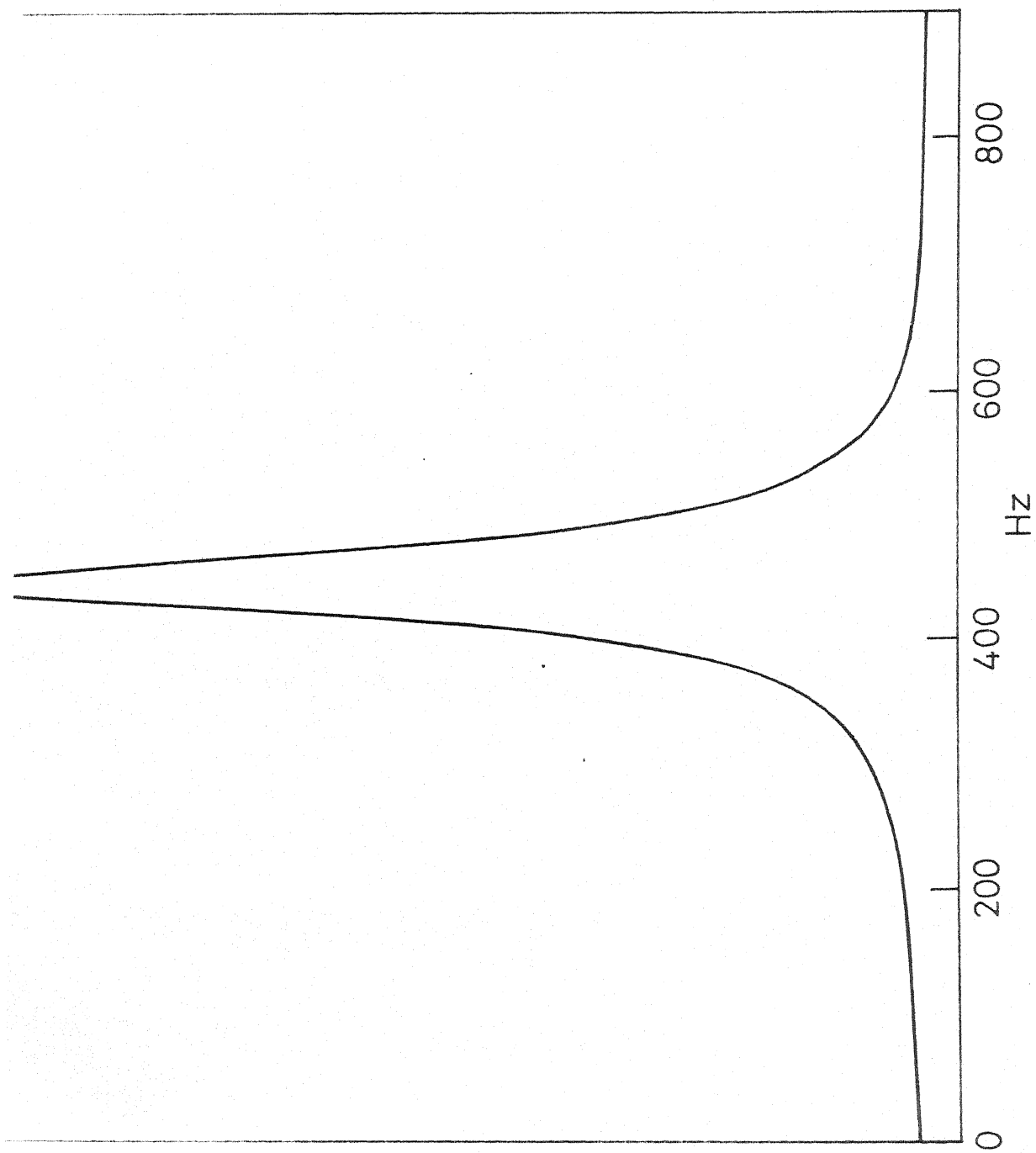


Fig. 5.4 30.71 MHz DMR Lineshape of PC-Cyclohexane -  $D_2O$  system at an R value of 3

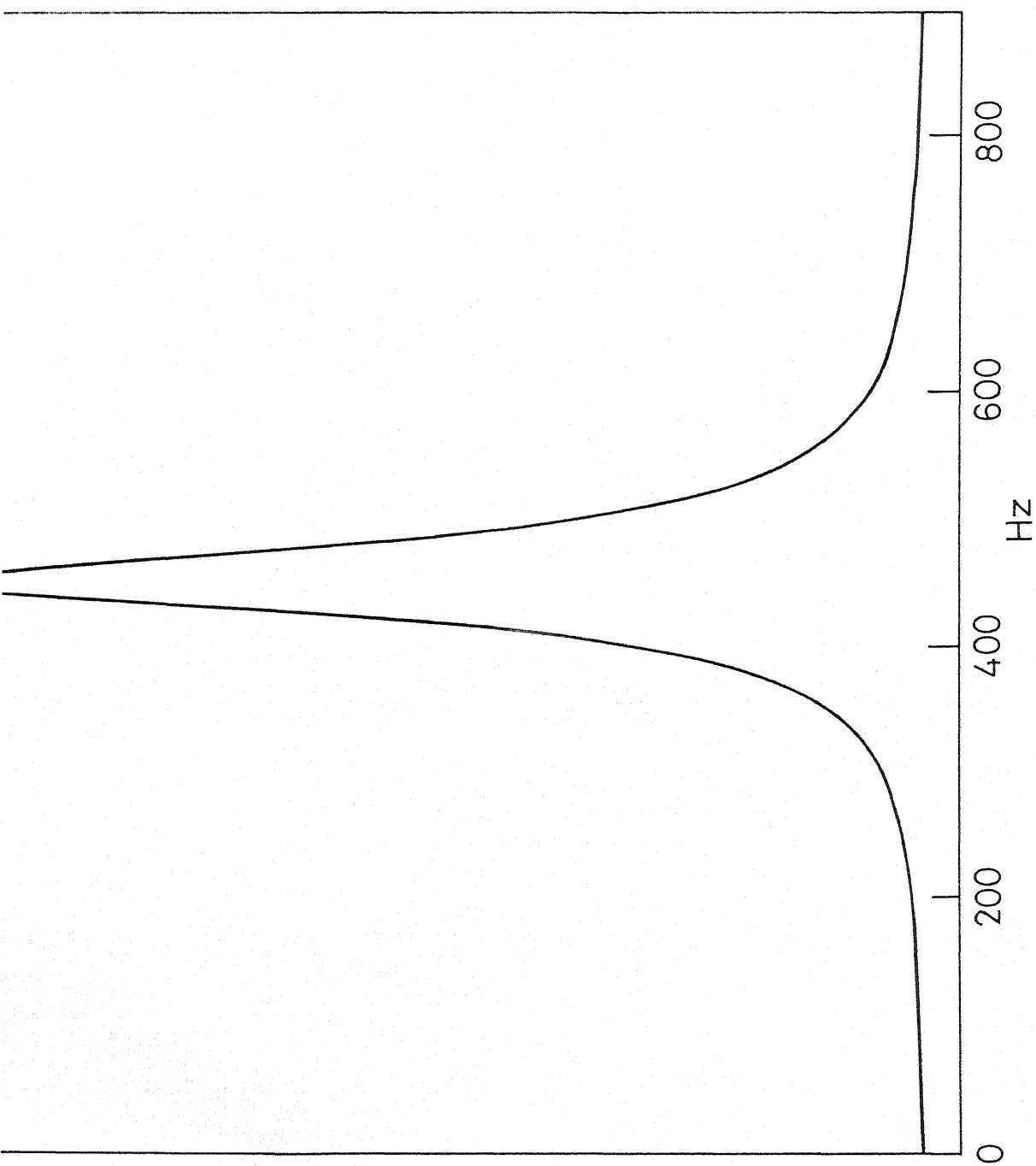


Fig. 5.5 30.71 MHz DMR Lineshape of PC-Cyclohexane- $D_2O$  system at an  $R$  value of 4

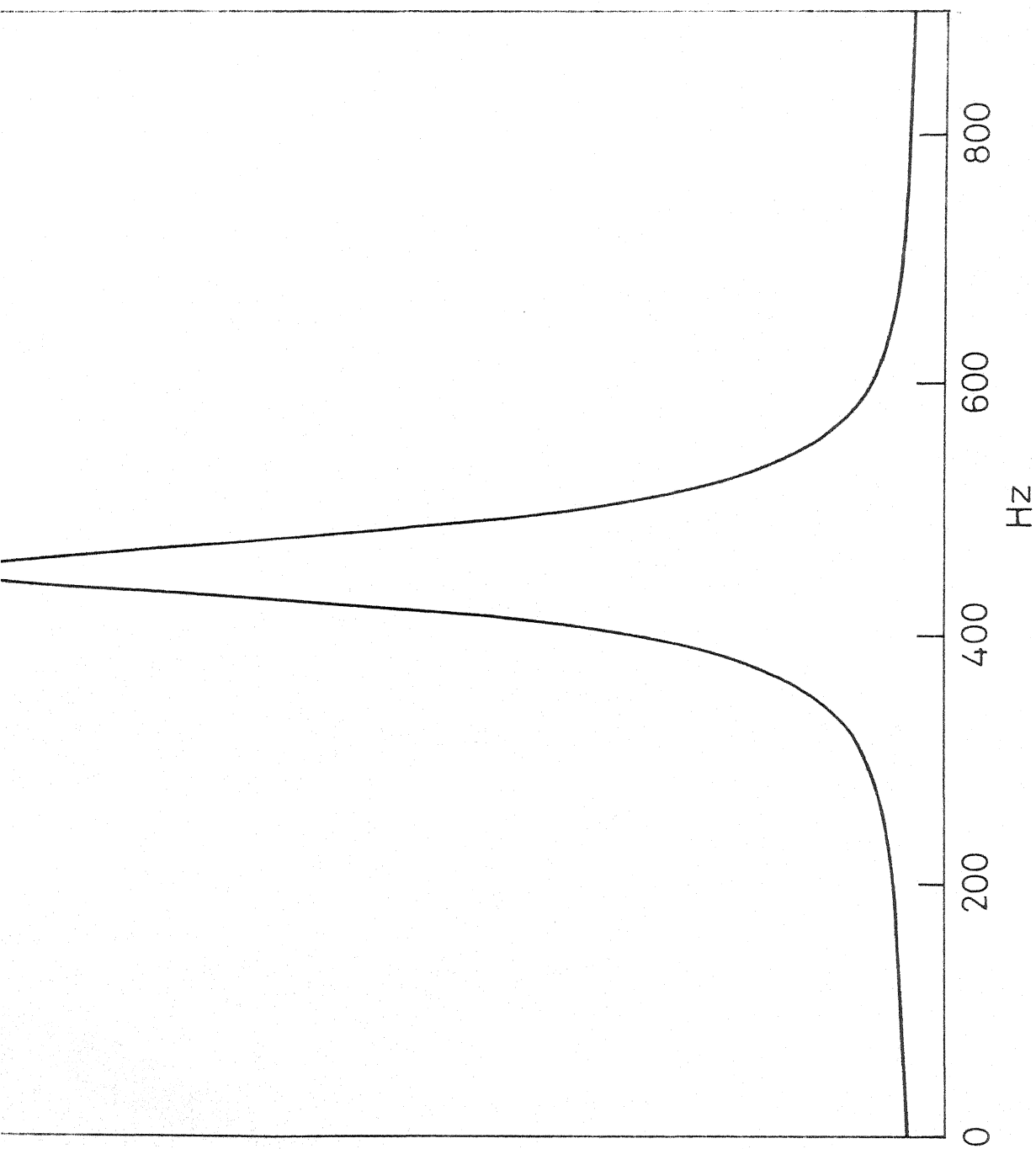


Fig. 5.6 30.71 MHz DMR Lineshape of PC - Cyclohexane -  $D_2O$  system at an R value of 5

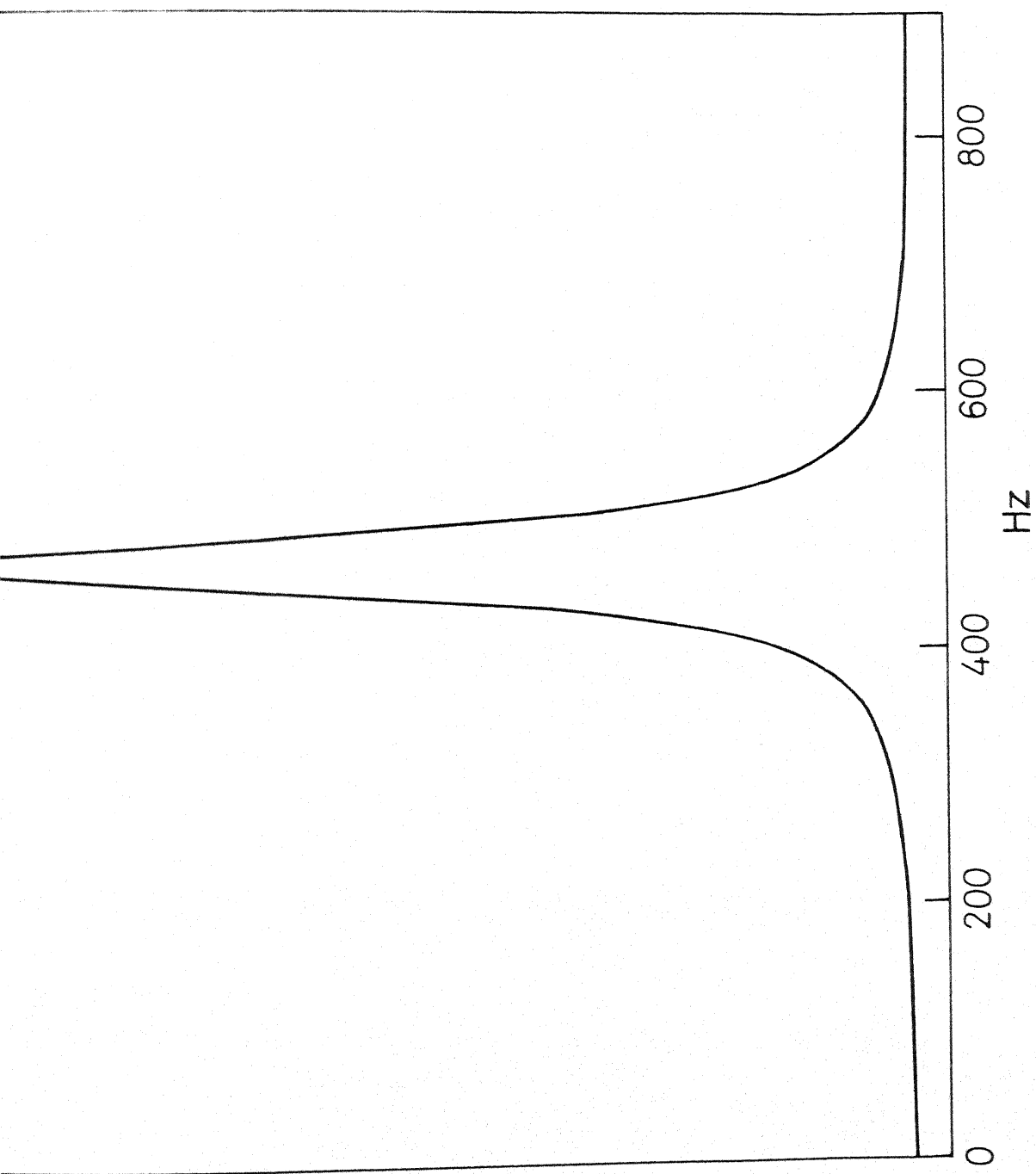


Fig. 5.7 30 71MHz DMR Lineshape of PC - Cyclohexane -  $D_2O$  system at an R value of 6.5

The time averaging of the efg, resulting eventually in a 4.7 kHz splitting, of Fig. 5.8 may be due to one or more of the following reasons: (a) exchange of water deuterons between the binding sites; (b) diffusion of water molecules along the aqueous channel; (c) tumbling motion of bound  $D_2O$  while being constantly bound and released from the binding site and (d) motion of the group to which water is bound.

Motional averaging occurs only if the frequency of the averaging processes is comparable to the energy range (expressed as radians  $\text{sec}^{-1}$ ) through which these averaging processes drive the nuclear energy levels (2). Considering that all orientations of the O-D bonds are possible in our system, it is difficult to get the exact value of this critical frequency. However, for a rigid water molecule, a mean value of  $e^2qQ/\hbar$  can be taken into account giving a critical time scale for the averaging processes of about  $10^{-6}$  secs. Those averaging processes taking place over a shorter time scale than this value ( $10^{-6}$  secs.) will contribute to the averaging of the electric field gradients.

In the limit of isotropic motion, the linewidth ( $\propto \frac{1}{T_2}$ ), of the DMR spectra may be related to the rotational correlation time of  $D_2O$  by Eq. 5.11:

$$\frac{1}{T_2} = \frac{3}{80} \left( \frac{e^2qQ}{\hbar} \right)^2 \left( 3\tau_c + \frac{5\tau_c}{1+\omega^2\tau_c^2} + \frac{2\tau_c}{1+4\omega^2\tau_c^2} \right) \quad \dots (5.11)$$

where  $e^2qQ/\hbar$  is the nuclear quadrupole coupling constant (240 kHz) of deuterium and  $\omega$  is its Larmor frequency. Application of

Eq. 5.11 is limited to cases where  $\frac{1}{T_2}$  does not have a contribution from exchange broadening. Indeed, exchange broadening effects are not observed for lecithin-water systems (2) and we assumed the same for our case. By incorporating the standard values, Eq. 5.11 may be simplified to

$$\frac{1}{T_2} = (8.53 \times 10^{11} \tau_c) \quad \dots (5.12)$$

Substituting the experimental values of  $T_2$  in Eq. 5.12, we get an estimate of  $\tau_c$ , the rotational correlation time of  $D_2O$ . Table 5.1 gives the value of  $\tau_c$  thus estimated at different R values.

Table 5.1

$\tau_c$  values of PC-cyclohexane- $D_2O$  system at different R values

R	$T_2$ (seconds)	$\tau_c$ (seconds)
1.0	$4.66 \times 10^{-3}$	$2.52 \times 10^{-10}$
2.0	$5.01 \times 10^{-3}$	$2.34 \times 10^{-10}$
3.0	$4.82 \times 10^{-3}$	$2.43 \times 10^{-10}$
4.0	$4.65 \times 10^{-3}$	$2.52 \times 10^{-10}$
5.0	$4.65 \times 10^{-3}$	$2.52 \times 10^{-10}$
6.5	$5.22 \times 10^{-3}$	$2.25 \times 10^{-10}$
8.0	$1.89 \times 10^{-6}$	$6.20 \times 10^{-7}$



From Table 5.1 it is seen that the  $D_2O$  experimental spectra at  $R$  values below 8 (Figs. 5.2 to 5.6) correspond to rotation of  $D_2O$  that is considerably faster compared to the averaging processes ( $10^{-6}$  secs). At an  $R$  value of 8, where the system becomes anisotropic, a doublet is seen (see Fig. 5.8) with a separation of 4.8 kHz suggesting a spectacular change in water dynamics. The  $\tau_c$  value at an  $R$  value of 8 is  $6.2 \times 10^{-7}$  (see Table 5.1) which is only shorter by an order of magnitude compared with the averaging processes and hence the low value of doublet splitting. The narrowing of the doublet may at least in part be attributed to motions of the head group that binds  $D_2O$ . The probable motion may be rapid rotations round the axis of phosphorylcholine group. Available estimates of the rotational correlation time,  $\tau_c$ , for the plausible motional modes of the lecithin polar groups in the multilamellar systems show that these motions may also contribute to the averaging of the electric field gradients. Some modes have  $\tau_c > 10^{-4}$  secs (21), while others have  $\tau_c < 10^{-9}$  secs (22).

The diffusion constant for water in this system at an  $R$  value of 6 has been shown to be  $2.16 \times 10^{-5} \text{ cm}^2/\text{sec}$  in Chapter IV giving a diffusion path of 1000 Å in  $10^{-5}$  secs. If the water molecule can have different orientations with respect to the long axis of the aqueous water channel along its diffusion path, this will narrow the splitting further.

In essence, then, the possible narrowing mechanisms in our cyclohexane system include motion of the binding group (i.e.,

head group), diffusion of water along the aqueous channel and tumbling of water in the potential energy well defined by the binding group.

Of the three mechanisms envisaged, the most probable one is motional modulation of water that is getting bound to the head group, as will be substantiated by our  $^{31}\text{P}$ -NMR study which follows.

### $^{31}\text{P}$ -NMR Lineshape Analysis

The use of  $^{31}\text{P}$ -NMR as an analytical technique for probing the polymorphic phase behaviour in lecithin-water systems is becoming increasingly important. When the phospholipids are present in non-bilayer environment, their lateral diffusion produces an additional narrowing mechanism. As a result of this, distinctive  $^{31}\text{P}$ -NMR spectra are obtained for lipids in the bilayer phase, hexagonal ( $\text{H}_{\text{II}}$ ) phase or phases such as the inverted micellar, cubic or rhombic (8,26).

The effective chemical shift anisotropy,  $\Delta\sigma_{\text{CSA}}^{\text{eff}}$ , may be defined as the chemical shift between the highfield peak and the lowfield shoulder. The value of this  $\Delta\sigma_{\text{CSA}}^{\text{eff}}$  for phospholipids in bilayer phase is of the order of -40 ppm for phosphatidylcholines (23) and phosphatidylethanolamines (24) and therefore such lipids in the hexagonal  $\text{H}_{\text{II}}$  phase exhibit lineshapes with a lowfield peak and a highfield shoulder where  $\Delta\sigma_{\text{CSA}}^{\text{eff}} \simeq 20$  ppm. The cubic or inverted micellar phases exhibit very narrow,

symmetric  $^{31}\text{P}$ -NMR spectra which have a chemical shift characteristic of diesterified phosphates which can undergo rapid isotropic averaging motion (30).

Taking account of the contribution of chemical shift anisotropy to phospholipid phosphorous, an appropriate spin Hamiltonian could be written as (30)

$$\mathcal{H}_{\text{CSA}} = \gamma_{\text{P}} \hbar (1 - \sigma_a) S_Z + \Delta\sigma_{\text{CSA}}^{\text{eff}} \gamma_{\text{P}} \hbar [^1_1 \text{ } ^{-2}_2] \cdot \underline{S} \quad \dots (5.13)$$

where  $\gamma_{\text{P}}$  is the phosphorous gyromagnetic ratio,  $\hbar$  is the magnetic field,  $S_Z$  is the Z component of spin  $\underline{S}$ . Eq.(5.13) takes into account the effects of rapid axial rotation about an axis perpendicular to the bilayer common to liquid-crystalline phospholipids (25) and the corresponding  $^{31}\text{P}$ -NMR lineshapes for different phases are presented in Fig. 5.9.

Lateral diffusion around the aqueous channels for phospholipids in the hexagonal  $\text{H}_{\text{II}}$  phase causes additional motional averaging. If we assume the long axis of the cylindrical aqueous channel to be labelled as the X-direction, the averaging out of the Y and Z components of the tensor of Eq. (5.13) may be mathematically expressed as

$$\mathcal{H}_{\text{CSA}} = \gamma_{\text{P}} \hbar (1 - \sigma_a) S_Z - \Delta\sigma_{\text{CSA}}^{\text{eff}} \gamma_{\text{P}} \hbar [^{-2}_1 \text{ } ^1_1] \cdot \underline{S} \quad \dots (5.14)$$

If  $\theta$  is the angle subtended by the X-axis with respect to  $\underline{H}$ ,

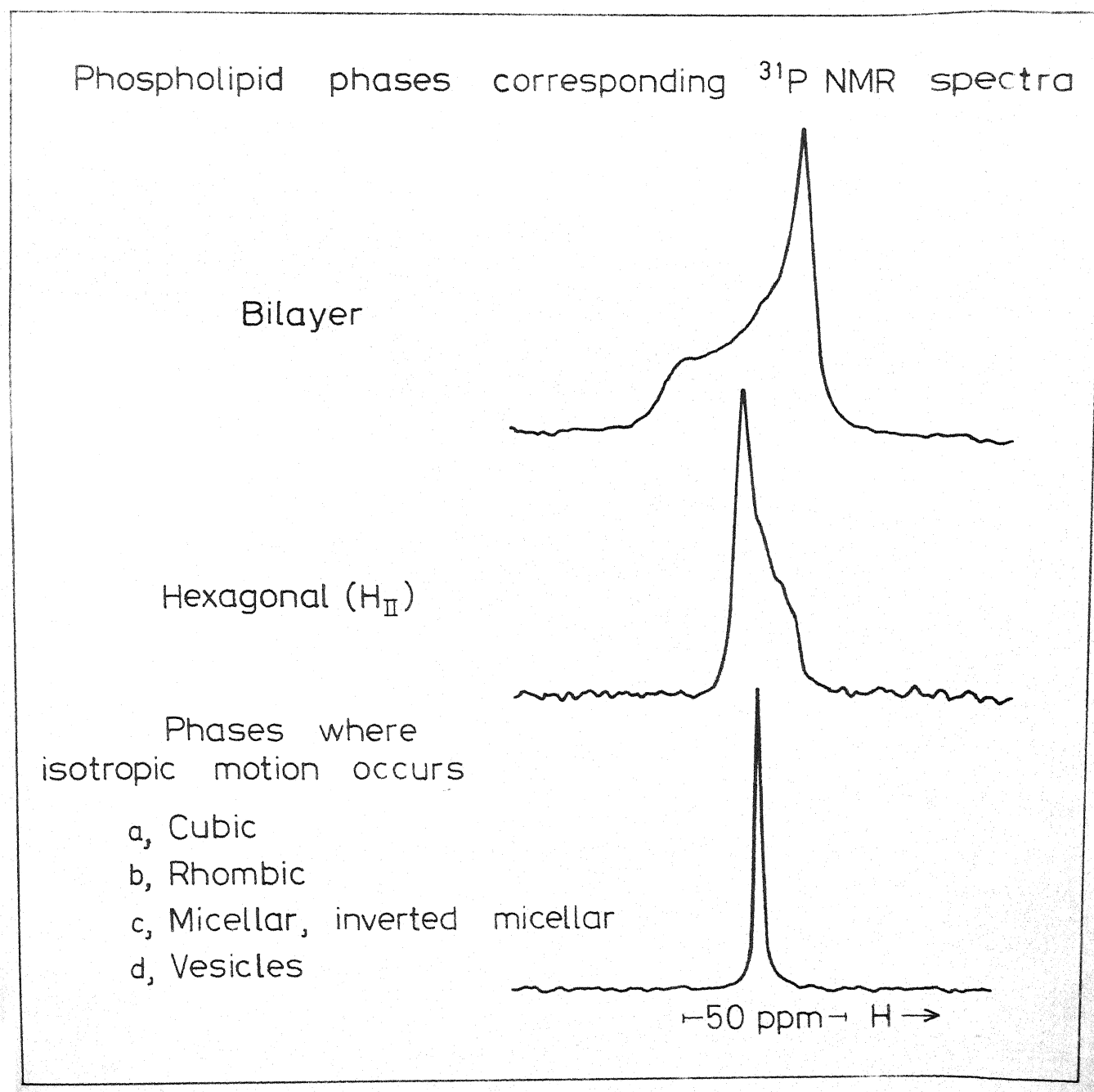


Fig. 5.9 Polymorphic phases of Phospholipids and the corresponding  $^{31}\text{P}$  NMR spectra.

then the chemical shift of the  $^{31}\text{P}$ -NMR signal from a particular lipid cylinder is given by

$$\Delta\nu(\theta) = -\gamma_{\text{P}} \text{H} \frac{\Delta\sigma_{\text{CSA}}^{\text{eff}} (3 \cos^2 \theta - 1)}{6} \quad \dots (5.15)$$

The lineshapes expected from hexagonal ( $\text{H}_{\text{II}}$ ) phase systems will have a reversed asymmetry and half the chemical shift anisotropy as compared with lineshapes expected for bilayer structures (see Fig. 5.9).

In Fig. 5.10 we present the experimental  $^{31}\text{P}$  NMR lineshape of the cyclohexane system at an R value of 6.5. Comparing the features of Fig. 5.10 with those of Fig. 5.9, it could be easily inferred that the liquid crystalline phase formed in cyclohexane system is of the hexagonal  $\text{H}_{\text{II}}$  type.

The chemical shift anisotropy of the experimental spectra presented in Fig. 5.10 is only 0.25 ppm at an observation frequency of 32.44 MHz. This value of CSA is less than by two orders of magnitude compared with the CSA values of the hexagonal  $\text{H}_{\text{II}}$  phase found in lecithin-water systems (27,29,30). For significant motional averaging to occur, the relation  $\omega^2 \ll 1$  must be obeyed where  $\omega^2 \simeq (\gamma_{\text{P}} \text{H} \Delta\sigma_{\text{CSA}}^{\text{eff}})^2$ . For  $\Delta\sigma_{\text{CSA}}^{\text{eff}} = 0.25$  ppm at an observation frequency of 32.44 MHz one would therefore require that  $\tau_{\text{c}} \ll 10^{-2}$  secs.

Fully detailed theories which are ideally suited for the  $^{31}\text{P}$  lineshape analysis based on Eqs. 5.13 to 5.15 for the  $^{31}\text{P}$

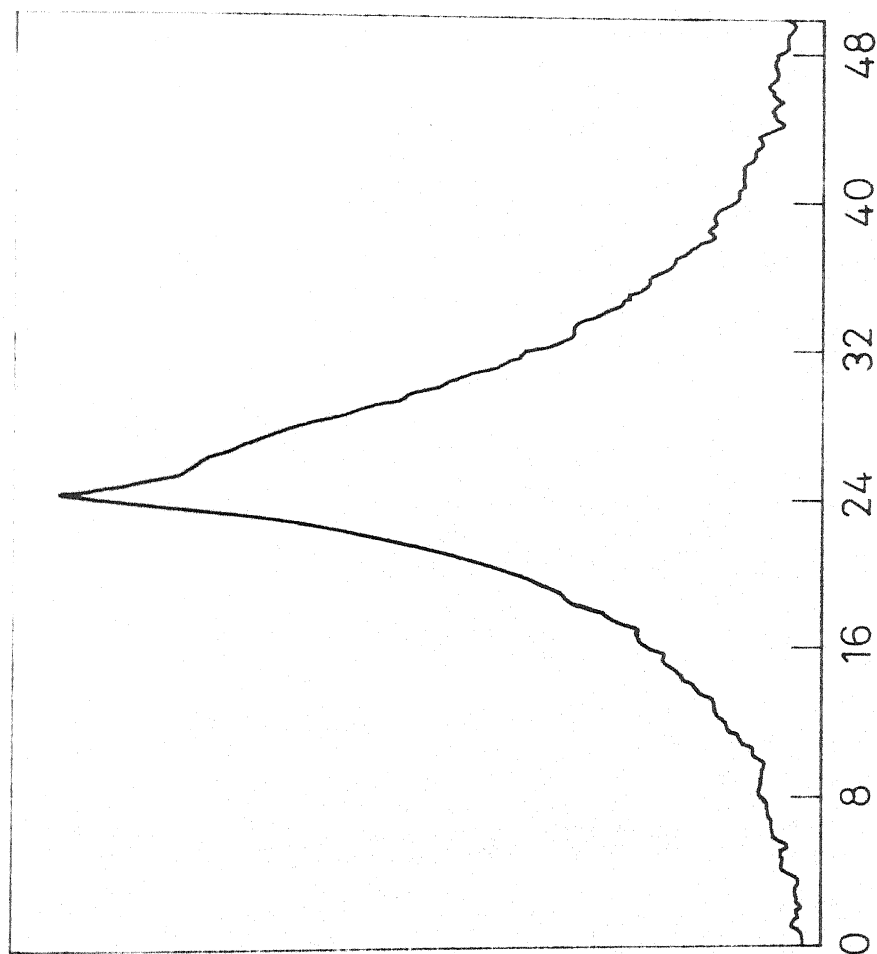
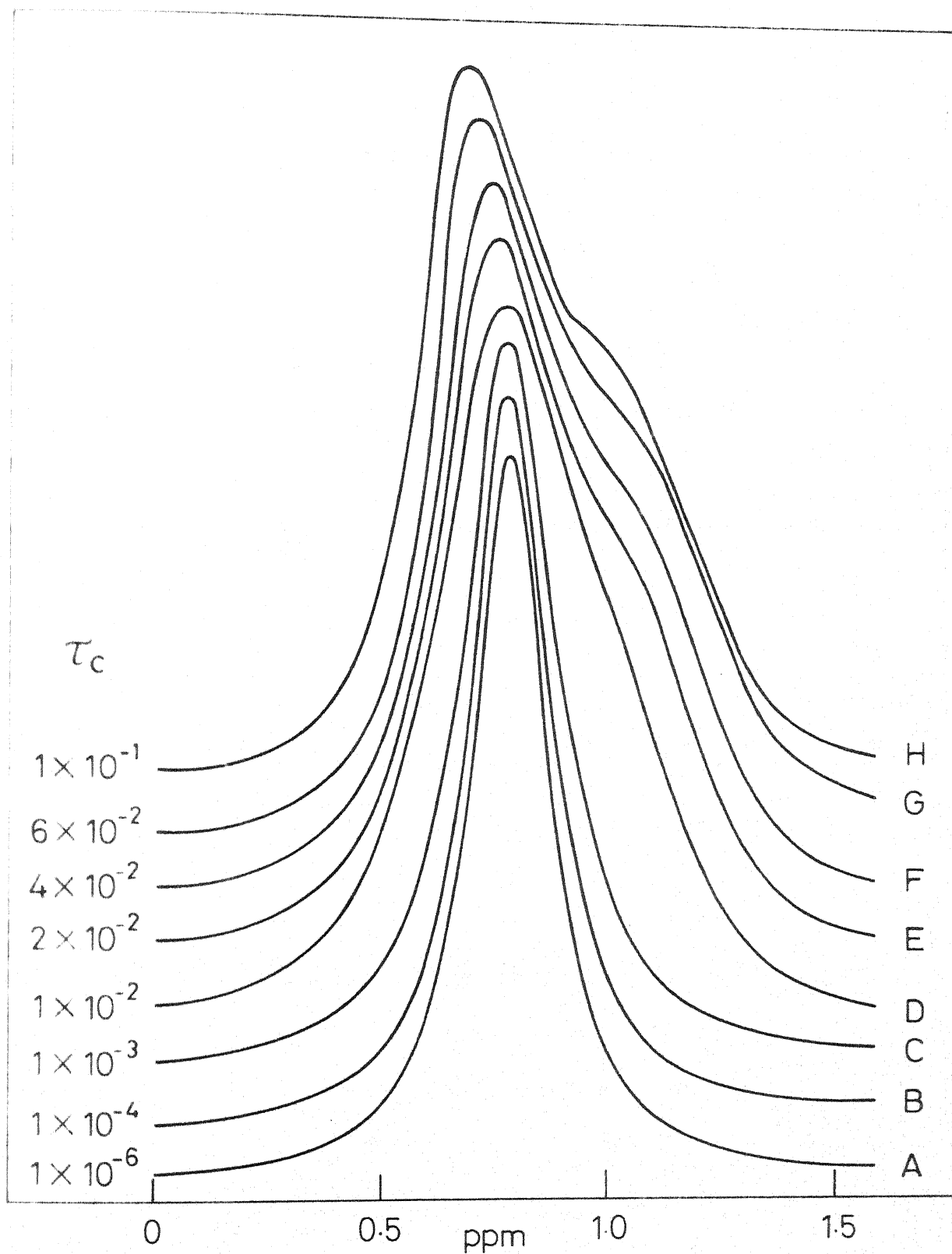


Fig. 5.10 32.44 MHz Phosphorous NMR spectrum of  
PC-Cyclohexane-D<sub>2</sub>O system at an R  
value of 6.5

chemical shift anisotropy are available in the literature (28,29), and will not be reviewed here. However, in recent work of Burnell et al. (27) on phospholipid systems, a computer calculation has been used which essentially incorporates the earlier theories (28,29) in a simple form, using  $\tau_c$  as the only adjustable parameter. We have used this computer calculation (reprogrammed to work on the IIT-Kanpur DEC-10 computer) to simulate our experimentally observed lineshape in the cyclohexane system. Representative simulations obtained for different  $\tau_c$  values are presented in Fig. 5.11. The 'best-fit' simulation to Fig. 5.10, is shown in Fig. 5.11E and corresponds to a correlation time of  $2 \times 10^{-2}$  secs. This value not only agrees well with the  $\tau_c$  estimated and presented earlier (i.e.  $\tau_c < 10^{-2}$  secs), but also reveals that a basic mechanism of slow motion of the head group is present which causes the above modulation.

How is an understanding of hexagonal  $H_{II}$  phase likely to be of importance? Here it should be first stated that our work is concerned with a non-bilayer phospholipid arrangement and its interaction with water. Now, several current models of biological membranes postulate that for the non-bilayer hexagonal  $H_{II}$  phase in an aqueous environment has a profound influence on the structure and function of biological membranes (25,30). This concept becomes especially valid if there are possibilities of segregation of phospholipids either in the plane of the membrane or across the membrane (30). As indicated in Fig. 1.6 of Chapter I, such a possibility could be envisaged to allow rapid



1 Computer Simulated Phosphorous NMR Lineshape for different values of  $\tau_c$



'flip-flop' of particular species of lipid across the membrane. Since local high concentrations of 'non-bilayer' lipid in one monolayer result in destabilisation of the monolayer, there occurs the intermediate formation of  $H_{II}$  or other inverted phase such as an inverted micelle. This subsequently leads to the redistribution of the 'non-bilayer' lipid on the monolayer of the membrane (30).

To test all such contemporary ideas in depth, and to provide proper diagnostics, approaches similar to ours based on a simple 'proto-type' model system should hopefully be of some value.

REFERENCES

1. N.J. Salsbury, A. Darke and D. Chapman, Chem. Phys. Lipids, 8, 142 (1972).
2. E.G. Finer, J. Chem. Soc. Faraday Trans. II, 69, 1590 (1973).
3. J. Seelig and A. Seelig, Biochem. Biophys. Res. Commun., 57, 406 (1974).
4. E.G. Finer and A. Darke, Chem. Phys. Lipids, 12, 1 (1974).
5. J. Ulminius, H. Wennerstrom, G. Lindblom and G. Arvidson, Biochemistry, 16, 5742 (1977).
6. K. Gawrisch, K. Arnold, T. Gottwald, G. Klose and F. Volke, Stud. Biophys., 74, 13 (1978).
7. D.G. Davis, Biochem. Biophys. Res. Commun., 46, 1492 (1972).
8. P.R. Cullis and B. De Kruijff, Biochim. Biophys. Acta, 559, 399 (1979). and references therein.
9. B. De Kruijff, P.R. Cullis, and A.J. Verkleij, Trends. Biochem. Sci., 5, 79 (1980) and references therein.
10. A Abragam, 'Principles of Nuclear Magnetism,' Oxford University Press, London, 1961, p. 232-234.
11. C.P. Slichter, 'Principles of Magnetic Resonance,' Springer. Verlag, New York, 1978, p. 275-291.
12. T.L. James, 'NMR in Biochemistry,' Academic Press, New York, 1975.
13. M.H. Cohen and F. Reif, Solid State Physics, 5, 321 (1957).
14. P. Waldstein, S.W. Rabideau and J.A. Jackson, J. Chem. Phys., 41, 3407 (1964).
15. S.W. Rabideau and J.A. Jackson, J. Chem. Phys., 41, 4008 (1964).
- 11 T. Chiba, J. Chem. Phys., 41, 1352 (1964).

17. H. Wennerstrom, G. Lindblom and B. Lindman, *Chemical Scripta*, 6, 97 (1974).
18. H. Wennerstrom, *Mol. Phys.*, 24, 69 (1972).
19. J.H. Davis, K.R. Jeffrey, M. Bloom, M.I. Valic, and T.P. Higgs, *Chem. Phys. Lett.*, 42, 390 (1976).
20. G. Soda and T. Chiba, *J. Chem. Phys.*, 50, 439 (1969).
21. D. Chapman, E. Oldfield, D. Doskocilova, and B. Schneider, *FEBS Lett.*, 25, 261 (1972).
22. E.G. Finer, A.G. Flook and H. Hauser, *Biochim. Biophys. Acta*, 260, 59 (1972).
23. P.R. Cullis, *FEBS Lett.*, 70, 223 (1976).
24. P.R. Cullis and B. De Kruijff, *Biochim. Biophys. Acta*, 436, 523 (1976).
25. P.R. Cullis and A.C. McLaughlin, *Trends. Biochem. Sci.*, 2, 196 (1977).
26. P.R. Cullis, B. De Kruijff and R.E. Richards, *Biochim. Biophys. Acta*, 426, 433 (1976).
27. E.E. Burnell, P.R. Cullis and B. De Kruijff, *Biochim. Biophys. Acta*, 603, 63 (1980).
28. S. Alexander, A. Baram and Z. Luz, *J. Chem. Phys.*, 61, 992 (1974).
29. R.F. Campbell, E. Meirovitch and J.H. Freed, *J. Phys. Chem.*, 83, 525 (1979).
30. P.R. Cullis and B. De Kruijff, *Biochim. Biophys. Acta*, 507, 207 (1978).

CONCLUSIONS  
AND  
SOME FURTHER PROSPECTS

On the basis of the extensive experimental results presented on the three systems, namely, Lecithin-Benzene-Water, Lecithin-Carbontetrachloride-Water and Lecithin-Cyclohexane-Water, the following conclusions have emerged.

(i) Though all the three solvents are highly non-polar (having almost the same dielectric constant of  $\sim 3$ ), the cyclohexane system behaves entirely differently in several respects. This leads to the conclusion that micellisation takes place in different ways in different solvents. It is, therefore, not perhaps warranted to extrapolate the apparent physical state of the micelle (e.g., size, shape and aggregation number) from one solvent to another. This incidentally also provides a rationalisation for the selection of the particular solvents used in this study.

(ii) A very important and interesting observation in cyclohexane system is the formation of an anisotropic (possibly liquid crystalline) phase around an R value of 6, which is

well characterised by our physical studies presented in Chapter II.

(iii) We have been able to characterise the dynamics of the pool water, bound water and phospholipid head group motion by means of a variety of nuclear magnetic resonance and other spectroscopic techniques presented in Chapter III.

(iv) The anisotropic phase in the cyclohexane system has been further examined by specific, specialised NMR experiments in Chapters IV and V. The results of these chapters provide a quantitative or at least semiquantitative estimate of such microscopic properties as (a) the diffusion dynamics of the water pool, (b) the bound-water interaction with the phospholipid head-group and (c) the phospholipid head-group dynamics itself.

After the completion of the work contained in this thesis, preliminary studies have been begun by us on the following systems:

1) Phosphatidylethanolamine (see Fig. 1.1 of Chapter I) contains a labile hydrogen in its head group which can form a hydrogen bond with the negative oxygen atom of the phosphate group. Furthermore, the head group in PE is not as bulky as in PC. Given these factors, it would be interesting to study the effect of water on PE head groups in non-polar organic solvents. We have already carried out some preliminary studies on PE-non-polar solvent-water system and PE is found to behave entirely differently as compared with PC.

2) In PC-diethyl ether systems, it has been reported by Wells ( cf. ref. 120 of Ch. I) that  $\text{Co}^{2+}$  exists as a tetrahedral blue complex. As a function of added water, there is gradual conversion of this blue, tetrahedral complex into a pink, octahedral complex. Such a phenomenon has not been observed by us when phosphatidylcholine (PC) is dissolved in  $\text{C}_6\text{H}_6$ ,  $\text{CCl}_4$  or cyclohexane. In the latter solvents, this behaviour may be due to the fact that the  $\Delta G$  (free energy difference) between  $\text{>N}^+ \text{---} \text{H}_2\text{O}$ ,  $\text{PO}_4^{3-} \text{---} \text{H}_2\text{O}$  and  $\text{>N}^+ \text{---} \text{PO}_4^{3-}$  is not larger than  $\Delta G$  for  $\text{Co}^{2+} \cdot 6\text{H}_2\text{O} \longrightarrow \text{Co}^{2+} \cdot 4\text{H}_2\text{O} + 2\text{H}_2\text{O}$  reaction. It is proposed to investigate further such interactions between phospholipid head-groups and water in a variety of solvent media.

VITAE

Born on October 9, 1954, at Guntur, Andhra Pradesh, Mr. V. Venkateswara Kumar had his early education at the Salvation Army High School, Bapatla. In 1973, he took his B.Sc. degree at C.S.R. Sarma College, Ongole and M.Sc. degree in Chemistry from Andhra University, Waltair in 1975. He has been working as Lecturer in Chemistry at C.S.R. Sarma College, Ongole since 1975 before being awarded a teacher fellowship under Faculty Improvement Programme of University Grants Commission in January 1979 for research at Indian Institute of Technology, Kanpur.

LIST OF PUBLICATIONSPAPERS

1. Physical Studies on Lecithin Reverse Micelles,  
J. Colloid Interface Science (communicated),  
V.V. Kumar, C. Kumar and P. Raghunathan.
2. Spectroscopic Studies on Lecithin Reverse Micelles,  
J. Phys. Chem. (communicated)  
V.V. Kumar and P. Raghunathan.
3. NMR of Water Diffusion in Lecithin-Cyclohexane-Water  
System,  
Biochim. Biophys. Acta (communicated)  
V.V. Kumar and P. Raghunathan.
4.  $^1\text{H}$  and  $^{31}\text{P}$ -NMR Studies of Lecithin Reverse Micelles,  
J. Mag. Res. (Manuscript under preparation),  
V.V. Kumar and P. Raghunathan.
5.  $^2\text{H}$  and  $^{31}\text{P}$ -NMR Studies of Lecithin-Cyclohexane- $\text{D}_2\text{O}$  System,  
J. Mag. Res. (Manuscript under preparation),  
V.V. Kumar and P. Raghunathan.
6.  $^{13}\text{C}$ -NMR Studies of Lecithin Reverse Micelles,  
J. Am. Chem. Soc. (Manuscript under preparation),  
V.V. Kumar and P. Raghunathan.

REVIEW

Lecithin Reverse Micelles - An Overview  
(Manuscript under preparation).